ARCHIVES OF MECHANICS **Appears since 1949**

Aims and Scope

ARCHIVES OF MECHANICS provides a forum for original research on mechanics of solids, fluids and discrete systems, including the development of mathematical methods for solving mechanical problems. The journal encompasses all aspects of the field, with the emphasis placed on:

- mechanics of materials: elasticity, plasticity, time-dependent phenomena, phase transformation, damage, fracture; physical and experimental foundations, micromechanics, thermodynamics, instabilities
- methods and problems in continuum mechanics: general theory and novel applications, thermomechanics, structural analysis, porous media, contact problems
- dynamics of material systems
- fluid flows and interactions with solids

Address of the Editorial Office:
Institute of Fundamental Technological Research
Świętokrzyska 21
PL 00-049 Warsaw, Poland

Tel.: (48-22) 826 60 22, Fax: (48-22) 826 98 15, E-mail: publikac@ippt.gov.pl

Abstracted/indexed in:

Applied Mechanics Reviews, Current Mathematical Publications, Mathematical Reviews, MathSci, Zentralblatt für Mathematik, UnCover.

Polish Academy of Sciences

Institute of Fundamental Technological Research

Archives of Mechanics

Archiwum Mechaniki Stosowanej

volume 52 issue 2

Agencja Reklamowo-Wydawnicza A. Grzegorczyk
Warszawa 2000

SUBSCRIPTIONS

Address of the Editorial Office: Archives of Mechanics
Institute of Fundamental Technological Research, Świętokrzyska 21
PL 00-049 Warsaw, Poland
Tel.: (48-22) 826 60 22, Fax: (48-22) 826 98 15, E-mail: publikac@ippt.gov.pl

Subscription orders for all journals edited by IFTR may be sent directly to the Editorial Office of the Institute of Fundamental Technological Research

Subscription rates

Annual subscription rate (2000) including postage is US $ 192.
Please transfer the subscription fee to our bank account: Payee: IPPT PAN,
Bank: PKO SA. IV O/Warszawa,
Account no. 12401053-40054492-3000-401112-001.
All journals edited by IFTR are available also through:

- Foreign Trade Enterprise ARS POLONA Krakowskie Przedmieście 7, 00-068 Warszawa, Poland fax: (48-22) 826 86 73
- RUCH S.A. ul. Towarowa 28, 00-958 Warszawa, Poland fax:(48-22) 620 17 62
- Agencja Reklamowo-Wydawnicza A. Grzegorczyk, Bitwy Warszawskiej 1920r. 3, 00-973 Warszawa, Poland tel./fax: (48-22) 822 49 36

Warunki prenumeraty

Redakcja przyjmuje prenumeratę na wszystkie czasopisma wydawane przez IPPT PAN. Bieżące numery można nabyć a także zaprenumerować roczne wydanie Archiwum Mechaniki Stosowanej bezpośrednio w Dziale Wydawnictw IPPT PAN, Świętokrzyska 21, 00-049 Warszawa, Tel.: (48-22) 826 60 22; Fax: (48-22) 826 98 15.
Cena rocznej prenumeraty z bonifikatą (na rok 2000) dla krajowego odbiorcy wynosi 150 zł

Również można je nabyć, a także zamówić (przesyłka za zaliczeniem pocztowym) we Wzorcowni Ośrodka Rozpowszechniania Wydawnictw Naukowych PAN,
00-818 Warszawa, ul. Twarda 51/55, tel. (48-22) 697 88 35.
Wpłaty na prenumeratę przyjmują także jednostki kolportażowe RUCH S.A. Oddział Krajowej Dystrybucji Prasy, 00-958 Warszawa, ul. Towarowa 28. Konto: PBK.S.A. XIII Oddział Warszawa nr 11101053-16551-2700-1-67. Dostawa odbywa się pocztą zwykłą w ramach opłaconej prenumeraty z wyjątkiem zlecenia dostawy pocztą lotniczą, której koszt w pełni pokrywa zleceniodawca. Tel.: (48-22) 620 10 39, fax: (48-22) 620 17 62

Arkuszy wydawniczych 10.4. Arkuszy drukarskich 12/A5.
Papier offset. kl III 70 g. B1.
Oddano do składania w lutym 2000 r. Druk ukończono w marcu 2000 r.
Skład i łamanie: G. Wasilewska. Druk i oprawa: Drukarnia OMIKRON, Stare Babice ul. Kutrzeby 15.

Arch. Mech., **52**, 2, pp. 203–223, Warszawa 2000

Modelling of nonstationary heat conduction problems in micro-periodic composites using homogenisation theory with corrective terms

M. LEFIK ([1]) and B. A. SCHREFLER ([2])

([1]) *Department of Mechanics of Materials, Technical University of Łódź, Poland*

([2]) *Dipartimento di Costruzioni e Trasporti, University of Padova, Italy*

HOMOGENISATION BASED on the asymptotic series expansion is used to model a nonstationary behaviour of a rigid heat conductor with micro-periodic structure. A usual first-order approximation (which cannot be assumed as a satisfactory solution for time-dependent problems) is treated as a suitable starting point for further corrections that make it admissible. An initial correction takes into account some fast processes acting on the level of the microstructure and guarantees that the initial condition is satisfied. Some higher-order correctors are intended to improve the first-order approximation far from the onset of the process, for composites with strongly different properties of components or for the case of a rough microstructure. A numerical example shows that the role of the initial corrector is prevailing in the model.

Notations

$\mathbf{x}$, $\mathbf{y}$	position vector in global and local co-ordinate system respectively,
t, τ	time,
$\Theta^k(\mathbf{x},\mathbf{y},t), T^k(\mathbf{x},t)$	temperature fields related to the k-th order of approximation,
$J^k(\mathbf{x},\mathbf{y},t)$	initial corrector to the temperature related to the k-th order of approximation,
$\mathbf{q}^k(\mathbf{x},\mathbf{y},t)$	heat flux related to k-th order of approximation,
$\chi^{(k)p}(\mathbf{y})$	p-th homogenisation function on the k-th level of approximation,
$k_{ij}(\mathbf{y}), c(\mathbf{y})$	tensor of thermal conductivity and coefficient of diffusivity,
K_{ij}	tensor of effective thermal conductivity,
$r(\mathbf{x})$	thermal sources,
$f_{,i(y)}, f_{,i(x)}, \dot{f}$	represent first derivatives of f with respect to y_i, x_i and t respectively,
$[f]_s$	represents the jump of a function f across a surface S,
$\tilde{f}(\mathbf{x},t)$ or $\langle f(\mathbf{x},t)\rangle$	represents the average value of a function $f(\mathbf{x},\mathbf{y},t)$,
meas Y	denotes a measure of an ensemble Y.

1. Introduction

WE ANALYSE here a nonstationary heat conduction problem in a rigid, microperiodic composite. For this purpose we construct a succession of approximate models using an asymptotic theory of homogenisation with some necessary correction due to the time-dependence of the problem.

The classical theory of homogenisation, resulting in effective moduli, provides a solution that cannot satisfy exactly the local boundary conditions or the initial conditions for time-dependent problems. The theory of homogenisation yields the effective constitutive law valid on the macrolevel, starting from the microdescription of the problem (without any *a priori* hypothesis about the macro-behaviour). This is the main idea of the micromechanical approach and it is obvious that boundary condition at the macro-level are then of minor importance. In fact, boundary and initial conditions cannot influence the effective material properties. On the other hand, the behaviour of the composite material in the vicinity of the border requires a special analysis. For the nonstationary process, because of the microheterogeneity, the global solution should also be analogously corrected at the initial moment.

The reason for this is given in a recent paper by WOŹNIAK *et al.* [12]. The authors show that the usual effective modulus theory leads to important errors in the prediction of the global, nonstationary thermal behaviour of the composite. A refined theory based on the concept of macrofunctions is applied there to solve correctly the problem of nonstationary heat conduction in composites.

Here we intend to adapt a classical, asymptotic theory of homogenisation to solve the problem of nonstationary heat conduction in a body with microstructure. We show that the improvement of this theory is possible and that some corrections can give a satisfactory approximation of the exact solution. Moreover, the algorithm of this correction process is similar to that described in [2, 4, 6] and applied by us in [7] and [8]. This algorithm assumes that the first order model, resulting from the theory of homogenisation, is a convenient starting point for the construction of an improvement of this approximation at the beginning of the process. The description of the heat and temperature distribution at the level of the microstructure can be refined as well. This assumption has been verified in the problem of boundary layers of the composite and results in an efficient numerical procedure.

We consider two kinds of corrections: first, the correction including the higher-order term in the asymptotic expansion of the exact solution in the power series of the small parameter characterising the microstructure, and second - a correction of the solution near the onset of the process, called the initial correction. This second type of correction seems to be new in the literature. We analyse the influence of these two corrections. It appears that the first correction

(that introduced via higher-order correctors) guarantees a weak convergence of the model to the exact solution. Hence the approximate solution far from the initial moment and inside of the body is very close to the exact one. However, the initial corrector changes qualitatively the solution at the beginning of the process and its role is still predominant, even until the process becomes steady. In this paper we present only some formal calculations. We do not analyse the regularity of the resulting family of boundary value problems because we do not expect any problem in this field. Finally, we present a simple, illustrative example which shows the efficiency of the proposed improvement.

2. Formulation of the problem and homogenization procedure

Let us consider the classical nonstationary heat conduction problem formulated for a rigid, micro-periodic composite body. Two systems of co-ordinates $\mathbf{x}$ and $\mathbf{y}$ describe the geometry of the body on the macro and micro-level, respectively. The assumed separation of scales between macro and micro phenomena is formally expressed by the following relation between two systems of co-ordinates $\mathbf{x}$ and $\mathbf{y}$ (see Fig. 1.):

$$\mathbf{y} = \varepsilon^{-1}\mathbf{x}. \tag{2.1}$$

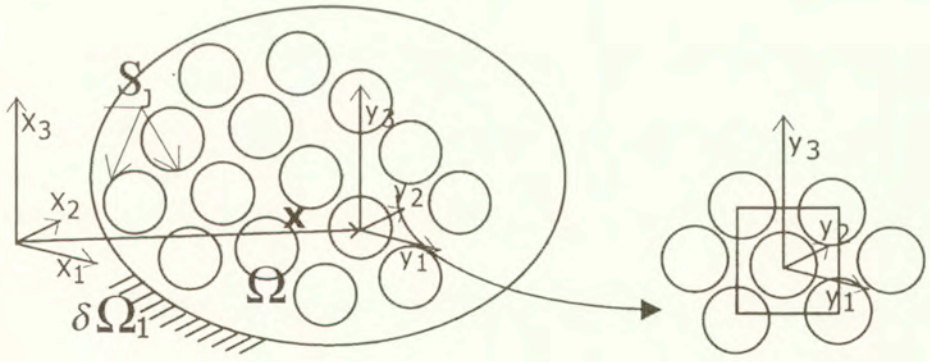

FIG. 1.

The small parameter ε, required by the homogenisation theory, is defined as the ratio between the characteristic dimension of the cell of periodicity and the diameter of Ω. This choice of the small parameter means that we are interested in the analysis of the behaviour of a solution when the microstructure is scaled down. The same symbol (used as a superscript will denote such a structure-dependent solution. Another possible choice of small parameter (such as for instance in [2]) seems to be not adequate for the analysis followed here.

The following equations define the problem under investigation:
Heat balance written for the body with diffusivity varying at the micro-level:

$$q_{i,i}(\mathbf{y},\mathbf{x},t) = \rho r(\mathbf{y},\mathbf{x},t) - c(\mathbf{y})\dot{\Theta}(\mathbf{y},\mathbf{x},t) \qquad \text{in } \Omega^{\varepsilon}. \tag{2.2}$$

Fourier law with rapidly oscillating conductivity tensor:

$$q_i(\mathbf{y},\mathbf{x},t) = -k_{ij}(\mathbf{y})\Theta_{,j}(\mathbf{y},\mathbf{x},t) \quad \text{in } \Omega^{\varepsilon}, \tag{2.3}$$

$$T(\mathbf{y},\mathbf{x},t) = T_b(\mathbf{y},\mathbf{x},t) \text{ on } \partial\Omega_T^{\varepsilon} \quad \text{and} \quad q_j(\mathbf{y},\mathbf{x},t)n_j = q_b(\mathbf{y},\mathbf{x},t) \quad \text{on} \quad \partial\Omega_h^{\varepsilon}, \tag{2.4}$$

$$T(\mathbf{y},\mathbf{x},t) = 0) = T_0(\mathbf{y},\mathbf{x}), \tag{2.5}$$

$$[T(\mathbf{y})] = 0 \; [q_j(\mathbf{y})n_j] = 0 \quad \text{on } S_J. \tag{2.6}$$

Of course, all the differentiations (appearing above and throughout the paper) are to be understood in the weak sense and will be replaced by equivalent variational formulations for detailed analysis if necessary. We assume also that all the usual requirements for the correctness of formulation hold. We suppose further that the periodicity of material characteristics imposes an analogous periodic perturbation on the studied quantities describing the thermal behaviour of the body. We will use hence the following representation for temperature:

$$\Theta^{\varepsilon}(\mathbf{x},t) \equiv \Theta^0(\mathbf{x},t) + \varepsilon^k\Theta^k(\mathbf{x},\mathbf{y},t), \tag{2.7}$$

where $k > 0$ and Θ^k are Y-periodic, i.e. takes the same values on the opposite sides of the cell of periodicity. The corresponding expansion of heat flux can be written as follows:

$$q_i^{\varepsilon}(\mathbf{x},t) = -k_{ij}(\mathbf{y})\left(\Theta^0_{,j(x)}(\mathbf{x},t) + \Theta^1_{,j(y)}(\mathbf{x},\mathbf{y},t)\right) + .. - \varepsilon^k k_{ij}(\mathbf{y})\left(\Theta^k_{,j(x)}(\mathbf{x},\mathbf{y},t) + \Theta^{k+1}_{,j(y)}(\mathbf{x},\mathbf{y},t)\right). \tag{2.8}$$

We will denote by $q_i^k(\mathbf{x},\mathbf{y})$ the flux component of order k, given in Eq. (2.8) by the expressions in parentheses, multiplied by ε^k.

We apply here and in the sequel the following notation for the chain rule of differentiation:

$$f_{,i} \equiv \frac{d}{dx_i}f = \left(\frac{\partial}{\partial x_i} + \frac{1}{\varepsilon}\frac{\partial}{\partial y_i}\right)f \equiv f_{,i(x)} + \frac{1}{\varepsilon}f_{,(y)}. \tag{2.9}$$

We are looking for some relationships analogous to (2.7) and (2.8) but formulated for some equivalent, homogeneous body and involving averaged (or global) quantities:

$$\tilde{\Theta}(\mathbf{x},t) = \frac{1}{\text{meas}Y}\int_Y \Theta(\mathbf{x},\mathbf{y},t)dY, \qquad \tilde{\mathbf{q}}(\mathbf{x},t) = \frac{1}{\text{meas}Y}\int_Y \mathbf{q}(\mathbf{x},\mathbf{y},t)dY. \tag{2.10}$$

By introducing Θ and q into (2.2) and (2.3) in the forms prescribed above, we split these equations into a pair of infinite systems of equations by equating terms of the same order. The first of these systems we will call "heat balance" (hb), the second one – the "Fourier law decomposition" (Fld). The first two terms of (hb) and the first term of (Fld) are taken into account to formulate the following well-known result of the homogenisation theory (see for example [1, 10]), called here "the first order approximation":

$$\tilde{q}_{i,i}(\mathbf{x},t) = \rho r(\mathbf{x},t) - \tilde{c}\dot{\tilde{\Theta}}(\mathbf{x},t) \quad \text{in } \Omega, \tag{2.11}$$

$$\tilde{q}_i(\mathbf{x},t) = -K_{ij}\tilde{\Theta}_{,j}(\mathbf{x},t) \quad \text{in } \Theta. \tag{2.12}$$

The tensor of effective thermal conductivity $\mathbf{K}$ is defined by a vector of homogenisation functions $\chi^{(0)p}(\mathbf{y})$:

$$K_{ij} = \frac{1}{\text{meas}Y}\int k_{ip}(y)\left(\delta_{pj} + \chi^{(0)p}_{,j}(\mathbf{y})\right)dY. \tag{2.13}$$

These functions satisfy the condition of local heat balance equation of order 0 ("local" means here: over the cell of periodicity):

$$\left(k_{ij}(\mathbf{y})(\delta_{ij} + \chi^{(0)p}_{,j(y)}(\mathbf{y})\right)_{,i(y)} = 0, \tag{2.14}$$

$$\left[k_{ij}(\mathbf{y})\left(\delta_{jp} + \chi^{(0)p}_{,j(y)}(\mathbf{y})\right)n_i\right] = 0, \tag{2.15}$$

(these equations express continuity of the heat flux across the interfaces of different materials inside Y),

$$\tilde{\chi}^{(0)p} = 0 \quad \text{and} \quad \chi^{(0)p}(\mathbf{y}) \quad \text{is } Y-\text{periodic}. \tag{2.16}$$

The variational counterpart of (2.14), (2.15) and (2.16) can be easily formulated (derivatives should be taken in the weak sense).

Mean form of the boundary and initial conditions complete the equivalent boundary value problem:

$$\tilde{T}(\mathbf{x},t) = \tilde{T}_b(\mathbf{x},t) \quad \text{on } \partial\Omega_T \quad \text{and} \quad \tilde{q}_j(\mathbf{x},t)n_j = \tilde{q}_b(\mathbf{x},t) \quad \text{on } \partial\Theta_h, \tag{2.17}$$

$$\tilde{T}(\mathbf{x},t=0) = \tilde{T}_0(\mathbf{x}). \tag{2.18}$$

It can be also deduced at this level of approximation that

$$\Theta^1(\mathbf{x},\mathbf{y},t) = T^1(\mathbf{x},t) + \chi^{(0)i}(\mathbf{y})T^0_{,i(x)}(\mathbf{x},t), \tag{2.19}$$

where $T^0(\mathbf{x},t) = \tilde{\Theta}(\mathbf{x},t)$ a solution of (2.11), (2.12) and $T^1(\mathbf{x},t)$ is to be defined on the next level of approximation. This fact is important since it defines a successive step of the solution of the system of equations.

In fact, the above solution, called here the "first approximation", is truncated at the term of zero order. According to the terminology adopted, all successive terms will be called "correctors", thus k-th order corrector corresponds to the temperature and heat flux with ε to the power of k in (2.7) and (2.8).

3. Higher order correctors

As a natural continuation of the approximation process initiated above, we attempt to compute the successive terms in (hb) and (Fld). We observe that the recurrent procedure initiated by (2.19) can be generalised by writing

$$\begin{aligned}\Theta^\varepsilon(\mathbf{x},\mathbf{y},t) = T^0(\mathbf{x},t) &+ \varepsilon(T^1(\mathbf{x},t) + \chi^{(0)i}(\mathbf{y})T^0_{,i(x)}(\mathbf{x},t)) \\ &+ \ldots + \varepsilon^k(T^k(\mathbf{x},t) + \chi^{(0)i}(\mathbf{y})T^{k-1}_{,i(x)}(\mathbf{x},t) \\ &+ \ldots + \chi^{(k-1)i..\times k..j}(\mathbf{y})T^0_{,i..\times k..j(x)}(\mathbf{x},t)).\end{aligned} \tag{3.1}$$

This form is given in [2], but our analysis differs from that which is shown in that reference. Using this representation, the equation number k in (hb) can be written in the form:

$$\begin{aligned}&k_{ij}(\mathbf{y})(\delta_{jp} + \chi^{(0)p}_{,j(y)})T^k_{,pi(x)}(\mathbf{x},t) + k_{ij}(\mathbf{y})(\delta_{jp}\chi^{(0)p} + \chi^{(1)pq}_{,j(y)})T^{k-1}_{,pqi(x)}(\mathbf{x},t) \\ &+ \ldots + k_{ij}(\mathbf{y})(\delta_{jp}\chi^{(k-1)p..\times(k-1)..r} + \chi^{(k)p..\times(k-1)..rq}_{,j(y)})T^0_{,p..\times(k-1)..rqi(x)}(\mathbf{x},t) \\ &+ (k_{ij}(\mathbf{y})(\delta_{jp} + \chi^{(0)p}_{,j(y)}))_{,i(y)}T^k_{,p(x)}(\mathbf{x},t) + (k_{ij}(\mathbf{y})(\delta_{jp}\chi^{(0)p} \\ &+ \chi^{(1)pq}_{,j(y)}))_{,i(y)}T^{k-1}_{,pq(x)}(\mathbf{x},t) \\ &+ \ldots + (k_{ij}(\mathbf{y})(\delta_{jp}\chi^{(k-1)p..\times(k-1)..r} + \chi^{(k)p..\times(k-1)..q}_{,j(y)}))_{,i(y)}T^0_{,p..\times(k-1)..rq(x)}(\mathbf{x},t) \\ &= c(\mathbf{y})(\dot{T}^k(\mathbf{x},t) + \chi^{(0)p}\dot{T}^{k-1}_{,p(x)}(\mathbf{x},t) + \ldots + \chi^{(k)p..\times k..q}\dot{T}^0_{,p..\times k..q(x)}(\mathbf{x},t)).\end{aligned} \tag{3.2}$$

We derive a partial differential equation defining the unknown temperature T^k by averaging over the cell of periodicity the equation number $k+1$ in (hb). We know at this step all previous T^i.

$$(3.3)\quad K_{ij}T^k_{,ij(x)}(\mathbf{x},t) + K^1_{ipq}T^{k-1}_{,pqi(x)}(\mathbf{x},t) + \ldots + K^k_{ip..\times k..q}T^0_{,p..\times..qi(x)}(\mathbf{x},t)$$
$$= \tilde{c}\dot{T}^k(\mathbf{x},t) + C^1_p\dot{T}^{k-1}_{,p(x)}(\mathbf{x},t) + \ldots + C^{(k)}_{p..\times k..q(x)}\dot{T}^0_{,p\times k...q(x)}(\mathbf{x},t),$$

where we define the "effective coefficients of order k":

$$(3.4)\quad K^k_{ip..\times k..q} = \int_Y k_{ij}(\mathbf{y})(\delta_{jp}\chi^{(k-1)p..\times(k-1)..r} + \chi^{(k)p..\times(k-1)..rq}_{,j(y)})dY,$$

$$(3.5)\quad C^{(k)}_{p..\times k..q} = \int_Y c(\mathbf{y})\chi^{(k)p..\times k..q}dY.$$

The general form of the homogenisation function associated with the k-th corrector is slightly more complicated. The boundary value problem defining it is formulated over the cell of periodicity. Remembering that we know at this step all previous $\chi^{(i)}(i<k)$ and assuming a weak sense of the differentiation symbol, we can write:

$$(3.6)\quad (k_{ij}(\mathbf{y})(\delta_{jp}\chi^{(k-1)p..\times(k-1)..r}(\mathbf{y}) + \chi^{(k)p..\times(k-1)..r}_{,j(y)}(\mathbf{y})))_{,i(y)}$$
$$= RHS^{(k)}_{p..\times(k-1)..r}(\mathbf{y}),$$

$$(3.7)\quad \left[k_{ij}(\mathbf{y})(\delta_{ij}\chi^{(k-1)p..\times(k-1)..r}(\mathbf{y}) + \chi^{(k)p..\times(k-1)..rq}_{,j(y)}(\mathbf{y})n_i\right] = 0$$
on the interfaces S_J,

$$(3.8)\quad \tilde{\chi}^{(k)p} = 0 \text{ and periodic boundary conditions are required for } \chi^{(k)p}(\mathbf{y}).$$

Right-hand side in (3.6) is a function of all known at this step, values $\chi^{(i)}$ and also K^k and C^k previously computed. The complicated formula for RHS can be given in a recurrent form. Equation (3.7) expresses a continuity of the contribution to the heat flux at the k-th step, across the interfaces of different materials in Y.

We understand that the pair of functions: T^k satisfying (3.3) and $\chi^{(k)p}(\mathbf{y})$, solution of (3.6) – (3.8), defines the higher-order correction (of order k) to the first approximation Θ^0.

We note immediately that the boundary value problem defining higher-order terms is always the same, only the right-hand side has to be updated. This is of a great advantage in the computational process. It is also clear that the successive approximation depends on the higher-order of the leading term T^0, thus some problems concerning the required higher-order differentiability of T^0 can arise. In this paper, we assume everywhere a sufficient regularity. The corresponding correction to the heat flux can be easily found using (2.8) at each step.

4. Initial corrector

Let us suppose that the given initial temperature is smooth everywhere in Ω^ε (in the domain of the real composite material, not in its equivalent homogenised medium). Obviously in this case at the initial moment, the temperature gradient is also continuous and, according to our constitutive equations, the continuity of the flux (2.8) is violated. We can accept such a situation only in the presence of some heat sources (not imposed as initial loads but rather spontaneously created at the initial moment of the process) at the interfaces between materials inside each cell of periodicity. The nature of such heat sources can be explained by a quick heat exchange between layers, described in the local co-ordinate system $\mathbf{y}$ related to a single layer.

We assume in what follows that, at the beginning of heat conduction, another micro-process of heat transfer on the level of microstructure (more or less the same in each layer) takes place. It is immediately seen from the solution derived until now that the gradient of temperature is discontinuous at each step of the approximation:

$$\begin{aligned}(4.1)\qquad \Theta^\varepsilon_{,i}(\mathbf{x},\mathbf{y},t) = T^0_{,i(x)}(\mathbf{x},t) + \chi^{(0)p}_{,i(y)}(\mathbf{y})T^0_{,p(x)}(\mathbf{x},t) + \ldots + \varepsilon^k(T^k_{,i(x)}(\mathbf{x},t)\\ +\chi^{(0)p}_{,i(y)}(\mathbf{y})T^k_{,p(x)}(\mathbf{x},t) + \ldots + \chi^{(k-1)p..\times k..q}(\mathbf{y})T^0_{,ip..\times k..q(x)}(\mathbf{x},t)\\ +\chi^{(k)p..\times k..qr}_{,i(y)}(\mathbf{y})T^0_{,p..\times(k+1)..qr(x)}(\mathbf{x},t)).\end{aligned}$$

The initial corrector will be defined to obtain the continuity of the initial temperature gradient at the moment $t = 0$. Since we intend to introduce the changes only at the beginning of the process, we define the time scaling via the following transformation:

$$(4.2)\qquad \tau = \delta^{-1}t.$$

A similar procedure can be found for example in [5] and is analogous to that employed in [7] for the spatial variables near the border. Velocities are computed now using the following expression:

$$\dot{f} \equiv \frac{d}{dt} f = \left(\frac{\partial}{\partial t} + \frac{1}{\delta} \frac{\partial}{\partial \tau} \right) f \equiv \dot{f}^t + \frac{1}{\delta} \dot{f}^\tau. \tag{4.3}$$

Instead of (2.7), we can use now the following representation for temperature, solution of (2.2) – (2.6):

$$\begin{aligned} \Theta^\varepsilon(\mathbf{x}, t) \equiv \Theta^{00}(\mathbf{x}, \mathbf{y}, t) + \delta \Theta^{01}(\mathbf{x}, \mathbf{y}, t, \tau) + .. + \delta^l \Theta^{0l}(\mathbf{x}, \mathbf{y}, t, \tau) \\ + ... + \varepsilon^k (\Theta^{k0}(\mathbf{x}, \mathbf{y}, t) + \delta \Theta^{k1}(\mathbf{x}, \mathbf{y}, t, \tau) + .. + \delta^l \Theta^{0l}(\mathbf{x}, \mathbf{y}, t, \tau)). \end{aligned} \tag{4.4}$$

It is probably possible to restart the whole analysis with this assumption, but we find this to be tedious and not necessary. Our idea is to correct "a posteriori" the solution obtained before. According to this we identify the first term in the new development (4.4) with the already known temperature field, depending only on t. In this paper we assume that the two small parameters ε and δ are of the same order. Identifying ε with δ in the above formulae we analyse Eq. (4.4) in the following simplified form:

$$\begin{aligned} \Theta^\varepsilon(\mathbf{x}, t) \equiv \Theta^0(\mathbf{x}, \mathbf{y}, t) + \varepsilon^1 (\Theta^1(\mathbf{x}, \mathbf{y}, t) + J^{01}(\mathbf{x}, \mathbf{y}, t, \tau)) \\ + ... + \varepsilon^k (\Theta^k(\mathbf{x}, \mathbf{y}, t) + J^{0k}(\mathbf{x}, \mathbf{y}, t, \tau) + J^{1k-1}(\mathbf{x}, \mathbf{y}, t.\tau) \\ + ... + J^{(k-1)1}(\mathbf{x}, \mathbf{y}, t, \tau)). \end{aligned} \tag{4.5}$$

The presence of the microstructure is at the origin of the corrective process under consideration, thus it is quite natural to deal with only one independent small parameter ε. Moreover, we do not intend to control any of the possibly time-dependent load parameters, like for example load frequency, since the only influence of the microstructure is the subject of our present analysis. It is easy to check that the following general representation of $J^k(\mathbf{x},\mathbf{y}, t)$ is suitable for our purpose:

Initial correctors of successive order to the known first order approximation

$$J^{0k}(\mathbf{x}, \mathbf{y}, t, \tau) = -\chi^{(0)p}(\mathbf{y}) I_p^{0k}(\mathbf{x}, \tau) + II^{0k}(\mathbf{x}, \tau). \tag{4.6}$$

Initial correctors of successive order to the known l-th order corrector

$$J^{lk}(\mathbf{x}, \mathbf{y}, t, \tau) = -\chi^{(l)p..q}(\mathbf{y}) I_{p..q}^{lk}(\mathbf{x}, \tau) + II^{lk}(\mathbf{x}, \tau). \tag{4.7}$$

In fact, with the initial condition:

$$I_p^{0k}(\mathbf{x}, \tau = 0) = T^0_{,p(x)}(\mathbf{x}, t = 0), \qquad I_p^{lk}(\mathbf{x}, \tau = 0) = T^l_{,p(x)}(\mathbf{x}, t = 0), \tag{4.8}$$

the initial continuity of the temperature gradient can be obtained for the first approximation and for each corrective term as well.

Using the improved representation (4.5), the equation of order 0 and k in (hb) can be written in the following form (we suppose that (3.2) is verified, therefore we write only the changes with respect to (3.2)):

$$
\begin{aligned}
(4.9)\qquad & k_{ij}(\mathbf{y})\chi^{(0)p}_{,j(y)} I^{01}_{p,i(x)}(\mathbf{x},\tau) + (k_{ij}(\mathbf{y})\chi^{(0)p}_{(y)})_{,i(y)} I^{01}_{p,j(x)}(\mathbf{x},t) \\
& + (k_{ij}(\mathbf{y})\chi^{(0)p}_{,j(y)})_{,i(y)} I^{02}_{p(x)}(\mathbf{x},t) + (k_{ij}(\mathbf{y})\chi^{(1)pq}_{,j(y)})_{,i(y)} I^{11}_{pq,j(x)}(\mathbf{x},t) \\
& = c(\mathbf{y})(\chi^{(0)p}\dot{I}^{\tau^{01}}_{p}(\mathbf{x},\tau) + \dot{I}I^{\tau^{01}}(\mathbf{x},\tau)),
\end{aligned}
$$

$$
\begin{aligned}
(4.10)\qquad & k_{ij}(\mathbf{y})\chi^{(k)p..\times(k-1)..rq}_{,j(y)} I^{k0}_{p..\times(k-1)..rq,i(x)}(\mathbf{x},t) \\
& + \left(k_{ij}(\mathbf{y})\chi^{(k)p..\times(k-1)..rq}_{(y)}\right)_{,i(y)} T^{k0}_{p..\times(k-1)..rq,j(x)}(\mathbf{x},t) \\
& + \left(k_{ij}(\mathbf{y})\chi^{(k)p..\times(k-1)..rq}_{,j(y)}\right)_{,i(y)} T^{k1}_{p..\times(k)..rq(x)}(\mathbf{x},t) \\
& = c(\mathbf{y})\left(\chi^{(k)p..\times k..q}\dot{I}^{\tau^{k0}}_{p..\times k..q}(\mathbf{x},t) + \dot{I}I^{\tau^{k0}}\right).
\end{aligned}
$$

It is easy to identify the right-hand side of the above equation as local heat sources arising at the beginning of the conduction process:

$$
(4.11)\qquad r^{k}(\mathbf{x},\mathbf{y},\tau) = c(\mathbf{y})\left(\chi^{(k)p..\times k..q}\dot{I}^{\tau^{k0}}_{p..\times k..q}(\mathbf{x},t) + \dot{I}I^{\tau^{k0}}(\mathbf{x},t)\right).
$$

The above equation serve us as a physical interpretation of the initial correctors. The micro-sources defined by (4.11) are associated with requirement of the smooth distribution of the initial temperature. It means that to obtain such an initial condition one should apply locally the micro-sources (4.11). It means also that if the graph of the temperature is smooth, the micro-sources of heat can be present at the level of the microstructure. The requirement of the zero mean values of these additional sources is natural in this problem and serves us as a first condition for the determination of the unknown initial corrector function,

$$
(4.12)\qquad \int_{Y} r^{k}\left(\dot{I}^{\tau^{k1}}_{p}, \dot{I}I^{\tau^{k+1,1}}\right) dY = 0.
$$

The known jump of the heat flux across the interface between two materials should be equal to the integral of the additional heat sources inside this material domain. This is another condition for the unknown initial corrector function:

$$\left[q_j^k(I_p^{k1}, II^{k+1,1})n_j\right]_{S_J} = \int_{Y_i} r^k\left(\dot{I}_p^{\tau^{k1}}, \dot{II}^{\tau^{k+1,1}}\right) dY_i. \tag{4.13}$$

Knowing I^{ik} satisfying Eqs. (4.12), (4.13), the initial correction J^{ik} is defined. It is easy to check that I^{ik} is always of the form:

$$I_p^{k1}(\mathbf{x}, t) = \exp(-\lambda^{(k)}t/\varepsilon)f(\mathbf{x}), \quad II_p^{k1}(\mathbf{x}, t) = 0, \tag{4.14}$$

$$\lambda^{(k)} = \frac{\int_{S_J} k_{ij}(\mathbf{y})\chi_{,j}^{(k)} n_i dS_J}{\int_{Y_i} c(\mathbf{y})\chi^{(k)} dY_i}. \tag{4.15}$$

The corresponding correction to the heat flux can be easily found using (2.8) and (4.5) at each step.

5. Example

The aim of this example is to illustrate the presented method by a simple calculation that can be carried out without any special software and can be presented in a relatively closed form. We consider a laminated domain Ω^ε bounded by two planes parallel to the layers. Each periodically repeated layer is made of two components. The thickness of the strip Ω^ε is $2L$, thickness of the components of the individual layer are l_1 and l_2. We assume that $l_1 + l_2 << L$. Thermal characteristics of these layers are respectively k_1, c_1 and k_2, c_2. It is natural to assume that the temperature field depends only on the co-ordinate x_1, perpendicular to the layers, with the origin in the middle of the composite strip (x_1 will be denoted simply by x). The local co-ordinate system is reduced to y, $\varepsilon = (l_1 + l_2)/L$.

We assume (as in [12]) the boundary condition in the form:

$$\Theta(L, y, t) = \Theta(L, t) = \Theta(-L, t) = \Theta_L. \tag{5.1}$$

The initial conditions are:

$$\Theta(x, y, 0) = \Theta(x, t) = \Theta_L + \Theta_0 \cos(\pi x_1/2L). \tag{5.2}$$

All computations have been performed symbolically, using the commercial code MAPLEV3.

Unfortunately, the resulting formulae defining the needed coefficients as functions of l_i, k_i, c_i are rather long, thus we present their behaviour in the form of graphs.

We start the analysis with the definition of successive homogenisation functions (the superscript p has been dropped since we deal with $\chi^{(k)1}(\mathbf{y})$ only). The local contribution to the flux vector is expressed by the formula

$$k(y)\left(\chi^{(k-1)} + \chi^{(k)}_{,y}(\mathbf{y})\right) = q^k(y)/T^0_{,k^*x} \equiv h^k(y). \tag{5.3}$$

The graphs of these two functions illustrate the local behaviour of the composite structure. They are to be extrapolated by periodicity to the whole domain Ω^ε, and then scaled with appropriate derivatives of the global solutions T^k.

In Fig. 2 and Fig. 3 we show the graphs of $\chi^{(k)}$and h^k for $l_1 = l_2$, or $l_1 = 5l_2$, $k_1 = 2k_2$, and $c_1 = c_2$. The influence of the ratio between the conductivities of components on the behaviour of $\chi^{(0)}(y)$ is shown in Fig. 4 for $l_1 = l_2$ and for $l_1 = 5l_2$. The influence of the ratio between conductivities and diffusivities of components on $\chi^{(1)}(y)$ is shown in Fig. 5 for $l_1 = l_2$ and for $l_1 = 5l_2$. Influence of the local geometry and material characteristics on K^0 and K^2 is shown in Fig. 7.

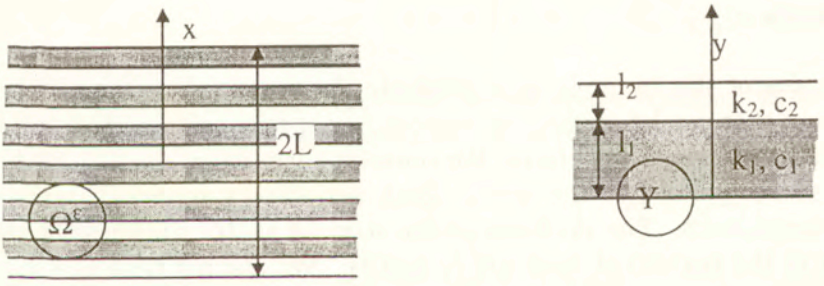

FIG. 2. Layered body and the single layer.

The next step consists of the computations of global unknowns of the model. The parabolic equations for the first approximation has the form:

$$K^0 \frac{\partial^2 T^0}{\partial x^2} - \tilde{c}\frac{\partial T^0}{\partial t} = 0 \quad \text{where} \quad K^0 = \frac{(l_1 + l_2)k_1 k_2}{l_1 k_2 + l_2 k_1}. \tag{5.4}$$

The first order corrector vanishes, the second order correctors verify the following equation:

$$K^0 \frac{\partial^0 T^2}{\partial x^2} - \tilde{c}\frac{\partial T^2}{\partial t} = \left(\frac{\langle c\chi^1\rangle}{\tilde{c}} - K^2\right)\frac{\partial^4 T^0}{\partial x^4} \tag{5.5}$$

where a symbolic formula for K^2 and averaging values involving c are rather long.

The following expressions stand for T^k, solutions of the above partial differential equations:

$$T^0(x,t) = \Theta_L + \Theta_0 \exp\left(-\frac{K^0}{\tilde{c}}\left(\frac{\pi}{2L}\right)^2 t\right)\cos\left(\frac{\pi}{2L}x\right), \tag{5.6}$$

$$T^2(x,t) = A t \exp\left(-\frac{K^0}{\tilde{c}}\left(\frac{\pi}{2L}\right)^2 t\right)\cos\left(\frac{\pi}{2L}x\right), \tag{5.7}$$

where $A = \Theta_0\left(\frac{\pi}{2L}\right)^4\left(\tilde{c}^{-1}\langle c\chi^1\rangle K^0 - K^{(2)}\right)$.

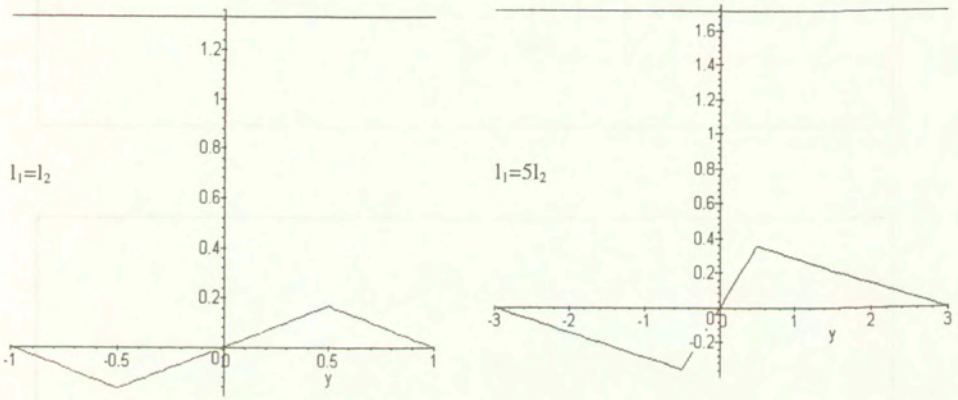

FIG. 3. Homogenisation function and corresponding heat flux for the first approximation.

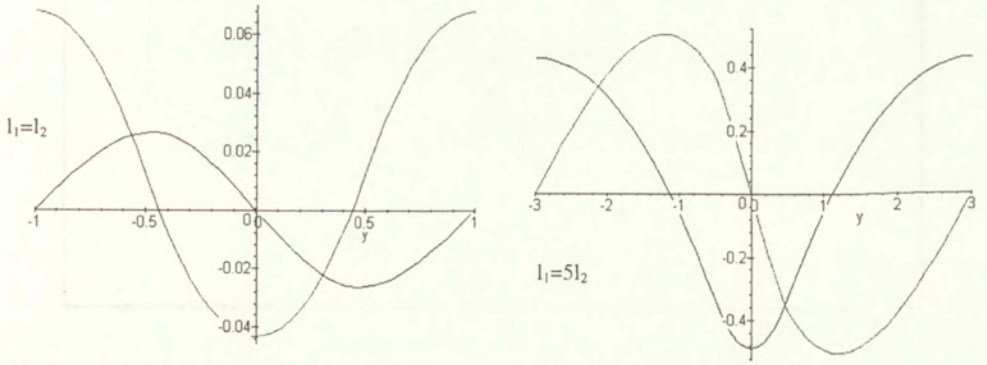

FIG. 4. Homogenisation function and corresponding heat flux for the second corrector.

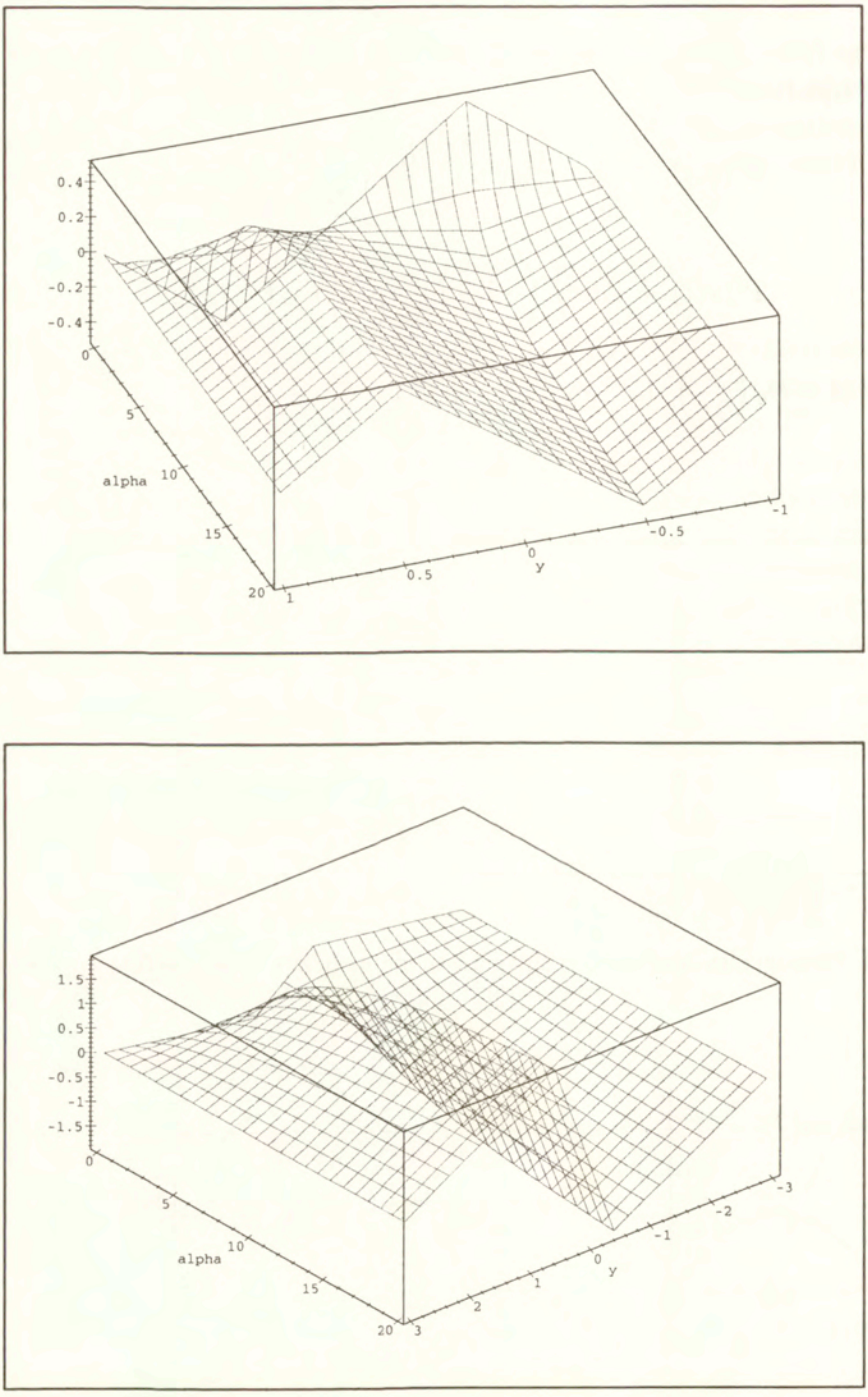

FIG. 5. Homogenisation function for the first approximation as a function of $\alpha = k_1/k_2$.

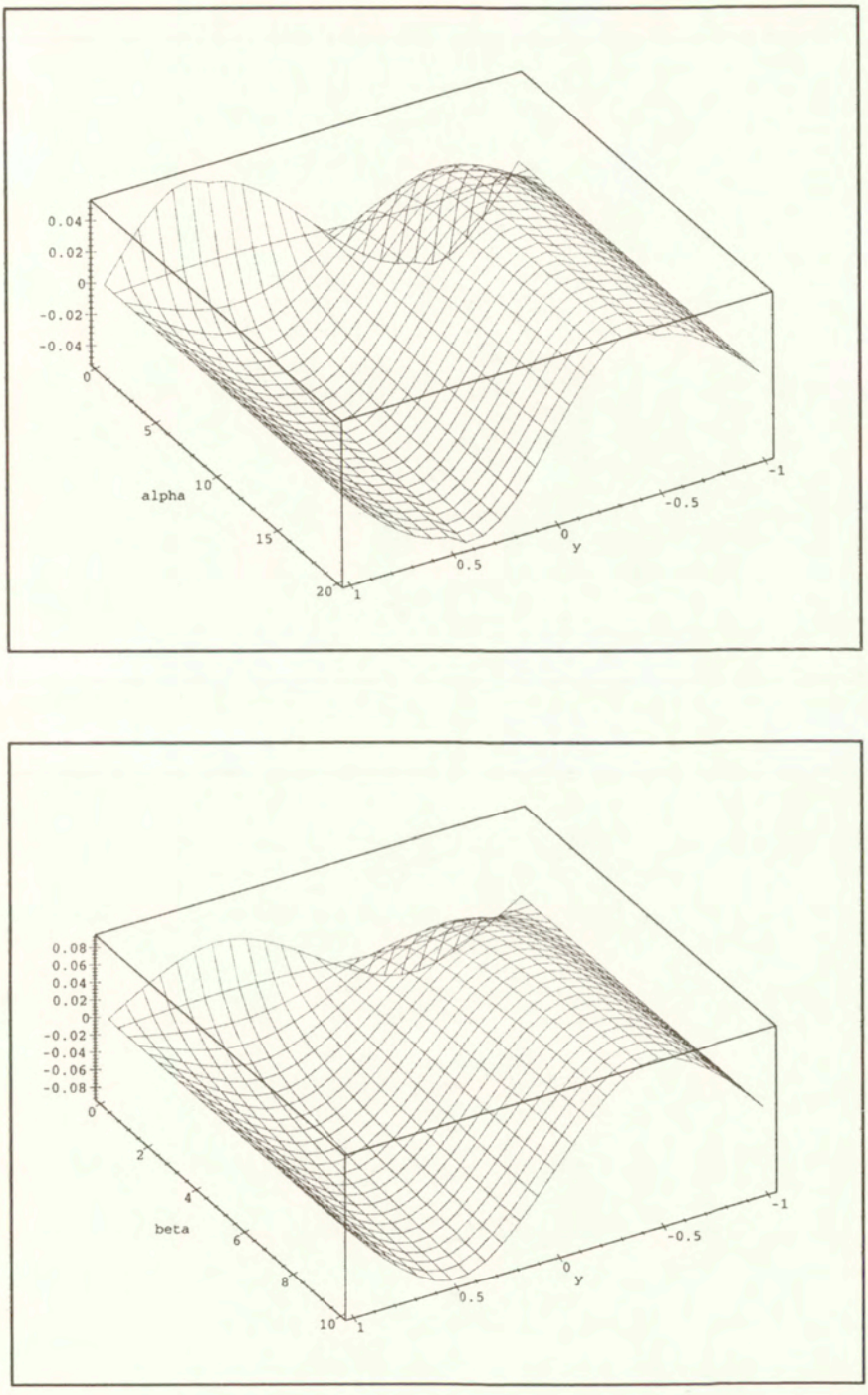

FIG. 6. Homogenisation function for the second corrector as a function of $\alpha = k_1/k_2$ and $\beta = c_1/c_2$.

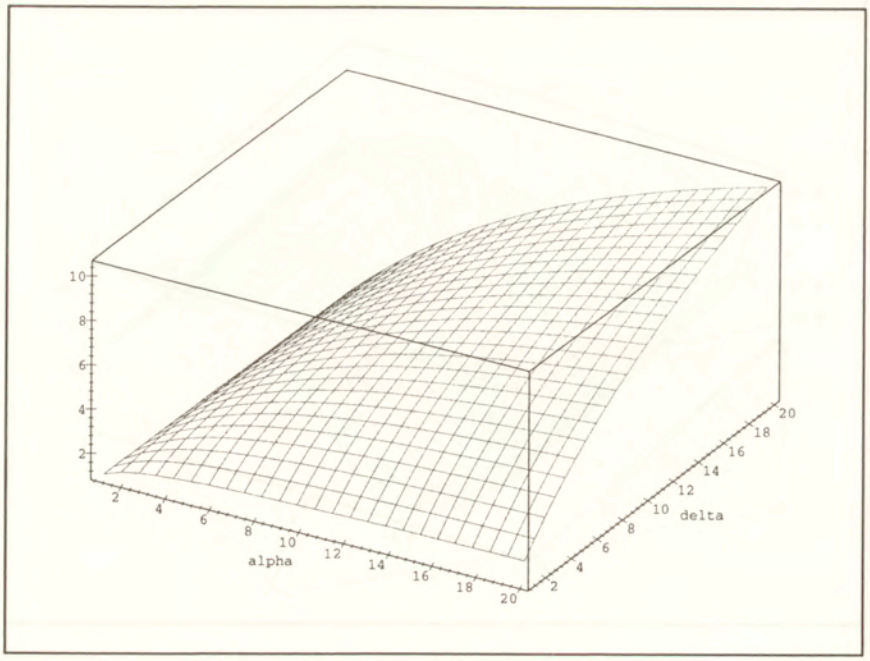

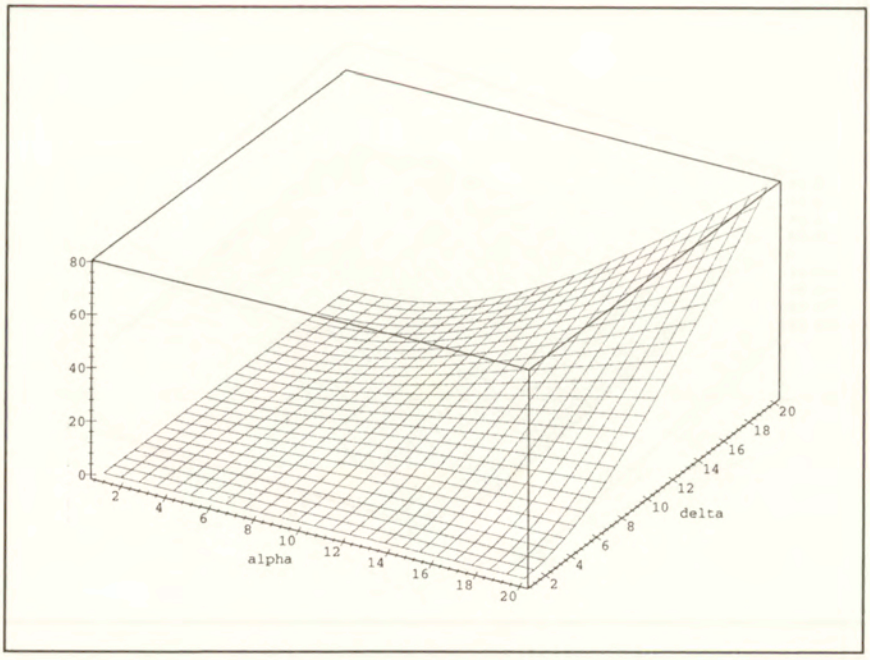

FIG. 7. Values of K^0 (first) and K^2 (second) in function of $\alpha = k_1/k_2$ and $\delta = l_1/l_2$.

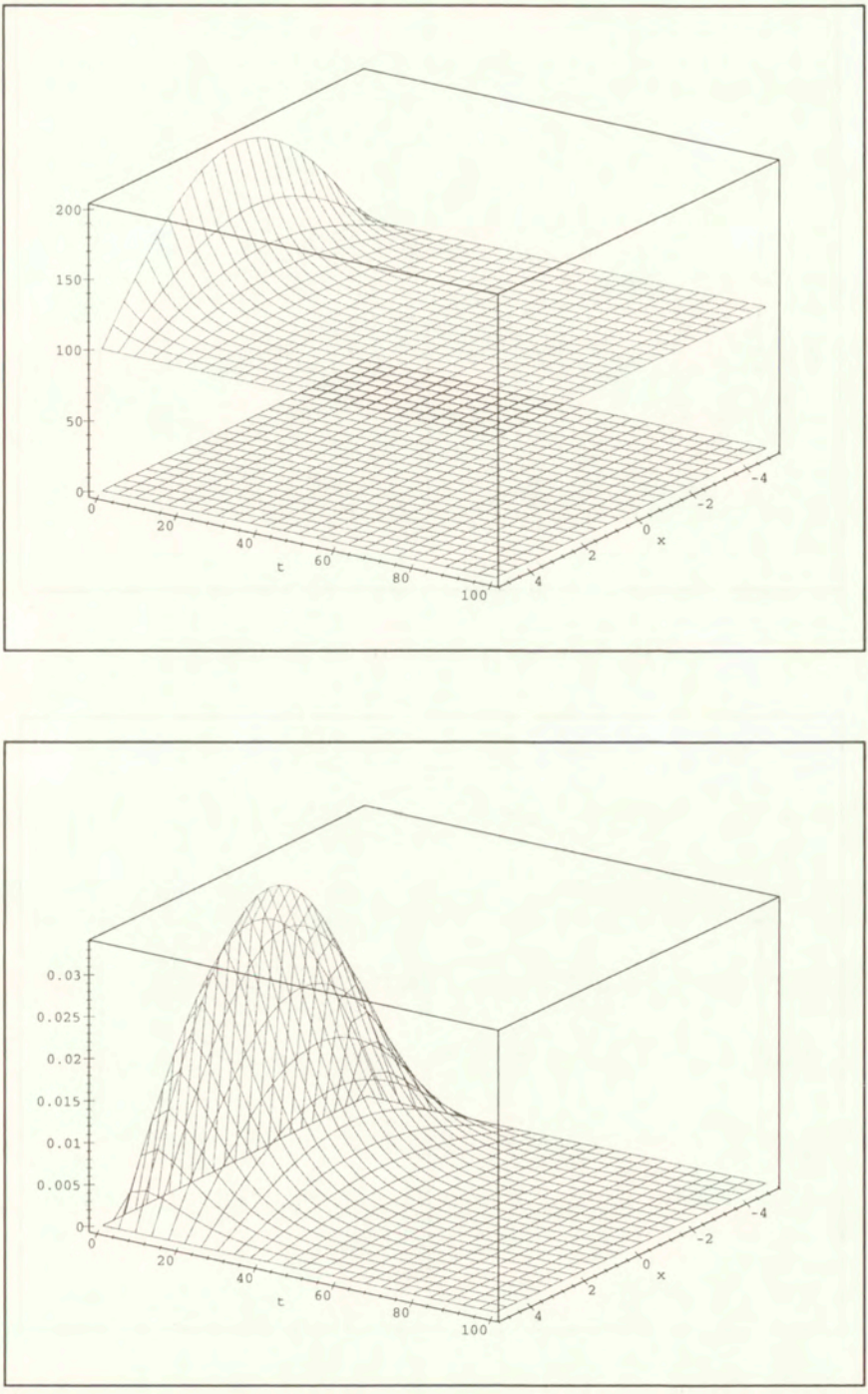

FIG. 8. $T^0(x,t)$ and the additive corrector $T^2(x,t)$ (first), the zoom of $T^2(x,t)$ (second).

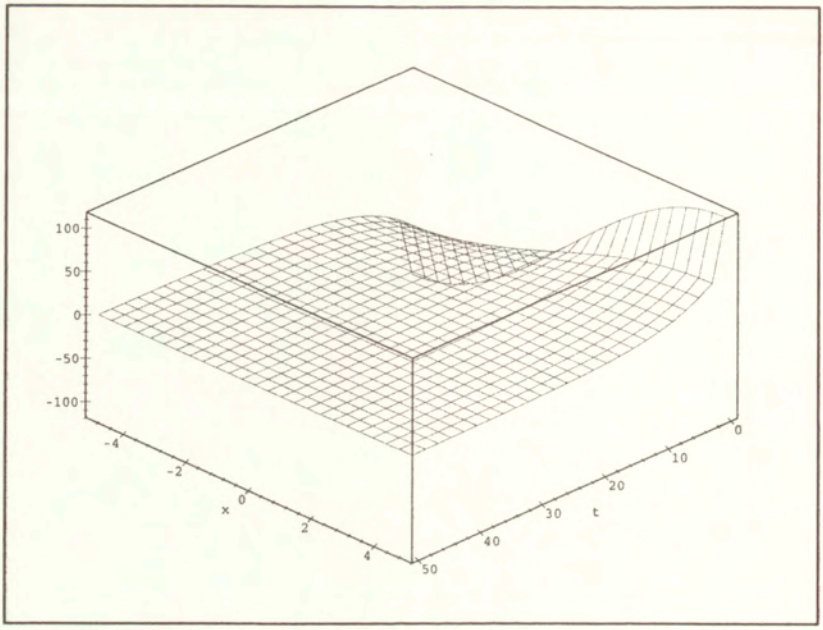

FIG. 9. Initial corrector of the first order.

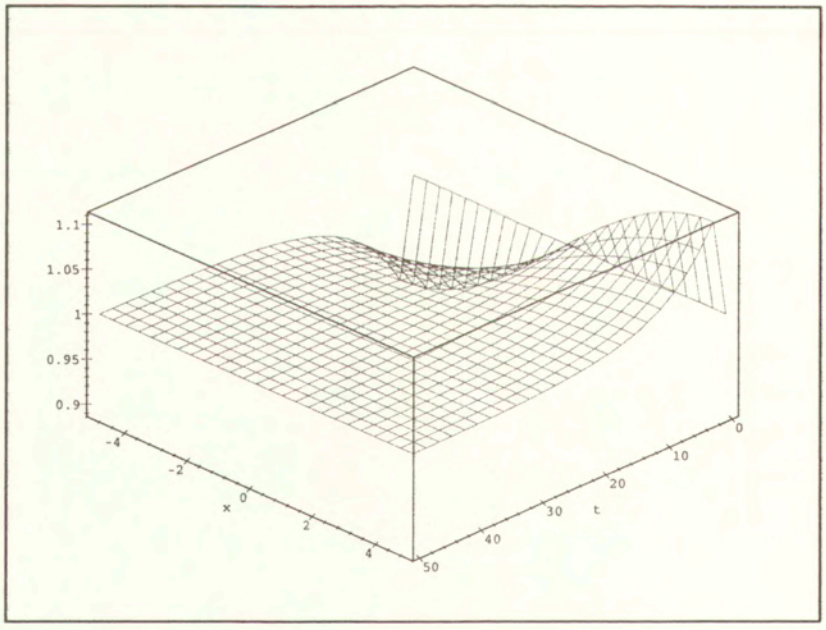

FIG. 10. Error in the average heat flux with respect to the refined solution given in [12]:

$$\text{error} = \frac{\text{our solution}}{\text{solution in[12]}}.$$

We present below (Fig. 8) both graphs: $T^0(x,t)$ and the additive corrector $T^2(x,t)$, then the zoom of $T^2(x,t)$.

In the third step of the analysis we compute the initial correctors. We limit ourselves to the first term. According to (4.14) and (4.15), the closed expression for $J^0(x,t)$ has the form:

$$J^{01}(\mathbf{x},t) = \Theta_0 \frac{\pi}{2L} \exp\left(-4 \frac{L}{(l_1+l_2)} \frac{|k_2-k_1|}{(c_1 l_1 + c_2 l_2)} t\right) \sin\left(\frac{\pi x}{2L}\right). \tag{5.8}$$

The set of Figures 9, 10, 11 below illustrates the behaviour of solution with initial corrector.

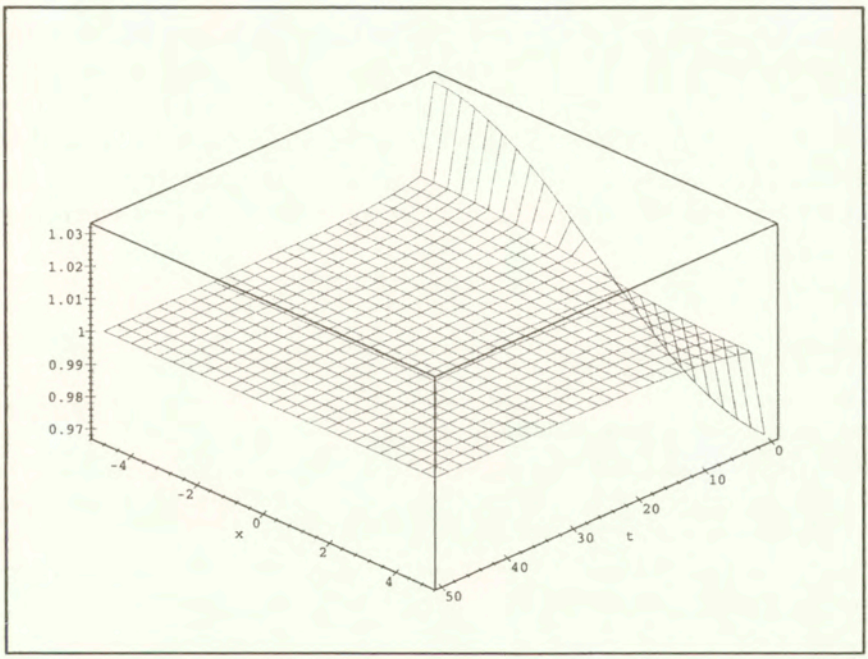

FIG. 11. Error in the average temperature gradient with respect to the refined solution given in [12]: error $= \dfrac{\text{our solution}}{\text{solution in[12]}}$.

6. Conclusions

We show in this paper that the procedure of successive corrections of the classical first order approximation resulting from the homogenisation theory is efficient. Improved approximation is qualitatively satisfactory: initial conditions

are satisfied within the given precision level, the simulated evolution of temperature and heat flux is close to the exact one. A numerical example reveals that our results are close to those obtained from the refined theory presented in [12].

The most important advantage of the proposed method is its recurrent character. The algorithm of the computations is thus composed of the same procedures in each step, using as the input the flux of data resulting from the preceding step. In the studied example, the influence of the higher-order corrector on the quantitative and qualitative behaviour of the solution was negligible. These correctors may be useful only for strongly differing values of the component parameters and in the case when the scale resolution is not sharp enough (small parameter larger than 0.1).

On the other hand, the improvement due to the initial corrector is remarkable. The initial correction changed qualitatively the approximate solution at the beginning of the process. In the studied example, the initial corrector is associated via (4.11) with a field of micro-sources of heat that is needed to satisfy the assumed initial conditions. Such a correction should always be used when a nonstationary process is modelled. In this case we estimate that even for composite with strongly different properties of components, the first corrective term is sufficient.

References

1. A. BENSOUSSAN, J.-L. LIONS and G. PAPANICOLAU, *Asymptotic analysis for periodic structures*, North-Holland, Amsterdam 1976.
2. C. BOUTIN, *Heat conduction with microstructural effects* [in:] Homogenisation, Theory of migration and granular bodies [Eds.] E. Dembicki, J.-L. Auriault, Z. Sikora, Gdańsk 1995, pp 53–63.
3. C. BOUTIN and J.L. AURIAULT, *Rayleigh scattering in elastic composite materials*, Int. J. Enging. Sci., **31**, 12, 1669–1689, 1993.
4. H. DUMONTET, *Homogeneisation et effets de bords dans les materiaux composites*, (These de Doctorat d'Etat), L'Université Pierre et Marie Curie, Paris 6 1990.
5. G. A. FRANCOFORT, *Homogenization and fast oscillations in linear thermoelasticity* [in:] Numerical methods for transient and coupled problems [Eds.] R. Lewis, E. Hinton, P. Betess and B. Schrefler, Pineridge Press, Swansea 1984, pp. 382–392.
6. P. LADEVEZE, *Local effects in the analysis of structures*, [Ed.] P. Ladeveze, Elsevier Publishers, 1985.
7. M. LEFIK and B. A. SCHREFLER, *FE modelling of a boundary layer correctors for composites, using the homogenization theory*, Engineering Computations, **13**, 6, 31–42, 1996.
8. M. LEFIK and B. A. SCHREFLER, *3D finite element analysis of composite beams with parallel fibres based on the homogenization theory*, Computational Mechanics, **14**, 1, 2–15, 1994.
9. M. LEFIK and B. A. SCHREFLER, *Application of the homogenization method to the analysis of superconducting coils*, Fusion Engineering and Design, **24**, 231–255, 1994.

10. E. SANCHEZ-PALENCIA, *Non-homogeneous media and vibration theory*, Springer V, Berlin 1980.

11. CZ. WOŹNIAK, *Refined macrodynamics of periodic structures*, Arch. Mech., **45**, 3, 295–304, 1993.

12. CZ. WOŹNIAK, Z. BACZYNSKI and M. WOŹNIAK, *Modelling of nonstationary heat conduction problems in micro-periodic composites*, ZAMM, Z. angew. Math. Mech., **76**, 4, 223–229, 1996.

Received April 14, 1999; revised version February 7, 2000.

Arch. Mech., **52**, 2, pp. 225–246, Warszawa 2000

Asymptotic analysis of heat propagation models

K. MOSZYŃSKI and A. PALCZEWSKI

Institute of Applied Mathematics and Mechanics,
Warsaw University

THE SUBJECT OF THIS PAPER is the analysis of different models of heat propagation. As is well known, one of essential disadvantages of the classical model proposed by Fourier is the infinite velocity at which heat propagates. To avoid that unphysical phenomenon, Cattaneo has proposed a hyperbolic model. An essential feature of that model is the introduction of a relaxation time for thermal processes. In recent years several new models have been proposed which retain the relaxation time phenomenon but are parabolic in their character. When the relaxation time is small, all these models lead to singularly perturbed equations. We analyze some of these models and prove that the solution of the classical heat equation (Fourier model) is a bulk approximation to exact solutions of these models. We show also that the behaviour of the Fourier model depends on the way in which it is applied. Finally, we present numerical comparison of exact solutions with the bulk solution for the test problem of heat propagation in thin metal films heated by a laser beam.

1. Models of heat propagation

A GENERAL PROBLEM IN MODELING heat propagation is the choice of a correct model connecting the heat flux with the temperature gradient. This problem has been thoroughly discussed in two papers by JOSEPH and PREZIOSI [13, 14] and the review of recent literature can be found in the paper by CHANDRASEKHARAIAH [4]. As is well known, the classical assumption of Fourier

$$q = -k_1 \nabla T$$

leads to the parabolic heat equation

$$\rho C_p \frac{\partial T}{\partial t} = k_1 \nabla^2 T, \tag{1.1}$$

where ρ is the density, C_p the specific heat and k_1 the thermal conductivity of the material. One of essential features of this model is the infinite velocity of propagation of heat disturbances. During experiments involving very low temperatures near the absolute zero, extremely short pulse laser heating or very high heat fluxes, investigators found that the heat propagation velocity becomes finite. To account for the phenomena involving the finite propagation velocity, the

classical Fourier heat flux model should be modified. CATTANEO [3] has proposed to model the heat flux as dependent on the history of the temperature gradient. This leads to the following differential relation between the heat flux and the temperature gradient:

$$\tau \frac{\partial q}{\partial t} + q = -k_2 \nabla T,$$

and the hyperbolic heat equation

$$\frac{\partial^2 T}{\partial t^2} + \frac{1}{\tau}\frac{\partial T}{\partial t} = c^2 \nabla^2 T\,, \tag{1.2}$$

where $c = \sqrt{k_2/\rho\tau C_p}$ is the velocity of propagation of thermal waves (τ is the relaxation time of thermal processes). For this model we obtain a finite velocity of propagation of heat waves but we loose a clear sense of the heat conductivity introduced in the Fourier model. In addition we encounter problems with the second law of thermodynamics (cf. [17]).

A different model has been proposed by JOSEPH and PREZIOSI [13] (called the Jeffreys-type model), which retains relaxation time phenomenon but also uses the effective Fourier conductivity k_1 explicitly

$$q(t) = -k_1 \nabla T - \frac{k_2}{\tau} \int_{-\infty}^{t} \exp(-\frac{t-t'}{\tau}) \nabla T(t') dt'\,. \tag{1.3}$$

For steady flows the thermal conductivity is given by

$$k = k_1 + k_2,$$

i.e. is the sum of the effective thermal conductivity k_1 and the elastic conductivity k_2. Equation (1.3) leads to the following equation for the temperature

$$\frac{\partial^2 T}{\partial t^2} + \frac{1}{\tau}\frac{\partial T}{\partial t} = c^2 \nabla^2 T + \kappa_1 \nabla^2 \frac{\partial T}{\partial t}\,, \tag{1.4}$$

where $c = \sqrt{k/\rho\tau C_p}$ is the velocity of propagation of heat impulses and $\kappa_1 = k_1/\rho C_p$.

Let us mention finally the inertial theory obtained as a limiting case of the Cattaneo model where $\tau \to \infty$ but $k_2/\tau = k^*$ remains finite. Then, we obtain the following law of heat conduction

$$\frac{\partial q}{\partial t} = -k^* \nabla T\,,$$

and the pure wave equation for the temperature

$$\frac{\partial^2 T}{\partial t^2} = c^2 \nabla^2 T\,, \tag{1.5}$$

where $c = \sqrt{k_2/\rho\tau C_p}$.

A nonlinear extension of the last model has been proposed by CIMMELLI and KOSIŃSKI [5, 6]. They have postulated the following law of thermal conductivity

$$q = -\chi \nabla \Theta\,,$$

where χ is a positive function representing the coefficient of thermal conductivity. Θ is the semi-empirical temperature representing a thermal history of the material and obey the evolution equation $\dot{\Theta} = F(T, \Theta)$. A particular linear version of this model was proposed earlier by IGNACZAK [11]

$$\frac{\partial q}{\partial t} = -k\nabla \frac{\partial T}{\partial t} - \frac{\kappa}{T_0}\nabla T\,.$$

The above model of heat conduction leads to the following equation for temperature

$$\rho C_p \frac{\partial^2 T}{\partial t^2} = k\nabla^2 \frac{\partial T}{\partial t} - \frac{\kappa}{T_0}\nabla^2 T\,.$$

The question which of these models is more realistic is difficult to answer. A number of papers defend the Fourier model (cf. [7, 8]) claiming that although the theoretical speed of heat impulses in this model is infinite, but the bulk of the heat energy propagates with a finite speed. The present paper can be considered as a voice in this discussion. We restrict our considerations to very short heat pulses at room temperature. This corresponds to a very short relaxation time τ. Hence we exclude from our comparison the analysis of inertial theory and its nonlinear extensions as they correspond to $\tau \to \infty$.

In what follows, we shall analyze the Fourier, Cattaneo and Jeffreys-type models. It is shown both by asymptotic analysis and numerical calculations that for the propagation time of macroscopic size there is no difference between predictions of all the three models. The situation changes for short distances of propagation and very short time. Here the predictions of the Fourier model differ form those of the Cattaneo and Jeffreys-type models. Which model is more realistic should be decided by comparison of numerical results with experimental data. For experimental results which we have found in the literature [2], the agreement is better with the Cattaneo and Jeffreys-type models (cf. Sec. 4).

2. Asymptotic analysis of the models

When the relaxation time is very small in comparison with the macroscopic time, Eqs. (1.2) and (1.4) are singularly perturbed. Hence we can apply singular

perturbation methods to find the behaviour of solutions in short time scale (initial layer) and in long time scale (bulk approximation).

We begin our analysis with the Cattaneo Eq. (1.2). Writing this equation in the dimensionless form as a first-order system, we obtain

$$\begin{aligned} \partial_t \theta + \partial_x \eta &= 0\,, \\ \tau \partial_t \eta + D^2 \partial_x \theta + \eta &= 0\,. \end{aligned} \tag{2.1}$$

In the above equations θ and η denote the dimensionless temperature and the heat flux, respectively, $D^2 = \dfrac{k_2 t_0}{\rho C_p x_0^2}$ is the dimensionless coefficient of thermal conductivity, where t_0 is the characteristic time and x_0 the characteristic length, and ∂_x denotes the nabla operator (*gradient* or *divergence,* depending on the context).

Now we apply the standard asymptotic procedure, i.e. we expand θ and η in power series of τ

$$\begin{aligned} \theta &= \theta_0 + \tau \theta_1 + \dots\,, \\ \eta &= \eta_0 + \tau \eta_1 + \dots\,. \end{aligned} \tag{2.2}$$

Inserting expansion (2.2) into Eq. (2.1) and comparing terms of the same order in τ, we obtain equations for consecutive terms of the bulk approximation. For the zeroth-order it gives

$$\begin{aligned} \partial_t \theta_0 + \partial_x \eta_0 &= 0\,, \\ D^2 \partial_x \theta_0 + \eta_0 &= 0\,. \end{aligned}$$

After rearranging the terms we obtain the classical heat Eq. (1.1) for the zeroth-order approximation to the temperature, and the Fourier formula of the heat flux

$$\begin{aligned} \partial_t \theta_0 &= D^2 \nabla^2 \theta_0\,, \\ \eta_0 &= -D^2 \nabla \theta_0\,. \end{aligned} \tag{2.3}$$

In the first-order we have

$$\partial_t \theta_1 + \partial_x \eta_1 = 0\,,$$

$$\partial_t \eta_0 + D^2 \partial_x \theta_1 + \eta_1 = 0\,,$$

which after rearrangement leads to the nonhomogeneous heat equation

$$\partial_t \theta_1 = D^2 \nabla^2 \theta_1 - D^2 \nabla^2 \partial_t \theta_0 .$$

To account for the short time effects we introduce the new time variable

$$\sigma = \frac{t}{\tau} .$$

Then Eq. (2.1) take the form

$$\begin{aligned} \frac{1}{\tau} \partial_\sigma \tilde{\theta} + \partial_x \tilde{\eta} &= 0 , \\ \partial_\sigma \tilde{\eta} + D^2 \partial_x \tilde{\theta} + \tilde{\eta} &= 0 , \end{aligned} \tag{2.4}$$

where *tilde* denotes the functions of the new variables (x, σ).

The above equations form again a singularly perturbed system with small parameter τ. We look for a solution of this system by expanding $\tilde{\theta}$ and $\tilde{\eta}$ in power series of τ. Then in the zeroth-order we obtain

$$\begin{aligned} \partial_\sigma \tilde{\theta}_0 &= 0 , \\ \partial_\sigma \tilde{\eta}_0 + \tilde{\eta}_0 &= 0 . \end{aligned} \tag{2.5}$$

Assuming that the initial layer solutions tend to zero at infinity, we get from (2.5)

$$\begin{aligned} \tilde{\theta}_0(\sigma, x) &= 0 , \\ \tilde{\eta}_0(\sigma, x) &= \tilde{\eta}_0(0, x) e^{-\sigma} . \end{aligned}$$

Let us observe that the initial layer equations are necessary to fulfill the initial conditions. Let $\theta(0, x)$ and $\eta(0, x)$ be the initial conditions to (2.1). If these initial functions are independent of τ then Eqs. (2.1), (2.3) and (2.5) give

$$\begin{aligned} \theta(0, x) &= \theta_0(0, x) , \\ \eta(0, x) &= \eta_0(0, x) + \tilde{\eta}_0(0, x) . \end{aligned}$$

Assuming that all the considered functions are extended down to the initial surface $t = 0$ and taking into account the equality

$$\eta_0(0) = -D^2 \partial_x \theta_0(0),$$

we can fulfill the initial data taking

$$\begin{aligned} \theta_0(0, x) &= \theta(0, x) , \\ \tilde{\eta}_0(0, x) &= \eta(0, x) + D^2 \partial_x \theta(0, x). \end{aligned}$$

An essential step in asymptotic analysis is the comparison of the approximate solution with the exact one. We shall carry on that procedure in the Hilbert space setting $H = L^2(\mathbb{R}^n)$. With some abuse of the notation we shall write $w \in H$ even if w is an n-dimensional vector, understanding in such a case that every component of w is in H and using the obvious extension of the norm in H to vector functions. Then the following result is standard in asymptotic analysis.

PROPOSITION 1. Let us consider the Cauchy problem for Eq. (2.1) with initial data belonging to $W_0^{2,1}(\mathbb{R}^n) \cap W^{2,2}(\mathbb{R}^n)$. Then both the exact Eq. (2.1) and the zeroth-order approximation (2.3) possess solutions in $C^1(\mathbb{R}^+, H)$ and the following estimate holds in the norm of H;

$$\|\theta(t) - \theta_0(t)\| = O(\tau)\,.$$

In addition for the heat flux we obtain

$$\|\eta(t) - \eta_0(t) - \tilde{\eta}_0(t/\tau)\| = O(\tau^{1/2})\,.$$

P r o o f: We omit the existence part of the proof as a standard one and concentrate on the error estimate. Let us define

$$\begin{aligned} y &= \theta - \theta_0\,, \\ z &= \eta - \eta_0 - \tilde{\eta}_0\,. \end{aligned}$$

Inserting y and z into Eq. (2.1) and making use of the fact that θ_0 and η_0 solve Eq. (2.3), and $\tilde{\eta}_0$ Eq. (2.5), we obtain

$$\begin{aligned} \partial_t y + \partial_x z &= -\partial_x \tilde{\eta}_0\,, \\ \tau\partial_t z + D^2\partial_x y + z &= \tau D^2 \partial_t \partial_x \theta_0\,. \end{aligned} \tag{2.6}$$

This equation can be written as an evolution equation in the matrix form

$$\partial_t u = \mathcal{S}u + \mathcal{C}u + g\,,$$

where

$$u = \begin{bmatrix} y \\ z \end{bmatrix}\,,$$

$$\mathcal{S} = \begin{bmatrix} 0 & -\partial_x \\ -\frac{D^2}{\tau}\partial_x & 0 \end{bmatrix}\,, \quad \mathcal{C} = \frac{1}{\tau}\begin{bmatrix} 0 & 0 \\ 0 & -1 \end{bmatrix}$$

and

$$g = \begin{bmatrix} -\partial_x \tilde{\eta}_0 \\ D^2 \partial_t \partial_x \theta_0 \end{bmatrix}$$

is the nonhomogeneous term.

We encounter a problem in this analysis because $\mathcal{S}$ is not a dissipative operator (cf. [1]). To avoid that difficulty we make a change of variables

$$\hat{u} = \begin{bmatrix} D & 0 \\ 0 & \sqrt{\tau} \end{bmatrix} u .$$

For $\hat{u}$ we get the equation

$$\partial_t \hat{u} = \mathcal{S}' \hat{u} + \mathcal{C} \hat{u} + g' ,$$

where

$$\mathcal{S}' = \frac{D}{\sqrt{\tau}} \begin{bmatrix} 0 & -\partial_x \\ -\partial_x & 0 \end{bmatrix} , \quad g = \begin{bmatrix} -D\partial_x \tilde{\eta}_0 \\ \sqrt{\tau} D^2 \partial_t \partial_x \theta_0 \end{bmatrix} .$$

Operator $\mathcal{S}'$ is already dissipative (it is in fact a conservative operator in H) and generates a semigroup of contractions in H. By standard methods of asymptotic analysis (cf. [1] Chap. 6) we obtain the estimate

$$\|\hat{u}(t)\| = O(\tau)$$

uniformly for $t \in [0, T]$, for any $T < \infty$.

Returning to the original variables y and z we obtain the assertion of the proposition.

■

Let us remark that the result of PROPOSITION 1 is well known in the literature (cf. GOLDSTEIN [9] Chap. 2 Sec. 11) and we present it only for the readers' convenience.

It is interesting to compare the above estimate with the result of JANSSEN [12] who analyzed the abstract telegraph equation. The result of Janssen in the Hilbert space $H = L^2(\mathbb{R}^n)$ setting has the form of

PROPOSITION 2. Let $\theta_0(t)$ be a bounded solution of the heat Eq. (2.3) for initial data belonging to $W_0^{2,1} \cap W^{2,2}$. Then the telegraph Eq. (1.2) with the same initial data possesses a solution $\theta(t)$ and for every $c_0 > 0$ there exists a constant C such that

$$\|\theta(t) - \theta_0(t)\| \leq C \left(\frac{1}{t/\tau} + \frac{1}{(t/\tau)^{1/2} c} \right) ,$$

for every $c > c_0$, $t > 0$ and $\tau > 0$, where $c^2 \tau = D^2$.

PROPOSITION 2 gives a long time convergence for solutions of the telegraph equation to solutions of the heat equation whereas PROPOSITION 1 gives only estimate on a bounded time interval. The term $\tau^{1/2}$ in the estimate of PROPOSITION 2 seems to be unexpected (we expect $O(\tau)$). Let us observe however, that

$c\tau^{1/2} = D$, where D is a constant. Hence the estimate in PROPOSITION 2 is in fact of order $O(\tau)$ which is standard for asymptotic analysis.

We proceed now to the analysis of the Jeffreys-type model of Joseph and Preziosi. As in the case of Cattaneo's model, we write this equation in the dimensionless form as a first-order system

$$\partial_t\theta + \partial_x\eta = 0\,,$$

$$\tau\partial_t\eta + D^2\partial_x\theta + \eta - \kappa^*\tau\partial_{xx}\eta = 0\,, \tag{2.7}$$

where $D^2 = \dfrac{kt_0}{\rho C_p x_0^2}$ and $\kappa^* = \dfrac{k_1 t_0}{\rho C_p x_0^2}$.

Carrying asymptotic analysis we obtain in the zeroth-order the result analogous to that obtained for the Cattaneo model, i.e. the classical heat equation and the Fourier formula of the heat flux

$$\partial_t\theta_0 = D^2\nabla^2\theta_0\,,$$

$$\eta_0 = -D^2\nabla\theta_0\,. \tag{2.8}$$

Proceeding like previously we obtain for the initial layer in the zeroth-order

$$\partial_\sigma\tilde{\theta}_0 = 0\,,$$

$$\partial_\sigma\tilde{\eta}_0 + \tilde{\eta}_0 = 0\,, \tag{2.9}$$

which are the same equations as for Cattaneo's model.

Then we can formulate our main result for the Jeffreys-type model.

PROPOSITION 3. Let us consider the Cauchy problems for Eqs. (2.7) and (2.8) with the same initial data belonging to $W_0^{2,1}(\mathbb{R}^n)\cap W^{2,2}(\mathbb{R}^n)$. Both these systems possess solutions in $C^1(\mathbb{R}^+, H)$ and the following estimate holds in the norm of H

$$\|\theta(t) - \theta_0(t)\| = O(\tau)\,.$$

In addition for the heat flux we obtain

$$\|\eta(t) - \eta_0(t) - \tilde{\eta}_0(t/\tau)\| = O(\tau^{1/2})\,.$$

P r o o f: The idea of the proof is analogous to the proof of PROPOSTION 1. We concentrate on an error estimate and define as previously

$$y = \theta - \theta_0\,,$$
$$z = \eta - \eta_0 - \tilde{\eta}_0\,.$$

Inserting y and z into Eq. (2.7) and making use of the fact that θ_0 and η_0 solve Eq. (2.8), and $\tilde{\eta}_0$ Eq. (2.9), we obtain

$$\begin{aligned} \partial_t y + \partial_x z &= -\partial_x \tilde{\eta}_0 \,, \\ \tau \partial_t z + D^2 \partial_x y + z - \kappa^* \tau \partial_{xx} z &= \tau (D^4 - \kappa^* D^2) \partial_{xxx} \theta_0 + \tau \kappa^* \partial_{xx} \tilde{\eta}_0 \,. \end{aligned} \tag{2.10}$$

With these equations we have similar problems as with (2.6). Changing variables

$$u = \begin{bmatrix} Dy \\ \sqrt{\tau} z \end{bmatrix},$$

we can write it in the matrix form

$$\partial_t u = \mathcal{S} u + \mathcal{C} u + g \,,$$

where

$$\mathcal{S} = \frac{D}{\sqrt{\tau}} \begin{bmatrix} 0 & -\partial_x \\ -\partial_x & \frac{\sqrt{\tau}\kappa^*}{D} \partial_{xx} \end{bmatrix}, \quad \mathcal{C} = \frac{1}{\tau} \begin{bmatrix} 0 & 0 \\ 0 & -1 \end{bmatrix}$$

and

$$g = \begin{bmatrix} -D \partial_x \tilde{\eta}_0 \\ \sqrt{\tau} (D^4 - \kappa^* D^2) \partial_{xxx} \theta_0 + \sqrt{\tau} \kappa^* \partial_{xx} \tilde{\eta}_0 \end{bmatrix}$$

is the nonhomogeneous term.

The operator $\mathcal{S}$ generates a contraction semigroup in H (cf. [16] for details). Then using standard methods of asymptotic analysis we obtain the estimate

$$\|u(t)\| = O(\tau)$$

uniformly for $t \in [0, T]$, for any $T < \infty$.

This estimate in terms of the original variables y and z is exactly the assertion of the proposition.

■

3. Jeffreys-type model revisited

Because Jeffreys-type model is not related straightforwardly to experimental results, it is very difficult to make any judgement on the relation between the thermal conductivity k and the effective conductivity k_1. The only relation which follows from considerations of Sec. 1 is that $c^2 \gg \kappa_1$. But recently another approach to the derivation of the Jeffreys-type model has been proposed (cf. [10, 19]). In this model, called *the dual-phase-lag model*, the following general relation between the heat flux and the temperature gradient has been proposed:

$$q(t + \tau_q) = -k \nabla T(t + \tau_T). \tag{3.1}$$

In this relation the delay time τ_T is interpreted as caused by phonon-electron interactions or phonon scattering. The other delay time τ_q is the relaxation time due to the fast transient effects of thermal inertia.

Expanding the left-hand side of (3.1) with respect to τ_q and the right-hand side with respect to τ_T and retaining only the first-order terms, we get

$$q + \tau_q \frac{\partial q}{\partial t} = -k\nabla T - k\tau_T \frac{\partial}{\partial t}\nabla T\,,$$

which leads to the following equation for the temperature:

$$\frac{\partial^2 T}{\partial t^2} + \frac{1}{\tau_q}\frac{\partial T}{\partial t} = c^2\nabla^2 T + \kappa_1 \frac{\tau_T}{\tau_q}\nabla^2 \frac{\partial T}{\partial t}\,, \tag{3.2}$$

where $c^2 = k/\rho\tau_q C_p$ and $\kappa_1 = k/\rho C_p$. The relation between terms in the right-hand side of (3.2) depends on the ratio τ_T/τ_q. For thin gold films for which we have made comparison with experimental data in both papers [10] and [19], it is reported that $\tau_T/\tau_q \approx 120$ which is $\gg 1$ and makes the analysis performed below justifiable.

We write Eq. (3.2) in the dimensionless form as a first order system

$$\begin{aligned} \partial_t\theta + \partial_x\eta &= 0\,, \\ \tau\partial_t\eta + D^2\partial_x\theta + \eta - \kappa_2\partial_{xx}\eta &= 0\,, \end{aligned} \tag{3.3}$$

where $D^2 = \dfrac{kt_0}{\rho C_p x_0^2}$, $\kappa_2 = \dfrac{k\tau_T}{\rho C_p x_0^2}$ and τ is the dimensionless value of τ_q.

Since $\tau_T \gg \tau_q$ coefficient κ_2 is of order $O(1)$ with respect to τ. Hence the standard procedure leads to the following zeroth-order approximation for the dimensionless temperature and the heat flux

$$\begin{aligned} \partial_t\theta_0 &= D^2\partial_{xx}\theta_0 + \kappa_2\partial_t\partial_{xx}\theta_0\,, \\ \eta_0 &= -D^2\partial_x\theta_0 - \kappa_2\partial_t\partial_x\theta_0\,. \end{aligned} \tag{3.4}$$

Let us observe the difference between this system and the system obtained in the zeroth-order for the original Jeffreys model. Also the initial layer equation has a different form. In the zeroth-order we obtain

$$\partial_\sigma\tilde{\eta}_0 = \kappa_2\partial_{xx}\tilde{\eta}_0 - \eta_0\,.$$

Then we can write the equation for the error term. Using the same notation as in the preceding section we obtain

$$\begin{aligned} \partial_t y + \partial_x z &= -\partial_x\tilde{\eta}_0\,, \\ \tau\partial_t z + D^2\partial_x y + z - \kappa_2\partial_{xx}z &= \tau D^2\partial_t\partial_x\theta_0 + \tau\kappa_2\partial_{tt}\partial_x\theta_0\,. \end{aligned} \tag{3.5}$$

The above system is analogous to Eq. (2.10) (the difference is only in the non-homogeneous term). Hence PROPOSITION 3 remains valid also for systems (3.4) and (3.5).

We can now return to Eq. (3.4). This is an example of Sobolev's equation (cf. [18]) and its analysis is relatively simple. First, let us write this equation in the more convenient form

$$\partial_t u = D^2(I - \kappa_2\Delta)^{-1}\Delta u\,. \tag{3.6}$$

To prove that Eq. (3.6) possesses smooth solutions let us take $K(x)$, the fundamental solution of the operator $I - \kappa_2\Delta$. Then Eq. (3.6) can be written as

$$\partial_t u = D^2 K \star \Delta u\,.$$

The following result is due to KARCH [15].

LEMMA 4. Let $A = D^2K \star \Delta$, then A has a unique extension to a bounded operator on $L^2(\mathbb{R}^n)$ and is the infinitesimal generator of uniformly continuous group $\mathcal{T}(t)$.

Let us consider the heat equation

$$\partial_t u = D^2\Delta u\,, \tag{3.7}$$

and let $\mathcal{T}_0(t)$ denote the semigroup generated by operator $D^2\Delta$. Then we have the following result.

PROPOSITION 5. Let $u_0(x) \in W_0^{2,1}(\mathbb{R}^n) \cap W^{2,2}(\mathbb{R}^n)$ denote initial data for Eqs. (3.6) and (3.7). Then in the Hilbert space $H = L^2(\mathbb{R}^n)$ we have the following time asymptotics for the solutions of these two equations:

$$t^{n/4}\|\mathcal{T}(t)u_0 - \mathcal{T}_0(t)u_0\| \to 0 \quad \text{as} \quad t \to \infty\,.$$

P r o o f: Passing to the Fourier transform we can write

$$\mathcal{T}(t)u_0 = (2\pi)^{-n/2}\int\limits_{\mathbb{R}^n} \exp\Big(\frac{-D^2\xi^2 t}{1+\kappa_2\xi^2} + ix\xi\Big)\hat{u}_0(\xi)d\xi\,,$$

$$\mathcal{T}_0(t)u_0 = (2\pi)^{-n/2}\int\limits_{\mathbb{R}^n} \exp\Big(-D^2\xi^2 t + ix\xi\Big)\hat{u}_0(\xi)d\xi\,.$$

Using the Plancherel formula we get

$$\|\mathcal{T}(t)u_0 - \mathcal{T}_0(t)u_0\|^2$$

$$= (2\pi)^{-n} \int_{\mathbb{R}^n} \left| \exp\left(\frac{-D^2\xi^2 t}{1+\kappa_2\xi^2}\right) - \exp\left(-D^2\xi^2 t\right) \right|^2 |\hat{u}_0(\xi)|^2 d\xi$$

$$\leq (2\pi)^{-n} \left(\int_{\mathbb{R}^n} \left| \exp\left(\frac{-D^2\xi^2 t}{1+\kappa_2\xi^2}\right) - \exp\left(-D^2\xi^2 t\right) \right|^2 d\xi \right)^{1/2}$$

$$\times \left(\int_{\mathbb{R}^n} \left| \exp\left(\frac{-D^2\xi^2 t}{1+\kappa_2\xi^2}\right) - \exp\left(-D^2\xi^2 t\right) \right|^2 |\hat{u}_0(\xi)|^4 d\xi \right)^{1/2}.$$

If u_0 is sufficiently smooth then the second integral is bounded. In the first integral we make a change of variables $w = t^{1/2}\xi$ to obtain

$$\int_{\mathbb{R}^n} \left| \exp\left(\frac{-D^2\xi^2 t}{1+\kappa_2\xi^2}\right) - \exp\left(-D^2\xi^2 t + ix\xi\right) \right|^2 d\xi$$

$$= t^{-n/2} \int_{\mathbb{R}^n} \left| \exp\left(\frac{-D^2 w^2}{1+\kappa_2 w^2 t^{-1}}\right) - \exp\left(-D^2 w^2\right) \right|^2 dw.$$

It is straightforward that the last integral tends to zero as $t \to \infty$.

■

4. Numerical results

The results of asymptotic analysis on the one hand, and the experimental results presented in [2] on the other, have been confronted with numerical calculations done for Fourier, Cattaneo, Jeffreys and dual-phase-lag models. Our aim was twofold: first, we would like to see how fast is the convergence of solutions of the Cattaneo, Jeffreys and dual-phase-lag models to solutions of the heat equation (Fourier model); second, we would like to compare different models with experimental results. In [2], the heat propagation in thin metal films (namely in gold films) undergoing very short impulses of laser irradiation were investigated. In these experiments heat waves of very large but finite velocity have been observed. Since the measurements were only one-dimensional, we restricted our numerical analysis also to one space dimension.

Since the Fourier model needs no special comments, we present here some technical details concerning only the Jeffreys-type model (the dual-phase-lag

model is defined by the same equations as Jeffreys model, while Cattaneo model can be treated as its special case). To account for short time effects and small sample thickness of metal films (200 to 3000 Å), we introduced the dimensionless variables in the form

$$t = \tau\hat{t}, \qquad x = v\tau\hat{x}, \tag{4.1}$$

where τ is the relaxation time and v is the sound velocity of electrons in metal. Such a change of variables is due to the assumption that heat is transported mostly by the flow of hot electrons. Following [2] we take $v = 0.8 \times 10^8$ cm/s. The same paper suggests also that the reference length should be taken as equal $74\,nm$ (the mean free path for hot electrons). This gives the relaxation time $\tau = 92\,fs$ which is almost equal to the duration of laser pulses ($96\,fs$).

In these new variables the original Jeffreys-type model (2.7) is replaced by the following system of equations

$$\begin{aligned} \partial_t T + \partial_x Q &= 0, \\ \partial_t Q + \hat{D}\partial_x T + Q - \kappa^* \partial_{xx} Q &= 0, \end{aligned} \tag{4.2}$$

where $\hat{D} = k/(\rho C_p \tau v^2)$ and $\kappa^* = k_1/(\rho C_p \tau v^2)$ (hats denoting independent variables have been omitted). T and Q are the dimensionless temperature and heat flux in the new variables, respectively. It is easy to see that if the pair $\{T, Q\}$ satisfies Eq. (4.2), then in the original independent variables Eq. (2.7) are satisfied. For the dual-phase-lag model we have the same equations but with $\kappa^* = k\tau_T/(\rho C_p \tau^2 v^2)$ (the value of κ_2 in the dimensionless variables (4.1)).

For numerical treatment of the problem, we replace system (4.2) by the following finite difference equations:

$$\begin{aligned} &\frac{u_j^{n+1} - u_j^n}{k} + \frac{A}{2}\left[\left(\frac{u_{j+1}^{n+1} - u_{j-1}^{n+1}}{2h}\right) + \left(\frac{u_{j+1}^n - u_{j-1}^n}{2h}\right)\right] \\ &+ \frac{B}{2}\left[\left(\frac{u_{j-1}^{n+1} - 2u_j^{n+1} + u_{j+1}^{n+1}}{h^2}\right) + \left(\frac{u_{j-1}^n - 2u_j^n + u_{j+1}^n}{h^2}\right)\right] \\ &+ \frac{C}{2}\left(u_j^{n+1} + u_j^n\right) = 0. \end{aligned} \tag{4.3}$$

Here h and k denote the space and time steps, respectively, n is the time level number and j the space node number of the rectangular space-time grid; u_j^n is the two-dimensional vector with the first coordinate corresponding to the approximation of T, and the second – to the approximation of Q. Matrices A, B, and

C are as follows

$$A = \begin{bmatrix} 0 & 1 \\ \hat{D} & 0 \end{bmatrix}, \qquad B = \begin{bmatrix} 0 & 0 \\ 0 & -\kappa^* \end{bmatrix}, \qquad C = \begin{bmatrix} 0 & 0 \\ 0 & 1 \end{bmatrix}.$$

The heat impulse is introduced by the left-hand side boundary condition depending on time. On the right-hand side we impose Dirichlet or Neumann zero conditions for both functions T and Q. As initial data we take the zero initial values for T and Q, however there are also other possibilities. Stability and convergence problems for finite difference schemes of this kind will be discussed elsewhere.

Let us now discuss the numerical experiments. We have done computations with a rectangular impulse of duration 96 fs (as in [2]) and amplitude equal to 1. The response to the impulse was observed at four distances from the insulation surface, equal to those used in experimental measurements of [2]. These distances are 500 Å, 1000 Å, 2000 Å, and 3000 Å.

On successive graphs we present the dimensionless temperature as a function of time in picoseconds counted from the start of the heat impulse. Since all the experimental curves are normalized up to their maxima (see Fig. 1), we have performed similar scaling for the numerical results. This, however, enables us to compare only the positions of extrema on the corresponding curves.

We have observed, that for the Jeffreys-type model the existence of extrema depends on the value of κ^*. For large κ^* and at a large distance from the insulation surface there is no clearly visible extremum. Hence we have chosen $\kappa^* = 0.01$ which is sufficiently small to give extrema for all the considered distances.

The best fitting in the Jeffreys and Cattaneo models has been obtained for $\hat{D} = 0.35$ (Fig. 2 Jeffreys, Fig. 3 Cattaneo). The small oscillations on the curves for the Cattaneo model are due to the hyperbolic nature of this model and a very low level of artificial diffusion in the numerical scheme. Thanks to this low diffusion we have obtained rather sharp jumps. Introducing some extra diffusion to our scheme we can diminish the oscillations but smear the jumps.

Similar results for the Fourier model are also presented ($\hat{D} = 0.35$, Fig. 4). It is visible that in the Fourier model maxima are traveling with slightly different speed than in experiments (cf. Fig. 1).

For dual-phase-lag model, which differs from the Jeffreys model only by the values of coefficients $\hat{D}$ and κ^*, computations were done for $\hat{D} = 0.0183$ and $\kappa^* = 2.06$ (Fig. 5). These values have been calculated using the data for gold from [10]. It is worth mentioning that the relaxation time suggested in this paper $\tau_q = 0.79$ ps is almost ten times larger than that used for the Cattaneo and Jeffreys-type models. On the other hand, it is not clear which value should be taken as the reference length. Therefore we have investigated how the numerical results depend on the value of the reference length and found that the position of maxima

is almost independent of this value. To obtain the above mentioned values of $\hat{D}$ and κ^* we have taken the same reference length as in other calculations ($74\,nm$). It is visible from Fig. 5 that in this model the heat waves travel too slowly with respect to experimental data of [2].

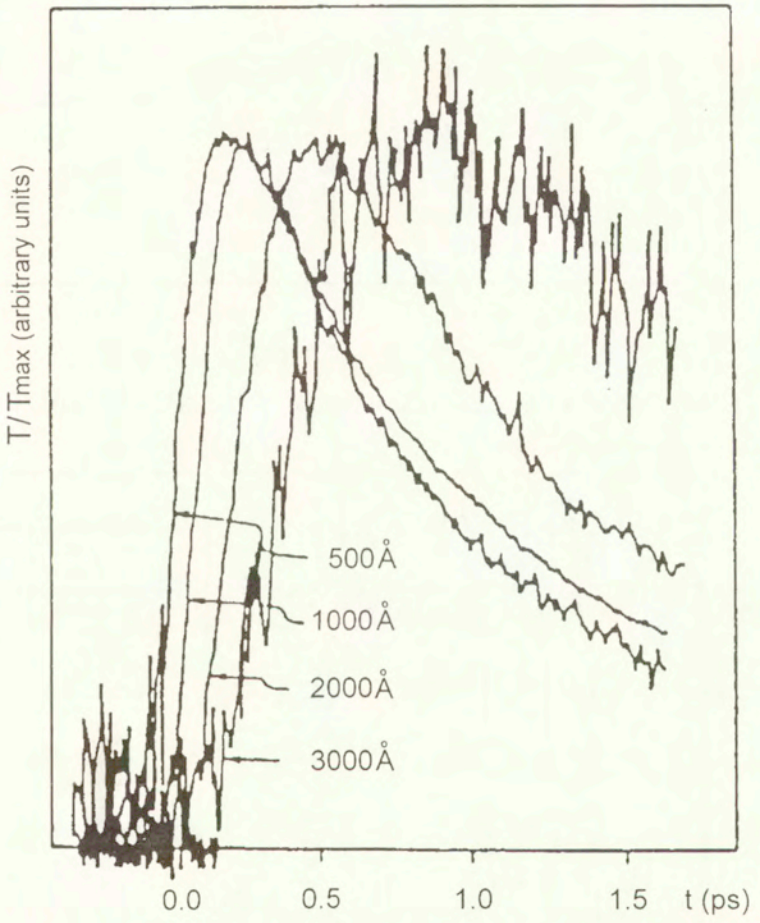

FIG. 1. Experimental data (taken from [2]).

Further, we would like to estimate the time of asymptotic confluence of the Cattaneo and Jeffreys-type models towards the Fourier model. To this end, we have done computations for the distance $x = 500\,\text{Å}$ and sufficiently long time (Fig. 8). It can be seen on this figure that the solutions are confluent, however, for data of the considered models, confluence is rather slow: curves stick after about 100 ps.

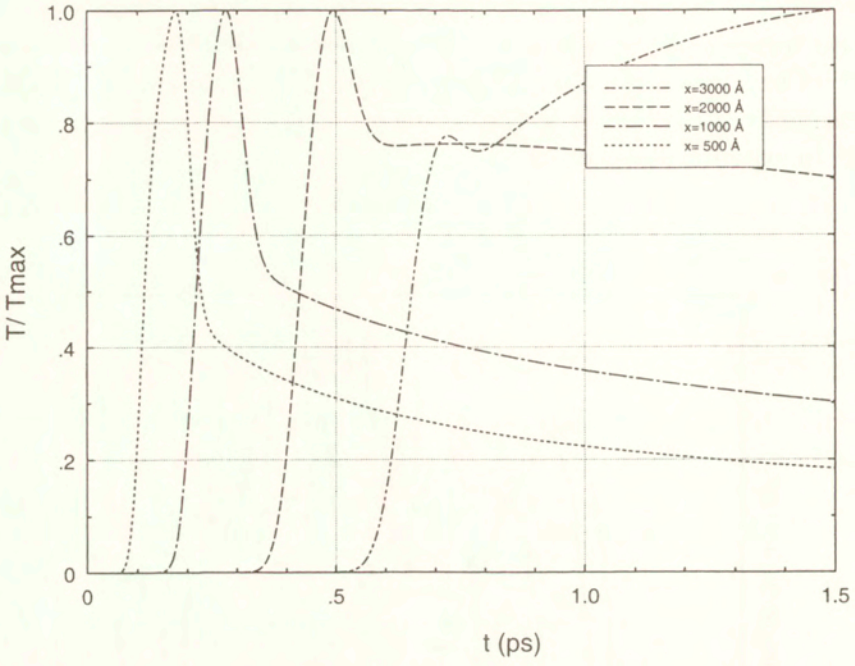

FIG. 2. Jeffreys model with rectangular impulse, $\hat{D} = 0.35$, $\kappa^* = 0.01$, $\tau = 92\, fs$.

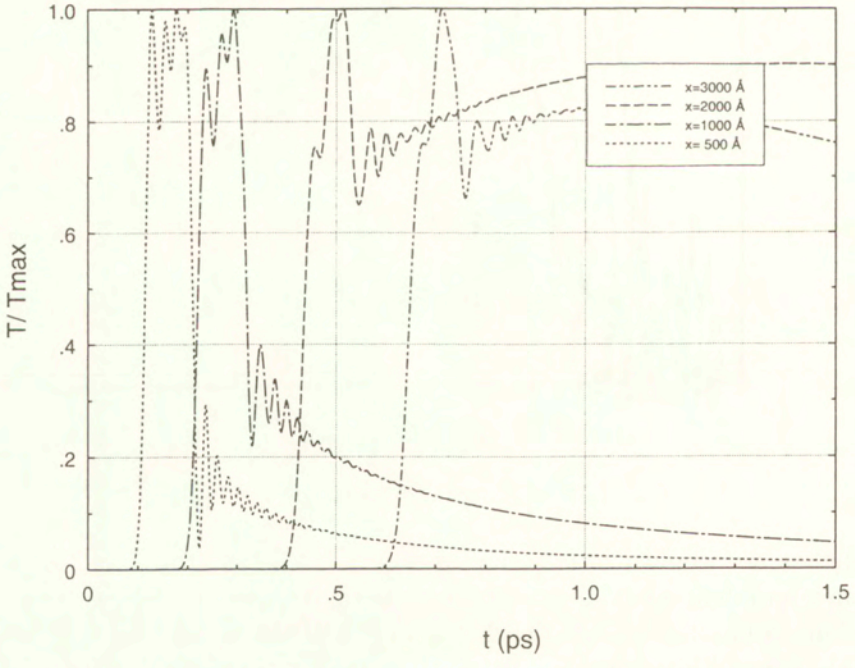

FIG. 3. Cattaneo's model with rectangular impulse, $\hat{D} = 0.35$, $\tau = 92\, fs$.

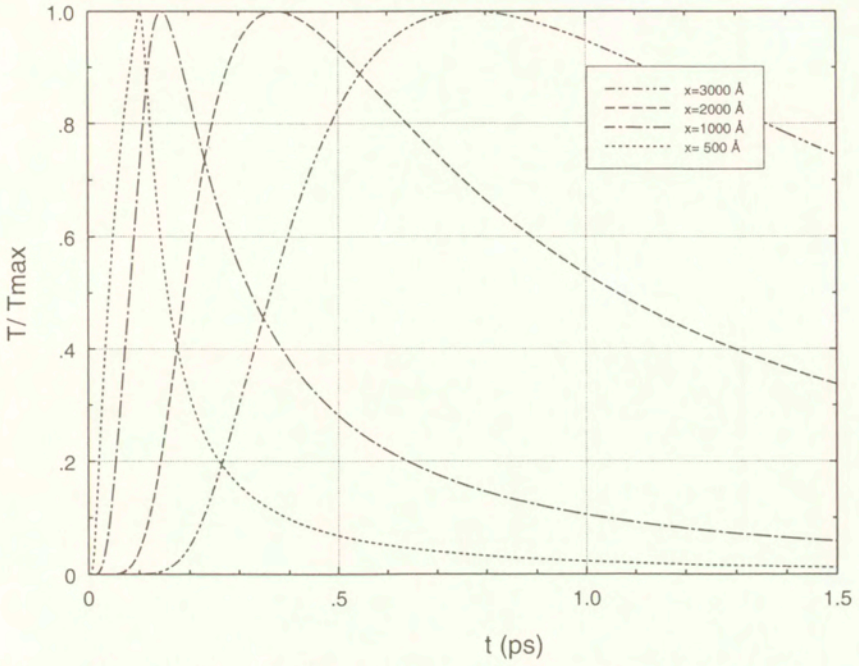

FIG. 4. Fourier model with rectangular impulse, $\hat{D} = 0.35$.

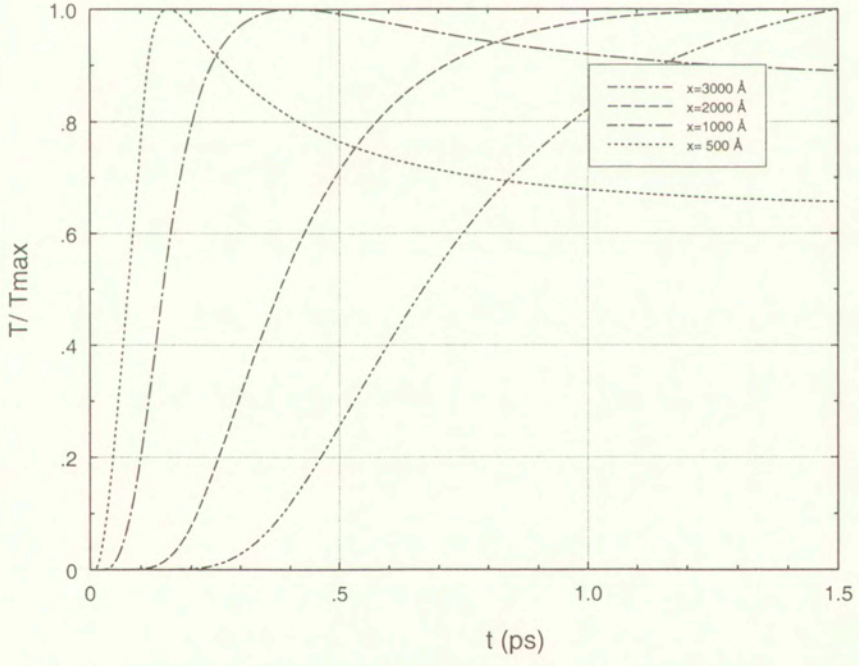

FIG. 5. Dual-phase-lag model with rectangular impulse, $\hat{D} = 0.0183$, $\kappa^* = 2.06$, $\tau = 790\, fs$.

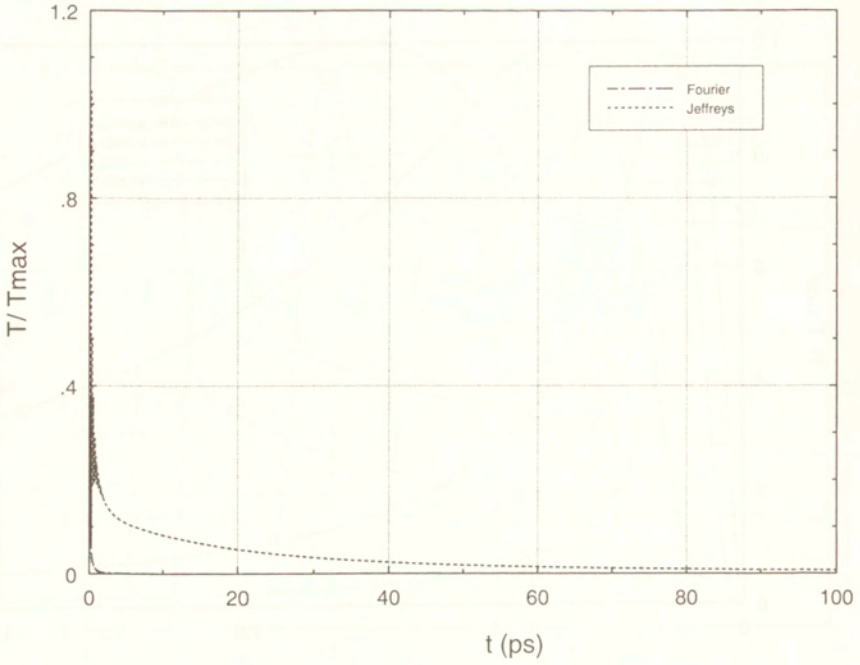

FIG. 6. Fourier and Jeffreys models confluence, temperature distribution at $x = 500$ Å, impulse via left the boundary.

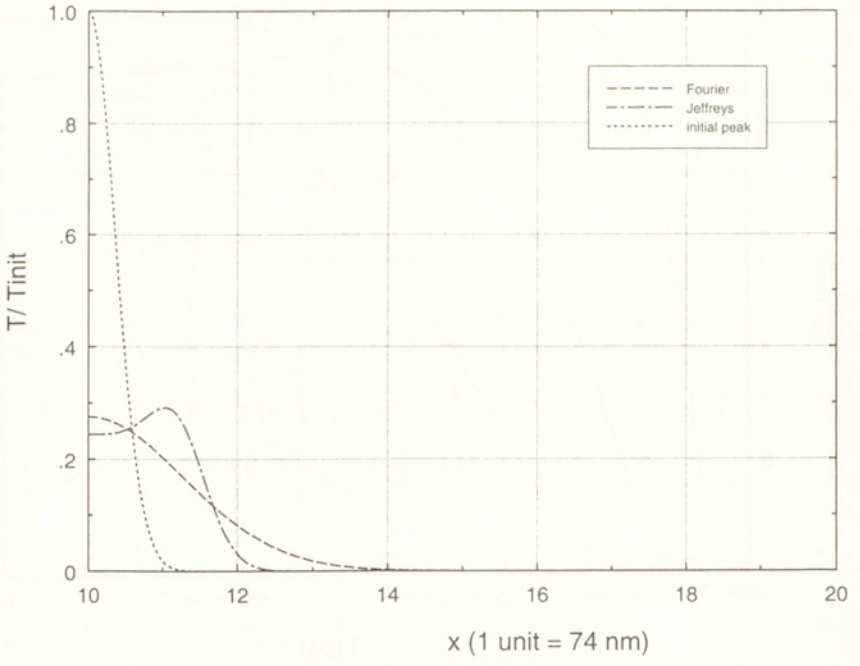

FIG. 7. Temperature distribution at $t = 0.2\,ps$ for Fourier and Jeffreys models, impulse via the initial conditions.

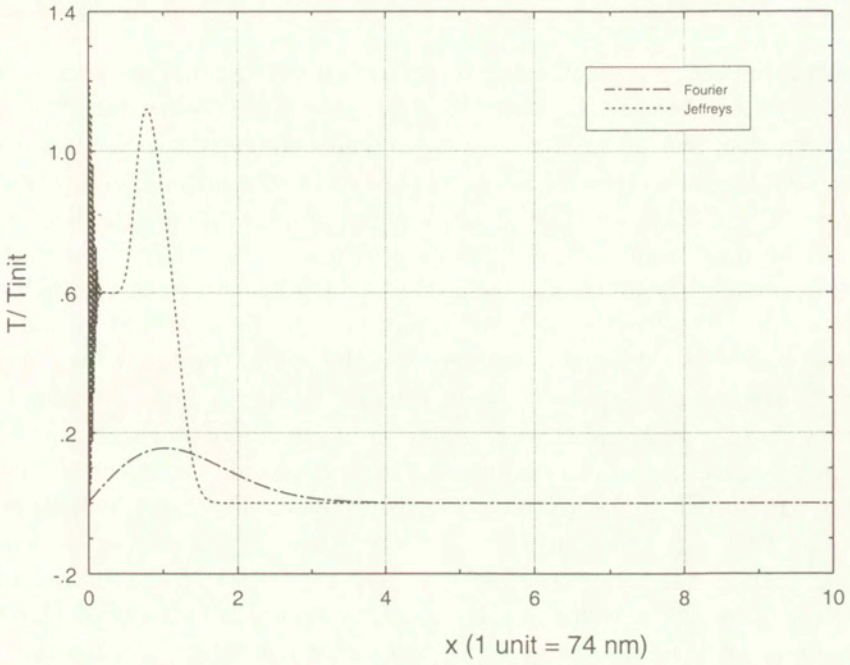

FIG. 8. Temperature distribution at $t = 0.2\,ps$ for Fourier and Jeffreys models, impulse via the left boundary.

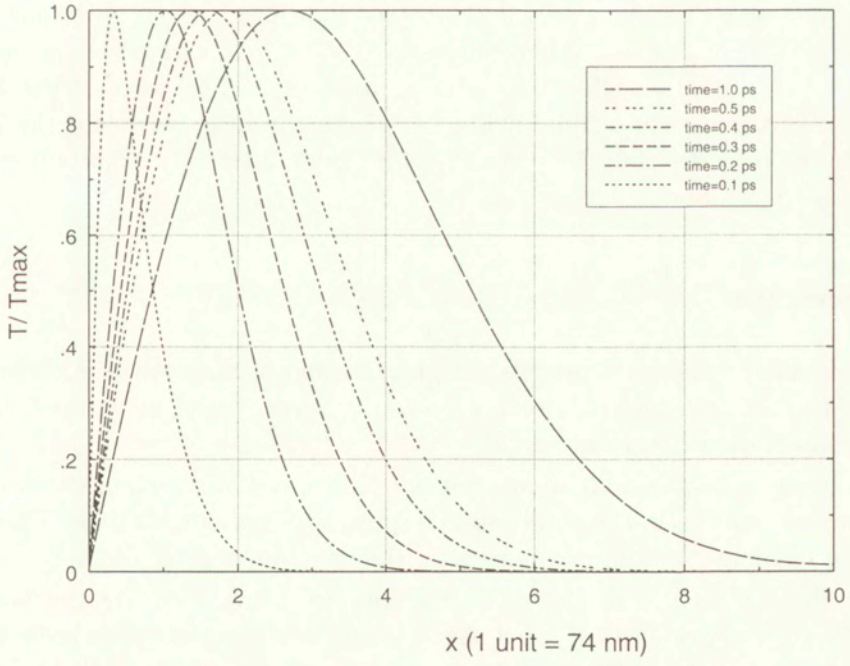

FIG. 9. Temperature distribution at different time instants for Fourier model.

Comparing the Jeffreys, Cattaneo and dual-phase-lag models with the Fourier model, it is worth to note the essential differences in the behaviour of the Fourier model from the point of view of the way in which the heat impulse is introduced: via the boundary conditions of Dirichlet type or via the initial conditions. Curves at Figures 7 and 8 present the dimensionless temperature (normalized with respect to the maximum of initial temperature) as a function of the distance x from the source of heat impulse after time $t = 0.2ps$, in both the Jeffreys and Fourier models. In Fig. 7 the heat impulse in the form of a slim and smooth peak centered at $x = 10$ was introduced via the initial condition for $t = 0$, while Figure 8 presents the same curves in the situation when the rectangular heat impulse enters through the left boundary. It is not important that the shapes of the impulses are different (rectangular impulse gives only the effect of oscillations near the left border of the graph in Fig. 8). We can see that the Jeffreys model behaves in both situations in a similar way: there is a traveling wave running from the source of the impulse. However, the behaviour of the Fourier model is completely different in each case. If the heat impulse is introduced through the initial condition (Fig. 7), there is no trace of a traveling wave for this model. With t growing, the temperature curve becomes more and more flat, its support blows up, but its maximal point is always at $x = 10$. If the heat impulse enters through the left boundary, the temperature curve in the Fourier model is completely different (see Fig. 8). It is important that its maximal point moves now to the right when t grows. When we observe the temperature curves as functions of time t this gives an effect very similar to the traveling wave of the Jeffreys model. This is clearly visible in Fig. 4, where the heat waves for the Fourier model are presented, and the positions of maxima differ only slightly from those of the Jeffreys model.

5. Conclusions

1. In all the discussed models the phenomenon of heat waves is present, but in the Fourier and dual-phase-lag models the waves travel at a speed different than that in the experiments of [2].

2. In the dual-phase-lag model not only the speed of traveling waves is lower than in experiments but, in addition this speed is decaying with time. This model gives in fact the worst approximation to the experimental results.

3. For the Fourier model (with the impulse introduced via the boundary condition), we have also observed that the speed of heat waves is lower than in experiments but the difference is not very significant. Also in this model the speed of heat waves is decaying with time (this effect is better visible in Fig. 9 where we have drawn the temperature profiles for different times).

4. There is no significant difference between the numerical results obtained by Cattaneo's and Jeffreys models. The positions of extrema in the Cattaneo and Jeffreys-type models are similar (visible instability in the Cattaneo model in the case of a rectangular impulse indicates that, perhaps the Jeffreys-type model fits better the reality).

5. The results of computations not presented here show that the positions of extrema in Jeffreys-type models depend only very weakly on the coefficient κ^*.

6. Long time computations made for the distance from the heat impulse source $x = 500$ Å show that the confluence of the Jeffreys and Fourier models occurs practically in about $100\,ps$ after the start of the initial impulse. This confirms the theoretical results we described in the preceding sections and shows that heat waves play an important role only in situations when very short impulses (of order of femtoseconds) and very thin films (of order of micrometers) are considered. The last statement is valid for experiments in room temperature and is not applicable to very low temperatures (for example in liquid helium).

7. Although the Cattaneo and Jeffreys-type models give the position of maxima of temperature profiles very close to the experimental results, the overall shape of numerical profiles is different than the experimental ones (rapid decay with time observed in experiment is not present in the numerical results for larger distances of 2000 Å and 3000 Å). This effect is maybe due to the nature of experimental data (we do not know to which temperature corresponds the bottom axis in Fig. 1 !).

8. The experimental material does not allow us to state in a decisive manner which model fits better the reality. In particular, the knowledge of the relative intensity of maxima can help in making distinction between the Fourier model, where the intensity of numerically calculated maxima is rapidly decreasing with x, and the Cattaneo and Jeffreys-type models, in which the calculated intensity of maxima is decaying much slower with x.

Acknowledgment

This work has been partially supported by the Committee for Scientific Research Grant No. 2P30100806.

References

1. J. BANASIAK and J. R. MIKA, *Singularly perturbed evolution equations with application to kinetic theory*, Word Scientific 1995.
2. S. D. BRORSON, J. G. FUJIMOTO and E. P. IPPEN, *Femtosecond electronic heat-transport dynamics in thin gold films*, Phys. Rev. Lett., **59**, 1962–1965, 1987.
3. C. CATTANEO, *Sulla conduzione de calore*, Atti del Semin. Mat. e Fis. Univ. Modena, **3**, 3, 1948.

4. D. S. CHANDRASEKHARAIAH, *Hyperbolic thermoelasticity: A review of recent literature*, Appl. Mech. Rev., **51**, 705–729, 1998.

5. V. A. CIMMELLI and W. KOSIŃSKI, *Nonequilibrium semi-empirical temperature in materials with thermal relaxation*, Arch. Mech., **43**, 753–767, 1991.

6. V. A. CIMMELLI and W. KOSIŃSKI, *Evolution hyperbolic equations for heat conduction* [in:] Thermodynamics and Kinetic Theory, Series on Advances in Mathematics for Applied Sciences, **12**, pp. 11–22, Word Scientific 1992.

7. W. A. DAY, *On rates of propagation of heat according to Fourier's theory*, Quart. Appl. Math., **55**, 127–138, 1997.

8. G. FICHERA, *Is the Fourier theory of heat propagation paradoxical?*, Rend. Circ. Mat. Palermo (2), **41**, 5–28, 1992.

9. J. E. GOLDSTEIN, *Semigroups of linear operators and applications*, Oxford University Press 1985.

10. K. J. HAYS-STANG and A. HAJI-SHEIKH, *A unified solution for heat conduction in thin films*, Int. J. Heat Mass Transfer, **42**, 455–465, 1999.

11. J. IGNACZAK, *Solitons in a non-linear rigid heat conductor*, J. Thermal Stresses, **12**, 403–423, 1989.

12. A. JANSSEN, *The distance between the Kac process and the Wiener process with applications to generalized telegraph equation*, J. Theoret. Prob.,**3**, 349–360, 1990.

13. D. D. JOSEPH and L. PREZIOSI, *Heat waves*, Rev. Mod. Phys., **61**, 41–73, 1989.

14. D. D. JOSEPH and L. PREZIOSI, *Addendum to the paper "Heat waves"*, Rev. Mod. Phys., **62**, 375–391, 1990.

15. G. KARCH, *Asymptotic behavior of solutions to some pseudoparabolic equations*, Math. Meth. Appl. Sci., **20**, 271–289, 1997.

16. F. NEUBRANDER, *Well-posedness of higher order abstract Cauchy problems*, Trans. Amer. Math. Soc., **295**, 257–290, 1986.

17. M. B. RUBIN, *Hyperbolic heat conduction and the second law*, Int. J. Engng. Sci., **30**, 1665–1676, 1992.

18. S. SOBOLEV, *Some new problems in mathematical physics*, Izv. Akad. Nauk SSSR Ser. Mat., **18**, 3–50, 1950.

19. D. Y. TZOU, *A unified approach for heat conduction from macro- to micro-scales*, J. Heat Transfer, **117**, 8–16, 1995.

Received April 29, 1999; new version February 2, 2000.

Arch. Mech., **52**, 2, pp. 247–273, Warszawa 2000

On the singular integral equations approach to the interface crack problem for piezoelectric materials

V. B. GOVORUKHA ([1]), D. MUNZ ([2]) and M. KAMLAH ([2])

([1]) *Department of Theoretical and Applied Mechanics, Dnepropetrovsk State University, Nauchny line 13, Dnepropetrovsk 320625, Ukraine*

([2]) *Forschungszentrum Karlsruhe, Institut für Materialforschung II, Postfach 3640, D-76021 Karlsruhe, Germany*

A PLANE STRAIN PROBLEM for an interface crack with poling axis orthogonal to the crack plane is considered. The contact zone model with an artificial contact zone is considered for electrically permeable crack. By means of the method of singular integral equations, the quasi-invariance of the energy release rate with respect to the contact zone length is demonstrated. The appearance of a singularity of real power type instead of an oscillating singularity for insulated crack faces for most combinations of ceramics is shown. In a numerical way, the comparison of stresses and electrical displacements corresponding to the different interface crack models is employed.

1. Introduction

FOR COMPOSITE MATERIALS and, in particular, for piezoelectric compounds, interfacial fracture is common and determines mainly the materials overall strength properties. Due to their significance in the areas of mechanics, material science, and engineering, interfacial cracks have been the focus of great interest in the last decades.

In the fundamental papers of WILLIAMS [1], CHEREPANOV [2], ENGLANG [3], RICE and SIH [4] and ERDOGAN [5], the oscillating model for cracks between two isotropic materials has been developed. This model was re-examined afterwards in numerous papers and particularly in the paper of RICE [6]. Interfacial cracks between anisotropic materials have been studied, for instance, by TING [7].

It is well known that the oscillating crack model leads to oscillations in the stress field near the crack tip, resulting in the physically unrealistic phenomenon of interpenetrating crack faces. Therefore, COMNINOU [8] proposed a crack model making use of zones of frictionless contact. This contact zone model was investigated numerically by COMNINOU [9], DUNDURS and COMNINOU [10] and con-

firmed in an analytical way by ATKINSON [11], SIMONOV [12], and GAUTSEN and DUNDURS [13].

Concerning piezoelectric materials, it is worth to note that there are few publications in the literature studying interfacial cracks. Such materials are of high interest in modern smart technology applications. In sensors, they allow for converting mechanical state changes into electric measuring signals, while in actuators, they offer the possibility to convert an electric control signal into mechanical action. In addition to the appearance of a large number of different constants, this case is connected with the coupling of mechanical and electric fields.

A further complication concerns the formulation of the electric boundary conditions at the crack faces in piezoelectric materials. Taking into account the permittivity of the medium filling the crack, increases the complexity of the problem significantly (DUNN [14], HAO and SHEN [15], BALKE *et al.* [16]). Therefore, it is common use to employ the idealised boundary conditions of permeable or insulating crack faces, respectively. Out of these two extreme cases, the permeable boundary condition which simply ignores the crack electrically, seems to be the more realistic one, if results are compared to the analyses taking into account the permittivity of the crack (GRUEBNER and KAMLAH [17]). There are also opposite opinions based on the fact that the permittivity of piezoceramics is three orders of magnitude higher than the one of air or vacuum (SUO *et al.* [18], PARK and SUN [19]). For a detailed discussion of this topic see MCMEEKING [20].

For permeable interfacial crack faces between piezoelectric materials, an exact oscillating solution for a crack between a conductor and a piezoelectric material was obtained in the paper of KUDRYAVTSEV *et al.* [21]. Recently, the character of the singularity at the interface crack tip of permeable and insulating crack faces has been investigated in the papers of KUO and BARNET [22] and SUO *et al.* [18] for piezoelectric compounds. In particular, the possibility of the existence of real as well as oscillating singularities at an interface crack tip was predicted in these papers.

A closed crack tip model for an interface crack in thermopiezoelectric materials was considered by QIN and MAI [23]. Insulated crack faces were considered in this paper and stress intensity factors and the size of the contact zone were found in a numerical way for a particular piezomaterial group.

In the present paper, a plane strain problem for an interface crack between two piezoelectric materials is considered. By means of the Fourier transform, the problem is reduced to a system of singular integral equations corresponding to different electric conditions at the crack faces and different interface crack models. The numerical solution of these systems gave the possibility to find the main fracture characteristics for all the considered cases. For the case of permeable crack faces, artificial contact zones are introduced and the important

property of the quasi-invariance of the energy release rate with respect to the contact zone length is proved. On the basis of this property, a numerical method for investigation of an interface crack problem for a finite-sized body is suggested. The real contact zone length is found for specific choices of the material constants. For insulating crack faces, the crack model without contact zone (open crack model) is considered. The possibility of the existence of a real as well as an oscillating singularity is revealed. Namely, the new principal result related to the most important class of piezoceramics concerning the simultaneous existence of a real non-square root singularity or an oscillating singularity and square root singularity is found out.

It is worth to note that the main advantage of the suggested approach is connected with its possibility to investigate completely different interface crack models and various conditions on the crack faces. Namely, this approach presents both a way for the determination of the singularities as well as a method for the solution of the boundary value problem.

2. Determination of the interface relations

A plane strain state of two bonded semi-infinite spaces $z < 0$ and $z > 0$ is considered. It is loaded by $\sigma_{zz}^{\pm} = \sigma_{zz}^{\infty}$, $D_z^{\pm} = D_z^{\infty}$ at infinity (the "+" sign refers to the upper domain, and "−" to the lower one). A plane crack $z = 0$, $|x| < b$ with free faces is situated in the interface (Fig. 1).

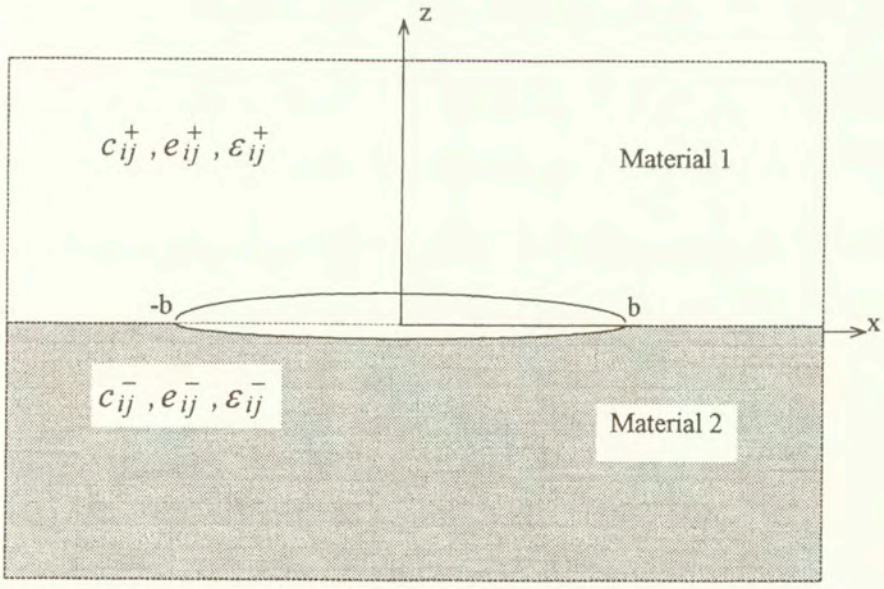

FIG. 1. An interface crack between two semi-infinite piezoelectric planes.

We assume that both materials belong to the hexagonal class of symmetry 6 mm. The plane deformation is orthogonal to the y axis and the z axis coincides with the vector of polarisation. We then find from the classical linear piezoelectric constitutive law the following equations (see e.g. PARTON and KUDRYAVTSEV [24]):

$$\begin{aligned}
\sigma_{xx} &= c_{11}\frac{\partial u}{\partial x} + c_{13}\frac{\partial w}{\partial z} + e_{31}\frac{\partial \varphi}{\partial z},\\
\sigma_{zz} &= c_{13}\frac{\partial u}{\partial x} + c_{33}\frac{\partial w}{\partial z} + e_{33}\frac{\partial \varphi}{\partial z},\\
\sigma_{xz} &= c_{44}\left(\frac{\partial u}{\partial z} + \frac{\partial w}{\partial x}\right) + e_{15}\frac{\partial \varphi}{\partial x},
\end{aligned} \tag{2.1}$$

$$\begin{aligned}
D_x &= e_{15}\left(\frac{\partial u}{\partial z} + \frac{\partial w}{\partial x}\right) - \varepsilon_{11}\frac{\partial \varphi}{\partial x},\\
D_z &= e_{31}\frac{\partial u}{\partial x} + e_{33}\frac{\partial w}{\partial z} - \varepsilon_{33}\frac{\partial \varphi}{\partial z}.
\end{aligned} \tag{2.2}$$

Here, $\{\sigma_{xx}, \sigma_{zz}, \sigma_{xz}\}$ represent the stress components, $\{u, w\}$ are the displacement components, $\{D_x, D_z\}$ are the electric displacement components and φ is the electric potential; $\{c_{11}, c_{13}, c_{33}, c_{44}\}$ are the elastic constants, $\{e_{31}, e_{33}, e_{15}\}$ are the piezoelectric constants and $\{\varepsilon_{11}, \varepsilon_{33}\}$ are the dielectric permittivities.

Taking into account (2.1), (2.2), the equations of equilibrium and electrostatic equations yield the following equations with respect to the displacements and electric potential:

$$\begin{aligned}
c_{11}\frac{\partial^2 u}{\partial x^2} + c_{44}\frac{\partial^2 u}{\partial z^2} + (c_{13}+c_{44})\frac{\partial^2 w}{\partial x \partial z} + (e_{31}+e_{15})\frac{\partial^2 \varphi}{\partial x \partial z} &= 0,\\
(c_{13}+c_{44})\frac{\partial^2 u}{\partial x \partial z} + c_{44}\frac{\partial^2 w}{\partial x^2} + c_{33}\frac{\partial^2 w}{\partial z^2} + e_{33}\frac{\partial^2 \varphi}{\partial z^2} + e_{15}\frac{\partial^2 \varphi}{\partial x^2} &= 0,\\
(e_{31}+e_{15})\frac{\partial^2 u}{\partial x \partial z} + e_{15}\frac{\partial^2 w}{\partial x^2} + e_{33}\frac{\partial^2 w}{\partial z^2} - \varepsilon_{11}\frac{\partial^2 \varphi}{\partial x^2} - \varepsilon_{33}\frac{\partial^2 \varphi}{\partial z^2} &= 0.
\end{aligned} \tag{2.3}$$

Due to the linearity of the Eqs. (2.1) – (2.3), the solution of the problem can be represented by a homogeneous electroelastic field and an additional field which ensures that the boundary conditions on the surface of the crack are fulfilled.

Applying the Fourier transform to Eqs. (2.3),

$$\overline{u}(p,z) = \int_0^\infty u(x,z)\sin(px)dx,$$

$$\overline{w}(p,z) = \int_0^\infty w(x,z)\cos(px)dx, \tag{2.4}$$

$$\overline{\varphi}(p,z) = \int_0^\infty \varphi(x,z)\cos(px)dx$$

we arrive at a system of ordinary differential equations with respect $\overline{u}$, $\overline{w}$, $\overline{\varphi}$. The form of the solution of this system depends on the roots of the characteristic equation

$$\det\|r_{ij}\| = 0, \qquad (i,j = 1,2,3), \tag{2.5}$$

where

$$r_{11} = c_{44}k^2 - c_{11}, \quad r_{12} = -r_{21} = k(c_{13} + c_{44}),$$

$$r_{13} = -r_{31} = k(e_{31} + e_{15}),$$

$$r_{22} = c_{33}k^2 - c_{44}, \quad r_{23} = r_{32} = e_{33}k^2 - e_{15}, \quad r_{33} = \varepsilon_{11} - \varepsilon_{33}k^2.$$

Analysis of Eq. (2.5) shows that for realistic values of the material constants of the considered class of materials, this equation has two real roots $\pm k_1$ and two pairs of complex conjugate roots $\pm\delta \pm i\omega$ (see e.g. PARTON and KUDRYAVTSEV [24]). Therefore the solution of the system (2.3) can be represented in the form

$$u(x,z) = \frac{2}{\pi}\int_0^\infty \Big\{\alpha_1 A(p)e^{-k_1 pz} + [\alpha_2 B(p) - \alpha_3 C(p)]e^{-\delta pz}\cos(\omega pz)$$

$$+[\alpha_3 B(p) + \alpha_2 C(p)]e^{-\delta pz}\sin(\omega pz)\Big\}\sin(px)dp,$$

$$w(x,z) = \frac{2}{\pi}\int_0^\infty \Big\{\beta_1 A(p)e^{-k_1 pz} + [\beta_2 B(p) - \beta_3 C(p)]e^{-\delta pz}\cos(\omega pz) \tag{2.6}$$

$$+ [\beta_3 B(p) + \beta_2 C(p)]e^{-\delta pz}\sin(\omega pz)\Big\}\cos(px)dp,$$

(2.6) [cont.]
$$\varphi(x,z) = \frac{2}{\pi}\int_0^\infty \Big\{\gamma_1 A(p)e^{-k_1 pz} + [\gamma_2 B(p) - \gamma_3 C(p)]e^{-\delta pz}\cos(\omega pz) + [\gamma_3 B(p) + \gamma_2 C(p)]e^{-\delta pz}\sin(\omega pz)\Big\}\cos(px)dp,$$

where

$$\alpha(k) = r_{12}r_{23} - r_{13}r_{22}, \quad \beta(k) = r_{13}r_{21} - r_{11}r_{23}, \quad \gamma(k) = r_{11}r_{22} - r_{12}r_{21},$$

$$\alpha_1 = \alpha(k_1), \quad \beta_1 = \beta(k_1), \quad \gamma_1 = \gamma(k_1),$$

$$\alpha_2 + i\alpha_3 = \alpha(\delta + i\omega), \quad \beta_2 + i\beta_3 = \beta(\delta + i\omega), \quad \gamma_2 + i\gamma_3 = \gamma(\delta + i\omega).$$

Taking into account these relations and the expressions (2.1), (2.2) for stresses and electric displacements via u, w, φ, one obtains at the interface $z = 0$ the following representations:

$$u^\pm(x,0) = \frac{2}{\pi}\int_0^\infty \left[\alpha_1^\pm A^\pm(p) + \alpha_2^\pm B^\pm(p) - \alpha_3^\pm C^\pm(p)\right]\sin(px)dp,$$

$$w^\pm(x,0) = \pm\frac{2}{\pi}\int_0^\infty \left[\beta_1^\pm A^\pm(p) + \beta_2^\pm B^\pm(p) - \beta_3^\pm C^\pm(p)\right]\cos(px)dp,$$

$$\varphi^\pm(x,0) = \pm\frac{2}{\pi}\int_0^\infty \left[\gamma_1^\pm A^\pm(p) + \gamma_2^\pm B^\pm(p) - \gamma_3^\pm C^\pm(p)\right]\cos(px)dp,$$

(2.7)
$$\sigma_{xz}^\pm(x,0) = \pm\frac{2}{\pi}\int_\pi^\infty \left[m_1^\pm A^\pm(p) + m_2^\pm B^\pm(p) - m_3^\pm C^\pm(p)\right]p\cdot\sin(px)dp,$$

$$\sigma_{zz}^\pm(x,0) = \frac{2}{\pi}\int_0^\infty \left[n_1^\pm A^\pm(p) + n_2^\pm B^\pm(p) - n_3^\pm C^\pm(p)\right]p\cdot\cos(px)dp + \sigma_{zz}^\infty,$$

$$D_z^\pm(x,0) = \frac{2}{\pi}\int_0^\infty \left[s_1^\pm A^\pm(p) + s_2^\pm B^\pm(p) - s_3^\pm C^\pm(p)\right]p\cdot\cos(px)dp + D_z^\infty.$$

The functions $A^{\pm}(p)$, $B^{\pm}(p)$, $C^{\pm}(p)$ are to be found from the boundary conditions. Expressions for $m_i^{\pm}$, $n_i^{\pm}$, $s_i^{\pm}$ $(i = 1, 2, 3)$ are given in the Appendix.

The conditions to be satisfied at the interface are:

$$\sigma_{xz}^{+}(x,0) = \sigma_{xz}^{-}(x,0), \quad \sigma_{zz}^{+}(x,0) = \sigma_{zz}^{-}(x,0), \quad D_z^{+}(x,0) = D_z^{-}(x,0). \tag{2.8}$$

Substituting the formulas (2.7) into (2.8), we obtain the relations

$$\begin{aligned} A^{-}(t) &= d_{11}A^{+}(t) + d_{12}B^{+}(t) + d_{13}C^{+}(t), \\ B^{-}(t) &= d_{21}A^{+}(t) + d_{22}B^{+}(t) + d_{23}C^{+}(t), \\ C^{-}(t) &= d_{31}A^{+}(t) + d_{32}B^{+}(t) + d_{33}C^{+}(t), \end{aligned}$$

where the constants d_{ij} $(i, j = 1, 2, 3)$ are given in the Appendix.

Next, we introduce the unknown functions

$$\begin{aligned} g_1(x) &= \sigma_{xz}^{+}(x,0) = \sigma_{xz}^{-}(x,0), \\ g_2(x) &= \frac{\partial w^{+}(x,0)}{\partial x} - \frac{\partial w^{-}(x,0)}{\partial x}, \\ g_3(x) &= \frac{\partial \varphi^{+}(x,0)}{\partial x} - \frac{\partial \varphi^{-}(x,0)}{\partial x}, \end{aligned} \tag{2.9}$$

and apply the Fourier transform to the expressions obtained after substituting $\sigma_{xz}^{\pm}(x,0)$, $w^{\pm}(x,0)$, $\varphi^{\pm}(x,0)$ from (2.7) into (2.9). This leads to a system of linear algebraic equations with respect to $A^{+}(t)$, $B^{+}(t)$ and $C^{+}(t)$ which has the following solutions:

$$\begin{aligned} A^{+}(t) &= \frac{1}{t}\left[a_{11}\overline{g}_1(t) + a_{12}\overline{g}_2(t) + a_{13}\overline{g}_3(t)\right], \\ B^{+}(t) &= \frac{1}{t}\left[a_{21}\overline{g}_1(t) + a_{22}\overline{g}_2(t) + a_{23}\overline{g}_3(t)\right], \\ C^{+}(t) &= \frac{1}{t}\left[a_{31}\overline{g}_1(t) + a_{32}\overline{g}_2(t) + a_{33}\overline{g}_3(t)\right], \end{aligned} \tag{2.10}$$

where

$$\overline{g}_k(t) = \int_0^{\infty} g_k(x)\sin(tx)dx, \quad k = 1, 2, 3,$$

and the constants $a_{ij}(i, j = 1, 2, 3)$ are given in the Appendix.

Substituting the formulas (2.10) into expressions for $\Delta(x,0) = \dfrac{\partial u^+(x,0)}{\partial x} - \dfrac{\partial u^-(x,0)}{\partial x}$, $\sigma_{zz}^+(x,0)$, $D_z^+(x,0)$ from (2.7) and taking into account that

$$\frac{2}{\pi}\int_0^\infty \overline{g}_k(t)\cos(tx)dt = \frac{1}{\pi}\int_{-\infty}^\infty \frac{1}{t-x}g_k(t)dt, \qquad k=1,2,3,$$

we arrive at the boundary relations

$$\Delta(x,0) = \frac{1}{\pi}\left\{\eta_{11}\int_{-\infty}^\infty \frac{g_1(t)dt}{t-x} + \eta_{12}\int_{-\infty}^\infty \frac{g_2(t)dt}{t-x} + \eta_{13}\int_{-\infty}^\infty \frac{g_3(t)dt}{t-x}\right\} + \Omega_1, \tag{2.11}$$

$$\sigma_{zz}^+(x,0) = \frac{1}{\pi}\left\{\eta_{21}\int_{-\infty}^\infty \frac{g_1(t)dt}{t-x} + \eta_{22}\int_{-\infty}^\infty \frac{g_2(t)dt}{t-x} + \eta_{23}\int_{-\infty}^\infty \frac{g_3(t)dt}{t-x}\right\} + \Omega_2, \tag{2.12}$$

$$D_z^+(x,0) = \frac{1}{\pi}\left\{\eta_{31}\int_{-\infty}^\infty \frac{g_1(t)dt}{t-x} + \eta_{32}\int_{-\infty}^\infty \frac{g_2(t)dt}{t-x} + \eta_{33}\int_{-\infty}^\infty \frac{g_3(t)dt}{t-x}\right\} + \Omega_3, \tag{2.13}$$

where $\Omega_1 = 0$, $\Omega_2 = \sigma_{zz}^\infty$, $\Omega_3 = D_z^\infty$, and the formulas for the constants $\eta_{ij}(i,j = 1,2,3)$ are given in the Appendix.

The boundary integral relations (2.11) – (2.13) play an important role in the following analysis because by means of these relations the singular integral equations for various mixed boundary conditions at the interface can be formulated.

3. Interface crack with permeable crack faces

We now turn to the permeable crack faces. Fracture mechanical parameters calculated by taking into account the permittivity of the crack medium, indicate that permeable crack faces are more realistic extreme case (DUNN [14], BALKE *et al.* [16], GRUEBNER and KAMLAH [17], MCMEEKING [20]).

So we now assume that the complete interface $z = 0$ is electrically permeable. In this case, the boundary conditions are the following

$$\sigma_{xz}^{+}(x,0) = 0, \quad \sigma_{zz}^{+}(x,0) = 0, \quad |x| < b;$$

$$u^{+}(x,0) - u^{-}(x,0) = 0, \quad w^{+}(x,0) - w^{-}(x,0) = 0, \quad |x| > b; \tag{3.1}$$

$$\varphi^{+}(x,0) - \varphi^{-}(x,0) = 0, \quad |x| < \infty.$$

Taking into account that according to (3.1), $g_1(x) = 0$ for $|x| < b$, $g_2(x) = 0$ for $|x| > b$, $g_3(x) \equiv 0$, and by satisfying the equation $\Delta(x,0) = 0$ as well as the second of the conditions (3.1), we arrive at the following system of singular integral equations (SIE):

$$\eta_{i1} \int_{c_1}^{d_1} \left[\frac{1}{t-x} + \frac{1}{t+x} \right] g_1(t)dt + \eta_{i2} \int_{c_2}^{d_2} \frac{1}{t-x} g_2(t)dt = -\pi \Omega_i. \tag{3.2}$$

Here, $x \in (c_i, d_i)$, $c_1 = -c_2 = d_2 = b$, $d_1 = \infty$, $i = 1, 2$.

In this case we obtain singularities which imply oscillations in the stress field near the tips of the crack, resulting in the unrealistic phenomenon of interpenetrating of crack faces, and leading to difficulties in the numerical analysis for the determination of the fracture mechanical parameters. For this reason, similar to COMNINOU [8] we introduce artificial frictionless contact zones $a < |x| < b$ to avoid the oscillating singularity, where the position of the point a is arbitrary for the time being. For an arbitrary position of the point a, an artificial contact zone model (ACZM) is not physically justified, but from this model the specific value of a for the real contact zone length (Comninou's model) can be found. Moreover, the quasi-invariance of the energy release rate (ERR) with respect to a, demonstrated later on for an ACZM can be used for a numerical (FEM or BEM) investigation of finite sized piezoelectrics with interface cracks.

The boundary conditions for considered model are the following:

$$\sigma_{xz}^{+}(x,0) = 0, \quad \sigma_{zz}^{+}(x,0) = 0, \quad |x| < a;$$

$$\sigma_{xz}^{+}(x,0) = 0, \quad w^{+}(x,0) - w^{-}(x,0) = 0, \quad a < |x| < b, |x| > h;$$

$$u^{+}(x,0) - u^{-}(x,0) = 0, \quad w^{+}(x,0) - w^{-}(x,0) = 0, \quad b < |x| < h; \tag{3.3}$$

$$\varphi^{+}(x,0) - \varphi^{-}(x,0) = 0, \quad |x| < \infty.$$

By these conditions, further zones of frictionless contact have been introduced for $|x| > h$. This assumption is not a principal one, since according to St.Venant's principle, it will not influence the state of stress near the crack, provided $h \gg b$.

However, in this case $g_1(x) = 0$ for $|x| < b$ and $|x| > h$, $g_2(x) = 0$ for $|x| > a$, $g_3(x) \equiv 0$ and from equation $\Delta(x, 0) = 0$ and the second of the conditions (16), we arrive at the very same system of SIE (3.2), in which now $x \in (c_i, d_i)$, $c_1 = b$, $d_1 = h$, $c_2 = -a$, $d_2 = a$, $i = 1, 2$. Note that we have finite upper limits in the integrals due to the further frictionless contact zones.

Additional conditions which must be satisfied to ensure that the displacements are single valued are (see e.g. COMNINOU and DUNDURS [25])

$$\int_{-b}^{b} \Delta(x, 0)dx = 0, \qquad \int_{-a}^{a} \left(\frac{\partial w^+(x, 0)}{\partial x} - \frac{\partial w^-(x, 0)}{\partial x} \right) dx = 0,$$

which, after substitution of relation (2.7) can be written in the form

$$2\eta_{11} \int_{b}^{h} \ln \left| \frac{t+b}{t-b} \right| g_1(t)dt + \eta_{12} \int_{-a}^{a} \ln \left| \frac{t+b}{t-b} \right| g_2(t)dt = 0, \tag{3.4}$$

$$\int_{-a}^{a} g_2(t)dt = 0.$$

Due to the absence of an oscillation in the singularity we can represent in this case the unknown functions $g_i(t)(i = 1, 2)$ in the form

$$g_i(t) = \frac{g_i^*(t)}{\sqrt{(d_i - t)(t - c_i)}}, \qquad g_i^*(t) \in H, \tag{3.5}$$

where H is the class of Hölder functions (see e.g. MUSKHELISHVILI [26]) in $[c_i, d_i]$, $i = 1, 2$.

Next, we introduce the stress intensity factors for the right-hand crack tip by

$$K_1 = \lim_{x \to a+0} \sqrt{2(x-a)}\sigma_{zz}^+(x, 0), \quad K_2 = \lim_{x \to b+0} \sqrt{2(x-b)}\sigma_{xz}^+(x, 0). \tag{3.6}$$

Due to (2.12), (3.5) and the results of MUSKHELISHVILI [26] for Cauchy type integrals behaviour, we can write

$$K_1 = -\frac{\eta_{22} g_2^*(a)}{\sqrt{a}}, \qquad K_2 = \sqrt{\frac{2}{h-b}} g_1^*(b). \tag{3.7}$$

The energy release rate G for the right crack tip can be represented by the virtual work integral

$$G = \lim_{\Delta l \to 0} \left\{ \frac{1}{2\Delta l} \int_{a}^{a+\Delta l} \tilde{\sigma}_{zz}^{+}(x)\tilde{w}(x+\Delta l)dx + \frac{1}{2\Delta l} \int_{b}^{b+\Delta l} \tilde{\sigma}_{xz}^{+}(x)\tilde{u}(x+\Delta l)dx \right\}. \tag{3.8}$$

The integrals in the last formula can be computed from the asymptotic behaviour of displacements and stresses near the singular points a and b.

Exploiting the asymptotic behaviour

$$g_2(x)|_{x\to a-0} = \frac{g_2^*(a)}{\sqrt{2a(a-x)}}$$

following from (3.5), the second of Eq. (2.9) gives

$$\left\{w^+(x,0) - w^-(x,0)\right\}\big|_{x\to a-0} = -\sqrt{\frac{2(a-x)}{a}}\, g_2^*(a).$$

Employing Cauchy-type integral properties [26] in Eq. (2.12) gives

$$\sigma_{zz}^{+}(x,0)\big|_{x\to a+0} = -\eta_{22}\frac{g_2^*(a)}{\sqrt{2a(x-a)}}.$$

Using the first of the relation (3.7) leads to the following formulas:

$$\tilde{w}(x) = \left\{w^+(x,0) - w^-(x,0)\right\}\big|_{x\to a-0} = \frac{\sqrt{2(a-x)}}{\eta_{22}}K_1,$$

$$\tilde{\sigma}_{zz}^{+}(x) = \sigma_{zz}^{+}(x,0)\big|_{x\to a+0} = \frac{K_1}{\sqrt{2(x-a)}}.$$

In a similar way it can be shown that

$$\tilde{u}(x) = \left\{u^+(x,0) - u^-(x,0)\right\}\big|_{x\to b-0} = -\eta_{11}\sqrt{2(b-x)}K_2,$$

$$\tilde{\sigma}_{xz}^{+}(x) = \sigma_{xz}^{+}(x,0)\big|_{x\to b+0} = \frac{K_2}{\sqrt{2(x-b)}}.$$

Substituting the last formulas into (3.8) and taking into account that

$$\int_0^{\Delta l} \sqrt{\frac{\Delta l - x}{x}}dx = \frac{\pi\Delta l}{2},$$

we obtain the following formula:

$$G = \frac{\pi}{4}\left[\overline{\alpha}K_1^2 + \overline{\beta}K_2^2\right], \quad \overline{\alpha} = 1/\eta_{22}, \quad \overline{\beta} = -\eta_{11}, \quad (\eta_{22} > 0,\ \eta_{11} < 0). \tag{3.9}$$

4. Interface crack with insulated crack faces

We now consider the second extreme case of electric boundary conditions, namely electrically insulating crack faces. Sometimes, they are thought to be more realistic since the permittivity of piezoceramics is three orders of magnitude higher than the one of air or vacuum (SUO *et al.* [18], PARK and SUN [19]). Thus we assume next that the crack faces are perfectly insulated. The boundary conditions for this case are the following:

$$
\begin{aligned}
&\sigma_{xz}^{+}(x,0)=0, \quad \sigma_{zz}^{+}(x,0)=0, \quad |x|<b;\\
&u^{+}(x,0)-u^{-}(x,0)=0, \quad w^{+}(x,0)-w^{-}(x,0)=0, \quad b<|x|<h;\\
&\sigma_{xz}^{+}(x,0)=0, \quad w^{+}(x,0)-w^{-}(x,0)=0, \quad |x|>h;\\
&D_{z}^{+}(x,0)=0, \quad |x|<b, \quad \varphi^{+}(x,0)-\varphi^{-}(x,0)=0, \quad |x|>b.
\end{aligned}
\tag{4.1}
$$

Taking into account that in this case $g_1(x)=0$, $(|x|<b, |x|>h)$, $g_2(x)=0$ $(|x|>b)$, and $g_3(x)=0$ $(|x|>b)$, we satisfy by means of relations (2.11) – (2.13) the relation $\Delta(x,0)=0$ $(b<|x|<h)$, the second, and the last but one of the boundary conditions (4.1), and we arrive at the following system of three SIE:

$$
\eta_{i1}\int_{b}^{h}\left[\frac{1}{t-x}+\frac{1}{t+x}\right]g_1(t)dt+\sum_{k=2}^{3}\eta_{ik}\int_{-b}^{b}\frac{1}{t-x}g_k(t)dt=-\pi\Omega_i,
\tag{4.2}
$$

where $x\in(b,h)$ for $i=1$ and $x\in(-b,b)$ for $i=2,3$.

Additional conditions which ensure that the displacements and the electrical potential are single valued, are taken to be in the form

$$
2\eta_{11}\int_{b}^{h}\ln\left|\frac{t+b}{t-b}\right|g_1(t)dt+\sum_{k=2}^{3}\eta_{1k}\int_{-b}^{b}\ln\left|\frac{t+b}{t-b}\right|g_k(t)dt=0,
\tag{4.3}
$$

$$
\int_{-b}^{b}g_k(t)dt=0, \qquad (k=2,3).
$$

We represent the unknown functions as

$$
g_1(t)=\frac{g_1^{*}(t)}{(t-b)^{\alpha}\sqrt{h-t}}, \quad g_k(t)=\frac{g_k^{*}(t)}{(b-t)^{\alpha}(b+t)^{\alpha}}, \quad (k=2,3),
\tag{4.4}
$$

where $g_i^{*}(t)\in H$ $(i=1,2,3)$ and $0\le \mathrm{Re}(\alpha)<1$.

Introducing the piecewise holomorphic functions

$$\Phi_1(x) = \frac{1}{\pi}\int_b^h \frac{g_1(t)}{t-x}dt, \qquad \Phi_k(x) = \frac{1}{\pi}\int_{-b}^b \frac{g_k(t)}{t-x}dt, \quad (k=2,3),$$

one can rewrite Eq. (4.2) as

$$\eta_{i1}\left[\Phi_1(x)+\Phi_1(-x)\right] + \sum_{k=2}^{3}\eta_{ik}\Phi_k(x) = -\Omega_i. \tag{4.5}$$

Using the approach described in the paper of MUSKHELISHVILI [26] for estimating Cauchy type integrals at the boundary points of the integration interval, one obtains for $x \to b+0$ and $x \to b-0$

$$\begin{aligned}
\Phi_1(x)|_{x\to b+0} &= \frac{\operatorname{ctg}(\pi\alpha)g_1^*(b)}{(x-b)^\alpha\sqrt{h-b}} + \Phi_1^*(x),\\
\Phi_1(x)|_{x\to b-0} &= \frac{g_1^*(b)}{\sin(\pi\alpha)(b-x)^\alpha\sqrt{h-b}} + \Phi_1^*(x),\\
\Phi_k|_{x\to b+0} &= -\frac{g_k^*(b)}{\sin(\pi\alpha)(x-b)^\alpha(2b)^\alpha} + \Phi_k^*(x),\\
\Phi_k(x)|_{x\to b-0} &= -\frac{\operatorname{ctg}(\pi\alpha)g_k^*(b)}{(2b)^\alpha(b-x)^\alpha} + \Phi_k^*(x).
\end{aligned} \tag{4.6}$$

Here $|\Phi_i^*(x)| \le \dfrac{C_i}{(x-b)^\gamma}$ with $\operatorname{Re}(\gamma) < \operatorname{Re}(\alpha)$ and $C_i (i=1,2,3)$ are real constants.

Substituting (4.6) into (4.5), we arrive to the following equations:

$$\begin{aligned}
\frac{\eta_{11}\cos(\pi\alpha)g_1^*(b)}{\sqrt{h-b}} - \frac{\eta_{12}g_2^*(b)}{(2b)^\alpha} - \frac{\eta_{13}g_3^*(b)}{(2b)^\alpha} &= (x-b)^\alpha\Phi_4^*(x),\\
\frac{\eta_{21}g_1^*(b)}{\sqrt{h-b}} - \frac{\eta_{22}\cos(\pi\alpha)g_2^*(b)}{(2b)^\alpha} - \frac{\eta_{23}\cos(\pi\alpha)g_3^*(b)}{(2b)^\alpha} &= (b-x)^\alpha\Phi_5^*(x),\\
\frac{\eta_{31}g_1^*(b)}{\sqrt{h-b}} - \frac{\eta_{32}\cos(\pi\alpha)g_2^*(b)}{(2b)^\alpha} - \frac{\eta_{33}\cos(\pi\alpha)g_3^*(b)}{(2b)^\alpha} &= (b-x)^\alpha\Phi_6^*(x).
\end{aligned}$$

This system has nonzero solutions for if

$$\det\|b_{ij}\| = 0, \qquad (i,j=1,2,3),$$

where

$$b_{11} = \eta_{11}\cos(\pi\alpha)/\sqrt{h-b}, \quad b_{12} = -\eta_{12}/(2b)^{\alpha}, \quad b_{13} = -\eta_{13}/(2b)^{\alpha},$$

$$b_{21} = \eta_{21}/\sqrt{h-b}, \quad b_{22} = -\eta_{22}\cos(\pi\alpha)/(2b)^{\alpha},$$

$$b_{23} = -\eta_{23}\cos(\pi\alpha)/(2b)^{\alpha}, \quad b_{31} = \eta_{31}/\sqrt{h-b},$$

$$b_{32} = -\eta_{32}\cos(\pi\alpha)/(2b)^{\alpha}, \quad b_{33} = -\eta_{33}\cos(\pi\alpha)/(2b)^{\alpha}.$$

This determinant can be rewritten in the form

$$\cos(\pi\alpha)\left[\mu_1\cos^2(\pi\alpha) + \mu_2\right] = 0, \tag{4.7}$$

where

$$\mu_1 = \eta_{11}\eta_{22}\eta_{33} - \eta_{11}\eta_{32}\eta_{23},$$

$$\mu_2 = \eta_{21}\eta_{32}\eta_{13} + \eta_{12}\eta_{23}\eta_{31} - \eta_{31}\eta_{22}\eta_{13} - \eta_{21}\eta_{12}\eta_{33}.$$

Equation (4.7) can be used for the determination of the power of singularity at the tip of interface crack for insulated crack surfaces.

5. Numerical results and discussion

First of all we pay our attention to the ACZM for the permeable crack faces. The values of the material constants of the piezoceramics PZT-4, PZT-19, PZT-5H, PZT-5 were adopted from the papers [19, 24, 27, 33], respectively.

A numerical solution of the system (3.2), (3.4) has been obtained by the method based on the Gauss-Chebyshev quadrature rule [28] which was described in detail in the paper of LOBODA [29] for equations similar to (3.2), (3.4).

The variation of the normal stress in the contact region corresponding to different $\lambda = \dfrac{b-a}{2b}$ are shown in Fig. 2. For the upper piezomaterial, fictitious material constants were taken as

$$c_{11} = 1.22\cdot 10^{10}(\mathrm{N/m^2}), \quad c_{12} = 7.78\cdot 10^{10}(\mathrm{N/m^2}),$$

$$c_{13} = 0.11\cdot 10^{10}(\mathrm{N/m^2}), \quad c_{33} = 1.23\cdot 10^{10}(\mathrm{N/m^2}),$$

$$c_{44} = 1.0\cdot 10^{10}(\mathrm{N/m^2}), \quad e_{31} = -6.50(\mathrm{C/m^2}),$$

$$e_{33} = 23.3(\mathrm{C/m^2}), \quad e_{15} = 17.0(\mathrm{C/m^2}),$$

$$\varepsilon_{11} = 15.1\cdot 10^{-9}(\mathrm{C/Vm}), \quad \varepsilon_{33} = 13.0\cdot 10^{-9}(\mathrm{C/Vm}),$$

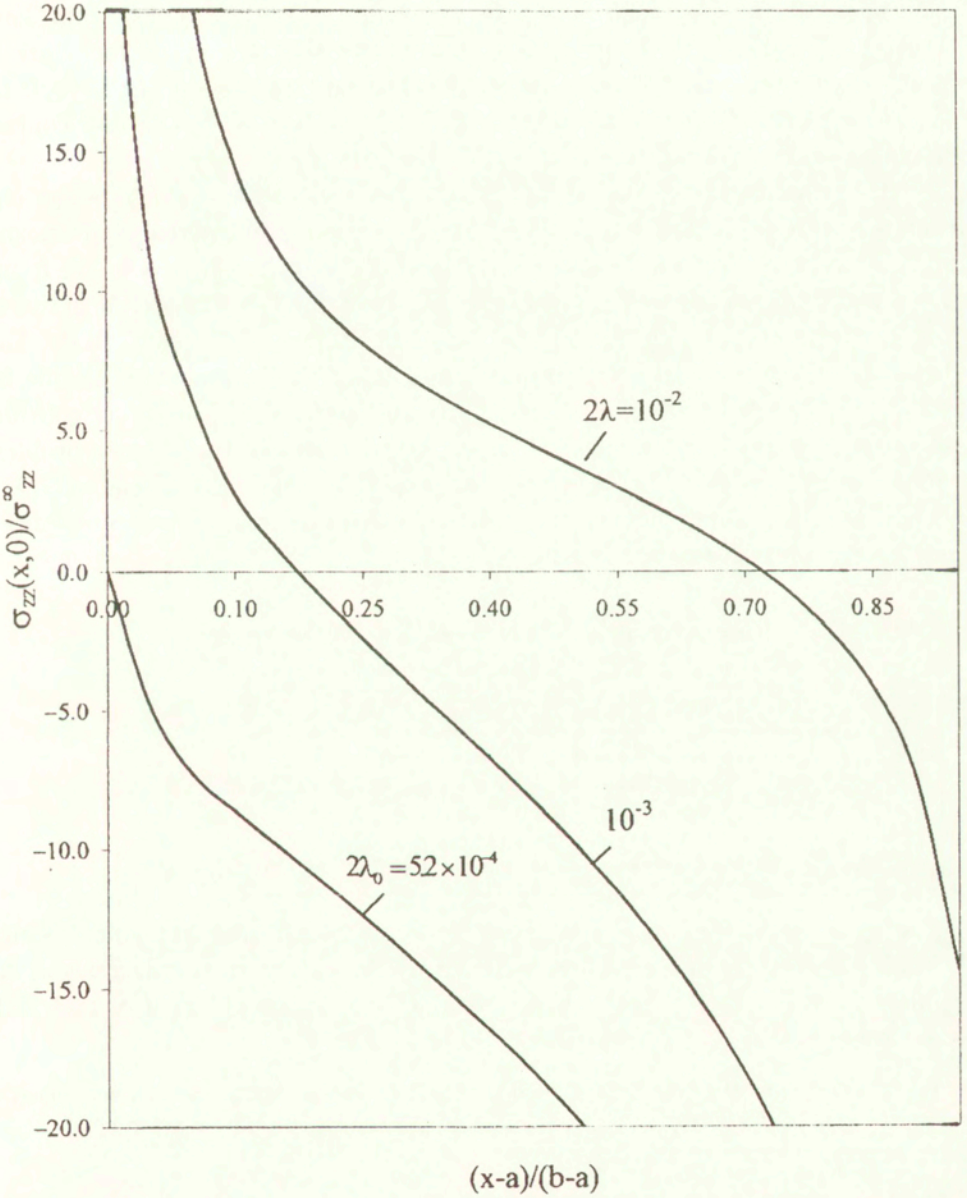

FIG. 2. Variation of the normal stress along the contact zone $[a, b]$ for different values of λ.

and PZT-4 was chosen as the lower piezomaterial. One can see that for sufficiently large λ, the values of $\sigma_{zz}(x,0)$ in the main part of $[a,b]$ are positive. Only at point b they are negative indicating a compressive stress. Decreasing λ leads to an increased relative length of the compressed zone with respect to the length of $[a,b]$. Finally, for $\lambda = \lambda_0 = 2.6 \times 10^{-4}$ the values of $\sigma_{zz}(x,0)$ becomes compressive in the complete contact region $[a,b]$. This means that the crack faces are in contact in all of $[a,b]$ and the boundary condition $w^+(x,0) - w^-(x,0) = 0$ for $x \in [a,b]$ is physically correct for $\lambda = \lambda_0$. In this sense, λ_0 is the real contact zone length.

Next, the values of K_1, K_2 and G for the same piezomaterials as before and various λ are shown in Table 1. The last line corresponds to the real contact zone length λ_0 and the maximum value of $|K_2|$ and $K_1 = 0$, i.e $g_2^*(a) = 0$, are found for $\lambda = \lambda_0$. This value for λ_0 is rather small (even for the considered fictitious upper piezomaterial) and it can not be found easily for a finite-sized body. But fortunately this is not necessary because the ERR $G(\lambda)$ is almost invariable for $\lambda_0 \leq \lambda \leq \lambda_*$ ($\lambda_* \sim 5 \times 10^{-2}$), and similarly to LOBODA [30] one may consider it as quasi-invariant with respect to λ. This fact permits to solve a problem in question for $\lambda = \lambda_* \gg \lambda_0$ and use the obtained value of G as $G_0 = G(\lambda_0)$. This approach simplifies the numerical solution of an interface crack problem for piezoelectric composites significantly.

Table 1. Dependence of the SIF-s K_i and the ERR G on the relative contact zone length λ for electrically permeable crack.

2λ	$K_2(\mathrm{Pa}\sqrt{m})$	$K_1(\mathrm{Pa}\sqrt{m})$	$G(\mathrm{N/m})$
5×10^{-2}	-0.861	1.016	0.165×10^{-9}
10^{-2}	-1.214	0.698	0.167×10^{-9}
5×10^{-3}	-1.319	0.531	0.167×10^{-9}
10^{-3}	-1.441	0.134	0.167×10^{-9}
$2\lambda_0 \approx 5.2 \times 10^{-4}$	-1.445	≈ 0	0.166×10^{-9}

The quasi-invariance of G with respect to λ is confirmed in Table 2 which has been obtained for the ceramics PZT-5H/PZT-4. Due to the decreasing K_1 and increasing K_2, it is reasonable to assume for this combination of materials the existence of $\lambda = \lambda_0$ for which $K_1 = 0$, too.

Table 2. Dependence of the SIFs K_i and the ERR G on the relative contact zone length λ for electrically permeable crack for the piezoceramics PZT-5H/PZT-4.

2λ	$K_2(\mathrm{Pa}\sqrt{m})$	$K_1(\mathrm{Pa}\sqrt{m})$	$G(\mathrm{N/m})$
10^{-2}	-0.106	0.986	0.331×10^{-10}
10^{-3}	-0.153	0.985	0.332×10^{-10}
10^{-4}	-0.178	0.982	0.332×10^{-10}
10^{-5}	-0.182	0.981	0.332×10^{-10}

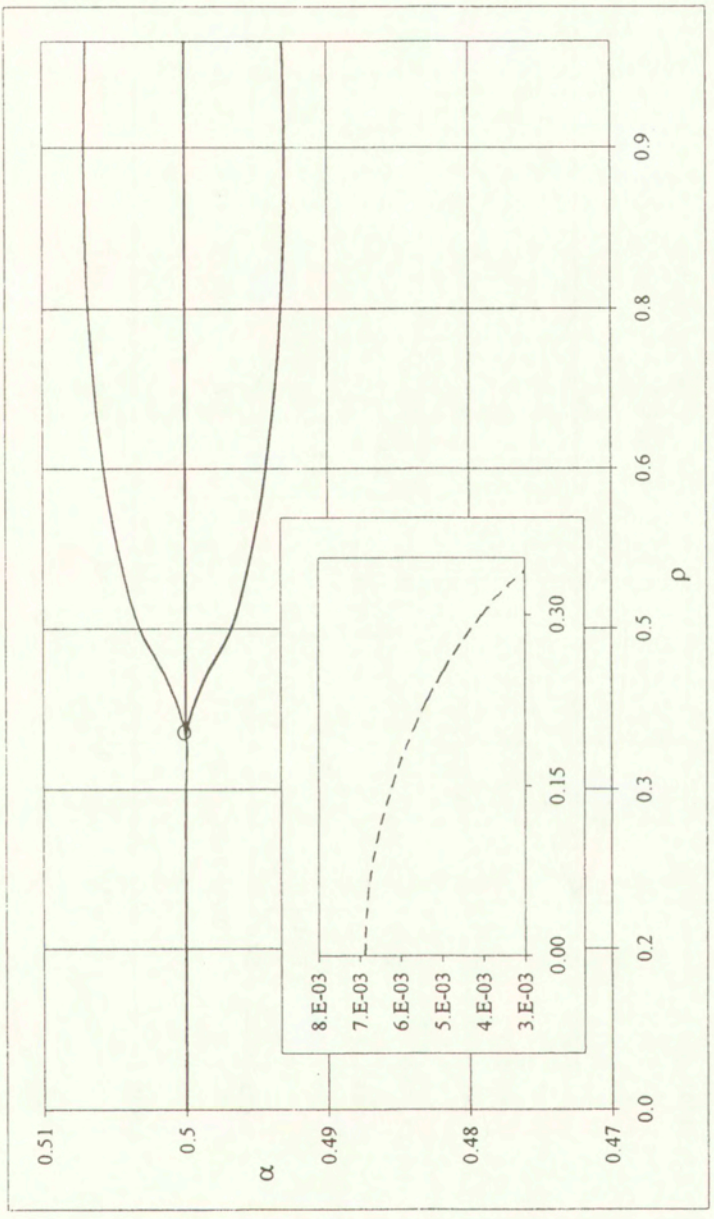

FIG. 3. Dependence of the power of singularity on the piezoelectric constants. The dielectric and elastic constants were chosen according to the combination of PZT-19/ PZT-5 piezoceramics. The solid lines represent the real and the dashed lines the imaginary part, respectively.

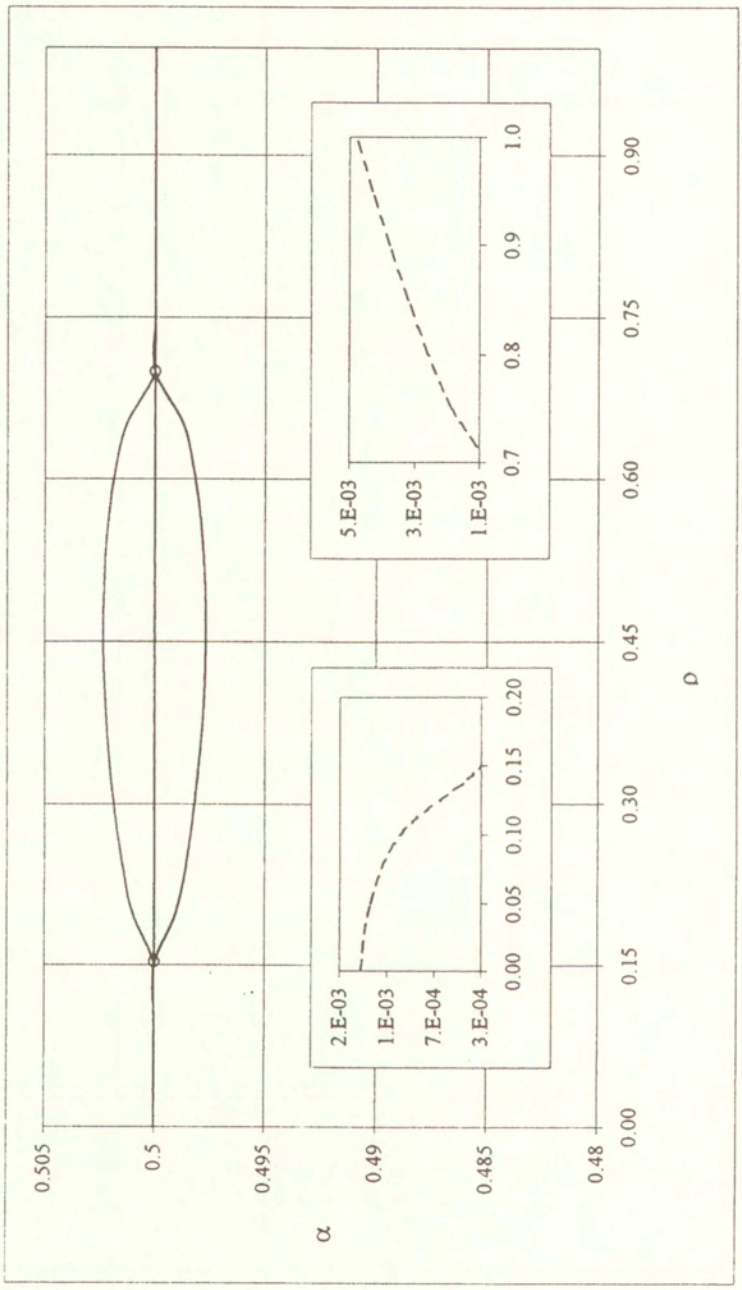

FIG. 4. Dependence of the power of singularity on the piezoelectric constants. The dielectric and elastic constants were chosen according to the combination of PZT-4/PZT-5 piezoceramics. The solid lines represent the real and the dashed lines the imaginary part, respectively.

Next, we consider the numerical solution of the system (4.2), (4.3) for insulated crack faces.

For this purpose the roots of the Eq. (4.7) were found numerically. Some of the most interesting results are shown in Fig. 3 and Fig. 4 where the dependence of the roots of Eq. (4.7) on the parameter ρ is displayed. Parameter ρ is introduced in order to investigate the influence of a varying degree of piezoelectric coupling in both piezomaterials: $\hat{e}_{31}^{\pm} = \rho e_{31}^{\pm}$, $\hat{e}_{33}^{\pm} = \rho e_{33}^{\pm}$, $\hat{e}_{15}^{\pm} = \rho e_{15}^{\pm}$. As ρ is increased from 0 to 1, the piezocoefficients in both the upper and the lower piezomaterials are increased from zero to their real value: $\hat{e}_{ij}^{\pm} = 0.0...e_{ij}^{\pm}$ for $\rho = 0.0...1.0$. The coefficients of $c_{11}^{\pm}$, $c_{13}^{\pm}$, $c_{33}^{\pm}$, $c_{44}^{\pm}$, $e_{31}^{\pm}$, $e_{33}^{\pm}$, $e_{15}^{\pm}$, $\varepsilon_{11}^{\pm}$, $\varepsilon_{33}^{\pm}$ were chosen according to piezomaterials PZT-19/PZT-5 (Fig. 3) and PZT-4/PZT-5 (Fig. 4), respectively. The rigid lines are related to the real parts of the roots while the dashed lines represent the corresponding imaginary parts (0.5 is a real root for any ρ). Circles on these lines indicate the transition from complex to real roots.

These results confirm the conclusion obtained earlier in another way in the papers [18, 22] concerning the possibility of a non-oscillating singularity for an interface crack in a piezomaterial compound. Here, we demonstrate additionally the rather complicated dependence of the power of singularity on the piezoelectric parameters and the appearance of both the real singularity for the ceramics PZT-19/PZT-5 (Fig. 3, $\rho = 1$) and the oscillating singularity for the ceramics PZT-4/PZT-5 (Fig. 4, $\rho = 1$).

The numerical solution of the system (4.2), (4.3) for the case of a real non-square root singularity was found by the numerical method based upon the Gauss-Jacobi quadrature rule suggested by ERDOGAN *et al.* [31] and described with some modifications by GOVORUKHA and LOBODA [32].

In Fig. 5 and Fig. 6, the variations of $\sigma_{zz}(x,0)$ and $D_z(x,0)$ respectively in the neighbourhood next to the right-hand crack tip are shown. The material parameters were taken for the combination PZT-19/PZT-4 and the crack faces were chosen to be perfectly insulated. The lines I are related to the remote tensile load $\sigma_{zz}^{\infty} = 1.0$ (MPa) while the lines II are related to the remote electric flux with $D_z^{\infty} = 1.0$ (C/m^2) (Fig. 5) and $D_z^{\infty} = 1.0(\times 10^{-8}$ C/m^2) (Fig. 6). The complicated behaviour of the fields at the crack tip can be seen, which can be explained by the influence of singularity occurring in this point. But it should be noted that for increasing x, the values of $\sigma_{zz}(x,0)$ and $D_z(x,0)$ rather stable tend to their values at infinity. This fact confirms the high accuracy of the applied analytical approach and the numerical method.

Finally, in Fig. 7 the values of $D_z(x,0)$ for the special case of a homogeneous material PZT-4 are shown. The solid line corresponds to permeable crack faces, the dashed line to – insulated crack faces. For comparison, the values of $D_z(x,0)$ calculated according to the analytical solution (see e.g. PARTON and

KUDRYAVTSEV [24]) are shown as well (such analytical solutions are only found for homogeneous materials). It is obvious that these values completely coincide with the numerical results obtained by the method developed in this paper. Note that in contrast to the mentioned analytical solution, the validity of our solution is not restricted to the neighbourhood of the crack tip.

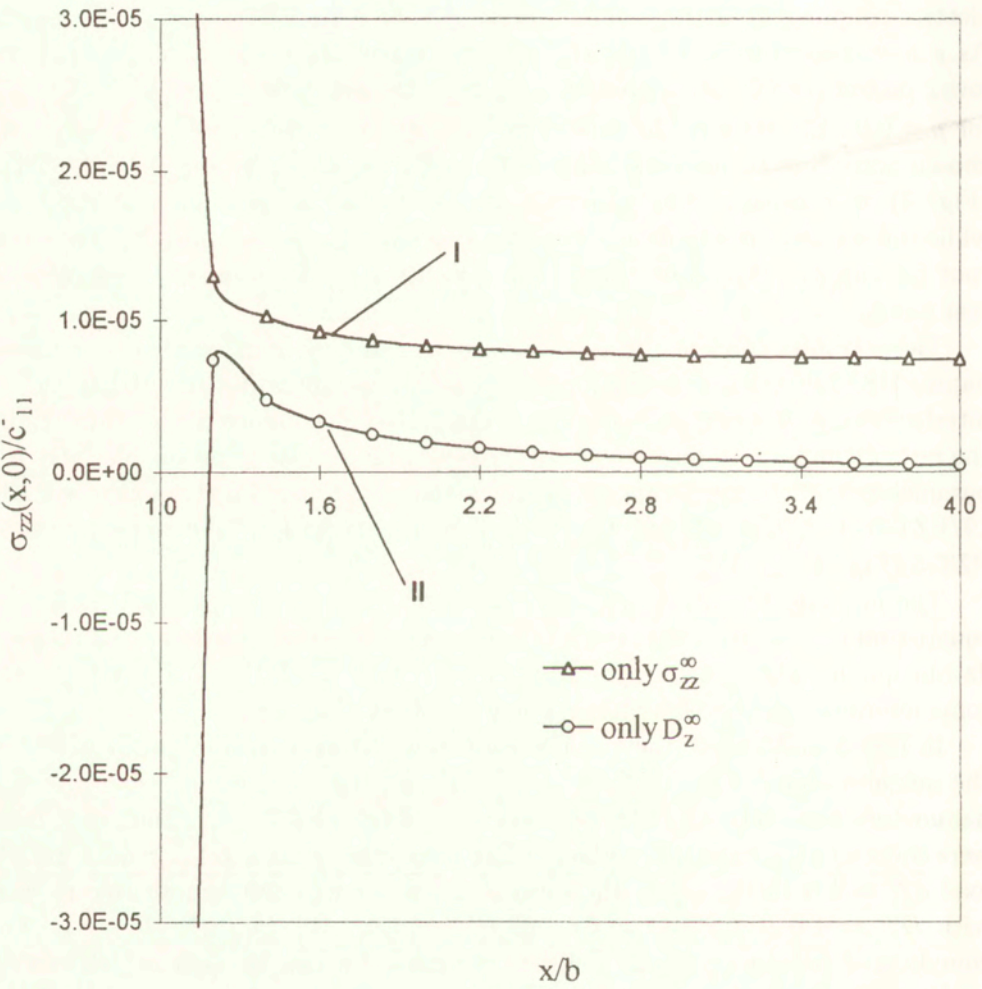

FIG. 5. Variations of the normal stresses for mechanical (line I) and electric (line II) loading.

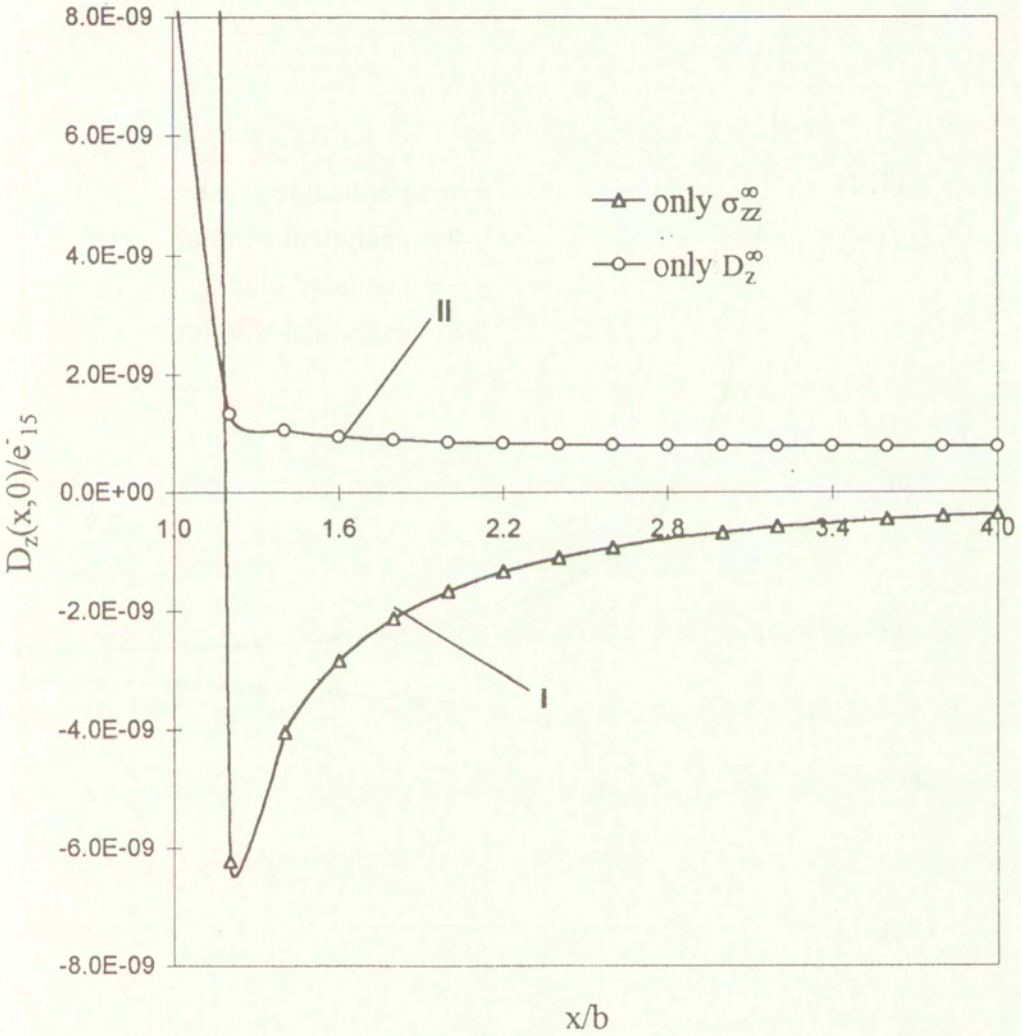

FIG. 6. Variations of the electric displacement for mechanical (line I) and electric (line II) loading.

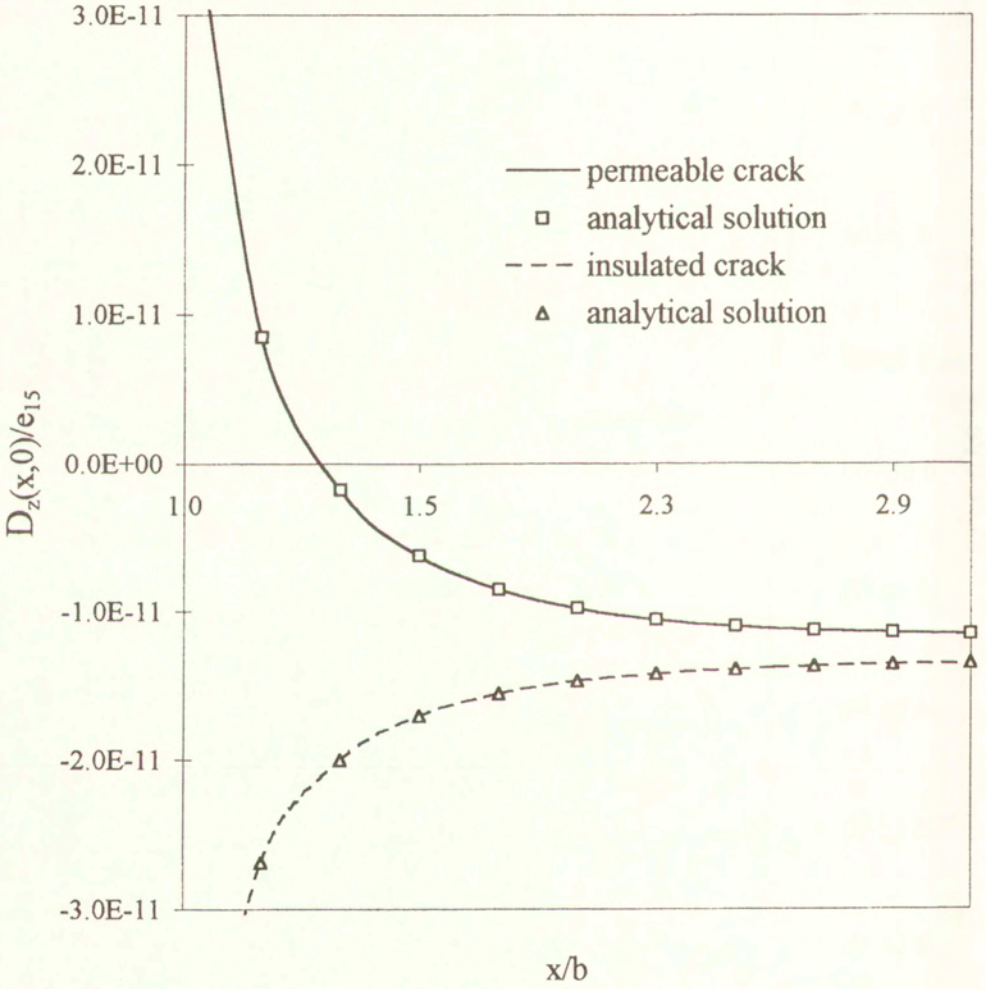

FIG. 7. Electric displacement for a crack in a homogeneous material. The solid line (our results) and marked line (analytical solution) – for electrically permeable crack; dashed line (our results) and marked line (analytical solution) – for insulated crack faces.

6. Conclusion

An interface crack between two piezoelectric semi-infinite planes is considered. The poling axis is assumed to be orthogonal to the crack plane and remote homogeneous tensile stresses and electric displacements act in infinite distance.

The methods of Fourier transforms and singular integral equations are utilised and both permeable and insulated crack faces are considered. For the first case, in addition to the open crack model, the contact zone model with an artificial contact zone is considered. Comninou's model with real contact zone is obtained as a particular case of this model and the quasi-invariance of the energy release rate with respect to the contact zone length is shown. The last property is rather useful from the point of view of the application of numerical methods for the investigation of finite-sized piezoelectric compounds with interface cracks because it permits to find the energy release rate for an artificial contact zone, and use approximately this value as the needed energy release rate.

The dependence of the power of singularity at a crack tip on the materials properties for perfectly insulated crack faces is investigated. The complete disappearance of an oscillating singularity in exchange for a real power singularity for most real ceramics of the considered class was revealed. The behaviour of stresses at the crack tip for both types of crack face conditions is obtained numerically and compared to an exact analytical solution for the special case of homogeneous materials.

Acknowledgment

V. B. GOVORUKHA is grateful to DAAD for financial support during his stay in Karlsruhe.

Appendix

$$m_1^{\pm} = -e_{15}^{\pm}\gamma_1^{\pm} - c_{44}^{\pm}(\alpha_1^{\pm}k_1^{\pm} + \beta_1^{\pm}),$$

$$m_2^{\pm} = -e_{15}^{\pm}\gamma_{21}^{\pm} - c_{44}^{\pm}(\alpha_2^{\pm}\delta^{\pm} - \alpha_3^{\pm}\omega^{\pm} + \beta_2^{\pm}),$$

$$m_3^{\pm} = -e_{15}^{\pm}\gamma_3^{\pm} - c_{44}^{\pm}(\alpha_2^{\pm}\omega^{\pm} + \alpha_3^{\pm}\delta^{\pm} + \beta_3^{\pm}),$$

$$n_1^{\pm} = c_{13}^{\pm}\alpha_1^{\pm} - c_{33}^{\pm}\beta_1^{\pm}k_1^{\pm} - e_{33}^{\pm}\gamma_1^{\pm}k_1^{\pm},$$

$$n_2^{\pm} = c_{13}^{\pm}\alpha_2^{\pm} - c_{33}^{\pm}(\beta_2^{\pm}\delta^{\pm} - \beta_3^{\pm}\omega^{\pm}) - e_{33}^{\pm}(\gamma_2^{\pm}\delta^{\pm} - \gamma_3^{\pm}\omega^{\pm}),$$

$$n_3^{\pm} = c_{13}^{\pm}\alpha_3^{\pm} - c_{33}^{\pm}(\beta_2^{\pm}\omega^{\pm} + \beta_3^{\pm}\delta^{\pm}) - e_{33}^{\pm}(\gamma_2^{\pm}\omega^{\pm} + \gamma_3^{\pm}\delta),$$

$$s_1^{\pm} = e_{31}^{\pm}\alpha_1^{\pm} - e_{33}^{\pm}\beta_1^{\pm}k_1^{\pm} + \varepsilon_{33}^{\pm}\gamma_1^{\pm}k_1^{\pm},$$

$$s_2^{\pm} = e_{31}^{\pm}\alpha_2^{\pm} - e_{33}^{\pm}(\beta_2^{\pm}\delta^{\pm} - \beta_3^{\pm}\omega^{\pm}) + \varepsilon_{33}^{\pm}(\gamma_2^{\pm}\delta^{\pm} - \gamma_3^{\pm}\omega^{\pm}),$$

$$s_3^{\pm} = e_{31}^{\pm}\alpha_3^{\pm} - e_{33}^{\pm}(\beta_2^{\pm}\omega^{\pm} + \beta_3^{\pm}\delta^{\pm}) + \varepsilon_{33}^{\pm}(\gamma_2^{\pm}\omega^{\pm} + \gamma_3^{\pm}\delta^{\pm}),$$

$$\Delta_1 = m_1^-(n_2^-s_3^- - n_3^-s_2^-) + m_2^-(n_3^-s_1^- - n_1^-s_3^-) + m_3^-(n_1^-s_2^- - n_2^-s_1^-)$$

$$p_{11} = (s_2^-n_3^- - s_3^-n_2^-)/\Delta_1, \quad p_{12} = (m_2^-s_3^- - m_3^-s_2^-)/\Delta_1,$$

$$p_{13} = (n_2^-m_3^- - n_3^-m_2^-)/\Delta_1, \quad p_{21} = (n_1^-s_3^- - n_3^-s_1^-)/\Delta_1,$$

$$p_{22} = (s_1^-m_3^- - s_3^-m_1^-)/\Delta_1, \quad p_{23} = (n_3^-m_1^- - n_1^-m_3^-)/\Delta_1,$$

$$p_{31} = (s_2^-n_1^- - s_1^-n_2^-)/\Delta_1, \quad p_{32} = (m_2^-s_1^- - m_1^-s_2^-)/\Delta_1,$$

$$p_{33} = (m_1^-n_2^- - m_2^-n_1^-)/\Delta_1,$$

$$d_{11} = p_{11}m_1^+ - p_{12}n_1^+ - p_{13}s_1^+, \quad d_{12} = p_{11}m_2^+ + p_{12}n_2^+ - p_{13}s_2^+,$$

$$d_{13} = -p_{11}m_3^+ + p_{12}n_3^+ + p_{13}s_3^+, \quad d_{21} = p_{21}m_1^+ - p_{22}n_1^+ - p_{23}s_1^+,$$

$$d_{22} = p_{21}m_2^+ - p_{22}n_2^+ - p_{23}s_2^+, \quad d_{23} = -p_{21}m_3^+ + p_{22}n_3^+ + p_{23}s_3^+,$$

$$d_{31} = p_{31}m_1^+ - p_{32}n_1^+ - p_{33}s_1^+, \quad d_{32} = p_{31}m_2^+ - p_{32}n_2^+ - p_{33}s_2^+,$$

$$d_{33} = -p_{31}m_3^+ + p_{32}n_3^+ + p_{33}s_3^+,$$

$$\rho_1 = \alpha_1^+ - \alpha_1^-d_{11} - \alpha_2^-d_{21} + \alpha_3^-d_{31},$$

$$\rho_2 = \alpha_2^+ - \alpha_1^-d_{12} - \alpha_2^-d_{22} + \alpha_3^-d_{32},$$

$$\rho_3 = \alpha_3^+ + \alpha_1^-d_{13} + \alpha_2^-d_{23} - \alpha_3^-d_{33},$$

$$\xi_1 = -\beta_1^+ - \beta_1^-d_{11} - \beta_2^-d_{21} + \beta_3^-d_{31},$$

$$\xi_2 = -\beta_2^+ - \beta_1^-d_{12} - \beta_2^-d_{22} + \beta_3^-d_{32},$$

$$\xi_3 = -\beta_3^+ + \beta_1^-d_{13} + \beta_2^-d_{23} - \beta_3^-d_{33},$$

$$q_1 = -\gamma_1^+ - \gamma_1^-d_{11} - \gamma_2^-d_{21} + \gamma_3^-d_{31},$$

$$q_2 = -\gamma_2^+ - \gamma_1^- d_{12} - \gamma_2^- d_{22} + \gamma_3^- d_{32},$$

$$q_3 = -\gamma_3^+ + \gamma_1^- d_{13} + \gamma_2^- d_{23} - \gamma_3^- d_{33},$$

$$\Delta_2 = q_1(\xi_2 m_3^+ - \xi_3 m_2^+) + q_2(\xi_3 m_1^+ - \xi_1 m_3^+) + q_3(\xi_1 m_2^+ - \xi_2 m_1^+),$$

$$a_{11} = (\xi_3 q_2 - \xi_2 q_3)/\Delta_2, \quad a_{12} = (q_3 m_2^+ - q_2 m_3^+)/\Delta_2,$$

$$a_{13} = (\xi_2 m_3^+ - \xi_3 m_2^+)/\Delta_2, \quad a_{21} = (\xi_1 q_3 - \xi_3 q_1)/\Delta_2,$$

$$a_{22} = (q_1 m_3^+ - q_3 m_1^+)/\Delta_2, \quad a_{23} = (\xi_3 m_1^+ - \xi_1 m_3^+)/\Delta_2,$$

$$a_{31} = (\xi_1 q_2 - \xi_2 q_1)/\Delta_2, \quad a_{32} = (q_1 m_2^+ - q_2 m_1^+)/\Delta_2,$$

$$a_{33} = (\xi_2 m_1^+ - \xi_1 m_2^+)/\Delta_2,$$

$$\eta_{11} = \rho_1 a_{11} + \rho_2 a_{21} - \rho_3 a_{31}, \quad \eta_{12} = \rho_1 a_{12} + \rho_2 a_{22} - \rho_3 a_{32},$$

$$\eta_{13} = \rho_1 a_{13} + \rho_2 a_{23} - \rho_3 a_{33}, \quad \eta_{21} = n_1^+ a_{11} + n_2^+ a_{21} - n_3^+ a_{31},$$

$$\eta_{22} = n_1^+ a_{12} + n_2^+ a_{22} - n_3^+ a_{32}, \quad \eta_{23} = n_1^+ a_{13} + n_2^+ a_{23} - n_3^+ a_{33},$$

$$\eta_{31} = s_1^+ a_{11} + s_2^+ a_{21} - s_3^+ a_{31}, \quad \eta_{32} = s_1^+ a_{12} + s_2^+ a_{22} - s_3^+ a_{32},$$

$$\eta_{33} = s_1^+ a_{13} + s_2^+ a_{23} - s_3^+ a_{33}.$$

References

1. M. L. WILLIAMS, *The stresses around a fault or cracks in dissimilar media*, Bull. Seismol. Soc. Am. **49**, 199–204, 1959.
2. G. P. CHEREPANOV, *The stress state in a heterogeneous plate with slits*, Isvestia AN SSSR, OTN, Mechan. i Mashin., **1**, 131–137, 1962 [in Russian].
3. A. H. ENGLAND, *A crack between dissimilar media*, J. Appl. Mech., **32**, 400–402, 1965.
4. J. R. RICE and G. C. SIH, *Plane problem of cracks in dissimilar media*, J. Appl. Mech., **32**, 418–423, 1965.
5. F. ERDOGAN, *Stress distribution in non-homogeneous elastic plane with cracks*, J. Appl. Mech., **32**, 403–410, 1965.
6. J. R. RICE, *Elastic fracture mechanics concept for interfacial cracks*, J. Appl. Mech., **55**, 98–103, 1988.
7. T. C. T. TING, *Explicit solution and invariance of the singularities at an interface crack in anisotropic composites*, Int. J. Solids Structures, **22**, 965–983, 1986.
8. M. COMNINOU, *The interface crack*, J. Appl. Mech., **44**, 631–636, 1977.

9. M. COMNINOU, *The interface crack in shear field*, J. Appl. Mech., **45**, 287–290, 1978.

10. J. DUNDURS and M. COMNINOU, *Revision and perspective of interface problem investigation*, Mechanics of Composite Materials, 387–396, 1979 [in Russian].

11. C. ATKINSON, *The interface crack with contact zone (an analytical treatment)*, Int. J. of Fracture, **18**, 161–177, 1982.

12. I. V. SIMONOV, *The interface crack in homogeneous field of stress*, Mechanics of Composite Materials, 969–976, 1985 [in Russian].

13. A. K. GAUTSEN and J. DUNDURS, *The interface crack in a tension field*, J. Appl. Mech., **55**, 580–585, 1988.

14. M. DUNN, *The effects of crack face boundary conditions on the fracture mechanics of piezoelectric solids*, Engng. Frac. Mech., **48**, 25–39, 1994.

15. T.-H. HAO and Z.-Y. SHEN, *A new electric boundary condition of electric fracture mechanics and its applications*, Engng. Frac. Mech., **47**, 793–802, 1994.

16. H. BALKE, G. KEMMER and J. DRESCHER, *Some remarks on fracture mechanics of piezoelectric solids*, [In:] B. MICHEL, T. WINKLER [Eds.] Proceedings of the Micro Materials Conference MicroMat'97, Berlin, pp. 398–401, 1997.

17. O. GRUEBNER and M. KAMLAH, *Effect of the electrical permittivity of cracks on the analysis of a piezoceramic CT specimen*, [In:] Jahresbericht 1998, Institut fuer Keramik im Maschinenbau, Universitaet Karlsruhe, Karlsruhe, 1999 [in German].

18. Z. SUO, C. M. KUO, D. M. BARNETT and J. R. WILLIS, *Fracture mechanics for piezoelectric ceramics*, J. Mech. Phys. Solids, **40**, 739–765, 1992.

19. S. V. PARK and G. T. SUN, *Effect of electric field on fracture of piezoelectric ceramics*, Int. J. of Fracture, **70**, 203–216, 1996.

20. R. MCMEEKING, *Crack tip energy release rate for a piezoelectric compact tension specimen*, Preprint submitted to Engng. Frac. Mech., University of California, Santa Barbara 1998.

21. B. A. KUDRYAVTSEV, V. Z. PARTON, and V. I. RAKITIN, *Fracture mechanics of piezoelectric materials. Rectilinear tunnel crack in the interface with conductor*, Prikladnaya Matematika and Mechanika, **39**, 149–159, 1975 [in Russian].

22. C. M. KUO and D. M. BARNET, *Stress singularities of interface crack in bonded piezoelectric half-spaces*, [In:] Modern Theory of Anisotropic Elasticity and Applications, [Ed.] J. J. WU, T. C. T. TING and D. M. BARNET, pp. 33–50, SIAM, 1991.

23. Q.-H. QIN and Y.-W. MAI, *A closed crack model for interface cracks in thermopiezoelectric materials*, Int. J. Solids Struct., **36**, 2463–2479, 1999.

24. V. Z. PARTON and B. A. KUDRYAVTSEV, *Electromagnetoelasticity*, Gordon and Breach Science Publishers, New York 1988.

25. M. COMNINOU and J. DUNDURS, *Partial closure of cracks at the interface between a layer and a half space*, Engng. Frac. Mech., **18**, 315–323, 1983.

26. N. I. MUSKHELISVILI, *Singular integral equations*, Noordhoff, Groningen 1953.

27. Y. E. PAK, *Linear electro-elastik fracture mechanics of piezoelectric materials*, Int. J. of Fracture, **54**, 79–100, 1992.

28. F. ERDOGAN and G. D. GUPTA, *On the numerical solution of a singular integral equations*, Quart. Appl. Math., **29**, 525–534, 1972.

29. V. V. LOBODA, *The problem of an orthotropic semi-infinite strip with a crack along the fixed end*, Engng. Frac. Mech., **55**, 7–17, 1996.

30. V. V. LOBODA, *The quasi-invariant in the theory of interface cracks*, Engng. Frac. Mech., **44**, 573–580, 1993.

31. F. ERDOGAN, G. D. GUPTA and T. S. COOK, *Numerical solution of singular integral equations*, [In:] Mechanics of Fracture, **1** - -Methods of analysis and solutions of crack problems [Ed.] G. C. SIH, Leyden: Nordhoff), pp. 368–425, 1973.

32. V. B. GOVORUKHA and V. V. LOBODA, *On the boundary integral equations approach to a semi-infinite strip investigation*, Acta Mechanica, **128**, 105–115, 1998.

33. M. L. DUNN and M. TAYA, *Micromechanics predictions of the effective electroelastic moduli of piezoelectric composites*, Int. J. Solids Struct., **30**, 161–175, 1993.

Received June 22, 1999; new version December 30, 1999.

Arch. Mech., **52**, 1, pp. 275–302, Warszawa 2000

Laminar dispersed two-phase flows at low concentration II Disturbance Equations

J. L. ACHARD and A. CARTELLIER

Laboratoire des Écoulements Géophysiques et Industriels
CNRS-UJF-INPG, B.P. 53X, 38041 Grenoble Cedex, France

IN A PRECEDING PAPER (Part I), a generalised system of equations was proposed to represent multi-D flows of particle-fluid mixtures. It was based on a coupling of two sets of equations, one for each phase: the Lundgren hierarchy for the continuous phase and an adaptation of the well-known B.B.G.K.Y. hierarchy for the dispersed phase. It happens that at any order, many of the equations obtained remain intricate: several important terms are difficult either to interpret or to compute effectively such as the averaged extra-deformation tensors, the interfacial force density and finally the pseudo-turbulent tensors in the momentum equations for both phases, arising from inclusion motions alone. That can be remedied by introducing the concept of an "averaged disturbance field" based on differences between two successive conditionally averaged variables. All the equations of both hierarchies are transformed in terms of these fields, which play a central role in our theory, except for the first-order equations of both hierarchies; these correspond to conservation equations of standard two-fluid models.

1. Introduction

A TRUNCATION PROCEDURE will ultimately have to cut the two hierarchies obtained in Part I using the same perturbation method based on diluteness. Besides the small dimensionless number, Θ, related to diluteness, we can expect some additional well-known parameters characterising the relevant dynamic processes, such as the inclusion Reynolds number, to appear. These parameters may be small or large and lead to some simplification. In order to take full advantage of the order of magnitude of these parameters while completing the truncation procedure in a subsequent part, it is advisable to introduce preliminary various disturbance flow fields, in the averaged sense, for both phases. These perturbations may be considered as being set up by one, two or more test inclusions, which locally modify the pre-existing averaged fluid flow which, in the absence of these test inclusions, would be created respectively by no, one or more test inclusions. One of the main goals of this paper is to replace the second-, third- and higher-order equations of both hierarchies by equations controlling these new disturbance fields.

In both new hierarchies, the equations controlling $\overline{\mathbf{v}}^{c1}(\mathbf{x})$ and $\overline{p}^{c1}(\mathbf{x})$ as well as $\overline{\mathbf{u}}^{1}(\mathbf{x})$ and $\overline{\boldsymbol{\omega}}^{1}(\mathbf{x})$ will remain unchanged. At each other order, the equations are combined in such a way that they control a particular disturbance field. The definition of disturbance fields will satisfy two requirements. First, they will vanish far from the test inclusions considered; conditional fields which move away from them lose their influence. Second, they must be symmetrical with respect to the locations of these inclusions.

A typical first-order disturbance field is:

$$\mathbf{u}^{*}(\mathbf{x}|\mathbf{x}^{\circ}) = \overline{\mathbf{u}}^{2}(\mathbf{x}|\mathbf{x}^{\circ}) - \overline{\mathbf{u}}^{1}(\mathbf{x}). \tag{1.1}$$

Similar definitions hold for $\boldsymbol{\omega}^{*}(\mathbf{x}|\mathbf{x}^{\circ})$, $\mathbf{v}^{*}(\mathbf{x}|\mathbf{x}^{\circ})$ and $p^{*}(\mathbf{x}|\mathbf{x}^{\circ})$. Attention must be paid to the definition of the first-order disturbance field relative to the dispersed-phase volume fraction, i.e., $\alpha^{*}(\mathbf{x}|\mathbf{x}^{\circ}) = \alpha^{\mathrm{d}2}(\mathbf{x}|\mathbf{x}^{\circ}) - \alpha^{\mathrm{d}1}(\mathbf{x}) = \alpha^{\mathrm{c}1}(\mathbf{x}) - \alpha^{\mathrm{c}2}(\mathbf{x}|\mathbf{x}^{\circ})$. In accordance with the convention introduced in Sec. 3.2 – Part I, the arguments which are understood in the shortened notations $\boldsymbol{\omega}^{\circ *}$, $\mathbf{v}^{\circ}$, $p^{\circ *}$ and $\alpha^{\circ *}$ are $(\mathbf{x}^{\circ}|\mathbf{x})$. Instead of disturbance densities, we will use conditional disturbance densities:

$$\chi^{*}(\mathbf{x}|\mathbf{x}^{\circ}) = \chi_2(\mathbf{x}|\mathbf{x}^{\circ}) - \phi_1(\mathbf{x}), \tag{1.2}$$

where the first conditional density $\chi_2(\mathbf{x}|\mathbf{x}^{\circ})$ is that introduced in ((4.32) – Part I). In unbounded physical domains, we can observe that $\mathbf{x}^{\circ}$ given $\chi^{*} \to 0$ as $\mathbf{x} \to \infty$, since inclusions which are far apart do not influence each other's position. As before, the arguments which will be understood in the shortened notation $\chi^{\circ *}$ are $(\mathbf{x}^{\circ}|\mathbf{x})$. The notion of correlation field, which is of standard use in Statistical Mechanics, is akin to that of disturbance field. Note that definition (1.2) is consistent with the double correlation fields, i.e. $\phi^{*}(\mathbf{x}, \mathbf{x}^{\circ}) = \phi_2(\mathbf{x}, \mathbf{x}^{\circ}) - \phi_1(\mathbf{x})\phi_1(\mathbf{x}^{\circ})$.

A typical second-order disturbance field to be introduced is:

$$\mathbf{v}^{**}(\mathbf{x}|\mathbf{x}^{\circ}, \mathbf{x}^{\circ\circ}) = \overline{\mathbf{v}}^{c3}(\mathbf{x}|\mathbf{x}^{\circ}, \mathbf{x}^{\circ\circ}) - \overline{\mathbf{v}}^{c2}(\mathbf{x}|\mathbf{x}^{\circ}) - \overline{\mathbf{v}}^{c2}(\mathbf{x}|\mathbf{x}^{\circ\circ}) + \overline{\mathbf{v}}^{c1}(\mathbf{x}). \tag{1.3}$$

The fields $p^{**}(\mathbf{x}|\mathbf{x}^{\circ}, \mathbf{x}^{\circ\circ})$ and $\alpha^{**}(\mathbf{x}|\mathbf{x}^{\circ}, \mathbf{x}^{\circ\circ})$ are defined in the same way. Note that the locations $\mathbf{x}^{\circ}$ and $\mathbf{x}^{\circ\circ}$ of the fixed inclusions are commutable. Incidentally, an extra convention will be adopted: the arguments which are understood in the shortened notations $\mathbf{v}^{\circ\circ **}$, $p^{\circ\circ **}$ and $\alpha^{\circ\circ **}$ are $(\mathbf{x}^{\circ\circ}|\mathbf{x}^{\circ}, \mathbf{x})$.

It should be recalled that for the theory being developed here, the B.B.G.K.Y. and Lundgren hierarchies were set up only up to the second and third orders respectively (cf. Part I) because the equations rapidly become unmanageable. As a consequence, a description of the dispersed phase does not imply second- (or higher-) order disturbance fields. However, it may be useful to introduce the triple number density $\phi^{(3)}(\mathbf{x}, \mathbf{x}^{\circ}, \mathbf{x}^{\circ\circ})$, the definition of which follows (see Sec. 3.2 – Part I):

$$\phi^{(3)}(\mathbf{x},\mathbf{x}^{\circ},\mathbf{x}^{\circ\circ}) = N(N-1)(N-2)\mathrm{E}[\varphi_1\varphi_2\varphi_3] = N(N-1)(N-2)\phi_3(\mathbf{x},\mathbf{x}^{\circ},\mathbf{x}^{\circ\circ}), \tag{1.4}$$

As conditional disturbance densities are being used, it is necessary to adopt:

$$\chi^{**}(\mathbf{x}|\mathbf{x}^{\circ},\mathbf{x}^{\circ\circ}) = \chi_3(\mathbf{x}|\mathbf{x}^{\circ},\mathbf{x}^{\circ\circ}) - \chi_2(\mathbf{x}|\mathbf{x}^{\circ}) - \chi_2(\mathbf{x}|\mathbf{x}^{\circ\circ}) + \phi_1(\mathbf{x}) \tag{1.5}$$

where a second conditional density $\chi_3(\mathbf{x}|\mathbf{x}^{\circ},\mathbf{x}^{\circ\circ}) = \phi_3(\mathbf{x},\mathbf{x}^{\circ},\mathbf{x}^{\circ\circ})/\phi_2(\mathbf{x}^{\circ},\mathbf{x}^{\circ\circ})$ has been introduced. Likewise, $\mathbf{x}^{\circ}$ and $\mathbf{x}^{\circ\circ}$ being given, it may be observed that $\chi^{**} \to 0$ as $\mathbf{x} \to \infty$. As before, the arguments understood in the shortened notation $\chi^{\circ\circ **}$ are $(\mathbf{x}^{\circ\circ}|\mathbf{x}^{\circ},\mathbf{x})$. Such a definition is not equivalent to the triple correlation fields of the S.M.

The continuous phase description does not imply either third- (or higher-) order disturbance fields but for the sake of completeness we will give its definition

$$\begin{aligned}\mathbf{v}^{***}(\mathbf{x}|\mathbf{x}^{\circ},\mathbf{x}^{\circ\circ},\mathbf{x}^{\circ\circ\circ}) = \overline{\mathbf{x}}^{c4}(\mathbf{x}|\mathbf{x}^{\circ},\mathbf{x}^{\circ\circ},\mathbf{x}^{\circ\circ\circ}) - \overline{\mathbf{v}}^{c3}(\mathbf{x}|\mathbf{x}^{\circ},\mathbf{x}^{\circ\circ}) \\ -\overline{\mathbf{v}}^{c3}(\mathbf{x}|\mathbf{x}^{\circ},\mathbf{x}^{\circ\circ\circ}) - \overline{\mathbf{v}}^{c3}(\mathbf{x}|\mathbf{x}^{\circ\circ},\mathbf{x}^{\circ\circ\circ}) \\ +\overline{\mathbf{v}}^{c2}(\mathbf{x}|\mathbf{x}^{\circ}) + \overline{\mathbf{v}}^{c2}(\mathbf{x}|\mathbf{x}^{\circ\circ}) + \overline{\mathbf{v}}^{c2}(\mathbf{x}|\mathbf{x}^{\circ\circ\circ}) - \overline{\mathbf{v}}^{c1}(\mathbf{x}).\end{aligned} \tag{1.6}$$

The first equations of the Lundgren hierarchy (continuous phase) and of the B.B.G.K.Y. hierarchy (dispersed phase) as well as corresponding boundary conditions in terms of these new disturbance fields, i.e. in terms of α^{d1}, $\overline{\mathbf{v}}^{c1}$, $\overline{p}^{c1}$, α^{*}, $\mathbf{v}^{*}$, p^{*}, α^{**}, $\mathbf{v}^{**}$, p^{**}, $\overline{\mathbf{u}}^{1}$, $\mathbf{u}^{*}$, $\overline{\boldsymbol{\omega}}^{1}$, $\boldsymbol{\omega}^{*}$, ϕ_1, χ^{*}, ... will be rewritten in Sec. 4. First, two preliminary studies have to be conducted to split the interaction terms between phases in both hierarchies. Any kind of interfacial field has indeed to be broken down properly at each order, yielding (i) disturbance forces and torques acting on an inclusion in the dispersed-phase equations (Sec. 2) and (ii) in the continous phase equations, disturbance extra-deformation tensors and disturbance interfacial force densities (Sec. 3). An extra advantage of this break-down is actually to cancel several terms which appear at the r.h.s. of the momentum equations presented in Part I. In this way true interaction terms between phases can be displayed in a similar way where such terms are usually introduced in classical two-fluid modelling. Note that all pseudo-turbulent tensors require a similar treatment. Breaking down pseudo-turbulent tensors happens to be much less straightforward; the entire paper (Part III) is devoted to this project.

Next, the resulting "extra-deformation tensors" and "disturbance interfacial density forces" that appear in the continuous phase momentum equations receive more appropriate expressions, which are presented in Sec. 5. For instance, interfacial density forces are expanded in multipoles and in this way they can

be related to the corresponding terms in the dispersed-phase equations. Finally some key results are recalled in Sec. 6.

2. Interaction terms in dispersed-phase equations

Interaction terms between phases which appear in the momentum equations obtained at the end of Part I are considered first. Beforehand, it should be pointed out that standard variables (see 3.8 and 3.9, Part I) appear naturally in these interaction terms. As they are simply considered as temporary variables in this model, they have to be expressed in terms of the moments derived from kinetic equations.

2.1. Standard dispersed-phase averaged variables

At the first-order, using (2.6), (3.3) and (3.8) of Part I, the following relations are obtained:

$$\alpha^{d1}(\mathbf{x}) = \sum_{j=1}^{N} E[H(a - |\mathbf{x} - \mathbf{x}_j|)] = NE[H(a - |\mathbf{x} - \mathbf{x}_1|)] \tag{2.1}$$

$$= NE\left[\int_{|\tilde{\mathbf{x}}-\mathbf{x}|\leq a} \delta(\tilde{\mathbf{x}} - \mathbf{x}_1)d\tilde{\mathbf{x}}\right] = N\int_{|\tilde{\mathbf{x}}-\mathbf{x}|\leq a} \phi_1(\tilde{\mathbf{x}})d\tilde{\mathbf{x}} = \int_{|\tilde{\mathbf{x}}-\mathbf{x}|\leq a} \phi^{(1)}d\tilde{\mathbf{x}}.$$

Without going into detail, the following are obtained at the next orders

$$\alpha^{d2}(\mathbf{x}^\circ|\mathbf{x}) = (N-1)\int_{|\tilde{\mathbf{x}}-\mathbf{x}^\circ|\leq a} \chi_2(\tilde{\mathbf{x}}|\mathbf{x})d\tilde{\mathbf{x}}$$

(2.2)

$$\alpha^{d3}(\mathbf{x}^{\circ\circ}|\mathbf{x}^\circ, \mathbf{x}) = (N-2)\int_{|\tilde{\mathbf{x}}-\mathbf{x}^{\circ\circ}|\leq a} \chi_3(\tilde{\mathbf{x}}|\mathbf{x}^\circ, \mathbf{x})d\tilde{\mathbf{x}}.$$

As for the dispersed-phase volume fractions, the standard velocities for the dispersed phase $\overline{\mathbf{v}}^{d1}$, $\overline{\mathbf{v}}^{d2}$ and $\overline{\mathbf{v}}^{d3}$ can be related to the dispersed-phase moments. Using (2.7), (3.4) and (3.8) of Part I, the first-order velocity is found to be:

$$\alpha^{d1}(\mathbf{x})\overline{\mathbf{v}}^{d1}(\mathbf{x}) = NE[H(a - |\mathbf{x} - \mathbf{x}_1|)[\mathbf{u}_1 + \boldsymbol{\omega}_1 \wedge (\mathbf{x} - \tilde{\mathbf{x}})] \tag{2.3}$$

$$= \int_{|\tilde{\mathbf{x}}-\mathbf{x}|\leq a} \left[\overline{\mathbf{u}}^1(\tilde{\mathbf{x}}) + \overline{\boldsymbol{\omega}}^1(\tilde{\mathbf{x}}) \wedge (\mathbf{x} - \tilde{\mathbf{x}})\right] \phi^{(1)}(\tilde{\mathbf{x}})d\tilde{\mathbf{x}}.$$

Likewise, based on (3.9), the second-order velocity becomes:

$$\alpha^{d2}(\mathbf{x}^\circ|\mathbf{x})\overline{\mathbf{v}}^{d2}(\mathbf{x}^\circ|\mathbf{x}) = (N-1)\int\limits_{|\tilde{\mathbf{x}}-\mathbf{x}^\circ|\leq a} [\overline{\mathbf{u}}^2(\tilde{\mathbf{x}}|\mathbf{x}) + \overline{\boldsymbol{\omega}}^2(\tilde{\mathbf{x}}|\mathbf{x}) \wedge (\mathbf{x}^\circ - \tilde{\mathbf{x}})]\chi_2(\tilde{\mathbf{x}}|\mathbf{x})d\tilde{\mathbf{x}}. \tag{2.4}$$

A similar expression can be derived at the third order. Integrals in the first-order Eqs. (2.1) and (2.3) can be approximated by expanding the typical fields $\mathbf{f}$ ($\phi^{(1)}, \overline{\mathbf{u}}^1, \overline{\boldsymbol{\omega}}^1, ...$) appearing in their integrands. Suppose that the averaged fields for both phases have L as a macroscopic length scale, which is much larger than a, the inclusion radius. This allows the preceding integrals to be expanded in terms of $\beta = a/L$. If $\mathbf{f}$ is expanded in a Taylor series around the centre $\mathbf{x}$ of the test inclusion, it may be written symbolically as (RAYLEIGH [14]) if $\mathbf{k} = \tilde{\mathbf{x}} - \mathbf{x}$:

$$\mathbf{f}(\tilde{\mathbf{x}}) = 1/\mathrm{m}! \sum_{\mathrm{m}=0}^{\infty} \mathbf{k}^{\mathrm{m}} \boxed{\mathrm{m}} \frac{\partial^{\mathrm{m}}}{\partial \mathbf{x}^{\mathrm{m}}} [\mathbf{f}(\mathbf{x})] = \exp\left(\mathbf{k} \cdot \frac{\partial}{\partial \mathbf{x}}\right) \mathbf{f}(\mathbf{x}), \tag{2.5}$$

where the m folded tensorial product of $\partial/\partial\mathbf{x}(\mathbf{k})$ is denoted by $\partial^{\mathrm{m}}/\partial\mathbf{x}^{\mathrm{m}}$ ($\mathbf{k}^{\mathrm{m}}$), while the symbol $\boxed{\mathrm{m}}$ indicates a full p-fold contraction between the tensors $\mathbf{k}^{\mathrm{m}}$ and $\partial^{\mathrm{m}}/\partial\mathbf{x}^{\mathrm{m}}$. Inserting (2.5) into (2.1) and (2.3) gives rise to two types of series:

$$\begin{aligned} &\int\limits_{|\mathbf{k}|<a} \mathbf{f}(\mathbf{x}+\mathbf{k})d\mathbf{k} = \left[\int\limits_{|\mathbf{k}|<a} \exp\left(\mathbf{k}\cdot\frac{\partial}{\partial\mathbf{x}}\right)d\mathbf{k}\right]\mathbf{f}(\mathbf{x}), \\ &\int\limits_{|\mathbf{k}|<a} \mathbf{k}\wedge\mathbf{f}(\mathbf{x}+\mathbf{k})d\mathbf{k} = \int\limits_{|\mathbf{k}|<a} \varepsilon : \mathbf{k}\,\mathbf{f}(\mathbf{x}+\mathbf{k})d\mathbf{k} \\ &\qquad = \varepsilon : \left[\int\limits_{|\mathbf{k}|<a} \mathbf{k}\exp\left(\mathbf{k}\cdot\frac{\partial}{\partial\mathbf{x}}\right)d\mathbf{k}\right]\mathbf{f}(\mathbf{x}), \end{aligned} \tag{2.6}$$

where $\partial/\partial\mathbf{x}$ is to be treated as a constant vector during the integration. Each type involves integrals which can be evaluated via a technique suggested by RAYLEIGH [14]) and GATIGNOL [7]). Then, by properly scaling lengths and velocities without changing their notations, we obtain:

$$\alpha^{d1} = \int\limits_{|\mathbf{k}|<a} \phi^{(1)}(\mathbf{x}+\mathbf{k})d\mathbf{k} = 4/3\pi a^3\left[\phi^{(1)} + \beta^2\nabla^2\phi^{(1)}/10 + O(\beta^4)\right], \tag{2.7}$$

and following LHUILLIER [10], who assumed that if no external couples are applied to inclusions, the order of magnitude of $\overline{\boldsymbol{\omega}}^1$ is the velocity scale over a:

$$\alpha^{d1}\overline{\mathbf{v}}^{d1} = 4/3\pi a^3[\phi^{(1)}\overline{\mathbf{u}}^1 + \beta\mathbf{curl}(\phi^{(1)}\overline{\boldsymbol{\omega}}^1)/5 + \beta^2\nabla^2(\phi^{(1)}\overline{\mathbf{u}}^1)/10 + O(\beta^3)], \tag{2.8}$$

where $\Delta^{\mathrm{m}} = \nabla^{2\mathrm{m}}$ denote m successive applications of the Laplace operator. Equation (2.7) has already been found by BUYEVICH and SHCHELCHKOVA [3] and an equation similar to (2.8) can be found in FELDERHOF [6]. As a matter of fact, the future paper will give a more refined scaling of various velocities: in particular, a specific scale has to be introduced for the relative velocity.

Likewise higher-order dispersed-phase volume fractions and velocities (2, 3, etc.) can be expanded and give rise to the same (two) types of series involving integrals which are computed using the same technique. However, it is impossible to arrange expansion terms with respect to β^2 since the space scale of the dependence of various higher-order conditioned variables equals a and not L. Instead, it may be useful to separate each type of series into two parts: a leading term and a general operator expressions for the remainder of the series:

$$\begin{aligned}
\mathbf{R}_1 &= \left[\frac{a^2}{10}\Delta + \frac{a^4}{280}\Delta^2 + \ldots + \frac{3(2n+2)}{(2n+3)!}a^{2n}\Delta^n + \ldots\right], \\
\mathbf{R}_2 &= \left[\frac{a^2}{14}\Delta + \frac{a^4}{504}\Delta^2 + \ldots + \frac{15(2n+2)(2n+4)}{(2n+5)!}a^{2n}\Delta^n + \ldots\right]\mathbf{curl}.
\end{aligned} \tag{2.9}$$

These remainders terminate after only a very few terms since the coefficients decrease rapidly.

Then the dispersed-phase volume fractions and the velocities assume the compact forms:

$$\begin{aligned}
\phi^{(1)}(\mathbf{x}^\circ)\alpha^{d2}(\mathbf{x}|\mathbf{x}^\circ) &= 4\pi/3a^3[\phi^{(2)}(\mathbf{x},\mathbf{x}^\circ) + \mathbf{R}_1(\phi^{(2)})], \\
\phi^{(2)}(\mathbf{x}^\circ,\mathbf{x}^{\circ\circ})\alpha^{d3}(\mathbf{x}|\mathbf{x}^\circ,\mathbf{x}^{\circ\circ}) &= 4\pi/3a^3[\phi^{(3)}(\mathbf{x},\mathbf{x}^\circ,\mathbf{x}^{\circ\circ}) + \mathbf{R}_1(\phi^{(3)})],
\end{aligned} \tag{2.10}$$

and

$$\begin{aligned}
\phi^{(1)}(\mathbf{x}^\circ)\alpha^{d2}(\mathbf{x}|\mathbf{x}^\circ)\overline{\mathbf{v}}^{d2}(\mathbf{x}|\mathbf{x}^\circ) &= 4\pi/3a^3[\phi^{(2)}\overline{\mathbf{u}}^2(\mathbf{x}|\mathbf{x}^\circ) \\
&\quad + a^2/5\,\mathbf{curl}\,(\phi^{(2)}\overline{\boldsymbol{\omega}}^2)(\mathbf{x}|\mathbf{x}^\circ) + \mathbf{R}_1(\phi^{(2)}\overline{\mathbf{u}}^2) + a^2/5\mathbf{R}_2(\phi^{(2)}\overline{\boldsymbol{\omega}}^2)], \\
\phi^{(2)}(\mathbf{x}^\circ,\mathbf{x}^{\circ\circ})\alpha^{d3}(\mathbf{x}|\mathbf{x}^\circ,\mathbf{x}^{\circ\circ})\overline{\mathbf{v}}^{d3}(\mathbf{x}|\mathbf{x}^\circ,\mathbf{x}^{\circ\circ}) &= 4\pi/3a^3[\phi^{(3)}\overline{\mathbf{u}}^3(\mathbf{x}|\mathbf{x}^\circ,\mathbf{x}^{\circ\circ}) \\
&\quad + a^2/5\,\mathbf{curl}\,(\phi^{(3)}\overline{\boldsymbol{\omega}}^3)(\mathbf{x}|\mathbf{x}^\circ,\mathbf{x}^{\circ\circ}) + \mathbf{R}_1(\phi^{(3)}\overline{\mathbf{u}}^3) + a^2/5\mathbf{R}_2(\phi^{(3)}\overline{\boldsymbol{\omega}}^3)].
\end{aligned} \tag{2.11}$$

Integral relations expressing standard dispersed-phase variables in terms of our variables at any order but the first may easily be restated as equations controlling disturbance fields. For instance:

$$\alpha^*(\mathbf{x}^\circ|\mathbf{x}) = (N-1)\int\limits_{|\tilde{\mathbf{x}}-\mathbf{x}^\circ|\le a} \chi^*(\tilde{\mathbf{x}}|\mathbf{x})d\tilde{\mathbf{x}} + O(1/N),$$

(2.12)

$$\alpha^{**}(\mathbf{x}^{\circ\circ}|\mathbf{x}^\circ,\mathbf{x}) = (N-2)\int\limits_{|\tilde{\mathbf{x}}-\mathbf{x}^\circ|\le a} \chi^{**}(\tilde{\mathbf{x}}|\mathbf{x}^\circ,\mathbf{x})d\tilde{\mathbf{x}} + O(1/N).$$

Moreover, transformation of all these relations involving volume integrals can be simplified into relations similar to (2.6), (2.7), (2.9) and (2.10). For instance:

$$\alpha^*(\mathbf{x}|\mathbf{x}^\circ) = (4\pi a^3/3)(N-1)\{\chi^*(\mathbf{x}|\mathbf{x}^\circ) + \mathbf{R}_1[\chi^*(\mathbf{x}|\mathbf{x}^\circ)]\} + O(1/N). \tag{2.13}$$

2.2. Disturbance-averaged interfacial forces and torques

The overall force $\overline{\mathbf{F}}^1(\mathbf{x})$ experienced at time t by an inclusion known to be centred at $\mathbf{x}$ given in ((4.14) and (5.11) – Part I) may be broken down according to (1.1):

$$\overline{\mathbf{F}}^1 = a^2\int\limits_{S(\mathbf{x})} \mathbf{n}\cdot\overline{X^c\mathbb{T}^c}^1 d\Omega + a^2\int\limits_{S(\mathbf{x})} [-\mathbf{n}p^* + 2\mu^c\mathbf{n}\cdot\mathbb{D}(\mathbf{v}^*)](\mathbf{x}+a\mathbf{n}|\mathbf{x})d\Omega, \tag{2.14}$$

where the last term in the r.h.s is the force exerted by the disturbance flows on the test inclusion. This involves the viscous drag force and other forces such as the added mass force; it will be denoted by $\mathbf{F}^*(\mathbf{x})$ (for short $\mathbf{F}^*$, or $\mathbf{F}^{\circ*}$ if the inclusion is centred at $\mathbf{x}^\circ$). Likewise, using (1.3), Eqs. (4.20) – (5.12) from Part I, giving $\overline{\mathbf{F}}^2(\mathbf{x}^\circ|\mathbf{x}) = \overline{\mathbf{F}^\circ}^2$ yields:

$$\overline{\mathbf{F}^\circ}^2 = \mathbf{F}^{\circ*} + a^2\int\limits_{S(\mathbf{x}^\circ)} \mathbf{n}\cdot\overline{X^c\mathbb{T}^c}^2(\mathbf{x}^\circ + a\mathbf{n}|\mathbf{x})d\Omega \tag{2.15}$$

$$+a^2\int\limits_{S(\mathbf{x}^\circ)} [-\mathbf{n}p^{**} + 2\mu^c\mathbf{n}\cdot\mathbb{D}(\mathbf{v}^{**})](\mathbf{x}^\circ + a\mathbf{n}|\mathbf{x},\mathbf{x}^\circ)d\Omega,$$

where the last term in the r.h.s is the force exerted by the disturbance flow on the test inclusion at $\mathbf{x}^\circ$ conditionally averaged upon the presence of another inclusion at $\mathbf{x}$. It will be denoted by $\mathbf{F}^{**}(\mathbf{x}^\circ|\mathbf{x})$ (for short $\mathbf{F}^{\circ**}$).

Overall torques ((4.15) – Part I) and ((4.21) – Part I) may similarly be broken down:

$$\overline{\mathbf{K}}^1 = a^3\varepsilon :\int\limits_{S(\mathbf{x})} \mathbf{nn}\cdot\overline{X^c\mathbb{T}^c}^1 d\Omega + a^3\varepsilon :\int\limits_{S(\mathbf{x})} [-\mathbf{nn}\,p^* \tag{2.16}$$

$$+2\mu^c\mathbf{nn}\cdot\mathbb{D}(\mathbf{v}^*)](\mathbf{x}+a\mathbf{n}|\mathbf{x})d\Omega$$

and

$$\overline{\mathbf{K}^{\circ}}^{2} = \mathbf{K}^{\circ *} + a^3\varepsilon \int_{S(\mathbf{x}^{\circ})} \mathbf{nn}\cdot\overline{X^c\mathbb{T}^c}^{2}d\Omega + a^3\varepsilon : \int_{S(\mathbf{x}^{\circ})} [-\mathbf{nn}\,p^{**} + 2\mu^c\mathbf{nn}\cdot\mathbb{D}(\mathbf{v}^{**})](\mathbf{x}^{\circ} + a\mathbf{n}|\mathbf{x},\mathbf{x}^{\circ})d\Omega, \tag{2.17}$$

where the last terms at the r.h.s are the torques exerted by the disturbance flows on the test inclusions. They will be denoted by $\mathbf{K}^{*}(\mathbf{x})$ and $\mathbf{K}^{**}(\mathbf{x}^{\circ}|\mathbf{x})$ (for short $\mathbf{K}^{*}$ and $\mathbf{K}^{\circ **}$ respectively).

The first-order averaged fields $\overline{X^c\mathbb{T}^c}^{1}(\mathbf{x}^{\circ})$ in (2.14) and (2.16) are defined inside the entire sphere $S(\mathbf{x})$, and the Gauss theorem can be used to transform the corresponding surface integrals into volume integrals:

$$a^2 \int_{S(\mathbf{x})} \mathbf{n}\cdot\overline{X^c\mathbb{T}^c}^{1}d\Omega = \int_{|\mathbf{k}|<a} \frac{\partial}{\partial\mathbf{k}}\cdot\left[-\overline{p}^{c1}\mathbb{I} + 2\mu^c\mathbb{D}(\overline{\mathbf{v}}^{c1})\right](\mathbf{x}+\mathbf{k})d\mathbf{k}, \tag{2.18}$$

$$a^3\varepsilon : \int_{S(\mathbf{x})} \mathbf{nn}\cdot\overline{X^c\mathbb{T}^c}^{1}d\Omega = \varepsilon : \int_{|\mathbf{k}|<a} \mathbf{k}\left[-\frac{\partial\overline{p}^{c1}}{\partial\mathbf{k}} + \mu^c\Delta(\overline{\mathbf{v}}^{c1}) + \mu^c\frac{\partial}{\partial\mathbf{k}}\left(\frac{\partial}{\partial\mathbf{k}}\cdot\overline{\mathbf{v}}^{c1}\right)\right]d\mathbf{k}. \tag{2.19}$$

The same transformation between the surface and the volume integrals holds for integrals involving the second-order averaged fields $\overline{X^c\mathbb{T}^c}^{2}(\mathbf{x}^{\circ} + a\mathbf{n}|\mathbf{x})$ in (2.15) and (2.17).

Introducing the expansion (2.6) of $\overline{X^c\mathbb{T}^c}^{1}$ about $\mathbf{x}$ and using the remainders of (2.9) yields:

$$a^2 \int_{S(\mathbf{x})} \mathbf{n}\cdot\overline{X^c\mathbb{T}^c}^{1}d\Omega = \frac{4\pi a^3}{3}\left\{-\frac{\partial\overline{p}^{c1}}{\partial\mathbf{x}} + \mu^c\Delta\overline{\mathbf{v}}^{c1} + \mu^c\frac{\partial}{\partial\mathbf{x}}\left(\frac{\partial}{\partial\mathbf{x}}\cdot\overline{\mathbf{v}}^{c1}\right) + \mathbf{R}_1\left[-\frac{\partial\overline{p}^{c1}}{\partial\mathbf{x}} + \mu^c\Delta\overline{\mathbf{v}}^{c1} + \mu^c\frac{\partial}{\partial\mathbf{x}}\left(\frac{\partial}{\partial\mathbf{x}}\cdot\overline{\mathbf{v}}^{c1}\right)\right]\right\} \tag{2.20}$$

and

$$a^3\varepsilon : \int_{S(\mathbf{x})} \mathbf{nn}\cdot\overline{X^c\mathbb{T}^c}^{1}d\Omega = 4\pi a^5\mu^c/15\{\mathbf{curl}\,(\Delta\overline{\mathbf{v}}^{c1}) + \mathbf{R}_2\,[\mathbf{curl}\,(\Delta\overline{\mathbf{v}}^{c1})]\}$$
$$= -4\pi a^5\mu^c/15\{\mathbf{curl}^3(\overline{\mathbf{v}}^{c1}) + \mathbf{R}_2\,[\mathbf{curl}^3(\overline{\mathbf{v}}^{c1})]\}. \tag{2.21}$$

In (2.20) and (2.21), it is possible to arrange terms with respect to β as in (2.7) and (2.8) for it is clear that $\mathbf{R}_1$ and $\mathbf{R}_2$ are $O(\beta^2)$. On the other hand, $\overline{X^c \mathbb{T}^c}^{c2}$ can be expanded about $\mathbf{x}$ and similar results are obtained where $\overline{p}^{c2}$ and $\overline{\mathbf{v}}^{c2}$ replaces $\overline{p}^{c1}$ and $\overline{\mathbf{v}}^{c1}$. However, $\mathbf{R}_1$ and $\mathbf{R}_2$ are not $O(\beta^2)$ when $\overline{p}^{c2}$ and $\overline{\mathbf{v}}^{c2}$ are involved, since they are not slowly varying.

3. Interaction terms in continuous phase equations

Both extra-deformation tensors and interfacial force densities have to be transformed according to the same procedure before being broken down.

3.1. Disturbance-averaged extra-deformation tensors

The averaged extra-deformation tensor for the field with no fixed inclusion is obtained by introducing the surface Dirac g.f. (Sec. 2 – Part I) and the generalised p.d.f. $\mathrm{f}_N(Z_N;t)$ (Sec. 3 – Part I) which allows averaging over Γ at any time:

$$(3.1)\qquad E[\mathbb{F}^c\delta_\Sigma](\mathbf{x}) = \sum_{j=1}^{N} E\{[\mathbf{n}_j^c\mathbf{v}_j^c]^s\delta(P_j)\} = \sum_{j=1}^{N}\int [\mathbf{n}_j^c\mathbf{v}_j^c]^s\delta(P_j)\mathrm{f}_N(Z_N)dZ_N$$

$$= N\int_{\mathcal{V}_x^d}\delta(a-|\mathbf{x}-\mathbf{x}_1|)\left[\int\{[\mathbf{n}_1^cX_1^c\mathbf{v}_1^c]^s\}(Z_N;\mathbf{x})\mathrm{f}_N(Z_N)d\xi_1d\mathbf{z}_2...d\mathbf{z}_N\right]d\mathbf{x}_1$$

$$= N\int_{\mathcal{V}_x^d}\delta(a-r_1)\left[\left[\int\{[\mathbf{n}_1^cX_1^c\mathbf{v}_1^c]^s\}(Z_N;\mathbf{x})\mathrm{f}_N(\mathbf{x}_1,\xi_1,Z_{N-1})d\xi_1d\mathbf{z}_2...d\mathbf{z}_N\right]\right.$$

$$\left.\times r_1^2d\Omega\right]dr_1 = a^2N\int_{S(\mathbf{x})}\left[\int\{[\mathbf{n}_1^cX_1^c\mathbf{v}_1^c]^s\}\,(Z_N;\mathbf{x})\mathrm{f}_N(\mathbf{x}_1,\xi_1,Z_{N-1})\right.$$

$$\left.d\xi_1d\mathbf{z}_2...d\mathbf{z}_N\right]d\Omega.$$

The second line results from the symmetry of f_N with respect to $\mathbf{z}_1$ and $\mathbf{z}_j$ and the third line is a simple change of integration variables: $d\mathbf{x}_1 = r_1^2d\Omega dr_1$ where $r_1(\mathbf{x}) = |\mathbf{x}-\mathbf{x}_1|$; finally, the volume integral can be converted into a surface integral (fourth line) taken over the surface of the sphere $S(\mathbf{x})$ i.e. such that $r_1(\mathbf{x}) = a$ or $\mathbf{x}_1 = \mathbf{x} + a\mathbf{n}_1^c$. By introducing the conditional velocity $\overline{\mathbf{v}}^{c2}$ ((3.7) – Part I), one obtains:

$$E[\mathbb{F}^c\delta_\Sigma](\mathbf{x}) = a^2 N \int_{S(\mathbf{x})} \Bigg[\int \{[\mathbf{n}_1^c \delta(\mathbf{x}_1 - \tilde{\mathbf{x}}) X_1^c \mathbf{v}_1^c]^s\} \tag{3.2}$$

$$(\tilde{\mathbf{x}}, \xi_1, Z_{N-1}; \mathbf{x}) \mathrm{f}_N(\tilde{\mathbf{x}}, \xi_1, Z_{N-1}) d\tilde{\mathbf{x}} d\xi_1 d\mathbf{z}_2 ... d\mathbf{z}_N \Bigg] d\Omega$$

$$= a^2 N \int_{S(\mathbf{x})} E[\{X^c \delta(\mathbf{x}_1 - \tilde{\mathbf{x}})[\mathbf{n}_1^c \mathbf{v}_1^c]^s\}] d\Omega = a^2 \int_{S(\mathbf{x})} [\mathbf{n}^c \overline{\mathbf{v}}^{c2}]^s (\mathbf{x}|\mathbf{x}_1) \phi^{(1)}(\mathbf{x}_1) d\Omega.$$

Now, $E[\mathbb{F}^c\delta_\Sigma]$ can be broken down by splitting $\overline{\mathbf{v}}^{c2}$ according to (1.1):

$$E[\mathbb{F}^c\delta_\Sigma](\mathbf{x}) = a^2 \int_{S(\mathbf{x})} [\mathbf{n}^c(\mathbf{x}|\mathbf{x}_1) \overline{\mathbf{v}}^{c1}(\mathbf{x})]^s \phi^{(1)}(\mathbf{x}_1) d\Omega \tag{3.3}$$

$$+ a_2 \int_{S(\mathbf{x})} [\mathbf{n}^c \mathbf{v}^*]^s (\mathbf{x}|\mathbf{x}_1) \phi^{(1)}(\mathbf{x}_1) d\Omega,$$

where the second r.h.s. term is admittedly the disturbance extra-deformation tensor $E[\mathbb{F}^*\delta_\Sigma]$. In relation to fields with no fixed inclusions, this tensor appears as an average, weighted by $\phi^{(1)}$, over all inclusion centre positions, $\mathbf{x}_1 = \mathbf{x} + a\mathbf{n}^c$ these positions being such that the inclusion surface touches $\mathbf{x}$. The first term at the r.h.s. is transformed using the Gauss theorem and the relation (2.1) giving the dispersed-phase volume fraction:

$$a^2 \int_{S(\mathbf{x})} [\mathbf{n}^c \overline{\mathbf{v}}^{c1}]^s \phi^{(1)}(\mathbf{x} + a\mathbf{n}^c) d\Omega = a^2 \left[\overline{\mathbf{v}}^{c1} \int_{S(\mathbf{x})} \mathbf{n}^c \phi^{(1)}(\mathbf{x} + a\mathbf{n}^c) d\Omega \right]^s \tag{3.4}$$

$$= \left[\overline{\mathbf{v}}^{c1} \int_{|\tilde{\mathbf{x}} - \mathbf{x}| \le a} \frac{\partial}{\partial \tilde{\mathbf{x}}} \phi^{(1)}(\tilde{\mathbf{x}}) d\tilde{\mathbf{x}} \right]^s = \left[\overline{\mathbf{v}}^{c1} \int_{|\mathbf{k}| \le a} \frac{\partial}{\partial \mathbf{x}} \phi^{(1)}(\mathbf{x} + \mathbf{k}) d\mathbf{k} \right]^s$$

$$= \left[\overline{\mathbf{v}}^{c1} \frac{\partial}{\partial \mathbf{x}} \alpha^{d1} \right]^s.$$

One advantage of this break-down is that one of the $O(\alpha^{d1})$ terms appearing at the r.h.s. of the momentum Eq. (5.18) derived at the end of Part I is cancelled.

Break-downs similar to (3.4) can be introduced in the next-order momentum Eqs. (5.19) and (5.20) of Part I, i.e.

$$E[\mathbb{F}^c \varphi_1 \delta_\Sigma^1](\mathbf{x}^\circ|\mathbf{x}) = \phi_1(\mathbf{x}) \left\{ \left[\overline{\mathbf{v}}^{c2} \frac{\partial}{\partial \mathbf{x}^\circ} \alpha^{d2} \right]^s (\mathbf{x}^\circ|\mathbf{x}) + E[\mathbb{F}^{**} \delta_\Sigma^1](\mathbf{x}^\circ|\mathbf{x}) \right\} \tag{3.5}$$

and:

$$E[\mathbb{F}^c\varphi_1\varphi_2\delta_\Sigma^{1,2}](\mathbf{x}^{\circ\circ}|\mathbf{x}^\circ,\mathbf{x}) = \phi_2(\mathbf{x}^\circ,\mathbf{x})\left\{\left[\overline{\mathbf{v}}^{c3}\frac{\partial}{\partial\mathbf{x}^{\circ\circ}}\alpha^{d3}\right]^s(\mathbf{x}^{\circ\circ}|\mathbf{x}^\circ,\mathbf{x}) + E[\mathbb{F}^{***}\delta_\Sigma^{1,2}](\mathbf{x}^{\circ\circ}|\mathbf{x}^\circ,\mathbf{x})\right\}, \tag{3.6}$$

where $E[\mathbb{F}^{**}\delta_\Sigma^1](\mathbf{x}^\circ|\mathbf{x})$ and $E[\mathbb{F}^{***}\delta_\Sigma^{1,2}](\mathbf{x}^{\circ\circ}|\mathbf{x}^\circ,\mathbf{x})$ are the higher-order disturbance-averaged extra-deformation tensors. For sake of brevity, only the first one will be given:

$$E[\mathbb{F}^{**}\delta_\Sigma^1](\mathbf{x}^\circ|\mathbf{x}) = a^2(N-1)\int\limits_{S(\mathbf{x}^\circ)}\{[\mathbf{n}^c\mathbf{v}^{**}]^s(\mathbf{x}^\circ|\mathbf{x}^\circ+a\mathbf{n}^c,\mathbf{x}) + [\mathbf{n}^c\mathbf{v}^*]^s(\mathbf{x}^\circ|\mathbf{x}^\circ+a\mathbf{n}^c)\}\{\phi_1(\mathbf{x}^\circ+a\mathbf{n}^c)+\chi^*(\mathbf{x}^\circ+a\mathbf{n}^c|\mathbf{x})\}d\Omega. \tag{3.7}$$

All these break-downs result in cancellations in the second and third-order momentum equations at the r.h.s.

3.2. Disturbance interfacial force density

The same arguments as those leading to (3.1) and (3.2) provide a new form of the averaged interfacial force density for the field with no fixed inclusions:

$$E[\mathbf{n}^c\cdot\mathbb{T}^c\delta_\Sigma](\mathbf{x}) = \sum_{j=1}^N E[\mathbf{n}_j^c\cdot\mathbb{T}_j^c\delta(P_j)] = \sum_{j=1}^N\int\mathbf{n}_j^c\cdot\mathbb{T}_j^c\delta(P_j)\mathrm{f}_N(Z_N)dZ_N$$

$$= a^2N\int\limits_{S(\mathbf{x})}\left[\int\{\mathbf{n}_1^c\cdot X_1^c\mathbb{T}_1^c\}(Z_N;\mathbf{x})\mathrm{f}_N(\mathbf{x}_1,\xi_1,Z_{N-1})d\xi_1 d\mathbf{z}_2...d\mathbf{z}_N\right]d\Omega$$

$$= a^2\int\limits_{S(\mathbf{x})}\mathbf{n}^c\cdot\overline{X_1^c\mathbb{T}^c}^2(\mathbf{x}|\mathbf{x}_1)\phi^{(1)}(\mathbf{x}_1)d\Omega, \tag{3.8}$$

where the simplified version of the local averaged stress upon an inclusion located at $\mathbf{x}_1$, $\overline{X_1^c\mathbb{T}^c}^2(\mathbf{x}|\mathbf{x}_1)$, ((5.11) – Part I) has been retained. Breaking down the conditional velocity and pressure $\overline{\mathbf{v}}^{c2}$ and $\overline{p}^{c2}$ appearing in it according to (1.1) gives:

$$E[\mathbf{n}^c\cdot\mathbb{T}^c\delta_\Sigma](\mathbf{x}) = a^2\int\limits_{S(\mathbf{x})}\mathbf{n}^c(\mathbf{x}|\mathbf{x}_1)\cdot[-\overline{p}^{c1}\mathbb{I}+2\mu^c\mathbb{D}(\overline{\mathbf{v}}^{c1})](\mathbf{x})\phi^{(1)}(\mathbf{x}_1)d\Omega + E[\mathbf{n}^c\cdot\mathbb{T}^*\delta_\Sigma], \tag{3.9}$$

where the disturbance interfacial force density $E[\mathbf{n}^c \cdot \mathbb{T}^* \delta_\Sigma]$ is defined by:

$$E[\mathbf{n}^c \cdot \mathbb{T}^* \delta_\Sigma] = a^2 \int_{S(\mathbf{x})} \mathbf{n}^c \cdot [-p^* \mathbb{I} + 2\mu^c \mathbb{D}(\mathbf{v}^*)](\mathbf{x}|\mathbf{x}_1) \phi^{(1)}(\mathbf{x}_1) d\Omega. \tag{3.10}$$

This term appears as an average of the local averaged stress weighted by $\phi^{(1)}$, over all inclusion centre positions, $\mathbf{x}_1 = \mathbf{x} + a\mathbf{n}^c$, these positions being such that the inclusion surfaces touch $\mathbf{x}$. Such a basic result was obtained previously by LUNDGREN [11]. The first term at the r.h.s. is transformed using the Gauss theorem and relation (2.1), which provides the dispersed-phase volume fraction:

$$\begin{aligned} a^2 \int_{S(\mathbf{x})} [-\overline{p^c}^1 \mathbb{I} + 2\mu^c \mathbb{D}(\overline{\mathbf{v}^c}^1)] \cdot \mathbf{n}^c \phi^{(1)}(\mathbf{x}_1) d\Omega] &= a^2 [-\overline{p^c}^1 \mathbb{I} + 2\mu^c \mathbb{D}(\overline{\mathbf{v}^c}^1)] \\ &\cdot \int_{S(\mathbf{x})} \mathbf{n}^c \phi^{(1)}(\mathbf{x} + a\mathbf{n}^c) d\Omega] = [-\overline{p^c}^1 \mathbb{I} + 2\mu^c \mathbb{D}(\overline{\mathbf{v}^c}^1)] \\ &\cdot \int_{|\tilde{\mathbf{x}} - \mathbf{x}| \leq a} \mathbf{n}^c \frac{\partial}{\partial \tilde{\mathbf{x}}} \phi^{(1)}(\tilde{\mathbf{x}}) d\tilde{\mathbf{x}} = [-\overline{p^c}^1 \mathbb{I} + 2\mu^c \mathbb{D}(\overline{\mathbf{v}^c}^1)] \cdot \frac{\partial}{\partial \mathbf{x}} \alpha^{d1}(\mathbf{x}). \end{aligned} \tag{3.11}$$

Our break-down exactly parallels the procedure followed in deterministic studies concerning hydrodynamic forces acting on a particle in arbitrary fields of flow. It is clearly $E[\mathbf{n}^c \cdot \mathbb{T}^* \delta_\Sigma]$ and not $E[\mathbf{n}^c \cdot \mathbb{T} \delta_\Sigma]$ which contains drag and lift forces as well as virtual mass effects. This break-down is also reminiscent of that introduced in classical two-fluid modelling (ISHII, [8]), where only the first-order equations are available; specific mean values, e.g. interfacial velocity and pressure, are therefore introduced to break down the interaction terms. In our approach, a different break-down, which can be made at any order, is based on averages that are conditional upon the presence of one or more inclusions.

This break-down of the overall interfacial force density has one advantage, which is exactly the same as that mentioned previously in breaking down the overall extra-deformation tensor: the remaining $O(\alpha^{d1})$ term appearing at the r.h.s. of the momentum Eq. ((5.18) – Part I) is cancelled. A second point is worth mentioning, namely that the disturbance interfacial force density $E[\mathbf{n}^c \cdot \mathbb{T}^* \delta_\Sigma]$ obtained here is not equal to the standard interfacial force density $\mathbb{M}_c^d$ (d in Ishii's book refers to "drag force" and c to "continuous phase"), for two reasons. As aforesaid, the reference fields in standard two-fluid modelling are interfacial averages and not averaged fields with one fixed inclusion; moreover in standard two-fluid modelling, there is an asymmetrical treatment of the interfacial pressure term and of the interfacial viscous stress term, which cannot be explained

very well. Note that in our approach they are logically placed on an equal footing. These odd characteristics of $\mathbb{M}_c^d$ which make it different from $E[\mathbf{n}^c \cdot \mathbb{T}^* \delta_\Sigma]$ have never prevented modellers from claiming that it must also contain drag and lift forces as well as virtual mass effects. Arbitrariness is usually so great in closing various unknown terms in a given application, that such statements can hardly be invalidated. Finally, the classical process somewhat artificially increases closure problems since, unlike our approach, it requires the difference between averaged interfacial pressure and bulk-averaged pressure to be expressed (STUHMILLER, [15]).

At the next order, the same process leads to:

$$E[\mathbf{n}^c \cdot \mathbb{T}^c \varphi_1 \delta_\Sigma^1](\mathbf{x}^\circ|\mathbf{x}) = \phi_1(\mathbf{x})\{[-\overline{p}^{c2}\mathbb{I} + 2\mu^c \mathbb{D}^\circ(\overline{\mathbf{v}}^{c2})] \cdot \frac{\partial}{\partial \mathbf{x}^\circ} \alpha^{d2}(\mathbf{x}^\circ|\mathbf{x}) + E[\mathbf{n}^c \cdot \mathbb{T}^{**} \delta_\Sigma^1](\mathbf{x}^\circ|\mathbf{x})\}, \tag{3.12}$$

where the disturbance interfacial force density relative to the fields with one fixed inclusion located at $\mathbf{x}$, denoted $E[\mathbf{n}^c \cdot \mathbb{T}^{**} \delta_\Sigma^1](\mathbf{x}^\circ|\mathbf{x})$, is defined by:

$$E[\mathbf{n}^c \cdot \mathbb{T}^{**} \delta_\Sigma^1](\mathbf{x}^\circ|\mathbf{x}) = a^2(N-1) \int_{S(\mathbf{x}^\circ)} \mathbf{n}^c \cdot \{[-p^{\circ **}\mathbb{I} + 2\mu^c \mathbb{D}^\circ (\mathbf{v}^{\circ **})(\mathbf{x}^\circ|\mathbf{x}^\circ + a\mathbf{n}^c, \mathbf{x})] + [-p^{\circ *}\mathbb{I} + 2\mu^c \mathbb{D}^\circ(\mathbf{v}^{\circ *})(\mathbf{x}^\circ|\mathbf{x}^\circ + a\mathbf{n}^c)]\} \{\phi_1(\mathbf{x}^\circ + a\mathbf{n}^c) + \chi^*(\mathbf{x}^\circ + a\mathbf{n}^c|\mathbf{x})\} d\Omega. \tag{3.13}$$

At the third order, a similar result is obtained:

$$E[\mathbf{n}^c \cdot \mathbb{T}^c \varphi_1 \varphi_2 \delta_\Sigma^{1,2}](\mathbf{x}^{\circ\circ}|\mathbf{x}, \mathbf{x}^\circ) = \phi_2(\mathbf{x}^\circ, \mathbf{x})\{[-\overline{p}^{c3} + 2\mu^c \mathbb{D}^{\circ\circ}(\overline{\mathbf{v}}^{c3})] \cdot \frac{\partial}{\partial \mathbf{x}^{\circ\circ}} \alpha^{d3}(\mathbf{x}^{\circ\circ}|\mathbf{x}^\circ, \mathbf{x}) + E[\mathbf{n}^c \cdot \mathbb{T}^{***} \delta_\Sigma^{1,2}](\mathbf{x}^{\circ\circ}|\mathbf{x}^\circ, \mathbf{x})\}, \tag{3.14}$$

where $E[\mathbf{n}^c \cdot \mathbb{T}^{***} \delta_\Sigma^{1,2}](\mathbf{x}^{\circ\circ}|\mathbf{x}^\circ, \mathbf{x})$ due to the third-order disturbance flows can be similarly defined. Analogous cancellations occur at the r.h.s. of the corresponding momentum equations.

4. New system of equations

All the equations of the Lundgren and B.B.G.K.Y. hierarchies as well as the boundary conditions between these two sets of equations at any order but the first one can now be transformed into equations for averaged disturbance flows.

Equations at the first order are still expressed in terms of their initial variables as presented at the end of Part I but they also require some simplifications.

4.1. New first-order equations for the continuous phase

The first-order momentum Eq. ((5.18) – Part I) can be simplified thanks to (3.3), (3.4), (3.9), (3.10) and (3.11):

$$\frac{\partial \overline{\mathbf{v}}^{c1}}{\partial t} + \overline{\mathbf{v}}^{c1} \cdot \frac{\partial}{\partial \mathbf{x}} \overline{\mathbf{v}}^{c1} + \left(\frac{\partial}{\partial \mathbf{x}} \overline{p}^{c1} \right) / \rho^c - \nu^c \Delta(\overline{\mathbf{v}}^{c1}) - \nu^c \frac{\partial}{\partial \mathbf{x}} \left[\frac{\partial}{\partial \mathbf{x}} \cdot \overline{\mathbf{v}}^{c1} \right]$$

$$-\mathbf{g} = 2\nu^c \frac{\partial}{\partial \mathbf{x}} \cdot [E(\mathbb{F}^* \delta_\Sigma)\mathbb{A}]/\alpha^{c1} + E[\mathbf{n}^c \cdot \mathbb{T}^* \delta_\Sigma]/\alpha^{c1} \rho^c - \frac{\partial}{\partial \mathbf{x}} \cdot \mathbb{A}^1_{vv}/\alpha^{c1}. \tag{4.1}$$

The l.h.s. comprises all the classical terms of the usual single-phase momentum equation for a compressible fluid whereas the r. h. s. displays three specific forcing functions due to the presence of the dispersed phase; note that these functions, which are multiplied by $(1-\alpha^{d1})^{-1}$, depend on first-order disturbance flow fields. This first-order momentum equation will ultimately remain in our modelling in the form of (4.1).

The first-order continuity Eq. ((5.7) – Part I) will be also kept as it is, and is repeated here for convenience

$$-\frac{\partial \alpha^{d1}}{\partial t} + \frac{\partial}{\partial \mathbf{x}} \cdot [(1-\alpha^{d1})\overline{\mathbf{v}}^{c1}] = 0. \tag{4.2}$$

Integral relations (2.1) and (2.3) linking standard dispersed-phase variables and new moments derived from the kinetic equations must be retained.

4.2. Disturbance equations for the continuous phase

Before transforming the second-order and third-order momentum equations into equations for averaged disturbance flows, all extra-deformation tensors and force densities they contain are split, as shown in Sec. 3. Equation ((5.18) – Part I) is then extended over $\mathcal{V}^c_{x,x^\circ}$ and after having set $\mathbf{x} = \mathbf{x}^\circ$, the resulting equation is subtracted from ((5.19) – Part I):

$$\frac{\partial \mathbf{v}^{\circ *}}{\partial t} + \mathbf{v}^{\circ *} \cdot \frac{\partial}{\partial \mathbf{x}^\circ} \mathbf{v}^{\circ *} + \left(\frac{\partial}{\partial \mathbf{x}^\circ} p^{\circ *} \right) / \rho^c - \nu^c \Delta^\circ(\mathbf{v}^{\circ *}) - \nu^c \frac{\partial}{\partial \mathbf{x}^\circ} \left[\frac{\partial}{\partial \mathbf{x}^\circ} \cdot \mathbf{v}^{\circ *} \right]$$

$$= -\overline{\mathbf{v}}^{c1}(\mathbf{x}^\circ) \cdot \frac{\partial}{\partial \mathbf{x}^\circ} \mathbf{v}^{\circ *} - \mathbf{v}^{\circ *} \cdot \frac{\partial}{\partial \mathbf{x}^\circ} \overline{\mathbf{v}}^{c1}(\mathbf{x}^\circ) \tag{4.3}$$

(4.3) [cont.)

$$+\frac{\partial}{\partial \mathbf{x}^{\circ}}\cdot[E(\mathbb{F}^{**}\delta_{\Sigma}^{1})](2\nu^{c}/\alpha^{c2})-\frac{\partial}{\partial \mathbf{x}^{\circ}}\cdot[E(\mathbb{F}^{*}\delta_{\Sigma})](2\nu^{c}/\alpha^{c1})$$

$$+E[\mathbf{n}^{c}\cdot\mathbb{T}^{**}\delta_{\Sigma}^{1}]/\rho^{c}\alpha^{c2}-E[\mathbf{n}^{c}\cdot\mathbb{T}^{*}\delta_{\Sigma}]/\rho^{c}\alpha^{c1}+C_{v}^{*}.$$

In the l.h.s. a usual single-phase momentum equation can be observed for the unknowns, $\mathbf{v}^{\circ *}=\mathbf{v}^{*}(\mathbf{x}^{\circ}|\mathbf{x})$ and $p^{\circ *}=p^{*}(\mathbf{x}^{\circ}|\mathbf{x})$. At the r.h.s., five types of source function are exhibited. First, two convective terms appear, expressing the influence of the first-order unperturbed fields. Second, there is a difference of two disturbance extra-deformation tensors involving the first-order and second-order averaged perturbation fields. Third, a similar combination of two disturbance interfacial force densities follows. Fourth, fluctuations effects are represented at the bulk level by two continuous-phase velocity variance tensors (pseudo-turbulent tensors). The last term C_{v}^{*} represents cross-correlations between the two phases:

(4.4)
$$C_{v(\mathbf{x}^{\circ}|\mathbf{x})}^{*}=-\frac{\partial}{\partial \mathbf{x}^{\circ}}\cdot\mathbb{A}_{v^{\circ}v^{\circ}}^{2}/\alpha^{c2}\phi^{(1)}+\frac{\partial}{\partial \mathbf{x}^{\circ}}\cdot\mathbb{A}_{v^{\circ}v^{\circ}}^{1}/\alpha^{c1}-\frac{\partial}{\partial \mathbf{x}}$$

$$\cdot E[\varphi_{1}X_{1}^{c}\mathbf{u}_{1}\mathbf{v}^{c}]/\alpha^{c2}\phi_{1}+\overline{\mathbf{v}}^{c2}(\mathbf{x}^{\circ}|\mathbf{x})\cdot\frac{\partial}{\partial \mathbf{x}}E[\varphi_{1}X_{1}^{c}\mathbf{u}_{1}]/\alpha^{c2}\phi_{1}.$$

These will be analysed in the next paper.

Equation ((5.19) – Part I) is then extended over $\mathcal{V}_{\mathbf{x},\mathbf{x}^{\circ},\mathbf{x}^{\circ\circ}}^{c}$; positing $\mathbf{x}^{\circ}=\mathbf{x}^{\circ\circ}$ and $\mathbf{x}=\mathbf{x}^{\circ}$, the resulting equation is subtracted from ((5.20) – Part I):

(4.5)
$$\frac{\partial \mathbf{v}^{\circ\circ **}}{\partial t}+\mathbf{v}^{\circ\circ **}\cdot\frac{\partial}{\partial \mathbf{x}^{\circ\circ}}\mathbf{v}^{\circ\circ **}+\left(\frac{\partial}{\partial \mathbf{x}^{\circ\circ}}p^{\circ\circ **}\right)/\rho^{c}-\nu^{c}\Delta^{\circ\circ}(\mathbf{v}^{\circ\circ **})$$

$$-\nu^{c}\frac{\partial}{\partial \mathbf{x}^{\circ\circ}}\left[\frac{\partial}{\partial \mathbf{x}^{\circ\circ}}\cdot\mathbf{v}^{\circ\circ **}\right]=-\mathbf{v}^{\circ\circ **}\cdot\frac{\partial}{\partial \mathbf{x}^{\circ\circ}}\{\overline{\mathbf{v}}^{c1}(\mathbf{x}^{\circ\circ})+\mathbf{v}^{*}(\mathbf{x}^{\circ\circ}|\mathbf{x})$$

$$+\mathbf{v}^{*}(\mathbf{x}^{\circ\circ}|\mathbf{x}^{\circ})\}-\overline{\mathbf{v}}^{c1}(\mathbf{x}^{\circ\circ})\cdot\frac{\partial}{\partial \mathbf{x}^{\circ\circ}}\mathbf{v}^{\circ\circ **}-\mathbf{v}^{*}(\mathbf{x}^{\circ\circ}|\mathbf{x})$$

$$\cdot\frac{\partial}{\partial \mathbf{x}^{\circ\circ}}\{\mathbf{v}^{\circ\circ **}+\mathbf{v}^{*}(\mathbf{x}^{\circ\circ}|\mathbf{x}^{\circ})\}-\mathbf{v}^{*}(\mathbf{x}^{\circ\circ}|\mathbf{x}^{\circ})\cdot\frac{\partial}{\partial \mathbf{x}^{\circ\circ}}\{\mathbf{v}^{\circ\circ **}+\mathbf{v}^{*}(\mathbf{x}^{\circ\circ}|\mathbf{x})\}$$

$$+2\nu^{c}\left\{\frac{\partial}{\partial \mathbf{x}^{\circ\circ}}\cdot[E(\mathbb{F}^{***}\delta_{\Sigma}^{1,2})]/\alpha^{c3}+\frac{\partial}{\partial \mathbf{x}^{\circ\circ}}\cdot[E(\mathbb{F}^{*}\delta_{\Sigma})](\mathbf{x}^{\circ\circ})]/\alpha^{c1}(\mathbf{x}^{\circ\circ})-\frac{\partial}{\partial \mathbf{x}^{\circ\circ}}\right.$$

$$\left.\cdot[E(\mathbb{F}^{**}\delta_{\Sigma}^{1})](\mathbf{x}^{\circ\circ}|\mathbf{x})]/\alpha^{c2}(\mathbf{x}^{\circ\circ}|\mathbf{x})-\frac{\partial}{\partial \mathbf{x}^{\circ\circ}}\cdot[E(\mathbb{F}^{**}\delta_{\Sigma}^{1})](\mathbf{x}^{\circ\circ}|\mathbf{x}^{\circ})]/\alpha^{c2}(\mathbf{x}^{\circ\circ}|\mathbf{x}^{\circ})\right\}$$

$$+(1/\rho^{c})\{E[\mathbf{n}^{c}\cdot\mathbb{T}^{***}\delta_{\Sigma}^{1,2}]/\alpha^{c3}+E[\mathbf{n}^{c}\cdot\mathbb{T}^{*}\delta_{\Sigma}](\mathbf{x}^{\circ\circ})/\alpha^{c1}$$

$$-E[\mathbf{n}^{c}\mathbb{T}^{**}\delta_{\Sigma}^{1}](\mathbf{x}^{\circ\circ}|\mathbf{x}^{\circ})/\alpha^{c2}(\mathbf{x}^{\circ\circ}|\mathbf{x}^{\circ})-E[\mathbf{n}^{c}\cdot\mathbb{T}^{**}\delta_{\Sigma}^{1}](\mathbf{x}^{\circ\circ}|\mathbf{x})/\alpha^{c2}(\mathbf{x}^{\circ\circ}|\mathbf{x})\}+C_{v}^{**},$$

which is a momentum equation for the unknowns $\mathbf{v}^{\circ\circ**} = \mathbf{v}^{**}(\mathbf{x}^{\circ\circ}|\mathbf{x}^{\circ}, \mathbf{x})$ and $p^{\circ\circ**} = p^{**}(\mathbf{x}^{\circ\circ}|\mathbf{x}^{\circ}, \mathbf{x})$. The forcing functions have exactly the same structure as in (4.3). The last term C_v^{**} represents correlation between the two phases.

$$
\begin{aligned}
(4.6)\quad C^{**}_{v(\mathbf{x}^{\circ\circ}|\mathbf{x}^{\circ},\mathbf{x})} = {} & -\frac{\partial}{\partial \mathbf{x}^{\circ\circ}} \cdot \mathbb{A}^3_{v^{\circ\circ}v^{\circ\circ}}/\alpha^{c3}\phi^{(2)} + \frac{\partial}{\partial \mathbf{x}^{\circ\circ}} \cdot \mathbb{A}^2_{v^{\circ\circ}v^{\circ\circ}}(\mathbf{x}^{\circ\circ}|\mathbf{x}^{\circ})/\alpha^{c2}(\mathbf{x}^{\circ\circ}|\mathbf{x}^{\circ}) \\
& \phi^{(1)}(\mathbf{x}^{\circ}) + \frac{\partial}{\partial \mathbf{x}^{\circ\circ}} \cdot \mathbb{A}^2_{v^{\circ\circ}v^{\circ\circ}}(\mathbf{x}^{\circ\circ}|\mathbf{x})/\alpha^{c2}(\mathbf{x}^{\circ\circ}|\mathbf{x})\phi^{(1)}(\mathbf{x}) \\
& + \frac{\partial}{\partial \mathbf{x}} \cdot E[X_1^c\varphi_1\mathbf{u}_1\mathbf{v}^c]/\alpha^{c2}(\mathbf{x}^{\circ\circ}|\mathbf{x})\phi_1(\mathbf{x}) - \overline{\mathbf{v}}^{c2}(\mathbf{x}^{\circ\circ}|\mathbf{x}^{\circ}) \cdot \frac{\partial}{\partial \mathbf{x}^{\circ}} E \\
& \times [X_2^c\varphi_2\mathbf{u}_2]/\alpha^{c2}(\mathbf{x}^{\circ\circ}|\mathbf{x}^{\circ})\phi_1(\mathbf{x}^{\circ}) + \frac{\partial}{\partial \mathbf{x}^{\circ}} \cdot E[X_2^c\varphi_2\mathbf{u}_2\mathbf{v}^c]/\alpha^{c2}(\mathbf{x}^{\circ\circ}|\mathbf{x}^{\circ})\phi_1(\mathbf{x}^{\circ}) \\
& -\overline{v}^{c2}(\mathbf{x}^{\circ\circ}|\mathbf{x}) \cdot \frac{\partial}{\partial \mathbf{x}} E[X_1^c\varphi_1\mathbf{u}_1]/\alpha^{c2}(\mathbf{x}^{\circ\circ}|\mathbf{x})\phi_1(\mathbf{x}) \\
& -\frac{\partial}{\partial \mathbf{x}} \cdot E[X^c_{1,2}\varphi_1\varphi_2\mathbf{u}_1\mathbf{v}^c]/\alpha^{c3}\phi_2 + \overline{\mathbf{v}}^{c3} \cdot \frac{\partial}{\partial \mathbf{x}} E[X^c_{1,2}\varphi_1\varphi_2\mathbf{u}_1]/\alpha^{c3}\phi_2 \\
& -\frac{\partial}{\partial \mathbf{x}^{\circ}} \cdot E[X^c_{1,2}\varphi_1\varphi_2\mathbf{u}_2\mathbf{v}^c]/\alpha^{c3}\phi_2 + \overline{\mathbf{v}}^{c3} \cdot \frac{\partial}{\partial \mathbf{x}^{\circ}} E[X^c_{1,2}\varphi_1\varphi_2\mathbf{u}_2]/\alpha^{c3}\phi_2.
\end{aligned}
$$

These convective terms, which have not yet been analysed, will also be considered in the next paper.

Finally, the second-order and third-order continuity equations of the Lundgren hierarchy can also be transformed into equations controlling disturbance fields $\alpha^{\circ*} = \alpha^*(\mathbf{x}^{\circ}|\mathbf{x})$ and $\alpha^{\circ\circ**} = \alpha^{**}(\mathbf{x}^{\circ\circ}|\mathbf{x}^{\circ}, \mathbf{x})$. Consider the first-order disturbance flow equation obtained by subtracting (4.2), in which $\mathbf{x} = \mathbf{x}^{\circ}$, from ((5.21) – Part I):

$$
(4.7)\quad \frac{\partial \alpha^{\circ*}}{\partial t} + \frac{\partial}{\partial \mathbf{x}^{\circ}} \cdot \left[\alpha^{\circ*}(\overline{\mathbf{v}}^{c1} + \mathbf{v}^{\circ*}) - \alpha^{c1}\mathbf{v}^{\circ*}\right] = -(\alpha^{c2}/\phi_1)\frac{\partial}{\partial \mathbf{x}} \cdot (\phi_1\overline{\mathbf{u}}^1) + C^*_\alpha,
$$

where $C^*_\alpha = (1/\phi_1)\dfrac{\partial}{\partial \mathbf{x}} \cdot E[\varphi_1 X_1^c\mathbf{u}_1]$. Setting $\mathbf{x}^{\circ} = \mathbf{x}^{\circ\circ}$ and $\mathbf{x} = \mathbf{x}^{\circ}$ in ((5.21) – Part I) and substracting the resulting equation from ((5.22) – Part I):

$$
\begin{aligned}
(4.8)\quad \frac{\partial \alpha^{\circ\circ**}}{\partial t} + \frac{\partial}{\partial \mathbf{x}^{\circ\circ}} \cdot \{\alpha^{\circ\circ**}[\overline{\mathbf{v}}^{c1}(\mathbf{x}^{\circ\circ}) + \mathbf{v}^*(\mathbf{x}^{\circ\circ}|\mathbf{x}^{\circ}) + \mathbf{v}^*(\mathbf{x}^{\circ\circ}|\mathbf{x}) \\
+\mathbf{v}^{\circ\circ**}]\} + \frac{\partial}{\partial \mathbf{x}^{\circ\circ}} \cdot \{\alpha^*(\mathbf{x}^{\circ\circ}|\mathbf{x}^{\circ})[\mathbf{v}^*(\mathbf{x}^{\circ\circ}|\mathbf{x}) + \mathbf{v}^{\circ\circ**}]\}
\end{aligned}
$$

(4.8) [cont.]
$$+\frac{\partial}{\partial \mathbf{x}^{\circ\circ}}\cdot\{\alpha^{*}(\mathbf{x}^{\circ\circ}|\mathbf{x})[\mathbf{v}^{*}(\mathbf{x}^{\circ\circ}|\mathbf{x}^{\circ})+\mathbf{v}^{\circ\circ **}]\}$$

$$-\frac{\partial}{\partial \mathbf{x}^{\circ\circ}}\cdot[\alpha^{c1}(\mathbf{x}^{\circ\circ})\mathbf{v}^{\circ\circ **}]$$

$$=[\alpha^{c2}(\mathbf{x}^{\circ\circ}|\mathbf{x})/\phi_1]\frac{\partial}{\partial \mathbf{x}}\cdot(\phi_1\overline{\mathbf{u}}^{1})+[\alpha^{c2}(\mathbf{x}^{\circ\circ}|\mathbf{x}^{\circ})/\phi_1^{\circ}]\frac{\partial}{\partial \mathbf{x}^{\circ}}\cdot(\phi_1^{\circ}\overline{\mathbf{u}^{\circ}}^{1})$$

$$-[\alpha^{c3}(\mathbf{x}^{\circ\circ}|\mathbf{x},\mathbf{x}^{\circ})/\phi_2]\left[\frac{\partial}{\partial \mathbf{x}}\cdot(\phi_2\overline{\mathbf{u}}^{2})+\frac{\partial}{\partial \mathbf{x}^{\circ}}\cdot(\phi_2\overline{\mathbf{u}^{\circ}}^{2})\right]+C_{\alpha}^{**},$$

where C_{α}^{**}, the correlation term, comprises composite divergence-type sources:

$$C_{\alpha}^{**}=-(1/\phi_1)\frac{\partial}{\partial \mathbf{x}}\cdot E[\varphi_1 X_1^{c}\mathbf{u}_1]-(1/\phi_1^{\circ})\frac{\partial}{\partial \mathbf{x}^{\circ}}\cdot E[\varphi_2 X_2^{c}\mathbf{u}_2] \tag{4.9}$$

$$+(1/\phi_2)\frac{\partial}{\partial \mathbf{x}}\cdot E[\varphi_1\varphi_2 X_{1,2}^{c}\mathbf{u}_1]+(1/\phi_2)\frac{\partial}{\partial \mathbf{x}^{\circ}}\cdot E[\varphi_1\varphi_2 X_{1,2}^{c}\mathbf{u}_2].$$

Integral relations linking (Sec. 2.1) standard dispersed-phase variables (basically α^{di}, $\mathbf{v}^{di}$, $i=2,3$) and new moments derived from the kinetic equations must be added in their initial integral form (see Eq. (2.12)) or their expanded form (see Eq. (2.13)).

4.3. New first-order equations for the dispersed phase

The first-order dispersed-phase linear momentum Eq. ((4.27) – Part I) becomes:

$$\rho^{d}\frac{\partial}{\partial t}\overline{\mathbf{u}}^{1}+\rho^{d}\overline{\mathbf{u}}^{1}\cdot\frac{\partial}{\partial \mathbf{x}}\overline{\mathbf{u}}^{1}+(1+\mathbf{R}_1)\left[\frac{\partial \overline{p}^{c1}}{\partial \mathbf{x}}-\mu^{c}\Delta\overline{\mathbf{v}}^{c1}\right. \tag{4.10}$$

$$\left.-\mu^{c}\frac{\partial}{\partial \mathbf{x}}\left(\frac{\partial}{\partial \mathbf{x}}\cdot\overline{\mathbf{v}}^{c1}\right)\right]-\rho^{d}\mathbf{g}=-\rho^{d}(\phi^{(1)})^{-1}\frac{\partial}{\partial \mathbf{x}}\cdot\mathbb{A}_{uu}^{1}+(3/4)\mathbf{F}^{*}/\pi a^{3}$$

considering (2.14) and (2.20). In this first-order equation, it should be recalled that $\mathbf{R}_1=O(\beta^2)$. It may appear surprising to meet a seemingly normal single-phase momentum equation written for an averaged "composite fluid" of a sort at the l.h.s. of (4.10). Its inertia is that of the inclusions while its viscosity is that of the carrying fluid. Two types of source terms are exhibited at the r.h.s. due to the presence of the continuous phase.

The first-order dispersed-phase angular momentum Eq. ((4.28) – Part I) may be similarly transformed by using (2.16) and (2.21)

$$\rho^d \frac{\partial}{\partial t}\overline{\omega}^1 + \rho^d \overline{\mathbf{u}}^1 \cdot \frac{\partial}{\partial \mathbf{x}}\overline{\omega}^1 = -\mu^c (1 + \mathbf{R}_2)\, \mathbf{curl}^3(\overline{\mathbf{v}}^{c1})/2 \tag{4.11}$$

$$+(15/8)\mathbf{K}^*/\pi a^5 - (\phi^{(1)})^{-1}\rho^d \frac{\partial}{\partial \mathbf{x}} \cdot \mathbb{A}^1_{\omega u}.$$

This first-order equation, where, similarly, $\mathbf{R}_2 = O(\beta^2)$, looks like a classical vorticity transport equation which could be written for the above "composite fluid", especially if the fluid spin is defined by $\overline{\omega}^{c1} = \mathbf{curl}\,(\overline{\mathbf{v}}^{c1})/2$. The viscous term at its r.h.s. is then the familiar $-\mu^c \mathbf{curl}^2(\overline{\omega}^{c1})$. However, several differences make this analogy irrelevant. The term $\overline{\omega}^1 \cdot \dfrac{\partial}{\partial \mathbf{x}}\overline{\mathbf{u}}^1$, which would give vorticity changes their distinctive character, is lacking. More basically, this is an equation in itself, juxtaposed to (4.11), and cannot be deduced from a more basic "Navier-Stokes equation".

For some applications, it is advantageous to transform the first-order dispersed-phase linear and angular momentum Eqs. (4.10) and (4.11) so that they directly provide the relative linear and angular velocities defined by:

$$\overline{\mathbf{u}}^r = \overline{\mathbf{u}}^1 - \overline{\mathbf{v}}^{c1}; \qquad \overline{\omega}^r = \overline{\omega}^1 - \overline{\omega}^{c1}. \tag{4.12}$$

The basic reason is the same as that leading to the introduction of disturbance field equations: estimating precisely the magnitude of various terms becomes easier. Moreover, $\mathbf{F}^*$ and $\mathbf{K}^*$ will appear as functions of these relative velocities. By introducing these velocities:

$$\rho^d \frac{\partial}{\partial t}\overline{\mathbf{u}}^r + \rho^d \overline{\mathbf{u}}^r \cdot \frac{\partial}{\partial \mathbf{x}}\overline{\mathbf{u}}^r - (3/4)\mathbf{F}^*/\pi a^3 + \rho^d (\phi^{(1)})^{-1} \frac{\partial}{\partial \mathbf{x}} \cdot \mathbb{A}^1_{uu} \tag{4.13}$$

$$+\rho^d \overline{\mathbf{u}}^r \cdot \frac{\partial}{\partial \mathbf{x}}\overline{\mathbf{v}}^{c1} + \rho^d \overline{\mathbf{v}}^{c1} \cdot \frac{\partial}{\partial \mathbf{x}}\overline{\mathbf{u}}^r = -\rho^d \frac{\partial}{\partial t}\overline{\mathbf{v}}^{c1} - \rho^d \overline{\mathbf{v}}^{c1} \cdot \frac{\partial}{\partial \mathbf{x}}\overline{\mathbf{v}}^{c1}$$

$$-(1 + \mathbf{R}_1)\left[\frac{\partial \overline{p}^{c1}}{\partial \mathbf{x}} - \mu^c \Delta \overline{\mathbf{v}}^{c1} - \mu^c \frac{\partial}{\partial \mathbf{x}}\left(\frac{\partial}{\partial \mathbf{x}} \cdot \overline{\mathbf{v}}^{c1}\right)\right] + \rho^d \mathbf{g},$$

and:

$$\rho^d \frac{\partial}{\partial t}\overline{\omega}^r + \rho^d \overline{\mathbf{u}}^r \cdot \frac{\partial}{\partial \mathbf{x}}\overline{\omega}^r - (15/8)\mathbf{K}^*/\pi a^5 + (\phi^{(1)})^{-1}\rho^d \frac{\partial}{\partial \mathbf{x}} \cdot \mathbb{A}^1_{\omega u} \tag{4.14}$$

$$+\rho^d \overline{\mathbf{v}}^{c1} \cdot \frac{\partial}{\partial \mathbf{x}}\overline{\omega}^r + \rho^d \overline{\mathbf{u}}^r \cdot \frac{\partial}{\partial \mathbf{x}}\overline{\omega}^{c1} = -\rho^d \frac{\partial}{\partial t}\overline{\omega}^{c1} - \rho^d \overline{\mathbf{v}}^{c1} \cdot \frac{\partial}{\partial \mathbf{x}}\overline{\omega}^{c1}$$

$$-\mu^c (1 + \mathbf{R}_2)\mathbf{curl}^3(\overline{\mathbf{v}}^{c1})/2.$$

In addition, the density dispersed-phase Eq. ((4.11) – Part I) itself becomes

$$\frac{\partial \phi_1}{\partial t} + \frac{\partial}{\partial \mathbf{x}} \cdot \phi_1 \overline{\mathbf{v}}^{c1} = -\frac{\partial}{\partial \mathbf{x}} \cdot \phi_1 \overline{\mathbf{u}}^{r}. \tag{4.15}$$

4.4. Disturbance flow equations for the dispersed phase

Using (2.15), (2.17) and results similar to (2.20) and (2.21), the second-order dispersed-phase momentum Eqs. ((4.29) and (4.30) – Part I) become:

$$\begin{aligned} \rho^d \left[\frac{\partial}{\partial t} \overline{\mathbf{u}}^{\circ 2} + \overline{\mathbf{u}^{\circ}}^2 \cdot \frac{\partial}{\partial \mathbf{x}^{\circ}} \overline{\mathbf{u}^{\circ}}^2 + \overline{\mathbf{u}}^2 \cdot \frac{\partial}{\partial \mathbf{x}} \overline{\mathbf{u}^{\circ}}^2 \right] \\ = (1 + \mathbf{R}_1^{\circ}) \left[-\frac{\partial \overline{p^{\circ}}^{c2}}{\partial \mathbf{x}^{\circ}} + \mu^c \Delta^{\circ} \overline{\mathbf{v}^{\circ}}^{c2} + \mu^c \frac{\partial}{\partial \mathbf{x}^{\circ}} \left(\frac{\partial}{\partial \mathbf{x}^{\circ}} \cdot \overline{\mathbf{v}^{\circ}}^{c2} \right) \right] \\ + \rho^d \left[-\left(\phi^{(2)}\right)^{-1} \frac{\partial}{\partial \mathbf{x}} \cdot \mathbb{A}^2_{uu^{\circ}} - \left(\phi^{(2)}\right)^{-1} \frac{\partial}{\partial \mathbf{x}^{\circ}} \cdot \mathbb{A}^2_{u^{\circ}u^{\circ}} + \mathbf{g} \right] \\ + (3/4)(\mathbf{F}^{\circ **} + \mathbf{F}^{\circ *})/\pi a^3, \end{aligned} \tag{4.16}$$

and

$$\begin{aligned} \rho^d \left[\frac{\partial}{\partial t} \overline{\boldsymbol{\omega}^{\circ}}^2 + \overline{\mathbf{u}^{\circ}}^2 \cdot \frac{\partial}{\partial \mathbf{x}^{\circ}} \overline{\boldsymbol{\omega}^{\circ}}^2 + \overline{\mathbf{u}}^2 \cdot \frac{\partial}{\partial \mathbf{x}} \overline{\boldsymbol{\omega}^{\circ}}^2 \right] = -\mu^c (1 + \mathbf{R}_2^{\circ}) \\ \mathbf{curl}^{\circ 3} (\overline{\mathbf{v}^{\circ}}^{c2})/2 - \rho^d (\phi^{(2)})^{-1} \left[\frac{\partial}{\partial \mathbf{x}^{\circ}} \cdot \mathbb{A}^2_{\omega^{\circ}u^{\circ}} + \frac{\partial}{\partial \mathbf{x}} \cdot \mathbb{A}^2_{\omega^{\circ}u} \right] \\ + (15/8)(\mathbf{K}^{\circ **} + \mathbf{K}^{\circ *})/\pi a^5. \end{aligned} \tag{4.17}$$

To establish the equation for $\mathbf{u}^{\circ *}$, the first-order Eq. (4.7) written at $\mathbf{x}^{\circ}$ is subtracted from the above second-order Eq. (4.16):

$$\begin{aligned} \rho^d \left[\frac{\partial}{\partial t} \mathbf{u}^{\circ *} + u^{\circ *} \cdot \frac{\partial}{\partial \mathbf{x}^{\circ}} \mathbf{u}^{\circ *} \right] + \frac{\partial p^{\circ *}}{\partial \mathbf{x}^{\circ}} - \mu^c \Delta^{\circ} \mathbf{v}^{\circ *} - \mu^c \frac{\partial}{\partial \mathbf{x}^{\circ}} \left(\frac{\partial}{\partial \mathbf{x}^{\circ}} \cdot \mathbf{v}^{\circ *} \right) \\ = +\mathbf{R}_1^{\circ} \left[-\frac{\partial p^{\circ *}}{\partial \mathbf{x}^{\circ}} + \mu^c \Delta \mathbf{v}^{\circ *} + \mu^c \frac{\partial}{\partial \mathbf{x}^{\circ}} \left(\frac{\partial}{\partial \mathbf{x}^{\circ}} \cdot \mathbf{v}^{\circ *} \right) \right] \\ - \rho^d \left[\overline{\mathbf{u}^{\circ}}^1 \cdot \frac{\partial}{\partial \mathbf{x}^{\circ}} \mathbf{u}^{\circ *} + \mathbf{u}^{\circ *} \cdot \frac{\partial}{\partial \mathbf{x}^{\circ}} \overline{\mathbf{u}^{\circ}}^1 + \overline{\mathbf{u}}^2 \cdot \frac{\partial}{\partial \mathbf{x}} \mathbf{u}^{\circ *} \right] \\ + \rho^d \left[-(\phi^{(2)})^{-1} \frac{\partial}{\partial \mathbf{x}^{\circ}} \cdot \mathbb{A}^2_{u^{\circ}u^{\circ}} - (\phi^{(2)})^{-1} \frac{\partial}{\partial \mathbf{x}} \cdot \mathbb{A}^2_{uu^{\circ}} \right. \\ \left. + (\phi^{(1)})^{-1} \frac{\partial}{\partial \mathbf{x}^{\circ}} \cdot \mathbb{A}^1_{u^{\circ}u^{\circ}} \right] + (3/4\pi a^3) \mathbf{F}^{\circ **}. \end{aligned} \tag{4.18}$$

The l.h.s. of (4.18) corresponds to the first-order averaged disturbance momentum equation relative to the afore-mentioned "composite fluid". At the r.h.s., the source terms bear some similarities to those encountered in the corresponding Eq. (4.3) of the Lundgren hierarchy.

Finally, by substracting the first-order equation for the angular velocity (4.11) written at $\mathbf{x}^\circ$ from the second-order Eq. (4.17), the equation for $\boldsymbol{\omega}^{\circ *}$ follows:

$$\rho^d \left[\frac{\partial}{\partial t}\boldsymbol{\omega}^{\circ *} + \mathbf{u}^{\circ *} \cdot \frac{\partial}{\partial \mathbf{x}^\circ}\boldsymbol{\omega}^{\circ *}\right] + \mu^c \, \mathbf{curl}^{\circ 3}(\mathbf{v}^{\circ *})/2$$

$$= -\mu^c \mathbf{R}_2^\circ[\mathbf{curl}^{\circ 3}(\mathbf{v}^{\circ *})]/2 - \rho^d \left[\overline{\mathbf{u}^\circ}^1 \cdot \frac{\partial}{\partial \mathbf{x}^\circ}\boldsymbol{\omega}^{\circ *} + \mathbf{u}^{\circ *} \cdot \frac{\partial}{\partial \mathbf{x}^\circ}\overline{\boldsymbol{\omega}^\circ}^1 + \overline{\mathbf{u}}^2 \cdot \frac{\partial}{\partial \mathbf{x}}\boldsymbol{\omega}^{\circ *}\right] + \rho^d \left[-(\phi^{(2)})^{-1}\frac{\partial}{\partial \mathbf{x}^\circ} \cdot \mathbb{A}^2_{\omega^\circ u^\circ} - (\phi^{(2)})^{-1}\frac{\partial}{\partial \mathbf{x}} \cdot \mathbb{A}^2_{\omega^\circ u}\right.$$

$$\left. + (\phi^{(1)})^{-1}\frac{\partial}{\partial \mathbf{x}^\circ} \cdot \mathbb{A}^1_{\omega^\circ u^\circ}\right] + (15/8\pi a^5)\mathbf{K}^{\circ **}. \tag{4.19}$$

The equation for the disturbance $\chi^{\circ *}$ defined in (1.2), is obtained by substracting ((4.11) – Part I) written for $\phi_1^\circ = \phi_1(\mathbf{x}^\circ)$ from ((4.31) – Part I):

$$\frac{\partial \chi^{\circ *}}{\partial t} + \frac{\partial}{\partial \mathbf{x}^\circ} \cdot \left[\phi_1^\circ \mathbf{u}^{\circ *} + \chi^{\circ *}\overline{\mathbf{u}^\circ}^1 + \chi^{\circ *}\mathbf{u}^{\circ *}\right]$$

$$= -(\phi_1^\circ + \chi^{\circ *})\frac{\partial}{\partial \mathbf{x}} \cdot \mathbf{u}^* - (\overline{\mathbf{u}}^1 + \mathbf{u}^*) \cdot \frac{\partial \chi^{\circ *}}{\partial \mathbf{x}} - \frac{\phi_1^\circ + \chi^{\circ *}}{\phi_1}\mathbf{u}^* \cdot \frac{\partial \phi_1}{\partial \mathbf{x}}, \tag{4.20}$$

where $\mathbf{u}^{\circ *}$ is the velocity disturbance at $\mathbf{x}^\circ$, knowing that an inclusion is located at $\mathbf{x}$.

4.5. Disturbance boundary continuity conditions

Boundary equations at the surfaces of test inclusions also have to be written in terms of disturbance flow. It should be recalled that these conditions express the continuity of tangential velocities (no-slip condition) and of normal velocity (no external fluid mass flows across the surface). From ((5.10) – Part I), at $\mathbf{x}^\circ = \mathbf{x} + a\mathbf{n}$ where $\mathbf{n}$ is the unit normal exterior to an inclusion, the first disturbance field satisfies:

$$\mathbf{v}^*(\mathbf{x} + a\mathbf{n}|\mathbf{x}) = \overline{\mathbf{u}}^1(\mathbf{x}) - \overline{\mathbf{v}}^{c1}(\mathbf{x}) + a\boldsymbol{\omega}^1(\mathbf{x}) \wedge \mathbf{n} + \overline{\mathbf{v}}^{c1}(\mathbf{x}) - \overline{\mathbf{v}}^{c1}(\mathbf{x} + a\mathbf{n})$$

$$= \overline{\mathbf{u}}^r(\mathbf{x}) + \overline{\boldsymbol{\omega}}^r(\mathbf{x}) \wedge \mathbf{n} - a\mathbb{D}[\overline{\mathbf{v}}^{c1}(\mathbf{x})] \cdot \mathbf{n} + (1/2)a^2 \nabla\nabla\overline{\mathbf{v}}^{c1}(\mathbf{x}) : \mathbf{nn} + \ldots \tag{4.21}$$

where ∇ and $\mathbb{D}$ are the gradient operator and its symmetrical part respectively. This equation may be viewed generally as relating the averaged disturbance field, $\mathbf{v}^*$, to three preponderant forcing functions:

• the relative dispersed-phase velocity, $\overline{\mathbf{u}}^r$, provided by the relative linear momentum equation for the dispersed phase,

• the relative dispersed-phase velocity, $\overline{\boldsymbol{\omega}}^r$, provided by the relative angular momentum equation for the dispersed phase,

• the simple shear flow, $a\mathbb{D}[\overline{\mathbf{v}}^{c1}(\mathbf{x}] \cdot \mathbf{n}$, provided by the first-order momentum equation for the continuous phase.

The second disturbance field satisfies two conditions, one at $\mathbf{x}^{\circ\circ} = \mathbf{x}^{\circ} + a\mathbf{n}$ and the other one at $\mathbf{x}^{\circ\circ} = \mathbf{x} + a\mathbf{n}$ derived from their mother condition ((5.10) – Part I):

$$\mathbf{v}^{**}(\mathbf{x}^{\circ} + a\mathbf{n}|\mathbf{x}^{\circ}, \mathbf{x}) = \mathbf{u}^{*}(\mathbf{x}^{\circ}|\mathbf{x}) + a\boldsymbol{\omega}^{*} \wedge \mathbf{n}(\mathbf{x}^{\circ}|\mathbf{x}) - \mathbf{v}^{*}(\mathbf{x}^{\circ} + a\mathbf{n}|\mathbf{x}) \tag{4.22}$$

and

$$\mathbf{v}^{**}(\mathbf{x} + a\mathbf{n}|\mathbf{x}^{\circ}, \mathbf{x}) = \mathbf{u}^{*}(\mathbf{x}|\mathbf{x}^{\circ}) + a\boldsymbol{\omega}^{*} \wedge \mathbf{n}(\mathbf{x}|\mathbf{x}^{\circ}) - \mathbf{v}^{*}(\mathbf{x} + a\mathbf{n}|\mathbf{x}^{\circ}). \tag{4.23}$$

These conditions, which are symmetrical with respect to $\mathbf{x}$ and $\mathbf{x}^{\circ}$, connect the third- and second-order disturbance flows.

On the external boundaries of $\mathcal{V}^c_{\mathbf{x},\mathbf{x}^{\circ}}$, $\mathcal{V}^c_{\mathbf{x},\mathbf{x}^{\circ},\mathbf{x}^{\circ\circ}}$ simple conditions result from ((5.9) – Part I):

$$\mathbf{v}^{*}(\mathbf{x}^{\circ}|\mathbf{x}) = 0, \quad \mathbf{x}^{\circ} \text{ on } \partial\mathcal{V}^c_w \quad \text{and} \quad \mathbf{v}^{**}(\mathbf{x}^{\circ\circ}|\mathbf{x}^{\circ}, \mathbf{x}) = 0, \quad \mathbf{x}^{\circ\circ} \text{ on } \partial\mathcal{V}^c_w \tag{4.24}$$

Regarding the dispersed phase, the condition in the vicinity of walls is derived from ((4.33) – Part I)

$$\mathbf{u}^{*}(\mathbf{x}^{\circ} - a\mathbf{n}^b|\mathbf{x}) + a\boldsymbol{\omega}^{*}(\mathbf{x}^{\circ} - a\mathbf{n}^b|\mathbf{x}) \wedge \mathbf{n}^b = 0, \quad \mathbf{x}^{\circ} \text{ on } \partial\mathcal{V}^c_w \tag{4.25}$$

while conditions on the fluid boundary of $\partial\mathcal{V}^d$ are obtained by combining Eqs. ((4.35) to (4.37) – Part I):

$$\chi^{*}(\mathbf{x}^{\circ}|\mathbf{x}) = \mathbf{u}^{*}(\mathbf{x}^{\circ}|\mathbf{x}) = \boldsymbol{\omega}^{*}(\mathbf{x}^{\circ}|\mathbf{x}) = 0, \quad \mathbf{x}^{\circ} \text{ on } \partial\mathcal{V}^d_f \tag{4.26}$$

Disturbance velocity fields satisfying conditions on the internal boundaries of $\mathcal{V}^d_{\mathbf{x},\mathbf{x}^{\circ}}$ result from ((4.34) – Part I)

$$\begin{aligned}\mathbf{u}^{*}(\mathbf{x}|\mathbf{x} + 2a\mathbf{n}) - \mathbf{u}^{*}(\mathbf{x} + 2a\mathbf{n}|\mathbf{x}) + 2a[\boldsymbol{\omega}^{*}(\mathbf{x}|\mathbf{x} + 2a\mathbf{n}) \\ + \boldsymbol{\omega}^{*}(\mathbf{x} + 2a\mathbf{n}|\mathbf{x})] \wedge \mathbf{n} + \overline{\mathbf{u}}^1(\mathbf{x}) - \overline{\mathbf{u}}^1(\mathbf{x} + 2a\mathbf{n}) + 2a[\overline{\boldsymbol{\omega}}^1(\mathbf{x}) \\ + \overline{\boldsymbol{\omega}}^1(\mathbf{x} + 2a\mathbf{n})] \wedge \mathbf{n} = 0,\end{aligned} \tag{4.27}$$

where $\mathbf{n}$ is the unit normal exterior to the inclusion centred at $\mathbf{x}$.

5. More about continuous-phase interaction terms

5.1. Various expressions of the extra-deformation tensors

The extra-deformation tensor given by (3.2) can be rewritten by introducing the boundary condition ((5.10) – Part I) and then by applying Gauss theorem:

$$E[\mathbb{F}^c\delta_\Sigma](\mathbf{x}) = a^2 \int_{S(\mathbf{x})} [\mathbf{n}^c\overline{\mathbf{v}}^{c2}]^s(\mathbf{x}|\mathbf{x}_1)\phi^{(1)}(\mathbf{x}_1)d\Omega \tag{5.1}$$

$$= a^2 \int_{S(\mathbf{x})} \{\mathbf{n}^c[\overline{\mathbf{u}}^1(\mathbf{x}_1) + \overline{\omega}^1(\mathbf{x}_1) \wedge (\mathbf{x} - \mathbf{x}_1)]\}^s \phi^{(1)}(\mathbf{x}_1)d\Omega$$

$$= \int_{|\tilde{\mathbf{x}}-\mathbf{x}|\leq a} \left\{ \frac{\partial}{\partial\tilde{\mathbf{x}}}[\overline{\mathbf{u}}^1(\tilde{\mathbf{x}}) + \overline{\omega}^1(\tilde{\mathbf{x}}) \wedge (\mathbf{x} - \tilde{\mathbf{x}})]\phi^{(1)}(\tilde{\mathbf{x}}) \right\}^s d\tilde{\mathbf{x}}$$

$$= \mathbb{D}\left\{ \int_{|\mathbf{k}|\leq a} [\overline{\mathbf{u}}^1(\mathbf{x}+\mathbf{k}) + \overline{\omega}^1(\mathbf{x}+\mathbf{k}) \wedge \mathbf{k}]\phi^{(1)}(\mathbf{x}+\mathbf{k})d\mathbf{k} \right\} = \mathbb{D}(\alpha^{d1}\overline{\mathbf{v}}^{d1}).$$

In the last line, the standard dispersed-phase velocity $\overline{\mathbf{v}}^{d1}$ (2.3) has been identified. Such a result has already been proposed by JOSEPH and LUNDGREN [9]. By averaging the fine-grained expression of the extra-deformation tensor $\mathbf{n}^c \cdot \mathbb{T}\delta_\Sigma = \mathbb{D}(X^d\mathbf{v}^d)$ (see (2.13) – Part I) they obtained directly the final term in Eq. (5.1). Besides several inferences were drawn.

Introducing the mixture velocity, $\mathbf{v}^m = X^c\mathbf{v}^c + X^d\mathbf{v}^d$, and taking the divergence of ((2.13) – Part I) yield:

$$\frac{\partial}{\partial\mathbf{x}} \cdot \{X^c\mathbb{T}^c\} = -\frac{\partial}{\partial\mathbf{x}}(X^c p^c) + \mu^c \Delta(\mathbf{v}^{\mathrm{m}}) + \frac{\partial}{\partial\mathbf{x}}\left[\frac{\partial}{\partial\mathbf{x}} \cdot (\mathbf{v}^{\mathrm{m}})\right] \tag{5.2}$$

$$= -\frac{\partial}{\partial\mathbf{x}}(X^c p^c) + \mu^c \Delta(\mathbf{v}^{\mathrm{m}})$$

since the continuity equations for both phases (i.e. the Eq. ((2.9) – Part I) and their dispersed-phase companion) give:

$$\frac{\partial}{\partial\mathbf{x}} \cdot \mathbf{v}^{\mathrm{m}} = 0. \tag{5.3}$$

Thus (5.2) offers an alternative expression for the fine-grained momentum Eq. ((2.15) – Part I). Once averaged, it is clear that all the averaged viscous terms except the averaged interfacial force density merge in the single term $\nu^c \Delta \overline{\mathbf{v}}^{m1}$, where the averaged mixture velocity has been introduced. Likewise, alternative expressions for the momentum equations at the second and third order can be obtained by averaging the appropriate fine-grained equations. These will not be presented for the sake of brevity.

Secondly, ISHII [8] discussed the form of the disturbance-averaged extra-deformation tensor $E[\mathbb{F}^* \delta_\Sigma]$ even if the above break-down was not explicitly given in his study. Employing (5.1), it is interesting to remark that $E[\mathbb{F}^* \delta_\Sigma]$ can be stated in the following form:

$$E[\mathbb{F}^* \delta_\Sigma](\mathbf{x}) = \alpha^{d1} \mathbb{D}(\overline{\mathbf{v}}^{c1})(\mathbf{x}) + \alpha^{d1} \mathbb{D}(\overline{\mathbf{v}}^{d1} - \overline{\mathbf{v}}^{c1})(\mathbf{x}) + \left[(\overline{\mathbf{v}}^{d1} - \overline{\mathbf{v}}^{c1}) \frac{\partial \alpha^{d1}}{\partial \mathbf{x}} \right]^s (\mathbf{x}), \tag{5.4}$$

so the disturbance-averaged extra-deformation tensor has three components. In the present type of modelling, the standard dispersed-phase velocity (2.7) defined in Part I has to be expressed via (2.8) in terms of our own dispersed phase (linear and angular) velocities. At the leading order, we have:

$$E[\mathbb{F}^* \delta_\Sigma] = \alpha^{d1} \mathbb{D}(\overline{\mathbf{v}}^{c1}) + \alpha^{d1} \mathbb{D}(\overline{\mathbf{u}}^r) + \left[\overline{\mathbf{u}}^r \frac{\partial \alpha^{d1}}{\partial \mathbf{x}} \right]^s + O(\beta). \tag{5.5}$$

This result is quite general and is valid for any type of dispersed inclusion as long as both phases may be considered incompressible. The third component in (5.4) is precisely the one discussed conjecturally by ISHII [8]: here it is proved. Somewhat anticipating the scale analysis to be performed in a future paper, it may be admitted that this component is important when the particulate Reynolds number based on linear movements is high. Such a component is often neglected in two-fluid models. A last remark is worth making; as the extra-deformation tensor appears in the momentum equation inserted into a divergence operator (see Eq. (4.1)) the above component gives rise to a diffusion-type term among other terms:

$$\left[(\overline{\mathbf{v}}^{d1} - \overline{\mathbf{v}}^{c1}) \Delta \alpha^{d1} + (\overline{\mathbf{v}}^{d1} - \overline{\mathbf{v}}^{c1}) \cdot \frac{\partial}{\partial \mathbf{x}} \frac{\partial}{\partial \mathbf{x}} \alpha^{d1} \right]. \tag{5.6}$$

The second component in (5.4) is also passed over by everyone. It is more difficult to ascertain but it is certainly important when the particulate Reynolds number based on rotational movements is high.

Finally, the first component which is important for low bulk flow Reynolds numbers appears as a systematic contribution to the continuous-phase viscosity.

It does not depend on inclusion flow regimes but becomes preponderant when the relative velocity between phases vanishes.

There are no similar alternative expressions for the second- and third-order extra-deformation tensors.

5.2. Expansion in multipoles of interfacial force densities

Interfacial force densities at a given observation point $\mathbf{x}$ involve continuous-phase interface fields resulting from the contributions of multiple inclusions placed at various positions all around the neighborhood of $\mathbf{x}$. This gives rise to various integrals that are difficult to handle. It is much easier to reverse the order namely fixing a single inclusion at $\mathbf{x}$ and integrating over its conditionally-averaged interface fields. Essentially, this is the multipole expansion method.

Furthermore, observe than in (4.1) the interfacial force density $E[\mathbf{n}^c \cdot \mathbb{T}^* \delta_\Sigma](\mathbf{x})$ differs from its counterpart $\alpha^{d1}(3/4\pi a^3)\mathbf{F}^*(\mathbf{x})$ in (4.18). The latter is viewed by the dispersed phase and the former by the continuous phase. The difference in fact results from the asymmetrical treatment of both phases. The link between these terms can just be shown by an expansion of $E[\mathbf{n}^c \cdot \mathbb{T}^* \delta_\Sigma](\mathbf{x})$ similar to the one performed by BUYEVICH and SHCHELCHKOVA [3] in terms of force multipoles. Their expansion involved all the overall stresses around the inclusions while the present expansion deals only with stresses arising from disturbance flows.

Let us introduce the $\mathrm{m}+1^{\mathrm{th}}$ tensor of order k, at $\mathrm{m} = 0, 1, 2$, which represents the monopole , dipole and other multipole moments of the local stress distribution over a test inclusion, due to the k^{th} order disturbance fields. In the calculations that follow, force multipoles of the first- and second-order disturbance flows are needed:

$$\mathbb{M}^*_{\mathrm{m}+1}(\mathbf{x}) = a^2 \frac{(-1)^{\mathrm{m}+1}}{\mathrm{m}!} \int_{S(\mathbf{x})} \mathbf{n}^{\mathrm{m}+1} \cdot \mathbb{T}^*(\mathbf{x} + a\mathbf{n}|\mathbf{x}) d\Omega, \tag{5.7}$$

where $\mathbf{n}^{\mathrm{m}+1}$ denotes a $\mathrm{m}+1$-fold tensor product of $\mathbf{n}$, and

$$\mathbb{M}^{**}_{\mathrm{m}+1}(\mathbf{x}^\circ|\mathbf{x}) = a^2 \frac{(-1)^{\mathrm{m}+1}}{\mathrm{m}!} \int_{S(\mathbf{x}^\circ)} \mathbf{n}^{\mathrm{m}+1} \cdot [\mathbb{T}^{**}(\mathbf{x}^\circ + a\mathbf{n}|\mathbf{x}^\circ, \mathbf{x}) + \mathbb{T}^*(\mathbf{x}^\circ + a\mathbf{n}|\mathbf{x}^\circ)] \, d\Omega. \tag{5.8}$$

These have the dimension of a force and are tensors of rank $\mathrm{m}+1$, that are symmetrical in their first m indices.

Firstly, it will be noted that $E[\mathbf{n}^c \cdot \mathbb{T}^* \delta_\Sigma](\mathbf{x})$ defined in (3.10) may be re-written as

$$E[\mathbf{n}^c \cdot \mathbb{T}^* \delta_\Sigma](\mathbf{x}) = -E[\mathbf{n} \cdot \mathbb{T}^* \delta_\Sigma](\mathbf{x}) \tag{5.9}$$

$$= -\int \delta(\tilde{\mathbf{x}} - \mathbf{x} + a\mathbf{n})\mathbf{n} \cdot \mathbb{T}^*(\tilde{\mathbf{x}} + a\mathbf{n}|\tilde{\mathbf{x}})\phi^{(1)}(\tilde{\mathbf{x}})d\tilde{\mathbf{x}}$$

$$= -\int \delta(\mathbf{k} + a\mathbf{n})\mathbf{n} \cdot \mathbb{T}^*(\mathbf{x} + \mathbf{k} + a\mathbf{n}|\mathbf{x} + \mathbf{k})\phi^{(1)}(\mathbf{x} + \mathbf{k})d\mathbf{k},$$

where $\mathbf{k} = \tilde{\mathbf{x}} - \mathbf{x}$. Then, by expanding $\mathbf{n} \cdot \mathbb{T}^*(\mathbf{x} + \mathbf{k} + a\mathbf{n}|\mathbf{x} + \mathbf{k})\phi^{(1)}(\mathbf{x} + \mathbf{k})$ in a Taylor series around $\mathbf{x}$, the integrand in (5.9)becomes according to the formula (2.5):

$$E[\mathbf{n}^c \cdot \mathbb{T}^* \delta_\Sigma](\mathbf{x}) = -\int \delta(\mathbf{k} + a\mathbf{n}) \sum_{\mathrm{m}=0}^{\infty} \frac{1}{\mathrm{m}!} \mathbf{k}^{\mathrm{m}} \boxed{\mathrm{m}} \frac{\partial^{\mathrm{m}}}{\partial \mathbf{x}^{\mathrm{m}}} \mathbf{n} \tag{5.10}$$

$$\cdot \mathbb{T}^*(\mathbf{x} + a\mathbf{n}|\mathbf{x})\phi^{(1)}(\mathbf{x})d\mathbf{k} = \sum_{\mathrm{m}=0}^{\infty} \frac{\partial^{\mathrm{m}}}{\partial \mathbf{x}} \boxed{\mathrm{m}} \phi^{(1)}(\mathbf{x}) a^2 \frac{(-1)^{\mathrm{m}+1}}{\mathrm{m}!}$$

$$\int (a\mathbf{n})^{\mathrm{m}} \mathbf{n} \cdot \mathbb{T}^*(\mathbf{x} + a\mathbf{n}|\mathbf{x})d\Omega,$$

where the second line results from a change in integration variables $d\mathbf{k} = r^2 d\Omega dr$, where $r(\mathbf{x}) = |\mathbf{k}|$. Finally, we succeeded in expanding:

$$E[\mathbf{n}^c \cdot \mathbb{T}^* \delta_\Sigma](\mathbf{x}) = \sum_{\mathrm{m}=0}^{\infty} a^{\mathrm{m}} \frac{\partial^{\mathrm{m}}}{\partial \mathbf{x}} \boxed{\mathrm{m}} [\phi^{(1)}(\mathbf{x}) \mathbb{M}^*_{\mathrm{m}+1}(\mathbf{x})] \tag{5.11}$$

$$= N\phi_1(\mathbf{x})\mathbb{M}^*_1(\mathbf{x}) + aN \frac{\partial}{\partial \mathbf{x}} \cdot [\phi_1(\mathbf{x})\mathbb{M}^*_2(\mathbf{x})] + \mathbb{R}^*(\mathbf{x}),$$

where the first and second terms represent the contributions of the monopole and dipole, while the remaining term $\mathbb{R}^*$ represents the total influence of all the other multipoles of higher order. As it will be shown in the future, the above expansion opens the way to various approximation schemes in which only the lowest-order multipoles are retained.

Consider $\overline{\mathbf{n}^{\mathrm{m}}}$, the irreducible tensor of rank m constructed with the vector $\mathbf{n}$, i.e. the traceless tensor that is symmetrical in any pair of its indices. If the tensor $\mathbf{n}^{\mathrm{m}}$ is replaced in (5.8) and (5.9) by $\overline{\mathbf{n}^{\mathrm{m}}}$, the resulting multipoles cannot be reduced and do not contain contributions of lower-rank multipoles. As shown by MAZUR and VAN SAARLOOS [12] in a different context, the above series can be transformed alternatively into a more convenient series of these irreducible multipoles; it should be noted that the monopole and dipole contributions remain the same. Moreover, it can be shown that the remaining contributions are still power expansions of $a\dfrac{\partial}{\partial \mathbf{x}}$ and thus $\mathbb{R}^* = O(\beta^2)$.

Furthermore, the first and second multipole in the multipole expansion (5.11), which are irreducible without transformation, can be easily related to the interaction term already found in the dispersed-phase model since comparing (2.14), (2.16) with (5.8) for $\mathrm{m} = 0, 1$ obviously yields:

$$\mathbf{F}^* = -\mathbb{M}_1^* \quad \text{and} \quad \mathbf{K}^* = a\varepsilon : \mathbb{M}_2^*. \tag{5.12}$$

In fact, the hydrodynamics torque $\mathbf{K}^*$ is only related to the antisymmetrical part $\mathbb{M}_2^{*a}$ of $\mathbb{M}_2$ and, conversely, $\mathbb{M}_2^{*a} = -(2a)^{-1}\varepsilon \cdot \mathbf{K}^*$. Similar relations were derived by MAZUR and VAN SAARLOOS [12]. Generally, the first two force multipoles have a clearer meaning and can be computed more easily than $E[\mathbf{n}^c \cdot \mathbb{T}^* \delta_\Sigma](\mathbf{x})$ as defined in (3.10).

The same arguments as before show that the averaged interfacial force density for the field with one fixed inclusion can be expanded according to:

$$E[\mathbf{n}^c \cdot \mathbb{T}^{**} \delta_\Sigma^1](\mathbf{x}^\circ|\mathbf{x}) = (N-1) \sum_{\mathrm{m}=0}^{\infty} a^{\mathrm{m}} \frac{\partial^{\mathrm{m}}}{\partial \mathbf{x}^{\circ \mathrm{m}}} \boxed{\mathrm{m}} [\chi_2(\mathbf{x}^\circ|\mathbf{x}) \mathbb{M}_{\mathrm{m}+1}^{**}(\mathbf{x}^\circ|\mathbf{x})] \tag{5.13}$$

$$= (N-1)\chi_2(\mathbf{x}^\circ|\mathbf{x})\mathbb{M}_1^{**}(\mathbf{x}^\circ|\mathbf{x}) + a(N-1)\frac{\partial}{\partial \mathbf{x}^\circ} \cdot [\chi_2(\mathbf{x}^\circ|\mathbf{x})\mathbb{M}_2^{**}(\mathbf{x}^\circ|\mathbf{x})]$$

$$+(N-1)\mathbb{R}^{**}(\mathbf{x}^\circ|\mathbf{x}).$$

Unlike the previous case, it is impossible to arrange the expansion terms with respect to β since the space scale of the dependence of various higher-order conditioned variables equals a and not L (see Sec. 2.1). The averaged interfacial force density for the continuous field with two fixed inclusions could equally have been treated in a similar way but its expression will not be presented here. Of course, we have $\mathbb{M}_1^{**}(\mathbf{x}^\circ|\mathbf{x}) = -\mathbf{F}^*(\mathbf{x}^\circ) - \mathbf{F}^{**}(\mathbf{x}^\circ|\mathbf{x})$.

Thus interaction terms in momentum equations could be expressed for any order and any phase in terms of force multipoles. A monopole and a dipole are simply required in the dispersed-phase equations at any order. An infinite sequence of multipoles is stricly necessary for the continuous phase; at the first order, the first two monopoles are clearly enough to provide a good approximation in most cases; at higher-order approximations schemes are more difficult to devise.

6. Conclusions

At the end of Part I, a double hierarchy of equations, one for each phase, was available to lay the fundations of a general description of laminar flows carrying spherical inclusions. Specific two-phase flow models could in principle be

extracted from these infinite hierarchies by proper truncation based on diluteness. This project could not in fact be undertaken readily as the form of several equations was very complicated. This is why the central concept of disturbance flow field in the averaged sense was defined for both phases. The equations for both hierarchies at any order but the first one have been replaced by equations controlling these new disturbance fields. In this way, the equations have proved to be not only simpler but easier to interpret.

The two first-order equations for each phase are not replaced but are just simplified. As they also form the basis of any usual two-fluid model approach, it is worth comparing the traditional position, where "unknown terms" make it necessary to guess the closure equations, to our new position, where these terms are naturally connected to higher-order equations, namely the afore-mentioned disturbance equations. Confining our attention to the momentum equation of the continuous phase, which contains the most difficult closure problems (DREW [4]), four specific "constitutive equations" are needed: the extra-deformation tensor, the interfacial force density, the pressure relation and the pseudo-turbulent stresses.

(i) The extra-deformation tensor is often by-passed in usual two-fluid models. Here, it is expressed in terms of the averaged dispersed-phase velocities and makes various contributions; some are important at low inclusion Reynolds numbers, and others at higher numbers. As far as solid particles are concerned, higher-order equations are not required; our expression was obtained previously by JOSEPH and LUNDGREN [9] in a different context.

(ii) Modelling the interfacial force density in a standard approach is tantamount to introducing various types of force exterted on an isolated inclusion calculated for a physical context defined in a relatively deterministic way: drag force, lift force, virtual mass force, etc. In our approach the isolated inclusion problem is perfectly defined: it is given by the first-order disturbance flow equations. Its solution leads to a sequence of force multipoles describing the interfacial stresses around a test inclusion with increasing precision; it may give some unexpected information, in particular near walls. In this case putting the interfacial force density in the same category as an overall force i.e. as a monopole, seems clearly inappropriate.

Incidentally, it should be noted that almost all the existing "theories" aimed at modelling two-phase flows rely on some typical small-scale hydrodynamics or thermal models for single-particle changes, in order to append the "constitutive relations" for the interfacial exchanges of momentum and energy in a heuristic manner. Our theory proposes a natural framework, the disturbance flow equations, for specifying the micro-problems that need to be solved to provide the missing information.

(iii) The pressure relation due to inclusion movements (STUHMILLER [15]) is simply not needed in our approach. Pressure differences between the averaged bulk pressure and the averaged interfacial pressure do not appear; in our case the extra averaged fields that are introduced are conditionally averaged upon the presence of one inclusion and lead on the contrary to consistent simplifications.

(iv) Unfortunately, a thorough analysis of pseudo-turbulent tensors and of correlation functions is still lacking, in both the continuous-phase momentum equation and in other equations. As they stand, they are just unclosed terms. It is not yet possible to commence the truncation procedure. What will be proposed in the next paper will be to derive expressions for any of them which can be effectively computed in terms of the selected main variables of the two hierarchies.

References

1. J.-L. ACHARD and A. CARTELLIER, *Laminar dispersed two-phase flows at low concentration. Part 1. Generalised system of equations*, Arch. Mech., **52**, 1, 25–53, 2000.
2. H. BRENNER, *The Stokes resistance of an arbitrary particle. Part V. Symbolic operator representation of intrinsic resistance*, Chem. Engng. Sci., **21**, 97–109, 1996.
3. YU. A. BUYEVICH and I. N. SHCHELCHKOVA, *Flow of dense suspensions*, Prog. Aerospace Sci., **18**, 121–150, 1978.
4. D. A. DREW, *Mathematical modeling of two-phase flow*, Ann. Rev. Fluid Mech., **15**, 261–291, 1983.
5. A. EINSTEIN, *Eine neue bestimmung der Moleküldimensionen*, J. Ann. Physik., **19**, 298–306, 1906 (Trans. in 1956 *Theory of Brownian Movement*, Dover).
6. B. U. FELDERHOF, *Dynamics of hard-sphere suspension*, Physica A, **169**, 1–16, 1990.
7. R. GATIGNOL, *The Faxen formulae for a rigid particle in an unsteady non uniform Stokes flow*, J. Mech. Th. Appl., **1**, 143–160, 1983.
8. M. ISHII, *Thermo fluid dynamic theory of two phase flow*, Eyrolles, Paris 1975.
9. D. D. JOSEPH and T. S. LUNDGREN, *Ensemble averaged and mixture theory equations for incompressible fluid-particle suspensions*, Int. Multiphase Flow, **16**, 35–42, 1990.
10. D. LHUILLIER, *Ensemble averaging in slightly non-uniform suspensions*, Eur. J. Mech., B/ Fluids, **11**, 649–661, 1992.
11. T. S. LUNDGREN, *Slow flow through stationary random beds and suspensions of spheres*, J. Fluid Mech., **51**, 273–299, 1972.
12. P. MAZUR and W. VAN SAARLOOS, *Many-sphere hydrodynamics interactions and mobilities in a suspension*, Physica, **115A**, 21–57, 1982.
13. R. I. NIGMATULIN, *Spatial averaging in the mechanics of heretogeneous and dispersed systems*, Int. J. Multiphase Flow., **5**, 353–385, 1979.
14. LORD RAYLEIGH, *The theory of sound*, vol. **II**, (2nd ed.), Dover, New York 1954.
15. J. H. STUHMILLER, *The influence of interfacial pressure forces on the character of two-phase flow model equations*, Int. J. Multiphase Flow, **3**, 551-560, 1977.

Received September 6, 1999; revised version November 18, 1999.

Arch. Mech., **52**, 2, pp. 303–318, Warszawa 2000

Magnetohydrodynamic convective flow in a rotating channel

S. K. GHOSH ([1]) and P. K. BHATTACHARJEE ([2])

([1]) *Department of Mathematics Narajole Raj College*
P.O.: Narajole, Dist: Midnapore West Bengal, India

([2]) *Department of Applied Mathematics Vidyasagar University*
Midnapore West Bengal, India

COMBINED FREE AND FORCED convective flow of an electrically conducting viscous incompressible fluid in a rotating parallel plate channel with perfectly conducting walls is investigated. Exact solutions of the governing equations for the fully developed flow are obtained in closed form. It is found that the resultant shear stresses at the walls decrease with the increase in both the rotation parameter K^2 and the magnetic parameter M^2. The rate of heat transfer at both walls decreases with the increase in the Grashof number G.

1. Introduction

THE STUDY OF FLUID FLOWS subject to the magnetic field and rotation finds wide applications in many fields of geophysical and astrophysical interest. VIDYANIDHI [1] has considered the effect of rotation on the hydromagnetic flow within a non-conducting parallel plate channel. On the other hand, NANDA and MOHANTY [2] have investigated the hydromagnetic flow in a rotating channel with perfectly conducting walls. However, the effect of combined free and forced convection flow does not receive much attention in literature. However, this study may have some bearings on the process of cooling of turbine blades, power generation, geophysical and astrophysical problems. Recently GUPTA [3] has studied the effect of combined free and forced convection on the flow of a viscous incompressible fluid in a parallel plate channel rotating with uniform angular velocity about an axis perpendicular to the plates.

In the present paper we have considered the combined free and forced convective flow of an electrically conducting viscous incompressible fluid confined between two horizontal perfectly conducting plates, rotating at a uniform angular velocity Ω about an axis perpendicular to their planes, in the presence of an applied uniform transverse magnetic field parallel to the axis of rotation. Exact solution of the governing equations for the fully developed flow is obtained in a closed form. The asymptotic behaviour of the solution is also analysed for both

small and large rotation parameter K^2 and the magnetic parameter M^2, to get some physical insight into the flow pattern. Heat transfer characteristics are also studied taking into account the viscous and Joule dissipations.

2. Mathematical formulation and its solution

Consider the steady, fully developed combined free and forced convection flow of an electrically conducting viscous incompressible fluid within a perfectly conducting parallel plate channel $z = \pm L$ due to a constant pressure gradient along the x-axis. A uniform magnetic flux density B_0 is imposed along the z-axis about which both the fluid and plates rotate at a uniform angular velocity Ω.

Since the plates of the channel are infinite in the x and y directions, all physical quantities except the pressure and temperature will be functions of z only. Rotation induces cross-flow, the velocity of fluid and magnetic field may be assumed as $q = (u^*, v^*, 0)$ and $B = \left(B_x^*, B_y^*, B_0\right)$, respectively, compatible with the fundamental equations of magnetohydrodynamics where $\mathbf{q}$ is the velocity vector and $\mathbf{B}$ is the magnetic field vector. The equation of continuity leads to a conservation of mass i.e. $\nabla \cdot q = 0$ and the solenoidal relation is $\nabla \cdot B = 0$. Therefore, under these assumptions, the equations of momentum and the magnetic induction in a rotating frame of reference can be written as

$$-2\rho\Omega v^* = -\frac{\partial P}{\partial x} + \mu\frac{\partial^2 u^*}{\partial z^2} + \frac{B_0}{\mu_e}\frac{\partial B_x^*}{\partial z}, \tag{2.1}$$

$$2\rho\Omega u^* = \mu\frac{\partial^2 v^*}{\partial z^2} + \frac{B_0}{\mu_e}\frac{\partial B_y^*}{\partial z}, \tag{2.2}$$

$$0 = -\frac{\partial p}{\partial z} - \rho g - \frac{1}{\mu_e}\left(B_x^*\frac{\partial B_x^*}{\partial z} + B_y^*\frac{\partial B_y^*}{\partial z}\right), \tag{2.3}$$

$$\frac{\partial^2 B_x^*}{\partial z^2} + \sigma\mu_e B_0\frac{\partial u^*}{\partial z} = 0, \tag{2.4}$$

$$\frac{\partial^2 B_y^*}{\partial z^2} + \sigma\mu_e B_0\frac{\partial v^*}{\partial z} = 0, \tag{2.5}$$

where ρ, μ, μ_e, σ, g and p are, respectively, the fluid density, coefficient of viscosity, magnetic permeability, electrical conductivity, acceleration due to gravity and modified pressure including the centrifugal force.

Assuming uniform axial temperature variation along the channel walls, the temperature of the fluid can be assumed in the form

$$T - T_0 = Nx + \phi(z), \tag{2.6}$$

where N is the uniform temperature gradient, T is the fluid temperature and T_0 is the temperature in the reference state.

Using the equation of state under the Boussinesq approximation

$$\rho = \rho_0[1 - \beta(T - T_0)]. \tag{2.7}$$

We obtain from Eq. (2.3) after integration

$$p = -\rho_0 g \int [1 - \beta(T - T_0)]\, dz - \frac{1}{2\mu_e}\left(B_x^{*2} + B_y^{*2}\right) + F^*(x), \tag{2.8}$$

where β is the coefficient of thermal expansion and ρ_0 is the density of reference state.

Making use of Eqs. (2.6) and (2.8) in Eq. (2.1), we obtain

$$-2\Omega v^* = -g\beta N z - \frac{1}{\rho_0}\frac{dF^*(x)}{dx} + \nu\frac{d^2u^*}{dz^2} + \frac{B_0}{\mu_e\rho_0}\frac{dB_x^*}{dz}, \tag{2.9}$$

where $\nu = \mu/\rho_0$.

Introducing non-dimensional variables

$$\eta = \frac{z}{L}, \quad u = \frac{u^*L}{\nu R}, \quad v = \frac{v^*L}{\nu R},$$

$$B_x = B_x^*/\sigma\mu_e\nu B_0 R, \quad B_y = B_y^*/\sigma\mu_e\nu B_0 R, \quad R = \left(L^3/\rho_0\nu^2\right)\left(-\frac{dF^*}{dx}\right), \tag{2.10}$$

Equations (2.9), (2.2), (2.4) and (2.5) reduce to

$$\frac{d^2u}{d\eta^2} + M^2\frac{dB_x}{d\eta} + 2K^2 v = -1 + G\eta, \tag{2.11}$$

$$\frac{d^2v}{d\eta^2} + M^2\frac{dB_y}{d\eta} - 2K^2 u = 0, \tag{2.12}$$

$$\frac{d^2B_x}{d\eta^2} + \frac{du}{d\eta} = 0, \tag{2.13}$$

$$\frac{d^2B_y}{d\eta^2} + \frac{dv}{d\eta} = 0, \tag{2.14}$$

where $M = B_0L(\sigma/\rho_0\nu)^{1/2}$ is the Hartmann number, $K^2 = \Omega L^2/\nu$ is the rotation parameter, and $G = g\beta NL^4/\nu^2 R$ is the Grashof number.

The boundary conditions for the velocity field are the usual no-slip conditions at the plates, i.e.

$$u = v = 0 \quad \text{at } \eta = \pm 1. \tag{2.15}$$

Since the plates are assumed to be perfectly conducting, the boundary conditions for magnetic field are

$$\frac{dB_x}{d\eta} = \frac{dB_y}{d\eta} = 0 \quad \text{at } \eta = \pm 1. \tag{2.16}$$

Combining Eqs. (2.11) and (2.13) with Eqs. (2.12) and (2.14) respectively, we obtain

$$\frac{d^2F}{d\eta^2} + M^2\frac{db}{d\eta} - 2iK^2F = -1 + G\eta, \tag{2.17}$$

$$\frac{d^2b}{d\eta^2} + \frac{dF}{d\eta} = 0, \tag{2.18}$$

where

$$F = u + iv \quad \text{and } b = B_x + iB_y. \tag{2.19}$$

The boundary conditions (2.15) and (2.16) become

$$F = 0 \quad \text{and} \frac{db}{d\eta} = 0 \quad \text{at } \eta = \pm 1. \tag{2.20}$$

The solution of Eqs. (2.17) and (2.18) subject to the boundary conditions (2.20) is

$$F(\eta) = \frac{(\alpha - i\beta)^2}{(\alpha^2+\beta^2)^2}\left[\left(1 - \frac{\operatorname{ch}(\alpha+i\beta)\eta}{\operatorname{ch}(\alpha+i\beta)}\right) + G\left(\frac{\operatorname{sh}(\alpha+i\beta)\eta}{\operatorname{sh}(\alpha+i\beta)} - \eta\right)\right], \tag{2.21}$$

$$b(\eta) = \frac{(\alpha - i\beta)^2}{(\alpha^2+\beta^2)^2}\left[\left(\frac{\operatorname{sh}(\alpha+i\beta)\eta}{(\alpha+i\beta)\operatorname{ch}(\alpha+i\beta)} - \eta\right) + \frac{G}{2}\left(\eta^2 - \frac{2\operatorname{ch}(\alpha+i\beta)\eta}{(\alpha+i\beta)\operatorname{sh}(\alpha+i\beta)} + \frac{2\operatorname{cth}(\alpha+i\beta)}{(\alpha+i\beta)} - 1\right)\right], \tag{2.22}$$

where

$$\alpha = \frac{1}{\sqrt{2}}\left[\left(M^4 + 4K^4\right)^{1/2} + M^2\right]^{1/2},$$
$$\beta = \frac{1}{\sqrt{2}}\left[\left(M^4 + 4K^4\right)^{1/2} - M^2\right]^{1/2}. \tag{2.23}$$

Considering the expressions of $F(\eta)$ and $b(\eta)$ given by (2.19), one can easily obtain the x and y components of the velocity and magnetic field from Eqs. (2.21) and (2.22), respectively.

In the absence of the buoyancy force (i.e. $G = 0$), the solutions (2.21) and (2.22) reduce to the results obtained by NANDA and MOHANTY [2].

Now we shall discuss a few particular cases of interest of the general solution given by Eqs. (2.21) and (2.22).

Case 1: $M^2 \ll 1$ and $K^2 \ll 1$

Since M^2 and K^2 are very small, neglecting higher powers of M^2 and K^2 in Eqs. (2.21) and (2.22), we obtain

$$u = \frac{1}{2}(1-\eta^2) + \frac{1}{3}G(\eta^3 - \eta) + M^2\left[-\frac{1}{24}(5 - 6\eta^2 + \eta^4) + \frac{G}{360}(7\eta - 10\eta^3 + 3\eta^5)\right] + \ldots, \tag{2.24}$$

$$v = K^2\left[-\frac{1}{12}(5 - 6\eta^2 + \eta^4) + \frac{G}{180}(7\eta - 10\eta^3 + 3\eta^5)\right] + \ldots, \tag{2.25}$$

$$B_x = \frac{1}{6}(\eta^3 - \eta) + \frac{G}{24}(-1 + 2\eta^2 - \eta^4) + M^2\left[\frac{1}{24}\left(5\eta - 2\eta^3 - \frac{1}{5}\eta^5\right) + \frac{G}{720}(7\eta^2 - 5\eta^4 + \eta^6)\right] + \ldots, \tag{2.26}$$

$$B_y = K^2\left[\frac{1}{12}\left(5\eta - 2\eta^3 + \frac{1}{5}\eta^5\right) - \frac{G}{360}(7\eta^2 - 5\eta^4 + \eta^6)\right] + \ldots. \tag{2.27}$$

Equations (2.24) – (2.27) reveal that in a slowly rotating system when the conductivity of fluid is low and the applied magnetic field is weak, the effect of magnetic field on the secondary flow v and on the induced magnetic field component B_y is negligible while the primary flow u and the induced magnetic field component B_x are uneffected by rotation. In absence of the rotation and magnetic fields, the problem reduces to the free and forced convection flow through a horizontal parallel plate channel due to a constant pressure gradient. In this case, the critical Grashof number $G_{\text{crit}} = \frac{1}{2}$.

Case 2: $K^2 \gg 1$ and $M^2 \sim O(1)$.

When rotation is very large and the applied magnetic field is weak, we can expect a boundary layer type of flow. For the boundary layer on the upper plate $\eta = 1$, writing $(1 - \eta) = \xi$, we obtain from Eqs. (2.21) and (2.22) the results

$$u = \frac{(1-G)}{2K^2} \exp\left[-K\left(1+\frac{M^2}{4K^2}\right)\xi\right] \sin\left[K\left(1-\frac{M^2}{4K^2}\right)\xi\right], \tag{2.28}$$

$$v = \frac{1}{2K^2}\left[-1+(1-\xi)\,G+(1-G)\exp\left\{-K\left(1+\frac{M^2}{4K^2}\right)\xi\right\} \times \cos\left\{K\left(1-\frac{M^2}{4K^2}\right)\xi\right\}\right], \tag{2.29}$$

$$B_x = -\frac{1}{2K^3}\left[\frac{1}{2}G+\frac{(1-G)}{\sqrt{2}}\exp\left\{-K\left(1+\frac{M^2}{4K^2}\right)\xi\right\} \times \sin\left\{K\left(1-\frac{M^2}{4K^2}\right)\xi+\frac{\pi}{4}\right\}\right], \tag{2.30}$$

$$B_y = -\frac{1}{2K^3}\left[K\left\{-1+\xi+\frac{1}{2}G\xi(\xi-2)\right\}+\frac{G}{2}+\frac{(1-G)}{\sqrt{2}} \times \exp\left\{-K\left(1+\frac{M^2}{4K^2}\right)\xi\right\}\cos\left\{K\left(1-\frac{M^2}{4K^2}\right)\xi+\frac{\pi}{4}\right\}\right]. \tag{2.31}$$

Equations (2.28) – (2.31) demonstrate the existence of a thin boundary layer of thickness $O\left\{K\left(1+\frac{M^2}{4K^2}\right)\right\}^{-1}$ in the vicinity of the wall ($\eta = 1$). This layer may be identified as a hydromagnetic Ekman layer and can be considered as a classical Ekman boundary layer modified by a uniform applied magnetic field parallel to the axis of rotation. The exponential terms in the expressions (2.28) – (2.31) damp out quickly as ξ increases. When $\xi \geq \frac{1}{K(1+M^2/4K^2)}$, we have

$$u \approx 0, \quad v \approx \frac{1}{2K^2}\left[-1+(1-\xi)G\right], \tag{2.32}$$

$$B_x \approx -\frac{G}{4K^3}, \quad B_y \approx -\frac{1}{2K^3}\left[K\left\{-1+\xi+\frac{1}{2}G\xi(\xi-2)\right\}+\frac{G}{2}\right]. \tag{2.33}$$

Equation (2.32) reveals that in the certain core, given by $\xi \geq 1/K(1+M^2/4K^2)$ about the axis of the channel, i.e. outside the boundary layer region, the velocity in the direction of pressure gradient vanishes while it remains in the y-direction. Thus, in the central core, the fluid will be moving in a direction normal to the pressure gradient and the axis of rotation. It is also evident from Eqs. (2.32) and (2.33) that, in the central core, the velocity and the magnetic field components

are independent of the applied magnetic field, and the magnetic field component B_x is very weak of order $O(G/4K^2)$.

Case 3: $M^2 \gg 1$ and $K^2 \sim O(1)$.

In this case also the flow has a boundary layer character and we obtain the velocity and magnetic field components from Eqs. (2.21) and (2.22) as

$$u = \frac{1}{M^2}\left[(1-\exp(-M\xi)\right\} + G\left\{-1+\xi+\exp(-M\xi)\right\}], \tag{2.34}$$

$$v = \frac{K^2}{M^4}\left[\left\{(2+M\xi)\exp(-M\xi) - 2\right\} + G\left\{2(1-\xi)\right.\right. \\ \left.\left. -(2+M\xi)\exp(-M\xi)\right\}\right], \tag{2.35}$$

$$B_x = \frac{1}{M^2}\left[\left\{-1+\xi+\frac{1}{M}\exp(-M\xi)\right\} + G\left\{\frac{1}{2}\xi(2-\xi)\right.\right. \\ \left.\left. +\frac{1}{M}(1-\exp(-M\xi))\right\}\right], \tag{2.36}$$

$$B_y = \frac{K^2}{M^4}\left[\left\{2-(2+\frac{1}{M}\exp(-M\xi))\xi - \frac{3}{M}\exp(-M\xi) + G\left\{\xi(2-\xi)\right.\right.\right. \\ \left.\left.\left. - \frac{1}{M}(3-\xi M\exp(-M\xi)) + \frac{3}{M}\exp(-M\xi)\right\}\right]. \tag{2.37}$$

Expressions (2.34) – (2.37) demonstrate the existence of a thin boundary layer of thickness $O(1/M)$ near the plate $\eta = 1$ which is independent of the rotation parameter K^2. This layer may be identified as the Hartmann layer. It is interesting to note that the secondary velocity v and magnetic field B_y are very weak being $O(K^2/M^4)$, while the primary velocity u and magnetic field B_x are unaffected by the rotation of the fluid. Therefore from expressions (2.34) and (2.35) we may conclude that in the central core given by $\xi \geq \frac{1}{4}$ the fluid will be moving in the direction of the pressure gradient.

3. Results and discussion

The non-dimensional shear stress components at the plates $\eta = \pm 1$ are

$$\left.\frac{du}{d\eta}\right|_{\eta=\pm1} = \frac{1}{(\alpha^2+\beta^2)}\left[\mp\frac{\alpha \mathrm{sh}2\alpha + \beta sin2\beta}{(\mathrm{ch}2\alpha + \cos 2\beta)} + G\left\{\frac{\alpha \mathrm{sh}2\alpha - \beta \sin 2\beta}{(\mathrm{ch}2\alpha - \cos 2\beta)} - \frac{(\alpha^2-\beta^2)}{(\alpha^2+\beta^2)}\right\}\right], \tag{3.1}$$

$$\left.\frac{dv}{d\eta}\right|_{\eta=\pm1} = -\frac{1}{(\alpha^2+\beta^2)}\left[\mp\frac{\beta \mathrm{sh}2\alpha - \alpha \sin 2\beta}{(\mathrm{ch}2\alpha + \cos 2\beta)} + G\left\{\frac{\beta \mathrm{sh}2\alpha + \alpha \sin 2\beta}{(\mathrm{ch}2\alpha - \cos 2\beta)} - \frac{2\alpha\beta}{(\alpha^2+\beta^2)}\right\}\right]. \tag{3.2}$$

The upper and lower signs in the Eqs. (3.1) and (3.2) correspond to values at the upper wall ($\eta = +1$) and the lower wall ($\eta = -1$), respectively.

The primary shear stress $\left.\frac{du}{d\eta}\right|_{\eta=-1}$ will vanish if the critical Grashof number equals

$$G_{cx} = -\frac{a_1(\alpha \mathrm{sh}2\alpha + \beta \sin 2\beta)}{(a_2 - a_3)}, \tag{3.3}$$

where

$$\begin{aligned} a &= \mathrm{ch}2\alpha - \cos 2\beta, \\ a_1 &= a(\alpha^2+\beta^2)/(\sigma \mathrm{ch}2\alpha + \cos 2\beta), \\ a_2 &= (\alpha^2+\beta^2)\alpha \mathrm{sh}2\alpha + a\beta^2, \\ a_3 &= (\alpha^2+\beta^2)\beta \sin 2\beta + a\alpha^2. \end{aligned} \tag{3.4}$$

The numerator in (3.3) is always positive, since $\mathrm{ch}2\alpha > \cos 2\beta$ for all values of M^2 and K^2. Thus when $a_2 > a_3$, there will be an incipient primary flow reversal at the lower plate when the temperature of the lower plate decreases.

Similarly, the secondary shear stress $\left.\frac{dv}{d\eta}\right|_{\eta=-1}$ will vanish if the critical Grashof number equals

$$G_{cy} = -\frac{a_1(\beta \mathrm{sh}2\alpha - \alpha \sin 2\beta)}{(a_4 - a_5)}, \tag{3.5}$$

where

$$\begin{aligned} a_4 &= (\alpha^2+\beta^2)(\beta \mathrm{sh}2\alpha + \alpha \sin 2\beta), \\ a_5 &= (2\alpha\beta)(\mathrm{ch}2\alpha - \cos 2\beta). \end{aligned} \tag{3.6}$$

Equations (3.5) and (3.6) show that for the decrease in the temperature at the lower wall, there will be an incipient reversed secondary flow near the lower wall ($\eta = -1$), $\beta \mathrm{sh}2\alpha > \alpha \sin 2\beta$ and $a_4 > a_5$ or $\beta \mathrm{sh}2\alpha < \alpha \sin 2\beta$ and $a_4 < a_5$. Also due to the increase in temperature in the axial direction of the lower plate, the secondary flow shows the reversal when $\beta \mathrm{sh}2\alpha > \alpha \sin 2\beta$ and $a_4 > a_5$ or $\beta \mathrm{sh}2\alpha < \alpha \sin 2\beta$ and $a_4 > a_5$. Proceeding exactly in the same way, we observe that the primary flow reversal near the upper plate $\eta = 1$ occurs, if

$$G_{cx} = \frac{a_1(\alpha \mathrm{sh}2\alpha + \beta \sin 2\beta)}{(a_2 - a_3)}. \tag{3.7}$$

Equation (3.7) reveals that the primary flow reversal occurs only when temperature of the upper wall increases in the axial direction.

Similarly, for secondary flow reversal at the upper plate $\eta = 1$, we get

$$G_{cy} = \frac{a_1(\beta \mathrm{sh}2\alpha - \alpha \sin 2\beta)}{(a_4 - a_5)}. \tag{3.8}$$

Equations (3.7) and (3.8) are the same as (3.3) and (3.5) respectively, taken with opposite sign.

The values of the critical Grashof numbers G_{cx} and G_{cy} given by (3.3) and (3.5), respectively, for which the primary and secondary flow reversal occur near the lower plate, are given in Tables 1 and 2 for various values of K^2 and M^2. It is observed that G_{cx} and G_{cy} decrease with the increase in the rotation parameter K^2. Hence we may conclude that rotation exerts a destabilizing effect on the primary as well as on the secondary flow.

Table 1. Critical Grashof number G_{cx}.

M^2/K^2	1.0	2.0	3.0	25.0	81.0
10	1.437079	1.403206	1.356935	1.036904	1.006681
15	1.340707	1.327579	1.307924	1.052206	1.009877
20	1.285041	1.278675	1.268736	1.065118	1.012967
25	1.248529	1.244960	1.239268	1.075641	1.015942

Table 2. Critical Grashof number G_{cy}.

M^2/K^2	1.0	2.0	3.0	25.0	81.0
10	2.439813	2.351326	2.229098	1.276532	1.129143
15	2.009786	1.979156	1.933043	1.285473	1.131058
20	1.791160	1.777421	1.755917	1.291425	1.132857
25	1.659765	1.652515	1.640924	1.294541	1.134537

The resultant shear stresses at the plates $\eta = 1$ and $\eta = -1$ are, respectively,

$$\tau_1 = \left\{ \left(\frac{du}{d\eta} \right)^2_{\eta=1} + \left(\frac{dv}{d\eta} \right)^2_{\eta=1} \right\}^{1/2}, \tag{3.9}$$

and

$$\tau_2 = \left\{ \left(\frac{du}{d\eta} \right)^2_{\eta=-1} + \left(\frac{dv}{d\eta} \right)^2_{\eta=-1} \right\}^{1/2}. \tag{3.10}$$

The values of τ_1 and τ_2 have been calculated numerically and are presented in Tables 3 and 4 for various values of K^2 and M^2. It is observed that both τ_1 and τ_2 decrease with the increase in either K^2 or M^2.

Table 3. Resultant shear stress τ_1 at the plate $\eta = 1$ for $G = 0.2$.

M^2/K^2	1.0	2.0	3.0	25.0	81.0
10	0.268977	0.261635	0.251059	0.115098	0.063697
15	0.218611	0.215692	0.211190	0.113824	0.063633
20	0.188317	0.186856	0.184539	0.112111	0.063539
25	0.167693	0.166853	0.165495	0.110057	0.063416

Table 4. Resultant shear stress τ_2 at the plate $\eta = -1$ for $G = 0.2$.

M^2/K^2	1.0	2.0	3.0	25.0	81.0
10	0.355559	0.347190	0.238894	0.165038	0.093297
15	0.295138	0.291708	0.505540	0.163032	0.093175
20	0.257682	0.255926	0.181505	0.160462	0.093105
25	0.231636	0.230604	0.163680	0.157465	0.092804

The primary and secondary velocity profiles have been plotted versus η for various values of K^2 and G (when flow does not separate) in Figs. 1 and 2. In Fig. 1 it is found that for fixed G, the primary velocity u decreases while the secondary flow is of an oscillatory nature with increase in K^2. Figure 2 reveals that when K^2 is small, the primary velocity increases near the lower wall $\eta = -1$ while it decreases near the upper wall $\eta = 1$ with the increase in G. The effect of G on the secondary velocity $(-v)$ is reversed as compared with the effect on the primary velocity u. It may be noted that due to the presence of buoyancy force, the velocity profiles are no longer symmetric.

The magnetic field components B_x and B_y have been depicted versus η for various values of K^2 and G in Figs. 3 and 4. It is observed from Fig. 3 that the magnetic field component B_x decreases with the increase in K^2 while the magnetic field component B_y is of oscillatory character with the increase in K^2.

Figure 4 reveals that the magnetic field components B_x and B_y decrease with the increase in G.

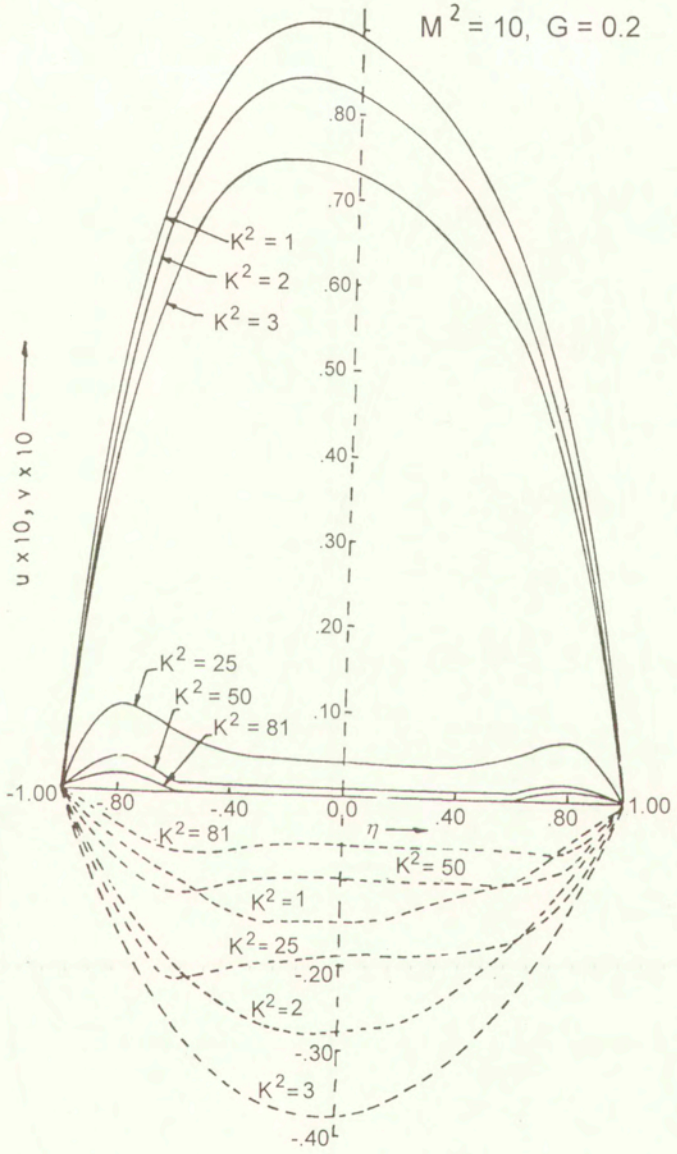

FIG. 1. Velocity distributions (— $u \times 10$, - - - - $v \times 10$) in primary and secondary flow directions.

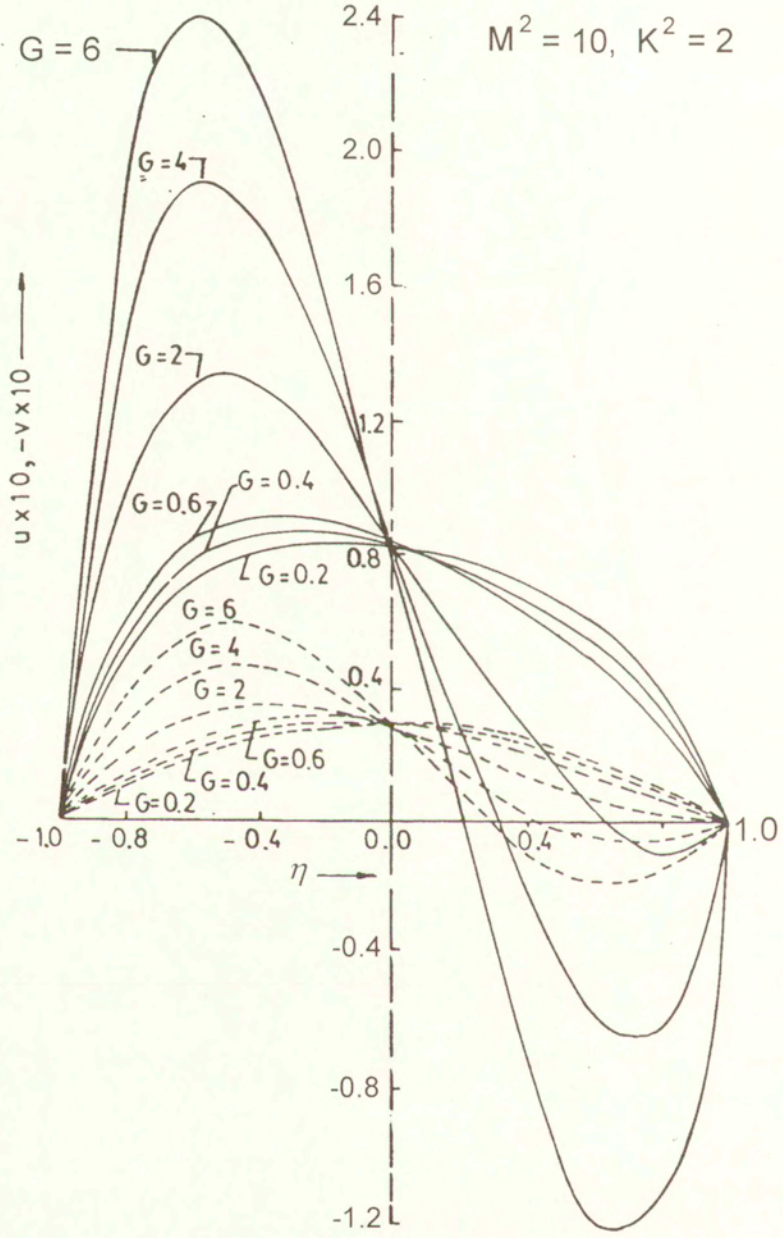

FIG. 2. Velocity distributions (— $u \times 10$, - - - - $v \times 10$) in primary and secondary flow directions.

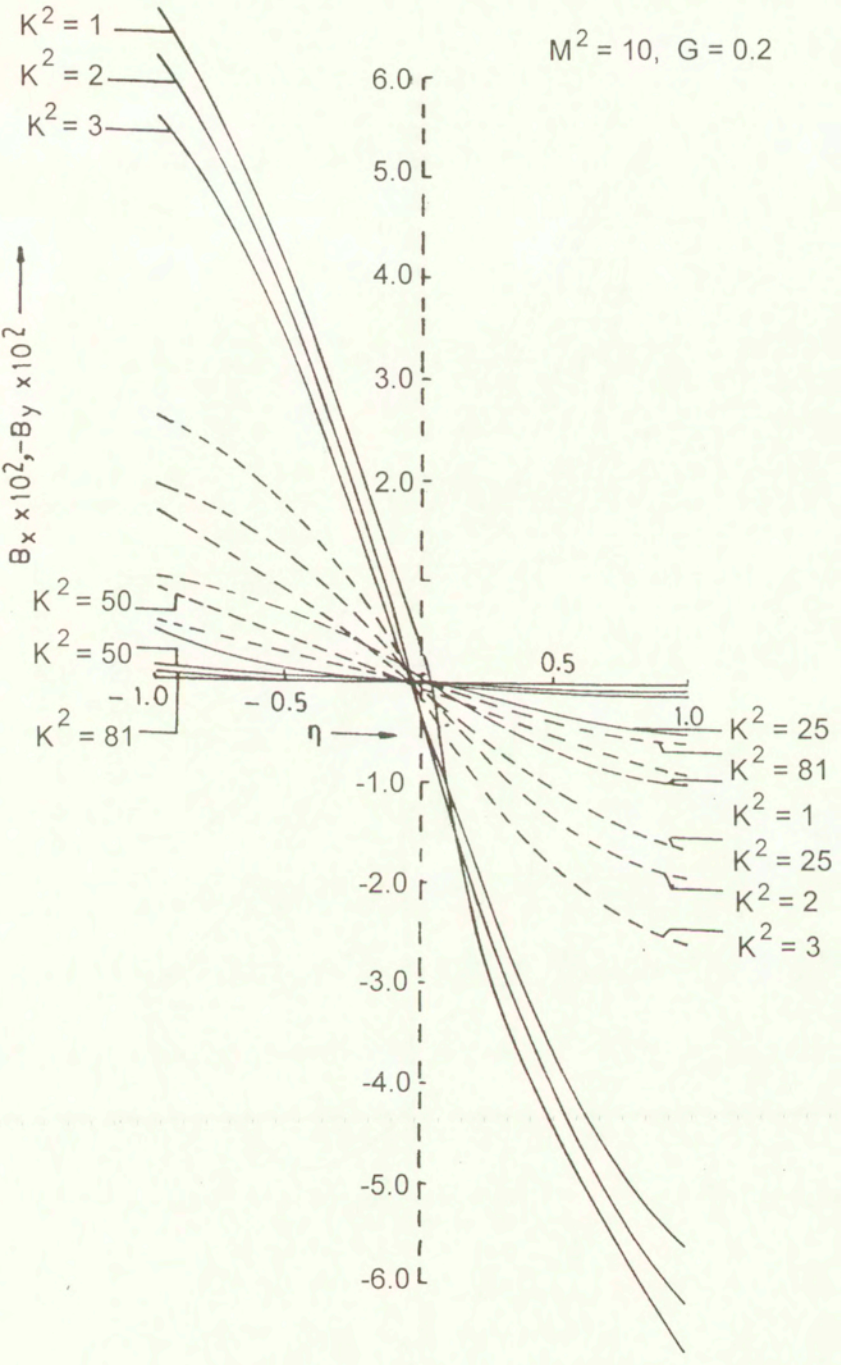

FIG. 3. Magnetic field distributions (— $B_x \times 10^2$, - - - - $B_y \times 10^2$) in primary and secondary flow directions.

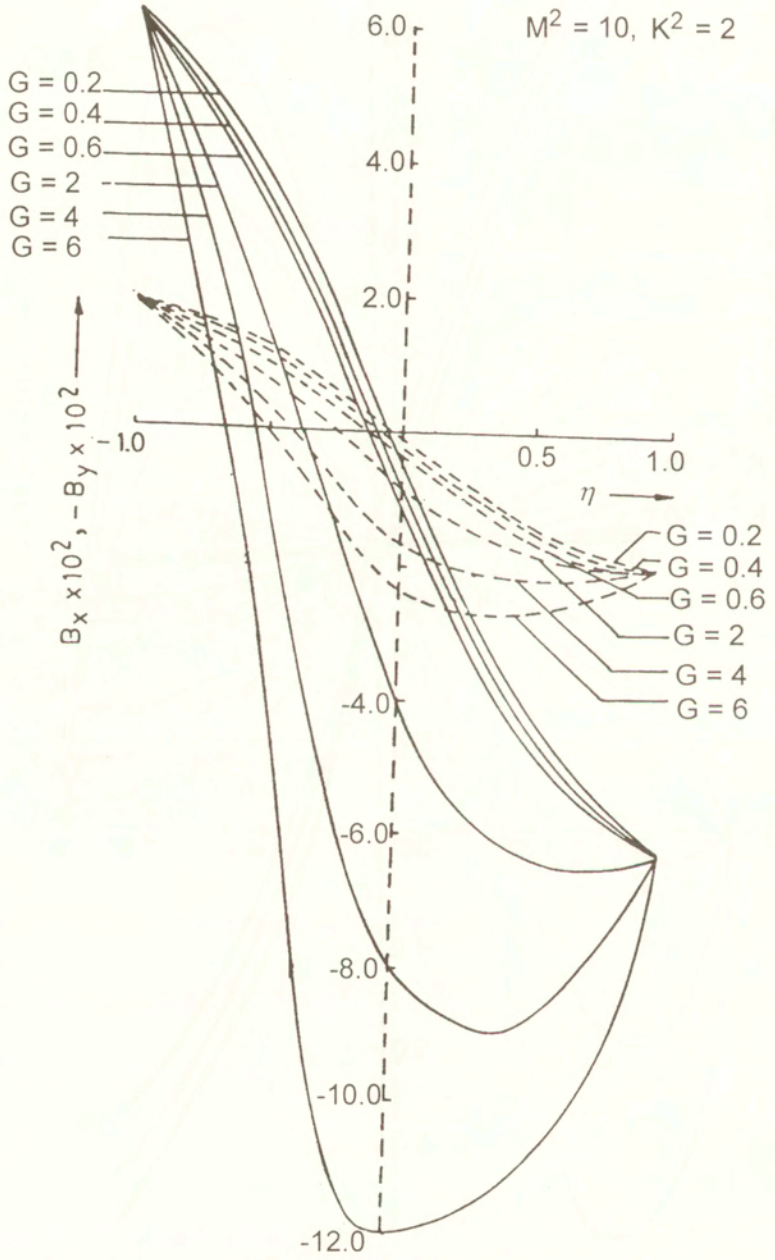

FIG. 4. Magnetic field distributions (— $B_x \times 10^2$, - - - - $B_y \times 10^2$) in primary and secondary flow directions.

4. Heat transfer

For the fully developed flow, the energy equation is

$$u^* \frac{\partial (T - T_0)}{\partial x} = \frac{K}{\rho_0 C_p} \frac{\partial^2 (T - T_0)}{\partial z^2} + \frac{\mu}{\rho_0 C_p} \left[\left(\frac{du^*}{dz} \right)^2 + \left(\frac{dv^*}{dz} \right)^2 \right] + \frac{1}{\mu_e^2 \rho_0 \sigma C_p} \left[\left(\frac{dB_x^*}{dz} \right)^2 + \left(\frac{dB_y^*}{dz} \right)^2 \right], \tag{4.1}$$

where C_p is the specific heat at constant pressure and k is the thermal conductivity. The last two terms in the parentheses are the viscous and Joule dissipation, respectively.

Using (2.6), (2.7), (2.10) and (2.19), Eq. (4.1) becomes

$$\frac{d^2\theta}{d\eta^2} = P_r u - K_1 \left[\frac{dF}{d\eta} \frac{\overline{dF}}{d\eta} + M^2 \frac{db}{d\eta} \frac{\overline{db}}{d\eta} \right], \tag{4.2}$$

where

$$P_r = (\mu/K) C_p, \qquad \theta(\eta) = \phi / NL, \qquad K_1 = \rho_0 \nu^2 R / KNL^3,$$

$$\frac{dF}{d\eta} \frac{\overline{dF}}{d\eta} = \left(\frac{du}{d\eta} \right)^2 + \left(\frac{dv}{d\eta} \right)^2, \quad \frac{db}{d\eta} \frac{\overline{db}}{d\eta} = \left(\frac{dB_x}{d\eta} \right)^2 + \left(\frac{dB_y}{d\eta} \right)^2.$$

We assume the reference temperature T_0 in such a way that temperature at the plate $\eta = -1$ is $T_0 + Nx$ and thus, by virtue of (2.6), we get $\phi(-1) = 0$. Hence the temperature boundary conditions are

$$\theta(-1) = 0 \quad \text{and} \quad \theta(1) = \phi(1)/NL = N_1 (\text{say}), \tag{4.3}$$

where N_1 is the wall temperature parameter.

Substituting the values of $F(\eta)$ and $b(\eta)$ from Eqs. (2.21) and (2.22) in Eq. (4.2) and solving the resulting differential equation subject to the boundary conditions (4.3), we obtain the expression for $\theta(\eta)$ which is rather complicated. We omit the details of calculations since they are lengthy. We have calculated numerically the rate of heat transfer at both the plates for various values of K^2 and G and presented the results in Tables 5 and 6. It is observed from Tables 5 and 6 that the rate of heat transfer at both the plates decreases with the increase in G. On the other hand, with increase in K^2 , the rate of heat transfer at the upper plate increases while that at the lower plate decreases.

Table 5. Rate of heat transfer $\left.\frac{d\theta}{d\eta}\right|_{\eta=1}$ **for** $P_r = 0.025$, $K_1 = 0.5$, $N_1 = 0.5$ **and** $M^2 = 10$.

G/K^2	1.0	2.0	3.0	25.0	81.0
0.0	0.218247	0.220370	0.223320	0.247559	0.249672
0.2	0.201979	0.204935	0.209022	0.244038	0.248510
0.4	0.185251	0.189052	0.194295	0.240429	0.247332

Table 6. Rate of heat transfer $\left.\frac{d\theta}{d\eta}\right|_{\eta=-1}$ **for** $P_r = 0.025$, $K_1 = 0.5$, $N_1 = 0.5$ **and** $M^2 = 10$.

G/K^2	1.0	2.0	3.0	25.0	81.0
0.0	0.134156	0.131785	0.128517	0.102536	0.100336
0.2	0.103589	0.102013	0.099832	0.084113	0.081915
0.4	0.073481	0.072689	0.071576	0.065779	0.068062

Acknowledgment

We are grateful to the referee for his helpful suggestion for the preparation of this paper. One of the authors (S.K. GHOSH) is sincerely acknowledged to University Grants Commission for financial support in persuing work under the scheme "Minor Research Project".

References

1. V. VIDYANIDHI, *Hydromagnetic flow in a channel with non-conducting walls*, J.Math. Phys. Sci., **3**, 193, 1969.
2. R. S. NANDA and H. K.MOHANTY, *Hydromagnetic flow in a rotating channel*, Appl. Sci. Res., **24**, 65, 1971.
3. P. S. GUPTA, *MHD combined free and forced convective flow in a rotating channel*, ZAMM, **54**, 359, 1974.

Received May 13, 1999; revised version January 10, 2000.

Arch. Mech., 2, pp. 319–327, Warszawa 2000

Brief Notes

Quasifractional approximants for effective conductivity of regular arrays of spheres [1]

I. ANDRIANOV (*), V. DANISHEVS'KYY (**)
and S. TOKARZEWSKI (***)

(*) *Department of Mathematics, Prydniprovska State Academy of Civil Engineering and Architecture,*
24a Chernyshevskogo St., Dnipropetrovsk 49600 Ukraine

(**) *Department of Heating and Ventilation,*
Prydniprovska State Academy of Civil Engineering and Architecture,
24a Chernyshevskogo St., Dnipropetrovsk 49600, Ukraine
e-mail: vdanish@lot.apex.dp.ua

(***) *Centre of Mechanics*
Institute of Fundamental Technological Research,
Świętokrzyska 21, 00-049 Warsaw, Poland
e-mail: stokarz@ippt.gov.pl

WE STUDY THE EFFECTIVE HEAT conductivity of regular arrays of perfectly conducting spheres embedded in a matrix with the unit conductivity. Quasifractional approximants allow us to derive an approximate analytical solution, valid for all values of the spheres volume fraction $\varphi \in [0; \varphi_{\max}]$ ($\varphi_{\max}$ is the maximum limiting volume of a sphere). As the bases we use a perturbation approach for $\varphi \to 0$ and an asymptotic solution for $\varphi \to \varphi_{\max}$. Three different types of the spheres space arrangement (simple, body and face-centred cubic arrays) are considered. The obtained results give a good agreement with numerical data.

1. Introduction

ONE OF THE MAIN TASKS of the theory of dispersed media is a theoretical prediction of effective transport properties. The problem could be formulated in a number of mathematically equivalent ways, but here we shall discuss it in the language

[1]) The main results of this paper were presented at the 32nd Solid Mechanics Conference (Zakopane, 1998) [12, 13].

of heat conductivity: we wish to determine the effective heat conductivity k of infinite regular arrays of identical, perfectly conducting spheres of the volume fraction φ, embedded in an isotropic matrix with the unit conductivity.

BATCHELOR [1] displayed a number of light distinct physical problems which can be solved by analogous mathematical methods. One of these is the above mentioned conductivity problem, while others involve calculating the dielectric constant, the magnetic permeability, the electric conductivity, elastic constants, etc. Thus, prediction of the effective conductivity of a two-phase medium spans many fields, and a great deal of efforts have been devoted to its resolution. Therefore, we can not possibly summarise even a small fraction of the previous investigations of the subject. A detailed review can be found, for example, in ref. [1]. Here we shall give a brief account of those papers of direct relevance to our work.

The calculation of k for general types of composites was originally discussed by J. C. MAXWELL [2], and subsequently has been considered by many others. The solution for the case of small spheres (φ tends to zero) was first examined by Lord RAYLEIGH [3], who described the polarization of each sphere in an external field by an infinite set of multipole moments. This method has recently been extended, with the aid of modern digital computers, so that a large number of multipoles can now be calculated [4, 5].

In the case of large, nearly touching spheres (φ tends to its maximum limiting value $\varphi_{\max}$), KELLER [6] derived an asymptotic solution of the problem. His work was extended by BATCHELOR and O'BRIEN [7] and by VAN TUYL [8]. However, there still remains a certain parameter range which is covered neither by the asymptotic approach nor by the solution based on the assumption of small φ.

Practically any physical or mechanical problem, which includes a variable parameter, can be approximately solved as this parameter approaches zero or infinity. How can this "limiting" information be used in the study of the system at the intermittent values of the parameter? This problem is one of the most complicated ones in asymptotic analysis. In many instances the answer to it is alleviated by two-point Padé approximants [9]. Some effective applications of two-point Padé approximants to the theory of dispersed media can be found in [10].

Unfortunately, the asymptotic formula for $\varphi \to \varphi_{\max}$ contains the logarithmic function; that is why two-point Padé approximants in its "pure form" can not be used in the problem under consideration. This point is most essential for two-point Padé approximants because, as a rule, one of the limits ($\lambda \to 0$ or $\lambda \to \infty$) for real mechanical problems gives expansions with logarithmic terms or other complicated functions. In order to overcome these obstacles, during the last few years the so-called quasifractional approximants are widely used in physics [11].

Here we use quasifractional approximants to derive an approximate analytical expression of k, valid for all values of the spheres volume fraction $\varphi \in [0; \varphi_{\max}]$

[12, 13]. As the bases we use the coefficients of the perturbation expansion of k at $\varphi = 0$ and the asymptotic formula for $\varphi \to \varphi_{\max}$. Three different types of the spheres space arrangement (simple cubic (SC), body-centred cubic (BCC) and face-centred cubic (FCC) arrays) are considered. The obtained results give a good agreement with numerical data.

This paper is organized as follows: in Sec. 2 and in Sec. 3 we define the "limiting" solutions for $\varphi \to 0$ and for $\varphi \to \varphi_{\max}$. The quasifractional approximant is developed in Sec. 4. In Sec. 5 the obtained results are compared with known numerical data, and in Sec. 6 we discuss the advantages and limitations of our method.

2. Solution for the case of small spheres

Lord RAYLEIGH [3] was the first to analyze the case when spheres are arranged in the SC array. He developed a solution for the case $\varphi \to 0$ by replacing the spheres by dipoles and higher-order multipoles, and obtained

$$k = 1 - 3\varphi \left(\frac{2+\lambda}{1-\lambda} + \varphi - \frac{1-\lambda}{4+3\lambda} d\varphi^{10/3} + O\left(\varphi^{14/3}\right) \right)^{-1}, \tag{2.1}$$

where φ is the spheres volume fraction; λ is the heat conductivity of spheres; $d = 1.57$.

MEREDITH and TOBIAS [14] extended Rayleigh's analysis and calculated the coefficient of the $O(\varphi^{14/3})$ term. The validity of Rayleigh's method, however, was questioned, because it involves the summation of non-absolutely convergent series. MCPHEDRAN and MCKENZIE [4] have modified Rayleigh's procedure in order to overcome these difficulties and, hence, this method has now a sound theoretical basis.

An alternative method, which avoids the difficulties encountered in Rayleigh's original treatment, was devised by ZUZOVSKY and BRENNER [15]. They used the method of generalized functions to develop a series expression for k to $O(\varphi^{20/3})$ and found that the coefficient of $O(\varphi^{14/3})$ in (2.1) reported by MEREDITH and TOBIAS [14] was in error. But, owing to a numerical slip in calculations, some results of Zuzovsky and Brenner were incorrect. The next development of this method was carried out by SANGANI and ACRIVOS [5], who corrected the previous errors and obtained the following perturbation expansion for k in terms of φ:

$$k = 1 - 3\varphi \left(-\frac{1}{L_1} + \varphi + a_1 L_2 \varphi^{10/3} \frac{1 + a_2 L_3 \varphi^{11/3}}{1 - a_3 L_2 \varphi^{7/3}} \right.$$
$$\left. + a_4 L_3 \varphi^{14/3} + a_5 L_4 \varphi^6 + a_6 L_5 \varphi^{22/3} + O(\varphi^{25/3}) \right)^{-1}, \tag{2.2}$$

where $L_i = \dfrac{\lambda - 1}{\lambda + 2i/(2i-1)}$, $i \in N$ (here we consider the case of perfectly conducting spheres, $\lambda = \infty$; $L_i = 1$); the constants $a_1, ..., a_6$ for the three cubic arrays are listed in Table 1.

Table 1. The constants $a_1, ..., a_6$.

	a_1	a_2	a_3	a_4	a_5	a_6
SC array	1.305	0.231	0.405	0.0723	0.153	0.0105
BCC array	0.129	−0.413	0.764	0.257	0.0113	0.00562
FCC array	0.0753	0.697	−0.741	0.0420	0.0231	$9.14 \cdot 10^{-7}$

It should be stressed that further development of this method by taking into account the terms of higher order in the perturbation expansion (2.2), however, does not allow us to calculate k correctly in the case of large spheres ($\varphi \to \varphi_{\max}$).

3. Solution for the case of large spheres

In the case of perfectly conducting large spheres ($\lambda = \infty, \varphi \to \varphi_{\max}$), the problem can be solved by means of a reasonable physical assumption that the flux of heat occurs entirely in the region where spheres are in near contact. Thus, the effective conductivity is determined in an asymptotic form for the flux between two spheres, which is logarithmically singular in the gap width, justifying the assumption. KELLER [6] solved this problem correctly to $O(\ln \chi)$, where χ is the dimensionless gap width ($\chi \to 0$). BATCHELOR and O'BRIEN [7] extended Keller's work to include touching spheres and near-perfect conductors, and derived the following asymptotic expansion for $\lambda = \infty$ and $\varphi \to \varphi_{\max}$:

$$k = -M_1 \ln \chi - M_2 + O(\chi^{-1}), \tag{3.1}$$

where $\chi = 1 - (\varphi/\varphi_{\max})^{1/3}$ is the nondimensional gap width between the neighbouring spheres, $\chi \to 0$; $M_1 = 0.5\varphi_{\max} p$, p is the number of contact points at the surface of a sphere; M_2 is a constant, dependent on the type of spheres space arrangement. The values of M_1, M_2 and $\varphi_{\max}$ for the three cubic arrays are listed in Table 2.

Table 2. The constants M_1, M_2 and $\varphi_{\max}$.

	M_1	M_2	$\varphi_{\max}$
SC array	$\pi/2$	0.7	$\pi/6$
BCC array	$\sqrt{3}\pi/2$	2.4	$\sqrt{3}\pi/8$
FCC array	$\sqrt{2}\pi$	7.1	$\sqrt{2}\pi/6$

VAN TUYL [8] has recently calculated the next higher order terms in the asymptotic expansion (3.1).

4. The quasifractional approximant

Now we go on to the problem of evaluating the effective conductivity k in terms of the quasifractional approximants [11, 12]. So, we consider a function of φ determined by the power series expansion (2.2) at $\varphi \to 0$ and knowing the asymptotic expansion (3.1) at $\varphi \to \varphi_{\max}$. A singularity of the searching solution involves the logarithmic function in the expression (3.1). In order to reproduce this singularity, the quasifractional approximant has to contain a similar term, so it can be written as follows:

$$k = \left(P_1(\varphi) + P_2\varphi^{(m+1)/3} + P_3 \ln\chi\right)/Q(\varphi), \tag{4.1}$$

where rational functions $P_1(\varphi)$, $Q(\varphi)$ and constants P_2, P_3 are determined from the following conditions: (i) the expansion of (4.1) in powers of φ at $\varphi \to 0$ coincides with m leading terms of the perturbation expansion (2.2), and (ii) the asymptotic behaviour of (4.1) at $\varphi \to \varphi_{\max}$ coincides with n leading terms of the asymptotic expansion (3.1). Thus, we obtain:

$$Q(\varphi) = 1 - \varphi - a_1\varphi^{10/3}; \qquad P_1(\varphi) = \sum_{i=0}^{m} \alpha_i \varphi^{i/3};$$

$$P_2 = \begin{cases} 0, & n = 1, \\ -\left(P_1(\varphi_{\max}) + Q(\varphi_{\max})M_2\right)/\varphi_{\max}^{(m+1)/3}, & n = 2; \end{cases}$$

here coefficients α_i are determined as follows: $\alpha_0 = 1$, $\alpha_3 = 2 - Q(\varphi_{\max})M_1/(3\varphi_{\max})$, $\alpha_{10} = -a_1 - Q(\varphi_{\max})M_1/(10\varphi_{\max}^{10/3})$, $\alpha_j = -Q(\varphi_{\max})M_1/(j\varphi_{\max}^{j/3})$, $j = 1, 2, 4, 5, ..., 8, 9, 11, 12, ..., m-1, m$.

5. Numerical results

The quasifractional approximant (4.1) represents an approximate analytical expression of k, valid for all values of the spheres volume fraction $\varphi \in [0; \varphi_{\max}]$. It should be stressed that taking into account more terms of the "limiting" expansions (2.2) and (3.1) (i.e., increment m and n) leads to the growth of the accuracy of the obtained solution (4.1). Let us illustrate this dependence for the case of the SC array. We calculated k for different values of m and n. In Fig. 1 our analytical results are compared with experimental measurements of KHARADLY, JACKSON [16] and MEREDITH, TOBIAS [14]. Finally, we restrict $m = 19$ and $n = 2$ for all types of arrays, so far as it provides a satisfactory agreement with numerical data and rather simple analytical form of the solution (4.1).

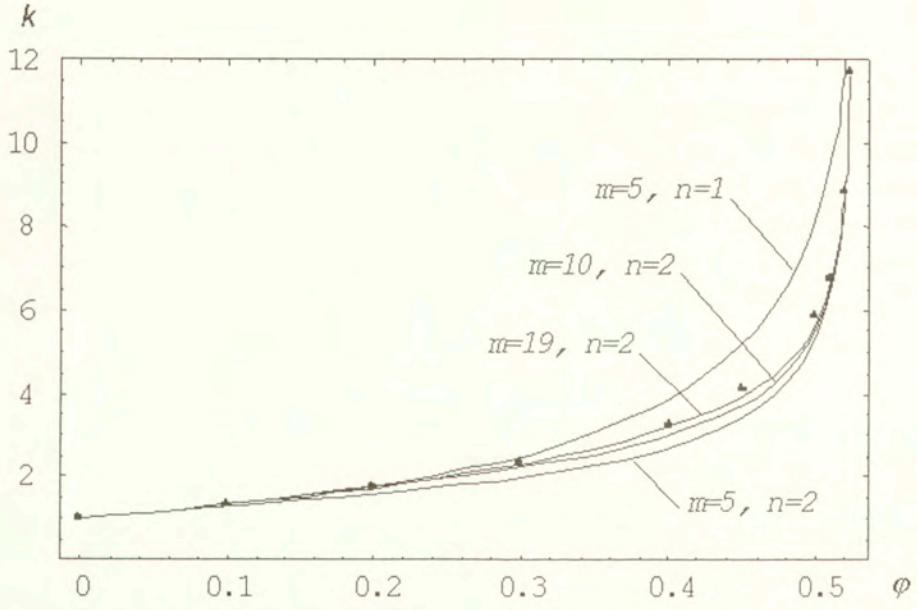

FIG. 1. Effective conductivity of the SC array. Analytical results (4.1) for different values of m, n (solid curves) are compared with experimental data [14, 16] (dots).

Numerical results for the BCC and the FCC arrays are displayed in Fig. 2 and Fig. 3 respectively. The obtained solution (4.1) is compared with experimental results of MCKENZIE *et al.* [17] for the BCC array and with numerical data [17] for the FCC array. The discrepancy between our analytical solution (4.1) and numerical results does not exceed 3.6%, 4.1% and 6.7% for, respectively, the SC, the BCC and the FCC arrays.

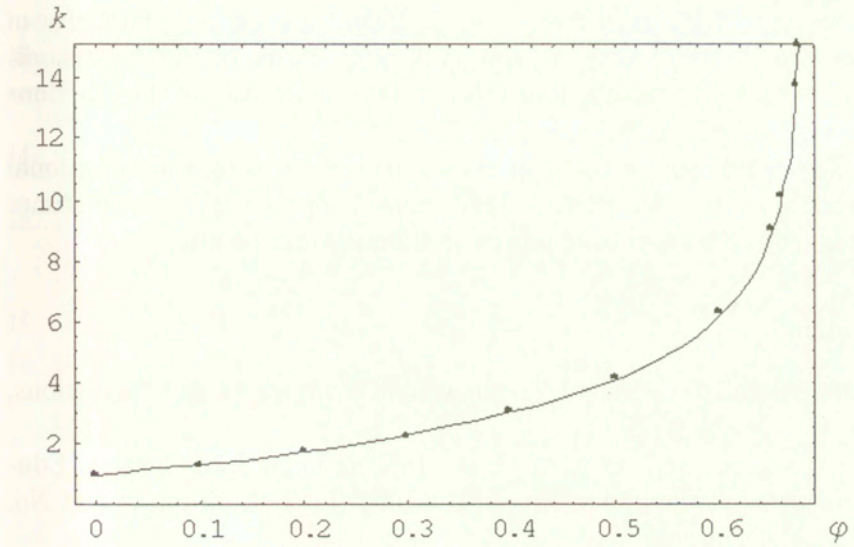

FIG. 2. The BCC array. Obtained analytical solution (4.1) (solid curve) is compared with experimental measurements [17] (dots). $m = 19$, $n = 2$.

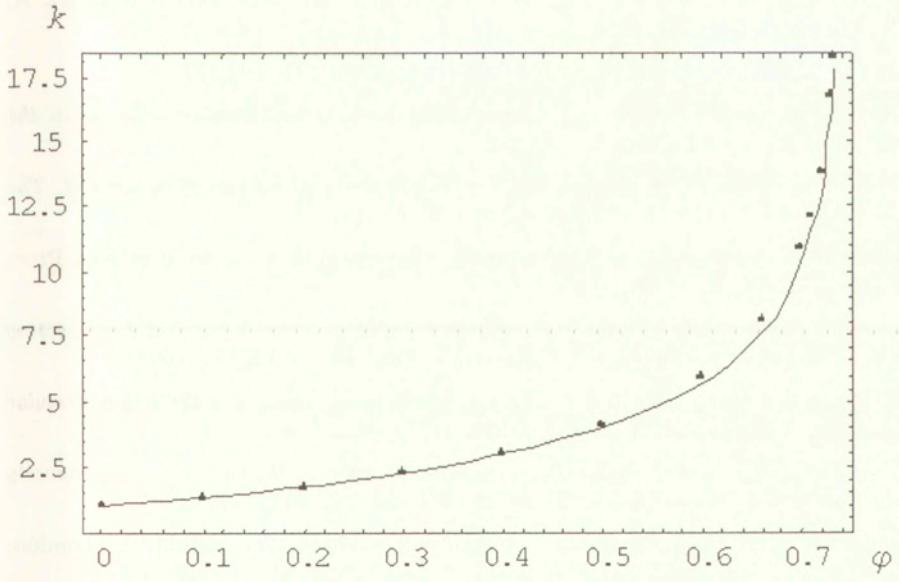

FIG. 3. The FCC array. Analytical results (4.1) (solid curve) is compared with numerical data [17] (dots). $m = 19$, $n = 2$.

6. Concluding remarks

Main advantages of the quasifractional approximants are the simplicity of the algorithms and the possibility of using only a few terms of the expansions. Besides, it is possible to take into account the known singularities of the functions defined.

On the other hand, one of the important features of using quasifractional approximants is the control of accuracy of the realized approximation. Sometimes to this end one can use numerical methods or experimental results.

Acknowledgment

Authors are grateful to the referee for the valuable comments and suggestions, which helped us to improve the paper.

This work was supported, in part, by the International Soros Science Education Program through the grants No. SPU061002 (for I. Andrianov) and No. PSU071071 (for V. Danishevs'kyy).

References

1. G. K. BATCHELOR, *Transport properties of two-phase materials with random structure*, A. Rev. Fluid Mech., **6**, 227–254, 1974.
2. J. C. MAXWELL, *Electricity and magnetism*, Clarendon Press, Oxford 1873.
3. R. S. RAYLEIGH, *On the influence of obstacles arranged in rectangular order upon the properties of medium*, Phil. Mag., **34**, 481–502, 1892.
4. R. C. MCPHEDRAN and D. R. MCKENZIE, *The conductivity of lattices of spheres. I. The simple cubic lattice*, Proc. R. Soc. Lond. A., **359**, 45–63, 1978.
5. A. S. SANGANI, A. ACRIVOS, *The effective conductivity of a periodic array of spheres*, Proc. R. Soc. Lond. A., **386**, 263–275, 1983.
6. J. B. KELLER, *Conductivity of a medium containing a dense array of perfectly conducting spheres or cylinders or nonconducting cylinders*, J. Appl. Phys., **34**, 991, 1963.
7. G. K. BATCHELOR and R. W. O'BRIEN, *Thermal or electrical conduction through a granular material*, Proc. R. Soc. Lond. A., **355**, 313–333, 1977.
8. A. H. VAN TUYL, *Asymptotic expansions with error bounds for the coefficients of capacity and induction of two spheres* , SIAM J. Math. Anal., **27**, 782–804, 1996.
9. G. BAKER and P. GRAVES-MORRIS, *Padé approximants*, Addison-Wesley Publ. Co., London, Tokyo 1995.
10. S. TOKARZEWSKI, J. BLAWZDZIEWICZ and I. ANDRIANOV, *Effective conductivity for densely packed highly conducting cylinders*, Appl. Phys. A., **59**, 601–604, 1994.
11. P. MARTIN and G. A. BAKER, *Two-point quasifractional approximant in physics. Truncation error*, J. Math. Phys., **32**, 1470–1477, 1991.

12. I. ANDRIANOV, G. STARUSHENKO and S. TOKARZEWSKI, *Asymptotic investigation of effective transport properties of composite materials*, Abstract of the 32nd Polish Solid Mechanics Conference, Zakopane (Poland) 1998, 47–48.

13. S. TOKARZEWSKI, I. ANDRIANOV and V. DANISHEVS'KYY, *Continued fraction approach to the torsionally oscillating viscoelastic beams reinforced with viscoelastic fibres*, Abstract of the 32nd Polish Solid Mechanics Conference, Zakopane (Poland), 1998, 377–378.

14. R. E. MEREDITH and C. W. TOBIAS, *Resistance to potential flow trough a cubical array of spheres*, J. Appl. Phys., **31**, 1270–1273, 1960.

15. M. ZUZOVSKY and H. BRENNER, *Effective conductivities of composite materials composed of cubic arrangements of spherical particles embedded in an isotropic matrix*, Z. angew. Math. Phys., **28**, 6, 979–992, 1977.

16. M. M. Z. KHARADLY and W. JACKSON, Proc. Elect. Engrs., **100**, 199–212, 1952.

17. D. R. MCKENZIE, R. C. MCPHEDRAN and G. H. DERRICK, *The conductivity of lattices of spheres. II. The body-centred and face-centred lattices*, Proc. R. Soc. Lond. A., **362**, 211–232, 1978.

Received July 8, 1999; revised version December 30, 1999.

Arch. Mech., **52**, 2, pp. 329–340, Warszawa 2000

On interactions of frictional cracks

M. BASISTA

Polish Academy of Sciences
Institute of Fundamental Technological Research
ul. Świętokrzyska 21, 00-049 Warszawa, Poland

THIS PAPER DEALS with the estimation of the stress intensity factors for interacting Mode-II cracks undergoing frictional sliding under overall compressive stresses. Crack interaction effects are examined via the Kachanov method that is extended here to account for frictional and cohesive resistance on crack faces. The accuracy of the obtained results is verified through comparison with the "exact" numerical solutions obtained using a boundary element method.

1. Introduction

THE PROBLEM OF A LINEAR ELASTIC solid with a multitude of interacting, arbitrarily located, open cracks under uniform remote loading $\boldsymbol{\sigma}^{\infty}$ has been considered by many authors over the past 20 years. A general algorithm of solving such a problem is as follows. Using the superposition principle, a multiple crack problem is reduced to a subproblem of a single crack but loaded by unknown tractions that are induced by the other cracks. The unknown tractions are then interrelated through singular integral equations which, except for a handful of special cases, do not lend themselves to rigorous analytical methods of solution. Consequently, one has to solve the problem numerically or resort to approximate techniques. As for the numerical approach, a boundary element method (BEM) proved quite effective in solving 2D multiple crack problems when formulated in terms of the complex variable method and the dislocation distribution along crack contours (cf. [1, 2]). A rather obvious reason behind the popularity of the BEM vs. FEM in crack problems is that in the BEM approach only the boundary of the problem geometry requires discretization. For multiple cracks, where a large number of model runs are necessary, this feature is of primary importance. On the other hand, the tractions on the interacting cracks were accurately approximated using Legendre or Chebyshev orthogonal polynomials ([3, 4, 5, 6, 7]). Recently, JU and TSENG [8] presented a comprehensive appraisal of these asymptotic polynomial techniques for crack interaction problems in plane elasticity.

The present note is focused on strong interactions of straight cracks randomly distributed in an infinite, homogeneous, linear elastic, two-dimensional matrix un-

der the action of compressive loading. It is assumed that the cracks are endowed with frictional-cohesive resistance and are constrained against normal opening. In compressive stress fields these cracks may slide in Mode-II provided they are inclined at nonzero angles to the direction of maximum compression. This problem is of practical importance for geotechnical applications where materials are typically deformed under compressive overall stresses. The basic mechanisms underlying inelastic deformation of brittle solids under compression are those of tension cracking and frictional slip. Usually, these two mechanisms are coupled but there are instances where frictional sliding takes the upper hand or precedes the crack growth. For example, in low-porosity rocks some of the preexisting flaws will close under external compression and slide with friction before they sprout curvilinear wings growing subparallel to the direction of maximum compression (the so-called sliding crack mechanism, e.g. [1, 9]).

The objective of this note is to compute the stress intensity factors (SIFs) at the tips of interacting closed cracks once sliding along their faces has been initiated. For this purpose, a relatively simple yet remarkably accurate method developed by KACHANOV [6] will be extended to account for the frictional contact of cracks faces. In order to illustrate the capabilities of the proposed framework, a number of test examples will be solved and the results confronted with the numerical solutions obtained using the boundary element method. Some aspects of this note are also addressed in the conference paper [10].

2. Method

In essence, the method devised in KACHANOV [6] is based on the following central assumption: *The unknown tractions induced on a considered crack by the presence of other cracks can be approximated by the tractions that would have been acted on the considered crack if the other cracks were loaded by uniform average (normal and shear) tractions.*

To assess the validity of this statement and to fully understand its impact on the calculation of SIFs, the reader is referred to the original paper [6] or related papers [11, 12]. On the other hand, since it is intended to keep this note self-contained, the key points of the Kachanov method will be made clear in the course of the analysis to follow. Note that this method yields very good predictions for freely opening cracks even if their tips are very close one to another. There are, however, some limitations to the method which will be discussed later on.

Consider two closed cracks in an infinite, linear elastic plate (Fig. 1) with the local (crack-attached) coordinate systems (x^L, y^L) and the global coordinate system (x_1, x_2). To facilitate drawing, only two cracks are shown but the ensuing equations are formulated for an arbitrary 2D crack array ($L = 1, 2, ..., N$). The

actual (contact) shear and normal stresses existing on the faces of L-th crack are denoted by τ_{xy}^L, σ_y^L. The boundary-value problem A can trivially be decomposed into two subproblems B, C. On the other hand, the problem C can be represented as a superposition of N subproblems, each involving only a single crack but subject to *unknown* shear and normal stresses τ_{xy}^{*L}, σ_y^{*L}. Unlike for open cracks considered in [6] where the sign convention for stresses was inconsequential thus omitted, the signs of the superimposed stresses in the compression case (Fig. 1 A-E) are strictly observed. Here, the adopted sign convention is that of continuum mechanics, i.e. compression is viewed negative. Consequently, for closed frictional cracks it follows from Fig. 1 that

$$\tau_{xy}^{*L} = \tau_{xy}^L - \left(\tau_{xy}^{\infty L} + \Delta\tau_{xy}^L\right), \tag{2.1}$$

$$\sigma_y^{*L} = \sigma_y^L - \left(\sigma_y^{\infty L} + \Delta\sigma_y^L\right), \tag{2.2}$$

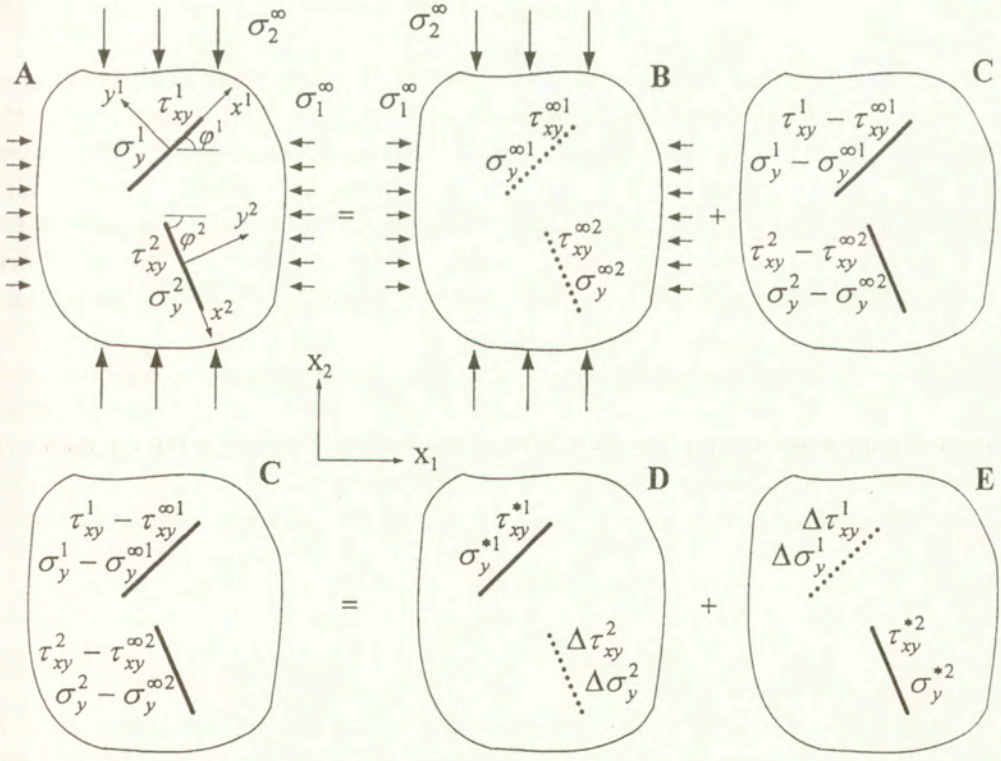

FIG. 1. Superposition of stress for interacting frictional cracks in infinite, linear elastic plate under compression.

where $\tau_{xy}^{\infty L}$, $\sigma_y^{\infty L}$ are the resolved (due to the remote loading $\boldsymbol{\sigma}^{\infty}$ shear and normal stresses in the continuous material along the line of L-th crack; $\Delta\tau_{xy}^L$, $\Delta\sigma_y^L$ are the interaction terms, i.e. shear and normal stresses generated by all other cracks along the line of L-th crack in the continuous material. Note that as long as the crack remains closed, it holds $\sigma_y^{*L} = 0$. Otherwise, $\sigma_y^{*L} = -\left(\sigma_y^{\infty L} + \Delta\sigma_y^L\right)$.

A necessary prerequisite for the computation of the SIFs is the determination of the loading of crack faces $(\tau_{xy}^{*L}, \sigma_y^{*L})$. Once τ_{xy}^{*L}, σ_y^{*L} are known, the SIFs can be computed according to the well-known formulas, [13]:

$$K_I^L(\pm c^L) = \frac{1}{\sqrt{\pi c^L}} \int_{-c^L}^{c^L} \sqrt{\frac{c^L \pm \zeta}{c^L \mp \zeta}} p^{*L}(\zeta) d\zeta, \tag{2.3}$$

$$K_{II}^L(\pm c^L) = \frac{1}{\sqrt{\pi c^L}} \int_{-c^L}^{c^L} \sqrt{\frac{c^L \pm \zeta}{c^L \mp \zeta}} \tau^{*L}(\zeta) d\zeta, \tag{2.4}$$

where $p^{*L} = -\sigma_y^{*L}$, $\tau^{*L} = -\tau_{xy}^{*L}$, due to the sign convention and c^L denotes the half-length of a straight crack. For closed cracks only (2.4) is relevant.

It is claimed here that irrespective of whether the interacting cracks are open or frictional, the central assumption of the Kachanov method remains valid: the unknown crack interaction stresses $\Delta\sigma_y^L$, $\Delta\tau_{xy}^L$ are induced only by uniform average tractions (as yet unknown) acting on the other cracks' faces. A far-reaching consequence of this assumption is that it yields a functional form for the unknown stresses $\Delta\sigma_y^L$, $\Delta\tau_{xy}^L$ since the problem of a single crack loaded by uniform tractions has analytical solution. Following KACHANOV [6], denote by P_{ij}^K and T_{ij}^K the standard stress fields that are generated in the continuous material by the K-th crack loaded by uniform normal and shear tractions of *unit intensity*, respectively. These standard stress fields can be computed using a suitable Westergaard function (as it is done in this paper) or can be found in textbooks on linear fracture mechanics. Hence, the crack interaction terms $\Delta\sigma_y^L$, $\Delta\tau_{xy}^L$, (generated in the continuous material) can be expressed in the following general form

$$\Delta\sigma_y^L = -n_i^{(L)} \left[P_{ij}^K \langle\sigma_y^{*K}\rangle + T_{ij}^K \langle\tau_{xy}^{*K}\rangle\right] n_j^{(L)}, \quad K, L = 1, ..., N; (K \neq L), \tag{2.5}$$

$$\Delta\tau_{xy}^L = -n_i^{(L)} \left[P_{ij}^K \langle\sigma_y^{*K}\rangle + T_{ij}^K \langle\tau_{xy}^{*K}\rangle\right] m_j^{(L)}, \quad K, L = 1, ..., N; (K \neq L). \tag{2.6}$$

In (2.5) and (2.6), the summation convention applies to the repeated indices K while it does not apply to the indices placed in parentheses i.e. (L); $\mathbf{n}^L$, $\mathbf{m}^L$ are crack-attached normal and tangential unit vectors; the Macauley bracket $\langle\ \rangle$ denotes the average value of the bracketed quantity. The standard stress fields

P_{ij}^K and T_{ij}^K are usually written assuming positive unit intensities of normal and shear tractions. However, in the considered case, the average normal stress (internal pressure) $\langle \sigma_y^{*K} \rangle$ and the average shear stress $\langle \tau_{xy}^{*K} \rangle$ acting on the crack faces are subject to the adopted sign convention. Hence, the minus signs in (2.5) and (2.6).

If the Eqs. (2.5) and (2.6) are to hold for the averages $\langle \sigma_y^{*K} \rangle$, $\langle \tau_{xy}^{*K} \rangle$ of an arbitrary crack, they also have to hold for $\langle \sigma_y^{*L} \rangle$, $\langle \tau_{xy}^{*L} \rangle$ of the L-th crack itself. This is nothing else but a rule of self-consistency. Applying this rule to the Eqs. (2.5) and (2.6), i.e. averaging them, leads to

$$\langle \Delta \sigma_y^L \rangle = -\Lambda_{11}^{KL} \langle \sigma_y^{*K} \rangle - \Lambda_{12}^{KL} \langle \tau_{xy}^{*K} \rangle, \tag{2.7}$$

$$\langle \Delta \tau_{xy}^L \rangle = -\Lambda_{21}^{KL} \langle \sigma_y^{*K} \rangle - \Lambda_{22}^{KL} \langle \tau_{xy}^{*K} \rangle, \tag{2.8}$$

where Λ_{ij}^{KL} are the Kachanov transmission factors (interaction matrices) defined as follows:

$$\left.\begin{aligned} \Lambda_{11}^{KL} &= n_i^{(L)} \langle P_{ij}^K \rangle^{(L)} n_j^{(L)} \\ \Lambda_{12}^{KL} &= n_i^{(L)} \langle T_{ij}^K \rangle^{(L)} n_j^{(L)} \\ \Lambda_{21}^{KL} &= n_i^{(L)} \langle P_{ij}^K \rangle^{(L)} m_j^{(L)} \\ \Lambda_{22}^{KL} &= n_i^{(L)} \langle T_{ij}^K \rangle^{(L)} m_j^{(L)} \end{aligned}\right\} (K \neq L) \tag{2.9}$$

$$\Lambda_{ij}^{KL} = 0; \quad (K = L). \tag{2.10}$$

For convenience, the notation of the transmission factors in (2.9) has been slightly changed as compared to that in the original paper [6]. For example, Λ_{21}^{KL} denotes the average shear stress (lower index 2) on crack L due to unit normal stress (lower index 1) on crack K. Incidentally, it seems that there is a misprint with regard to the formula (13b) in the original paper. Namely, in the limit case of $K = L$ (crack interaction with itself) it should be $\Lambda_{ij}^{KK} = 0$, (2.10), and not $\Lambda_{ij}^{KK} = \delta_{ij}$, as in [6]. Note that to compute the transmission factors, the standard stress fields generated by the uniformly loaded K-th crack have to be integrated along the line of the L-th crack. For a given configuration of N cracks this is usually done by numerical integration.

The actual stresses τ_{xy}, σ_y induced by the frictional-cohesive contact on the crack faces are interrelated through a law of dry friction. A simple Coulomb-Mohr law is adopted for this purpose:

$$\tau_{xy}^L = \mp \tau_c \pm \mu \sigma_y^L, \tag{2.11}$$

where τ_c is the cohesion and μ is the coefficient of dry friction, both being positive constants. In Eq. (2.11) and the equations to follow, the upper signs hold for cracks oriented at $0 < \varphi^L < \pi/2$ while the lower ones for $-\pi/2 < \varphi^L < 0$, Fig. 1.

Making use of (2.1), (2.2) and (2.11), it follows that

$$\tau_{xy}^{*L} = \mp\tau_c \pm \mu\sigma_y^{\infty L} - \tau_{xy}^{\infty L} \pm \mu\Delta\sigma_y^L - \Delta\tau_{xy}^L. \tag{2.12}$$

Averaging (2.12) and using (2.7), (2.8), the following system of N linear equations is obtained

$$\left(\delta^{KL} \pm \mu\Lambda_{12}^{KL} - \Lambda_{22}^{KL}\right)\langle\tau_{xy}^{*K}\rangle = \mp\tau_c \pm \mu\sigma_y^{\infty L} - \tau_{xy}^{\infty L}, \quad (K, L = 1, 2, ..., N). \tag{2.13}$$

The right-hand side of (2.13) specifies the remote loading conditions and the friction-cohesion resistance on each crack's faces. In other words, it represents the effective (net) shear stress that drives the crack sliding. The crack array geometry and the influence of friction on the transmission of shear stresses are reflected by the left-hand side. The system of equations (2.13) with the transmission factors (2.9), (2.10) and a given load $(\sigma_y^{\infty L}, \tau_{xy}^{\infty L})$ of the crack faces constitute the governing system of linear algebraic equations from which the average shear stresses $\langle\tau_{xy}^{*K}\rangle$ can be computed.

If the average values of shear stresses $\langle\tau_{xy}^{*K}\rangle$ are known, it is straightforward to compute the whole distribution of τ_{xy}^{*K}. From (2.12), when combined with (2.5) and (2.6), it follows that

$$\tau_{xy}^{*L} = \mp\tau_c \pm \mu\sigma_y^{\infty L} - \tau_{xy}^{\infty L} + n_i^{(L)} T_{ij}^K \langle\tau_{xy}^{*K}\rangle \left(\mp\mu n_j^{(L)} + m_j^{(L)}\right). \tag{2.14}$$

Finally, combining (2.14) and (2.4), the K_{II} factors for interacting frictional cracks read

$$K_{II}^L(+c) = \sqrt{\pi c^{(L)}}\left(\tau_{xy}^{\infty(L)} \pm \tau_c \mp \mu\sigma_y^{\infty(L)}\right) + \frac{\langle\tau_{xy}^{*K}\rangle}{\sqrt{\pi c^{(L)}}}\left[n_i^{(L)}\left(\int_{-c^L}^{c^L}\sqrt{\frac{c^L+\zeta}{c^L-\zeta}}T_{ij}^K\,d\zeta\right)\left(\pm\mu n_j^{(L)} - m_j^{(L)}\right)\right]$$

$$K_{II}^L(-c) = \sqrt{\pi c^{(L)}}\left(\tau_{xy}^{\infty(L)} \pm \tau_c \mp \mu\sigma_y^{\infty(L)}\right) + \frac{\langle\tau_{xy}^{*K}\rangle}{\sqrt{\pi c^{(L)}}}\left[n_i^{(L)}\left(\int_{-c^L}^{c^L}\sqrt{\frac{c^L-\zeta}{c^L+\zeta}}T_{ij}^K\,d\zeta\right)\left(\pm\mu n_j^{(L)} - m_j^{(L)}\right)\right]. \tag{2.15}$$

3. Test examples

To evaluate the predictive capability of the present model, the basic Eqs. (2.13), (2.14) (2.15) have been implemented numerically. For this purpose, a source FORTRAN code has been assembled based on a similar code for open cracks [14]. The numerical algorithm is relatively simple except for the weighted integrals in (2.15) which required some special treatment. The following three test examples of an infinite, linear elastic plate under uniaxial compression with:

- a pair of collinear inclined cracks (Fig. 2, insert),
- a pair of symmetrically inclined cracks (Fig. 3, insert),
- a pair of stacked cracks (Fig. 5, insert),

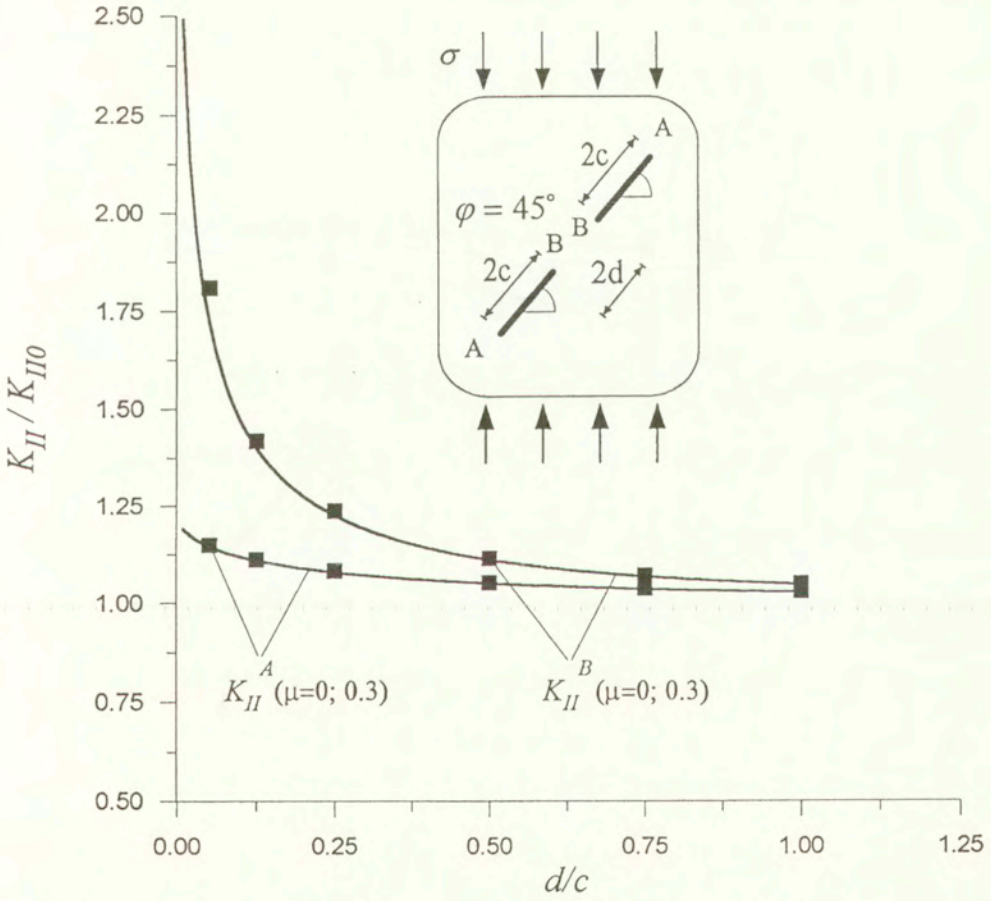

FIG. 2. Two collinear cracks under uniaxial compression. Normalized K_{II} factors vs. relative distance of crack tips for $\mu = 0.3$ and $\tau_c = 0$. Solid lines depict present solution, squares – BEM solution.

have been solved using the developed code. In parallel, the same three test problems have been solved using the BEM source code [15, 16].

In Figures 2, 3, 4, 5 the present solutions are compared with the 'exact' numerical ones obtained by means of the BEM. For the selected test examples the normalized K_{II} factors vs. the relative distance of crack tips d/c are plotted for frictionless ($\mu = 0$) and frictional contact ($\mu = 0.3$) on crack faces. The normalization factor K_{II0} is the stress intensity factor for the respective single crack under a given load with all other cracks absent. On the example of the inclined cracks (insert in Fig. 3), an intermediate step of the method, namely the computed average shear stress $\langle \tau_{xy}^{*1} \rangle$ vs. d/c, is also illustrated and compared with the respective BEM data in Fig. 4.

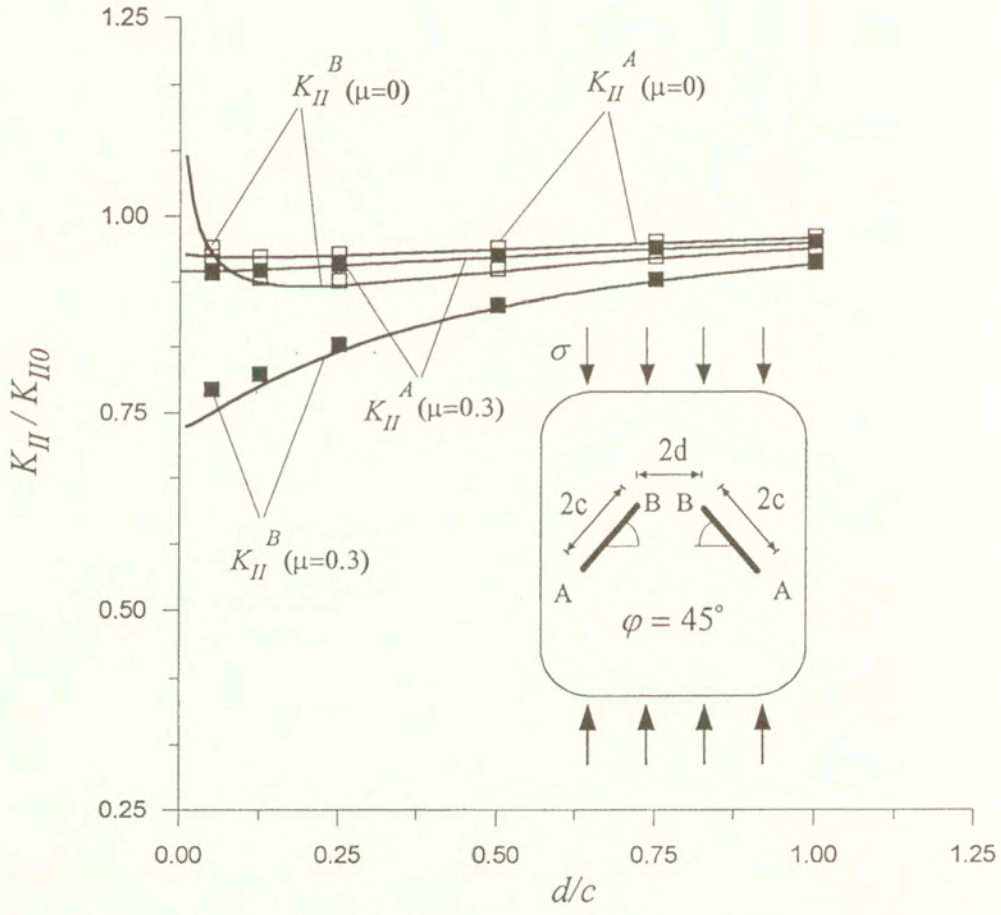

FIG. 3. Two symmetrically inclined crack under uniaxial compression. Normalized K_{II} factors vs. relative distance of crack tips. Solid curves – present solution, squares – BEM data for $\mu = 0$, $\mu = 0.3$ at $\tau_c = 0$.

Typically of open cracks, collinear configurations induce amplification of stresses and stress intensity factors as cracks approach one another. In the case of frictional cracks this effect is maintained, as can be seen in Fig. 2. On the other hand, the stacked crack configurations (Figs. 3, 4, 5) promote shielding (for the most part) as d/c becomes smaller.

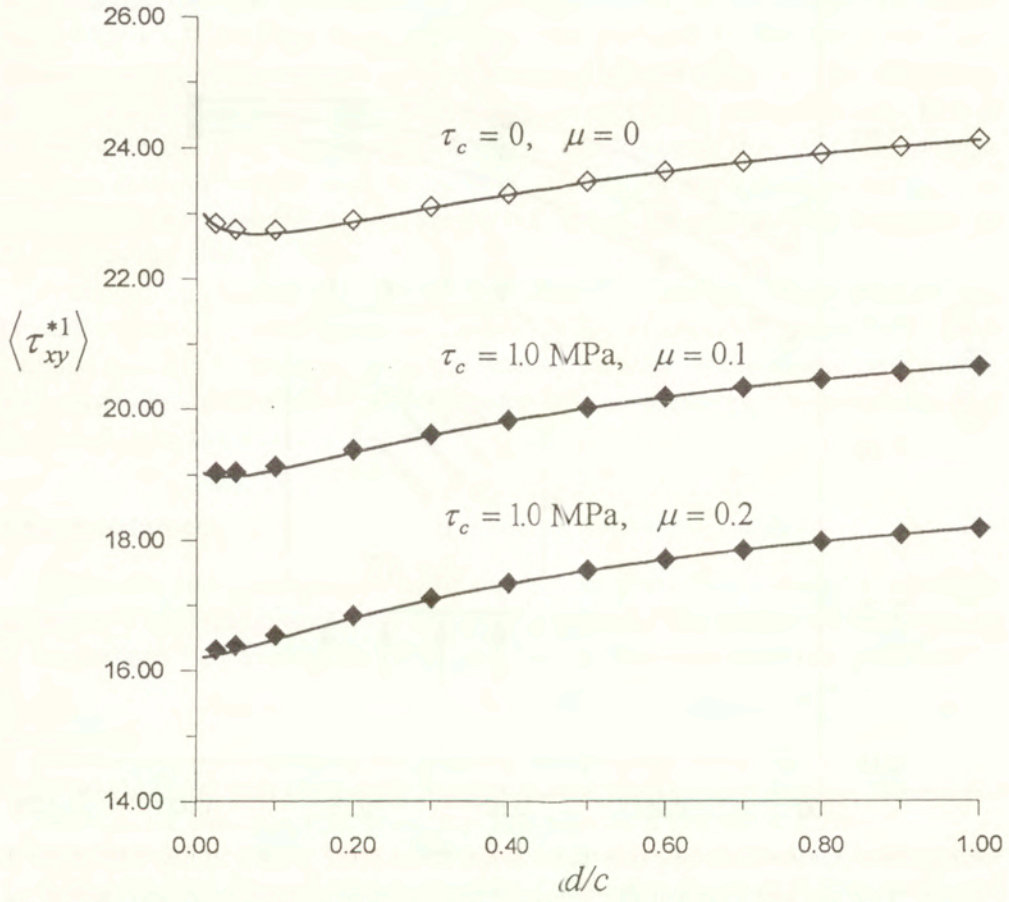

FIG. 4. Average shear stress $\langle \tau_{xy}^{*1} \rangle$ as predicted by Eq. (2.13) vs. BEM data (diamonds) for inclined cracks of Fig. 3.

All figures clearly show that the accuracy of the extended Kachanov method is excellent even at very small distances between the crack tips. This could have been expected for the aligned cracks since Kachanov's method has always been working fine for collinear crack arrays. However, stacked crack configurations are an acid test for the method. Surprisingly enough, for two parallel stacked cracks (Fig. 5) the present results and the BEM data are practically indistinguishable with the exception of the outer tip at $\mu = 0.3$ and $d/c = 0.05$. But even there

the error is merely 0.8%. The least accurate results are obtained in the case of inclined cracks for inner tips (labeled B in Fig. 3) at $\mu = 0.3$ and $d/c = 0.05$. Nevertheless, the error in this case is less than 3% which is still reasonable for practical applications.

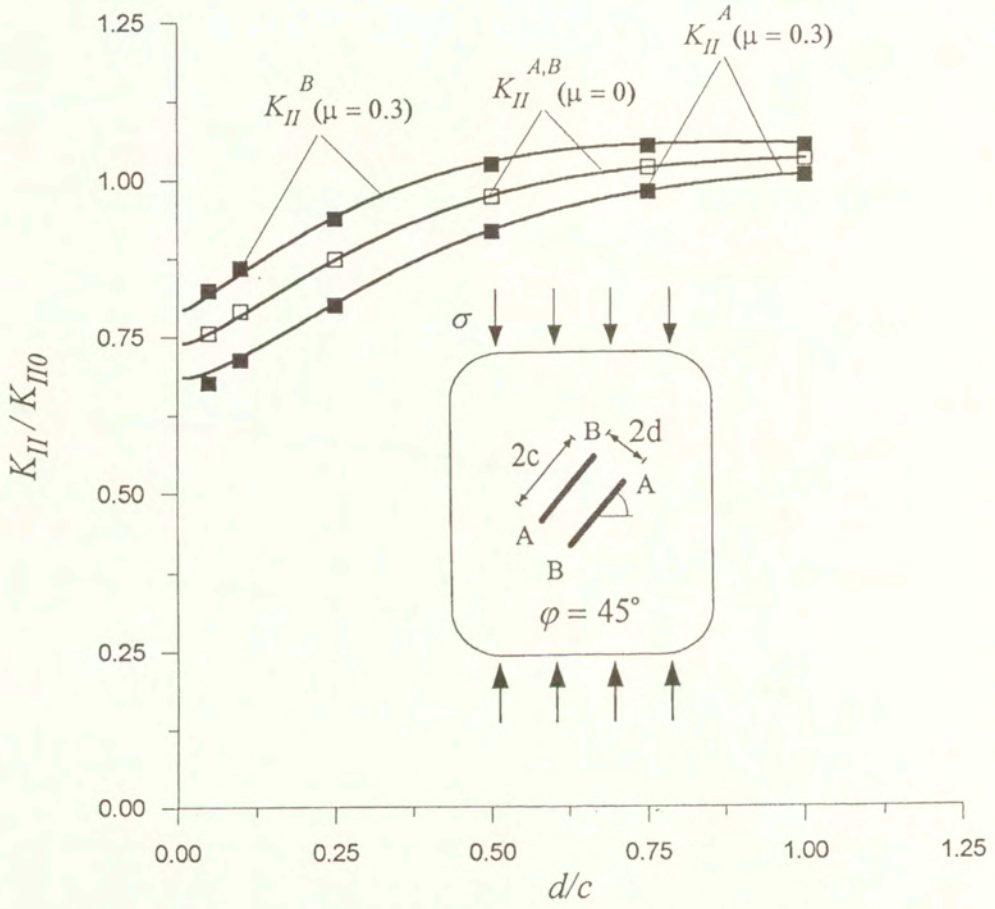

FIG. 5. Two stacked cracks under uniaxial compression. Normalized K_{II} factors vs. relative distance of crack tips. Solid curves – present solution, squares – BEM data, for $\mu = 0$, $\mu = 0.3$ at $\tau_c = 0$.

4. Conclusions

It has been shown in this paper that the Kachanov method of crack interaction analysis can successfully be extended to the case of frictionally sliding cracks. Introducing the Coulomb-Mohr law for the frictional contact on crack faces, the basic equations of the original model were modified accordingly and implemented

numerically. The test examples were solved in a twofold manner: using the present code and the BEM program. The agreement between the obtained results is remarkably good even at crack tip distances as small as 0.05 of the crack length.

There are at least two reasons for the observed accuracy of the present model. First of all we have been dealing with somewhat biased, though important, situations of straight cracks and distributed loading on crack faces. For such situations the Kachanov scheme is best suited. The applicability of the method in case of point-force loads on crack faces has yet to be checked. To this end, some preliminary results are presented in [17]. Secondly, the formulas for the SIFs (2.3), (2.4) involve the unknown crack-face tractions only in an integral sense. This is in tune with the basic assumption of the method stating that it is the average tractions that contribute most to the SIFs. As for 3D crack configurations, it is known from the analysis of open cracks (cf. [11]) that the method performs in 3D even better than in 2D cases.

It should be pointed out though that this effective and elegant method has its limitations. It is contingent on the knowledge of standard stress fields, thus confined actually to straight (or penny-shaped) cracks. If the cracks grow out of their original planes, which is often the case in real situations, the simplicity and applicability of the method decrease.

Acknowledgment

This work has been supported by the Polish State Committee for Scientific Research (KBN) under the Grant no. 7 T07A 050 15. The author wishes to thank B. Lauterbach for running the BEM program in the considered test problems.

References

1. H. HORII and S. NEMAT-NASSER, *Brittle failure in compression: splitting, faulting and brittle-ductile transition*, Phil. Trans. Roy. Soc. London, **A 319**, 337–374, 1986.
2. A. BETTIN and D. GROSS, *Crack propagation in materials with local inhomogeneities under thermal load* [in:] *Thermal Effects in Fracture of Multiphase Materials*, K.P. Herrmann and Z.S. Olesiak [Eds.], Lecture Notes in Engineering, Springer Verlag, **59**, 85–93, 1990.
3. D. GROSS, *Spannungsintensitaetsfaktoren von Risssystemen*, Ing. Archiv, **51**, 301–310, 1982.
4. Y. Z. CHEN, *General case of multiple crack problems in an infinite plate*, Eng. Fracture Mech., **20**, 591–597, 1984.
5. H. HORII and S. NEMAT-NASSER, *Elastic fields of interacting inhomogeneities*, Int. J. Solids Structures, **21**, 731–745, 1985.
6. M. KACHANOV, *Elastic solids with many cracks – a simple method of analysis*, Int. J. Solids Structures, **23**, 23–43, 1987.
7. Y. BENVENISTE, G. J. DVORAK, J. ZARZOUR and E. C. J. WUNG, *On interacting cracks and complex crack configurations in linear elastic media*, Int. J. Solids Structures, **25**, 1279–1293, 1989.

8. J. W. JU and K. H. TSENG, *An improved two-dimensional micromechanical theory for brittle solids with randomly located interacting microcracks*, Int. J. Damage Mech., **4**, 23–57, 1995.

9. M. BASISTA and D. GROSS, *The sliding crack model of brittle deformation: an internal variable approach*, Int. J. Solids Structures, **35**, 487–509, 1998.

10. M. BASISTA, *Micromechanical, phenomenological, and lattice modeling of brittle damage* [in:] *Modeling of Damage and Fracture Processes in Engineering Materials*, M. BASISTA and W. K. NOWACKI [Eds.], IPPT PAN, Warszawa, 236–298, 1999.

11. M. KACHANOV, *Elastic solids with many cracks and related problems*, Advances Appl. Mech., J. Hutchinson and T. Wu [Eds.], 30, Academic Press, New York, 259–445, 1993.

12. C. MAUGE and M. KACHANOV, *Effective elastic properties of an anisotropic material with arbitrary oriented interacting cracks*, J. Mech. Phys. Solids, **42**, 561–584, 1994.

13. H. TADA, P. PARIS and G. IRWIN, *The Stress Analysis of Cracks Handbook*, Paris Productions Inc., St. Louis, MO, 1985.

14. CH. WAGNER and D. GROSS, *Untersuchungen zur Wechselwirkung zwischen Defekten und einem Einzelriss*, DFG-Arbeitsbericht, Gr 596/15-1, Institut für Mechanik, Technische Hochschule Darmstadt, Germany 1988.

15. B. LAUTERBACH and D. GROSS, *Crack growth in brittle solids under compression*, Mech. Mater., **29**, 81–92, 1998.

16. B. LAUTERBACH and D. GROSS, *Analysis of microcrack interaction in brittle solids* [in:] *Fracture and Damage Mechanics*, M.H. Aliabadi [Ed.], University of London, UK, 213–222, 1999.

17. M. BASISTA and D. GROSS, *A note on crack interactions under compression*, Int. J. Fracture, accepted for publication.

Received December 6, 1999.

SERIES: TRENDS IN MECHANICS OF MATERIALS

Modeling of damage and fracture processes in engineering materials

M. BASISTA and W. K. NOWACKI [Eds.]

This book deals with diverse failure phenomena observed in engineering materials when exposed to mechanical loading. Its main objective is to present analytical, numerical and experimental tools used in applied mechanics to investigate and mathematically describe the processes of damage and fracture occuring under static or dynamic loading conditions. For obvious reasons, failure phenomena are of primary interest to modern technology and engineering. This continuing interest has provided impetus to development of damage and fracture mechanics. These fields have been very active in the recent years and continue to experience rapid growth as new materials appear. The book is based on the general lectures presented at the Workshop on *Modeling of Damage, Localization, and Fracture Processes in engineering Materials* held at Kazimierz Dolny, Poland in June 1998.

Contents and Contributors. Preface **1**. Recent results in the dynamics of stationary and running cracks; *D. Gross*. **2**. Analysis of stable and unstable crack growth; *A. Neimitz*. **3**. Fracture dynamics in one-dimensional strain; *J. R. Klepaczko, P. Chevrier*. **4**. Multiaxial fatigue and damage conditions; *Z. Mróz, A. Seweryn*. **5**. Continuum damage mechanics modeling of creepdamage and elastic-damage-fracture in materials and structures; *J. Skrzypek, H. Kuna-Ciskał, A. Ganczarski*. **6**. Micromechanical, phenomenological, and lattice modeling of brittle damage; *M. Basista*.

Hardbound, ISBN 83-910387-2-6
1999, 298 pages

To order please contact

Editorial Office
Świętokrzyska 21, 00-049 Warsaw, Poland
Email: publikac@ippt.gov.pl
Fax: +48 22 826 98 15
Phone: +48 22 826 60 22

DIRECTIONS FOR THE AUTHORS

The journal *ARCHIVES OF MECHANICS (ARCHIWUM MECHANIKI STOSOWANEJ)* deals with the printing of original papers which should not appear in other periodicals.

As a rule, the volume of a paper should not exceed 40 000 typographic signs, that is about 20 type-written pages, format: 210×297 mm, leaded. The papers should be submitted in two copies. They must be set in accordance with the norms established by the Editorial Office. Special importance is attached to the following directions:

1. The title of the paper should be as short as possible.

2. The text should be preceded by a brief introduction; it is also desirable that a list of notations used in the paper should be given.

3. The formula number consists of two figures: the first represents the section number and the other the formula number in that section. Thus the division into subsections does not influence the numbering of formulae. Only such formulae should be numbered to which the author refers throughout the paper, and also the resulting formulae. The formula number should be written on the left-hand side of the formula; round brackets are necessary to avoid any misunderstanding. For instance, if the author refers to the third formula of the set (2.1), a subscript should be added to denote the formula, viz. $(2.1)_3$.

4. All the notations should be written very distinctly. Special care must be taken to write small and capital letters as precisely as possible. Semi-bold type should be underlined in black pencil. Explanations should be given on the margin of the manuscript in case of special type face.

5. It has been established to denote vectors by semi-bold type. Trigonometric functions are denoted by sin, cos, tg and ctg, inverse functions – by arc sin, arc cos, arc tg and arc ctg; hyperbolic functions are denoted by sh, ch, th and cth, inverse functions – by Arsh, Arch, Arth and Arcth.

6. Figures in square brackets denote reference titles. Items appearing in the reference list should include the initials of the first name of the author and his surname, also the full title of the paper (in the language of the original paper); moreover;

a) In the case of books, the publisher's name, the place and year of publication should be given, e.g.,

5. S. Ziemba, *Vibration analysis*, PWN, Warszawa 1970;

b) In the case of a periodical, the full title of the periodical, consecutive volume number, current issue number, pp. from ... to ..., year of publication should be mentioned; the annual volume number must be marked in black pencil so as to distinguish it from the current issue number, e.g.,

6. M. Sokołowski, *A thermoelastic problem for a strip with discontinuous boundary conditions*, Arch. Mech., **13**, 3, 337–354, 1961.

7. The authors should enclose a summary of the paper. The volume of the summary is to be about 100 words.

8. The authors are kindly requested to enclose the figures prepared on diskettes (format PCX, BitMap or PostScript).

Upon receipt of the paper, the Editorial Office forwards it to the reviewer. His opinion is the basis for the Editorial Committee to determine whether the paper can be accepted for publication or not.

The printing of the paper completed, the author receives 25 copies of reprints free of charge. The authors wishing to get more copies should advise the Editorial Office accordingly, not later than the date of obtaining the galley proofs.

The papers submitted for publication in the journal should be written in English. No royalty is paid to the authors.

Please send us, in addition to the typescript, the same text prepared on a diskette (flopy disk) 3 1/2″ as an ASCII file, preferably in the TEX or LATEX format in Dos or Unix format.

EDITORIAL COMMITTEE

ARCHIVES OF MECHANICS

(ARCHIWUM MECHANIKI STOSOWANEJ)

INSTITUTE OF FUNDAMENTAL TECHNOLOGICAL RESEARCH
is publishing the following periodicals:

ARCHIVES OF MECHANICS – bimontly (in English)
ARCHIVES OF ACOUSTICS – quarterly (in English)
ARCHIVES OF CIVIL ENGINEERING – quarterly (in English)
ENGINEERING TRANSACTIONS – quarterly (in English)
COMPUTER ASSISTED MECHANICS AND ENGINEERING SCIENCES – quarterly (in English)
JOURNAL OF TECHNICAL PHYSICS – quarterly (in English)

Subscription orders for the journals edit by IFTR may be sent directly to the
Editorial Office
Institute of Fundamental Technological Research,
Świętokrzyska 21, p. 508,
00-049 WARSZAWA, Poland.

DIRECTIONS FOR THE AUTHORS

The journal *ARCHIVES OF MECHANICS (ARCHIWUM MECHANIKI STOSOWANEJ)* deals with the printing of original papers which should not appear in other periodicals.

As a rule, the volume of a paper should not exceed 40 000 typographic signs, that is about 20 type-written pages, format: 210×297 mm, leaded. The papers should be submitted in two copies. They must be set in accordance with the norms established by the Editorial Office. Special importance is attached to the following directions:

1. The title of the paper should be as short as possible.

2. The text should be preceded by a brief introduction; it is also desirable that a list of notations used in the paper should be given.

3. The formula number consists of two figures: the first represents the section number and the other the formula number in that section. Thus the division into subsections does not influence the numbering of formulae. Only such formulae should be numbered to which the author refers throughout the paper, and also the resulting formulae. The formula number should be written on the left-hand side of the formula; round brackets are necessary to avoid any misunderstanding. For instance, if the author refers to the third formula of the set (2.1), a subscript should be added to denote the formula, viz. $(2.1)_3$.

4. All the notations should be written very distinctly. Special care must be taken to write small and capital letters as precisely as possible. Semi-bold type should be underlined in black pencil. Explanations should be given on the margin of the manuscript in case of special type face.

5. It has been established to denote vectors by semi-bold type. Trigonometric functions are denoted by sin, cos, tg and ctg, inverse functions – by arc sin, arc cos, arc tg and arc ctg; hyperbolic functions are denoted by sh, ch, th and cth, inverse functions – by Arsh, Arch, Arth and Arcth.

6. Figures in square brackets denote reference titles. Items appearing in the reference list should include the initials of the first name of the author and his surname, also the full title of the paper (in the language of the original paper); moreover;

a) In the case of books, the publisher's name, the place and year of publication should be given, e.g.,

5. S. Ziemba, *Vibration analysis*, PWN, Warszawa 1970;

b) In the case of a periodical, the full title of the periodical, consecutive volume number, current issue number, pp. from ... to ..., year of publication should be mentioned; the annual volume number must be marked in black pencil so as to distinguish it from the current issue number, e.g.,

6. M. Sokołowski, *A thermoelastic problem for a strip with discontinuous boundary conditions*, Arch. Mech., **13**, 3, 337–354, 1961.

7. The authors should enclose a summary of the paper. The volume of the summary is to be about 100 words.

8. The authors are kindly requested to enclose the figures prepared on diskettes (format PCX, BitMap or PostScript).

Upon receipt of the paper, the Editorial Office forwards it to the reviewer. His opinion is the basis for the Editorial Committee to determine whether the paper can be accepted for publication or not.

The printing of the paper completed, the author receives 25 copies of reprints free of charge. The authors wishing to get more copies should advise the Editorial Office accordingly, not later than the date of obtaining the galley proofs.

The papers submitted for publication in the journal should be written in English. No royalty is paid to the authors.

Please send us, in addition to the typescript, the same text prepared on a diskette (flopy disk) 3 1/2″ as an ASCII file, preferably in the TEX or LATEX format in Dos or Unix format.

EDITORIAL COMMITTEE
ARCHIVES OF MECHANICS
(ARCHIWUM MECHANIKI STOSOWANEJ)

Archives of Mechanics

Contents of issue 2 vol. 52

Arch. Mech., **52**, nr 2, str. 201–344, Warszawa 2000